USAAVLABS TECHNICAL REPORT 66-85

ADVANCEMENT OF SPUR GEAR DESIGN TECHNOLOGY

Final Report

By

W. L. McIntire

R. C. Malott

December 1966

U. S. ARMY AVIATION MATERIEL LABORATORIES
FORT EUSTIS, VIRGINIA

CONTRACT DA 44-177-AMC-318(T)

ALLISON DIVISION - GENERAL MOTORS
INDIANAPOLIS, INDIANA

Distribution of this document is unlimited

Disclaimers

The findings in this report are not to be construed as an official Department of the Army position unless so designated by other authorized documents.

When Government drawings, specifications, or other data are used for any purpose other than in connection with a definitely related Government procurement operation, the United States Government thereby incurs no responsibility nor any obligation whatsoever; and the fact that the Government may have formulated, furnished, or in any way supplied the said drawings, specifications, or other data is not to be regarded by implication or other wise as in any manner licensing the holder or any other person or corporation, or conveying any rights or permission, to manufacture, use, or sell any patented invention that may in any way be related thereto.

Trade names cited in this report do not constitute an official endorsement or approval of the use of such commercial hardware or software.

Disposition Instructions

Destroy this report when no longer needed. Do not return it to originator.

DEPARTMENT OF THE ARMY
U. S. ARMY AVIATION MATERIEL LABORATORIES
FORT EUSTIS, VIRGINIA 23604

The objective of this program was to conduct an analytical and experimental study to derive or establish accurate factors for inclusion in spur gear design formula for the accurate appraisal of gear bending strength.

This report presents the results of this investigation. An accurate spur gear bending strength formula was determined and an IBM 7090 computer program using the substantiated formula was provided.

This command concurs in the conclusions made by the contractor.

Task 1M121401D14414
Contract DA 44-177-AMC-318(T)
USAAVLABS Technical Report 66-85
December 1966

ADVANCEMENT OF SPUR GEAR DESIGN TECHNOLOGY

Final Report

EDR 4743

by
W. L. McIntire and R. C. Malott

Prepared by

Allison Division ● General Motors
Indianapolis, Indiana

for

U.S. ARMY AVIATION MATERIEL LABORATORIES
FORT EUSTIS, VIRGINIA

Distribution of this
document is unlimited

FOREWORD

This is the final report on the Allison project entitled "Advancement of Spur Gear Design Technology." This project was conducted during the 13-month period from 29 June 1965 through 28 July 1966 for the U.S. Army Aviation Materiel Laboratories (USAAVLABS) under contract DA 44-177-AMC-318(T).

USAAVLABS technical direction was provided by Mr. R. Givens. Mr. W. L. McIntire served as the Allison project engineer. The principal investigators at Allison were Mr. R. C. Malott, Mr. F. G. Leland, Mr. K. V. Young, and Mr. W. W. Gunkel. The project was reviewed periodically with Mr. R. L. Mattson of General Motors Research for suggestions and comments.

Permission was obtained from the American Gear Manufacturers Association (AGMA) to print AGMA 220.02, Tentative AGMA Standard for Rating the Strength of Spur Gear Teeth, in this final report.

SUMMARY

This report presents the results of an analytical and experimental program to derive and substantiate a bending strength design formula for spur gears. The program consisted of:

- Static single tooth fatigue testing of 16 gear designs in a design experiment to determine the effect of four geometric variables—diametral pitch, pressure angle, fillet size, and fillet configuration (full form ground or protuberant hobbed).
- Evaluation of the ability of five current calculation methods—AGMA, Dolan-Broghamer, Heywood, Kelley-Pedersen, and Lewis—to predict the relative ranking of the 16 fatigue test gear endurance limits.
- Statistical analyses of the fatigue test data to develop a predictive formula and relative significance values of the four geometric variables and their two- and three-factor interactions.
- A strain gage and photostress experimental evaluation to measure stress on eight of the fatigue test gears for comparison with calculated stresses and fatigue test endurance limits.
- R. R. Moore rotating beam fatigue tests of the gear material to establish basic material strength for comparison with fatigue test endurance limits.
- Measurement of the fatigue test gear crack location for comparison with location of the weakest section as predicted by the Lewis and Dolan-Broghamer calculation methods.
- Metallurgical examination of five representative fatigue test gears to verify material processing and mode of failure.
- A dynamic test at high pitch line velocities—up to 26,000 feet per minute—to determine speed effect on gear tooth bending stress.
- Development of a computer program to calculate gear tooth bending stress from the basic gear geometry, thus eliminating the need for a gear tooth layout.

The results of the program were as follows:

- The AGMA method of calculating gear tooth bending stress predicted the greatest number of correct rankings of the 16 fatigue test gear endurance limits. This method also predicted the rank position with the least average error.
- Comparison of endurance limits, based on applied load, calculated from the fatigue test data for each of the 16 gear designs was made by statistical tests of significance. Diametral pitch and pressure angle had a significant effect on gear tooth bending fatigue strength. The AGMA formula successfully compensated for the significant variables determined by the base-line applied load analyses.

- The strain gage stress values obtained tend to verify the AGMA calculated stresses. The average strain rate measured on the fatigue test gears was within 2.5 percent of the strain rate calculated by the AGMA formula.
- The basic gear material endurance limit determined by the R. R. Moore rotating beam test was 182,000 p.s.i. when modified for single-direction bending. The fatigue test gear average endurance limit based on AGMA calculated stress was 182,000 p.s.i. It appears, therefore, that basic material strength can be very closely related to AGMA calculated gear stress and endurance limit.
- Fatigue test gear crack location was nearer the Dolan-Broghamer than the Lewis predicted location, as expected.
- Metallurgical examinations verified good processing of the fatigue test gears and fatigue as the mode of failure. Failures were initiated at random locations across the face width of the gears, indicating minimal influence of surface finish, material inclusions, corner edge break, and test rig alignment.
- Steady hoop stresses were measured in the dynamic test at the weakest section. The measured stresses were 70 percent of the calculated root diameter hoop stress. The measured stress was 14,000 p.s.i. which is considered sufficient to necessitate its inclusion in bending stress determinations for high-speed gears.
- The dynamic test also measured dynamic fluctuating gear tooth level stresses. Stresses indicated a dynamic stress factor increasing with the square of the rotational speed. The dynamic factor was 1.8 at 26,000-feet-per-minute-pitch-line velocity.
- The computer program developed accurately determined the root fillet configuration by calculating the true radius or trochoidal fillet depending on the manufacturing method and the tool (hob) dimensions. The Lewis weakest section is determined by iteration. The gear tooth dimensions determined are used in the AGMA formula to determine bending stress. A hoop stress at the root diameter is then calculated to account for the effect of speed on gear tooth bending stress. The steady hoop stress and the fluctuating bending stresses are then combined by means of a modified Goodman diagram to produce a combined stress and an expected failure life. The modified Goodman diagram was based on the average S/N curve determined by the fatigue test gears.

TABLE OF CONTENTS

Page

APPENDIXES

LIST OF ILLUSTRATIONS

Figure		Page

LIST OF TABLES

BLANK PAGE

INTRODUCTION

The purpose of the project was to conduct an analytical and experimental investigation to derive factors and formulae which can be used to appraise accurately spur gear tooth bending strength for aircraft applications.

The objective of the project was twofold—to substantiate an accurate spur gear bending strength formula and to provide an IBM 7090 computer program using the substantiated formula. Correlation of a basic material strength with this formula was desired.

There are four common modes of gear failure—tooth breakage, surface pitting, scoring, and wear. Tooth breakage is the most severe and often causes considerable secondary damage and sometimes catastrophic failure of an entire gear unit. It may be caused accidentally, such as when a foreign object passes through a tooth mesh, or it may be caused by the repetitive high bending stresses near the root of the tooth when under load.

Many factors affecting the bending fatigue strength of gear teeth are not treated with precision in current spur gear design formulae. This is because the magnitude and interrelationships of the various factors have not been accurately assessed. Gear tooth bending strength is a function of geometric variables such as pressure angle, diametral pitch, tooth width, root fillet form, and root fillet radius. It is also influenced by manufacturing variables such as surface finish, residual stress, material, and processing technique. Operating variables such as speed, alignment, dynamic loading, and vibration affect the fatigue life. A thorough analysis of these variables will permit more accurate assessment of gear life expectancy.

Considerable research has been accomplished in analyzing gear tooth bending strength; however, there is wide variation in the type of analysis, test data, and field experience. In many instances extensive extrapolation has been required to apply these data to carburized gears designed to current standard geometric proportions. The program described herein was conducted in an effort to establish correlation between analytical methods and actual test results for lightweight aircraft gearing.

Current methods of calculating gear tooth bending stress are based on analytical studies and photoelastic tests. These methods produce calculated stresses which are appreciably lower than measured gear stresses and basic material strengths. Thus the calculations are most often used to compare similar designs. An "ideal" gear tooth bending strength formula would relate the operating gear tooth stress to the basic material strength in such a way as to produce a gear life which has been substantiated by fatigue test. It was therefore the intent of the subject program to provide a more accurate bending stress formula by also relating calculated stress and fatigue test results to the basic material strength. R. R. Moore tests of carburized specimens were used to provide a basic material strength.

To accomplish the program, the following analytical and experimental analyses were conducted.

- Design Analysis—An analytical review was made of current spur gear tooth bending strength formulae. Each formula was analyzed and compared to determine the effects of design variables.
- Experimental Evaluation—A photostress analysis was conducted to evaluate the location and distribution of the maximum stress on actual fatigue test gears. Strain gage stress measurements were obtained for correlation with stress calculations.

- **Gear Tooth Fatigue Tests**—A single tooth fatigue test was conducted to investigate the effect of diametral pitch, pressure angle, root fillet size, and root fillet configuration on fatigue life. Eighty gears were manufactured. Extreme care was taken to reduce all possible manufacturing variances which might affect fatigue life. Metallurgical investigations of the fatigue failures were also made to ensure that the basic material was sound and was properly heat treated. Four teeth on each gear were available for fatigue testing.
- R. R. Moore Tests—R. R. Moore tests were conducted using the same heat of material used for the test gears. The data obtained were used for comparison with the bending endurance strengths from the gear fatigue tests.
- Dynamic Tests—An existing accessory gear in an Allison 501-D13 gearbox was instrumented with strain gages. The gear was operated at high speed (pitch line velocity of 27,000 feet/minute) at load and no-load conditions to investigate the effect of speed on bending stress. The data obtained were reduced to determine the effect of centrifugal and dynamic loads on bending stress.
- Final Computer Program—Data from the previously mentioned items were formulated into an IBM 7090 computer program for spur gear bending strength.

ANALYSIS OF PROBLEM

HISTORICAL REVIEW

A review of gear tooth bending strength theory was made. The results of this review are discussed in the following paragraphs.

In 1887, Mr. A. B. Couch in an American Society of Mechanical Engineers (ASME) meeting was asked for a rule to determine safe gear loads (reference 62). He expressed surprise and replied that "the rules furnished (available) are in number bountiful and in variety nearly infinite." He reported that a fellow ASME member had compiled a list of 30 to 40 such rules. In these different rules, safe load varied directly as the square and in a few instances even as the cube of circular pitch. Face width was the only other widely considered factor. The same discussion group expressed an awareness of dynamic loads when they commented, "The cog gearing of power levers used in threshing, owing to the irregular draft of horses, is subjected to heavier strains."

In 1892, Mr. Wilfred Lewis presented a paper which related gear tooth bending strength to tooth geometry. The formula derived in this paper is the basis for most bending stress calculation methods used today. Publication of the Lewis formula did not result in its immediate unanimous adoption. However, it did accelerate further analytical and experimental investigations. Charts and computer programs based on the Lewis formula were developed to expedite gear designs (references 27 and 44). A cantilever beam bending formula for a rectangular section was used to calculate bending stress from 100-times size gear tooth layouts at successive sections 0.100-inch apart to determine the minimum load section for an arbitrary constant stress (reference 31). This work served to verify the principles of the Lewis formula. The improved accuracy required and the higher peripheral speeds of gears necessitated three basic changes to the Lewis formula which have been accepted by general usage—the addition of the Dolan-Broghamer stress concentration factor, the addition of a compressive stress term, and consideration of tooth loading at the high point of single tooth contact or at the pitch diameter rather than at the tip.

The Dolan-Broghamer stress concentration formula is based on photoelastic stress work accomplished at the University of Illinois Engineering Experiment Station in 1942 (reference 16). Their formula is included in the current AGMA Standard 220:02 which is included in this report as Appendix VI. This formula is included in many stress and engineering handbooks as a modified Lewis formula or as a part of the AGMA standard.

Other investigators have obtained photoelastic stress results in close agreement with those of Dolan and Broghamer (references 1 and 10). Prior to the Dolan-Broghamer formula, the stress concentration factors included only a limited number of geometric variables and thus were not as universally applicable (reference 58).

The existence of stresses other than bending stresses in the critical root area of a gear tooth was recognized at an early date. Calculation and vectorial addition of shear stress, from the tangential (circumferential) component of the tooth load, were accomplished and published in 1897 (reference 31). Several current tooth strength formulae include shear stress; the AGMA standard does not. See Appendix VI. For a given tooth load, shear stress would be greate. . a pressure angle gear of 14.5 degrees than for a similar one of 25 degrees.

Compressive stress from the tooth load radial component has been accepted for summation with the gear tooth bending stress. The AGMA standard (Appendix VI) includes a compressive stress term. More recently, an additional compressive stress at the tensile root fillet has been expressed. This additional stress is due to the moment about the gear tooth radial center line from the radial component of the tooth load. An unsymmetrical stress distribution across the weakest section results, which tends to relieve the bending stresses in both the tensile (load side) and compressive (unloaded side) root fillet areas. The gear tooth load components are shown in Figure 1. These static stresses are present in the photoelastic models used to determine stress concentration factors. Thus, their effect is included in the stress concentration factor if the calculated stress used as a basis does not include any such component load stress.

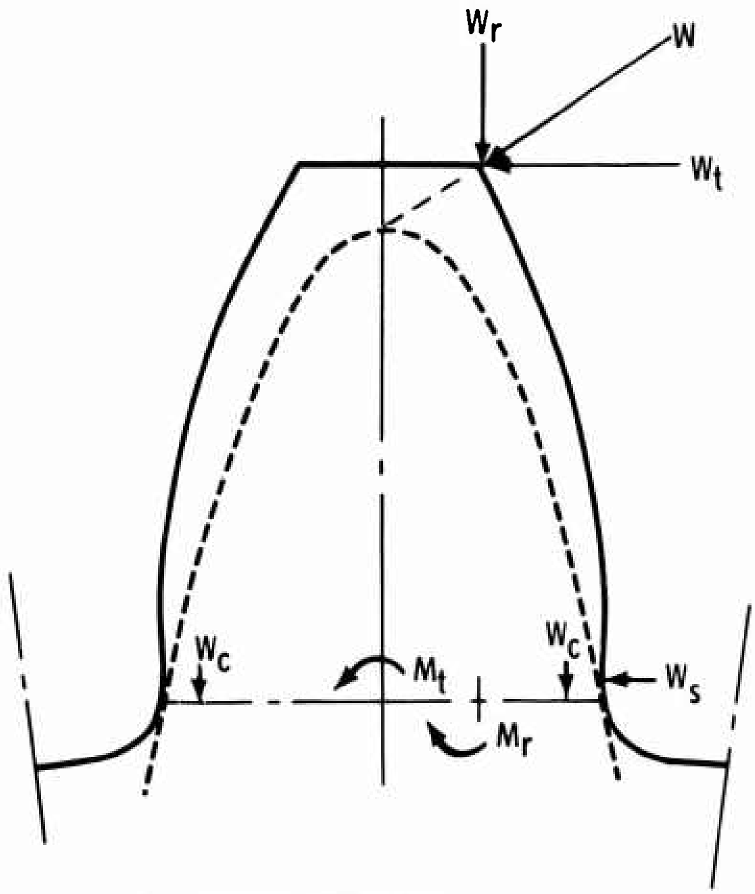

W —normal applied load

W_t—tangential component of W

W_r—radial component of W

W_c—compressive load at weakest section from W_r

W_s—shear load at weakest section from W_t

M_t—bending moment at weakest section from W_t

M_r—bending moment at weakest section from W_r

Figure 1. Gear Tooth Static Load Analysis.

Tip loading, as used in the original Lewis formula, was often changed to pitch line loading to account for load sharing at the tip. It was only recently that the exact point of maximum loading for spur gears was recognized (reference 61). This latest refinement permitted more accurate assessment of safety and/or dynamic factors.

Speed effect curves were developed from experimental data on cast iron gears which had been operated under increasing load until tooth breakage occurred (reference 42). The shape of the curves was similar to the curves currently in the AGMA standard (speed effect becomes constant at higher speeds). The same curve shape can also be observed in current gear scoring versus speed work curves (reference 8).

A review of the Engineering Index volumes for 1950 through 1965 reveals approximately 1255 abstracts on gears. Ten percent of these involve gear tooth bending strength calculation, fatigue testing, or dynamic factors. Almost 20 percent are from foreign sources, mostly German. The yearly output of such articles is nearly constant over this time period.

Several gear tooth strength formulas are of current interest. Five have been investigated and applied to the 16 fatigue test gear configurations—Lewis, Dolan-Broghamer, Heywood, Kelley-Pedersen, and AGMA. A full ground root fillet radius was assumed for all gears in this study. The stresses for each configuration are listed in Table I. The average, range, and variation in stress for each method relative to the Lewis stress are shown in Figure 2. The Kelley-Pedersen method produced a high average stress and by far the greatest range of stress (75 percent of the average Lewis stress). The average stress of the 16 gears as computed by the five formulas varied from 150 to 187 percent of the average Lewis stress. The AGMA method produced the smallest average stress and the smallest range (20 percent of the average Lewis stress). In contrast, the Lewis stresses calculated for the 16 test gear configurations loaded to 1000 pounds per inch of face width varied by over 400 percent. All five formulas identify the same configurations as having the highest and the lowest stresses (boxed numbers in Table I). The highest stresses are most often calculated by the Heywood method, while the lowest stresses in all cases were determined by the Lewis formula, which does not consider stress concentration.

The geometric construction and formula for each of the five gear tooth strength calculation methods are shown in Figures 3, 4, and 5 and in Tables II and III. The Dolan-Broghamer and AGMA methods use Lewis geometric construction (Figure 3) and thus are similar to each other. A detailed discussion of the Dolan-Broghamer and AGMA methods and factors is given in the section titled Discussion of Results.

The Heywood and Kelley-Pedersen construction methods (Figures 4 and 5, respectively) incorporate features which generally lower the position of the weakest section. The Heywood construction method contains several arbitrary features which are not suitable for use with all gear design systems. Variations such as nonstandard addendums and dedendums, which are often used in aircraft designs to balance bending strength or sliding velocity, are examples.

The Kelley-Pedersen method constructs the Lewis parabola, then rotates the tangent line around the root fillet through a "stress shift" angle. Both the Kelley-Pedersen and Heywood methods contain stress concentration factor terms.

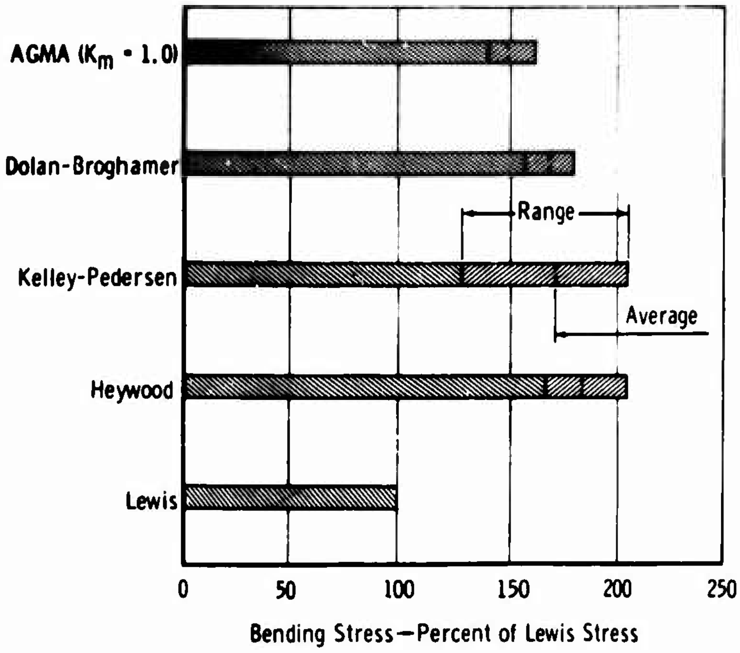

Figure 2. Relative Gear Tooth Bending Stress.

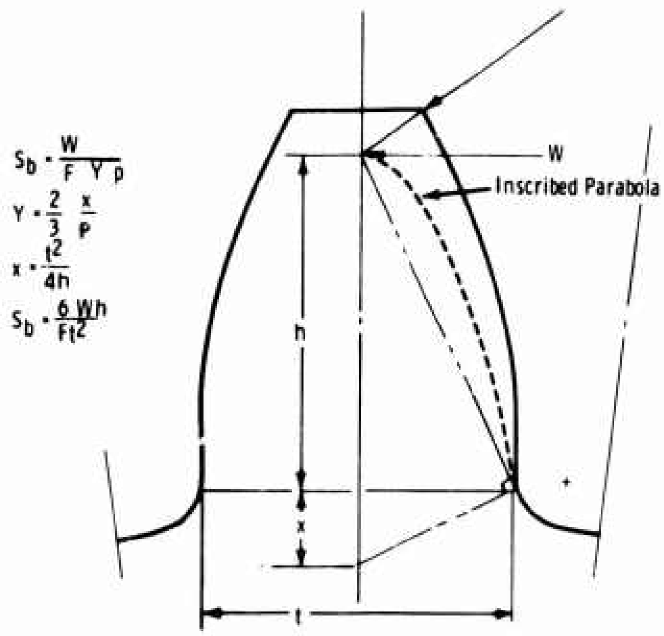

where :

W = tangential component of load applied at vertex of inscribed parabola

F = face width of tooth

S_b = maximum bending stress

h = height of equivalent constant stress parabolic beam

t = thickness of beam at weakest section

p = circular pitch

Figure 3. Lewis Construction and Gear Tooth Bending Stress Formula.

TABLE I
COMPARISON OF GEAR TOOTH BENDING STRESSES CALCULATED BY VARIOUS METHODS

Gear Configuration					Gear Tooth Str			
Gear	Pitch	Pressure Angle (deg)	Radius (in.)	Unit Load (lb)	Lewis	Dolan-Broghamer	Dolan-Broghamer	A
1	6	20	0.050	6,000	12,692	22,682	179 xx	2
3	6	20	0.080	6,000	11,020	19,382	176	1
5	6	20	0.050*	6,000	17,572	28,385	162	2
7	6	20	0.080*	6,000	14,023	22,796	163	2
9	6	25	0.050	6,000	9,871	17,583	178	1
11	6	25	0.067	6,000	$\boxed{9,447}$	$\boxed{16,651}$	176	1
13	6	25	0.050*	6,000	11,028	18,673	169	1
15	6	25	0.067*	6,000	10,468	17,574	168	1
2	12	20	0.025	12,000	27,391	47,781	174	4
4	12	20	0.040	12,000	23,869	40,944	171	3
6	12	20	0.025*	12,000	$\boxed{38,497}$	$\boxed{60,520}$	157 x	5
8	12	20	0.040*	12,000	30,687	48,562	158	4
10	12	25	0.025	12,000	21,159	36,732	174	3
12	12	25	0.033	12,000	20,306	34,893	172	2
14	12	25	0.025*	12,000	23,630	39,044	165	3
16	12	25	0.033*	12,000	22,448	36,806	164	3
Average					19,007	31,813	167.4	2
Variation (Max ÷ Min)					4.075	3.635	1.140	[illegible]

* Root diameter for protuberance cut.
x designates low stress range configuration.
xx designates high stress range configuration.

Notes:
A value of 1.0 was used for K_m (load distribution factor).
High and low calculated stress configurations are boxed.

A

Tooth Stress at High Point of Single Tooth Contact (p. s. i.)

mer	AGMA	AGMA as % of Lewis	Heywood	Heywood as % of Lewis	Kelley-Pedersen	Kelley-Pedersen % of Lewis
	20,484	161 xx	24,504	193	24,229	191
	17,300	157	19,750	179	19,654	178
	26,152	149	31,266	178	27,770	158
	20,729	148	23,614	168	19,518	139
	14,952	151	20,279	205 xx	20,305	206 xx
	$\boxed{14,063}$	149	$\boxed{18,093}$	192	$\boxed{17,512}$	185
	16,148	146	21,900	199	21,767	197
	15,099	144	19,398	185	18,619	178
	43,006	157	51,737	189	51,859	189
	36,447	153	41,710	175	41,848	175
	$\boxed{55,548}$	144	$\boxed{67,120}$	174	$\boxed{57,038}$	148
	44,015	143	50,531	165 x	39,402	128 x
	31,196	147	42,527	201	40,272	190
	29,456	145	38,093	188	34,754	171
	33,680	143	45,997	195	43,453	184
	31,562	141 x	40,888	182	37,195	166
	28,115	147.9	34,838	183.3	33,233	169.4
	3.950	1.142	3.710	1.242	3.257	1.493

B

$$S_b = \left[1 + 0.26\left(\frac{e}{R}\right)^{0.7}\right]\left[\frac{1.5\,a}{e^2} + \left(\frac{0.36}{be}\right)^{0.5}(1 + 0.25\sin\gamma)\right]\frac{P}{F}$$

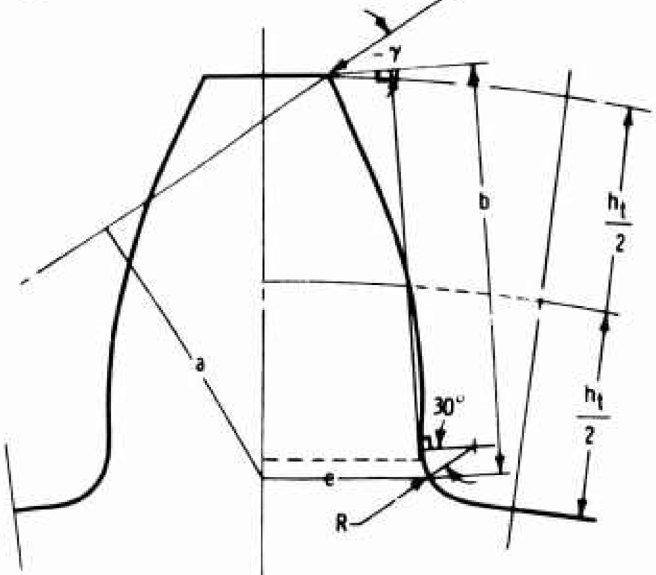

where:

- h_t = tooth depth
- F = face width
- a = moment arm
- e = resisting material
- R = fillet radius
- P = normal load
- γ = angle deviation of load from the point of loading to the point of maximum stress
- b = distance parallel to equivalent straight-sided projection from the point of loading to the point of maximum stress
- S_b = maximum fillet stress

Figure 4. Heywood Construction and Gear Tooth Bending Stress Formula.

$$S_b = \frac{W}{F}\left[1 + 0.26\left(\frac{e}{r_f}\right)^{0.7}\right]\left[\frac{1.5\,a}{e^2} + \frac{\sin\beta}{2\,e} + \frac{0.45}{(be)^{0.5}}\right]$$

where:

- S_b = maximum fillet stress
- W = normal load
- F = tooth face width
- e = dimension of resisting material
- r_f = fillet radius at the point of maximum stress
- b = distance from point of load application to maximum stress
- β = deviation of load line from direction of principal stress

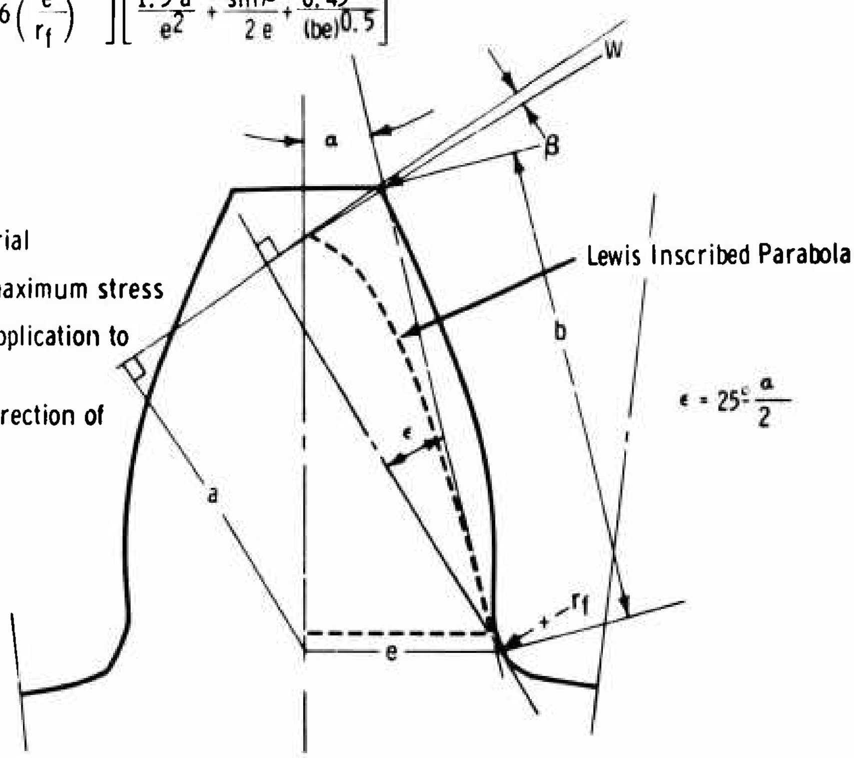

Figure 5. Kelley-Pedersen Construction and Gear Tooth Bending Stress Formula.

TABLE II
DOLAN-BROGHAMER GEAR TOOTH BENDING STRESS FORMULA

$$S_b = K \left[\frac{6\ Wh}{t^2 F} - \frac{W}{tF} \tan \phi_L\right]$$

where

W	=	tangential load at load point
ϕ_L	=	pressure angle at load point
h, t	=	load height and maximum stress section tooth thickness from gear tooth layout (Lewis construction)
F	=	gear tooth face width
S_b	=	combined stress (from radial and flexural components of load) at the tensile fillet
K	=	concentration factor for combined stress at tensile fillet
	=	$\dfrac{\text{maximum observed tensile stress}}{\text{computed combined stress}}$
	=	$0.22 + \left(\frac{t}{r_f}\right)^{0.2} \left(\frac{t}{h}\right)^{0.4}$ for 14.5-degree pressure angle
	=	$0.18 + \left(\frac{t}{r_f}\right)^{0.15} \left(\frac{t}{h}\right)^{0.45}$ for 20-degree pressure angle
r_f	=	minimum fillet radius at bottom of the trochoidal fillet of a generated tooth as determined by procedure developed by Mr. A. H. Candee.
	=	$r_i + r_t$
r_i	=	$b_i^2/(R = b_i)$ = minimum radius of curvature of trochoid at center of edge radius
b_i	=	$b - r_t$ = dedendum to center of tool edge radius
r_t	=	tool edge radius
b	=	length of dedendum of the gear
R	=	radius of the pitch circle
t	=	thickness of tooth at theoretical weakest section (Lewis)
h	=	height of load position above the theoretical weakest section

TABLE III
AGMA GEAR TOOTH BENDING STRESS FORMULA

$$S_t = \frac{W_t K_o}{K_v} \left(\frac{P_d}{F}\right) \frac{K_s\ K_m}{J}$$

where

S_t	=	calculated tensile stress at the root of the tooth	
W_t	=	transmitted tangential load at operating pitch diameter	Load
K_o	=	overload factor	Load
K_v	=	dynamic factor	Load
P_d	=	transverse diametral pitch	Tooth Size
F	=	net face width	Tooth Size

TABLE III (CONT)

AGMA GEAR TOOTH BENDING STRESS FORMULA

Ks = size factor
Km = load distribution factor
J = geometry factor

} Stress Distribution

$J = \dfrac{Y}{K_f\, m_N}$ for spur gears

Y = tooth form factor
K_f = stress correction factor
m_N = load sharing ratio

$$K_f = H + \left(\frac{t}{r_f}\right)^J \left(\frac{t}{h}\right)^L$$ = Dolan-Broghamer Stress Concentration Factor

			Pressure Angle (Degrees)
H	=	0.22	14.5
		0.18	20
J	=	0.20	14.5
		0.15	20
L	=	0.40	14.5
		0.45	20

t, h, and r_f from gear tooth layout (Lewis construction)

m_N = normally 1 for spur gears

$$Y = \frac{1}{\dfrac{\cos\phi_L}{\cos\phi}\left(\dfrac{1.5}{X} - \dfrac{\tan\phi_L}{t}\right)}$$ for spur gears

ϕ = tooth pressure angle
ϕ_L = load pressure angle
t = tooth thickness at the section of maximum stress (Lewis construction)
X = tooth strength factor from layout (Lewis construction)

r_f = radius of curvature of fillet at point tangent to root circle (may also be calculated)

$$S_t \leq \frac{Sa\ K_L}{K_T\ K_R}$$

where

Sa = allowable stress for material
K_L = life factor
K_T = temperature factor
K_R = factor of safety

In summary, review of the literature indicated that wide variations of bending strength could be calculated for a given configuration. Little data are available which attempt to correlate basic material strengths from laboratory tests with actual gears. It was thus apparent that a controlled fatigue experiment with full-size tooth proportions could aid the development of a more accurate method of calculating bending strength. Basic material strength data from R. R. Moore tests for correlation would also enhance the analysis.

DESIGN OF EXPERIMENT

Four factors of gear tooth geometry were investigated in a statistically designed experiment. Each of the factors selected was expected to affect gear tooth life. The experiment was designed to indicate if these factors interacted and if the observed results were statistically significant. The geometric factors evaluated were:

Factor	Levels	Values assigned
● Diametral pitch	2	6 and 12
● Pressure angle	2	20 and 25 degrees
● Root radius size	2	Small and large (exact values dependent on diametral pitch)
● Fillet configuration	2	Full form ground and protuberance hobbed

The experiment planned involved cycling three gear teeth to failure at each of four stress levels for each of the 16 possible combinations of the four geometric factors investigated. Evaluation of the effects of the four geometric factors was to be based on the finite life portion of the resulting fatigue (S/N) curves.

DESIGN OF FATIGUE TEST GEARS

Drawings of the 16 fatigue test gears are presented in Appendix I. Table IV lists the pertinent dimensions for the 16 fatigue test gear configurations.

Diametral pitch values of 6 and 12 were selected. A diametral pitch of 6 is typical for main power train gears in turboprop and helicopter aircraft engine transmissions. A diametral pitch of 12 provides a reasonable 2:1 variation; it also represents typical aircraft engine accessory drive train practice.

The pressure angles of 20 and 25 degrees were selected since they represent aircraft engine design practice.

Each gear tooth design has a maximum fillet radius size that can be accommodated between the active profile diameter and the root diameter. Using this maximum value of 100 percent, the minimum fillet radii for the test gears were specified as 80 percent for one design experiment level. The other level was set at 50 percent for the 20-degree pressure angle gears and 60 percent for the 25-degree gears to maintain a minimum actual fillet radius of 0. 025 inch. A manufacturing tolerance of 20 percent was thus provided with a minimum variation of 20 percent in fillet size.

The fatigue test gears were made without a rim and web to eliminate possible complications. Twenty-four tooth gears were chosen to avoid undercutting and to provide reasonable gear sizes.

TABLE IV
FATIGUE TEST GEAR DIMENSIONS

Configuration	1	2	3	4	5	6	7	8	
Part number	EX-78772	EX-78773	EX-78774	EX-78775	EX-78776	EX-78777	EX-78778	EX-78779	EX-7
Number of teeth	24	24	24	24	24	24	24	24	24
Pressure angle, degrees	20	20	20	20	20	20	20	20	25
Diametral pitch	6	12	6	12	6	12	6	12	6
Pitch diameter, inches	4.0	2.0	4.0	2.0	4.0	2.0	4.0	2.0	4.0
Base circle diameter, inches	3.7588	1.8794	3.7588	1.8794	3.7588	1.8794	3.7588	1.8794	3.62
Diameter at HPSTC*, inches	4.08289	2.04748	4.08289	2.04748	4.08289	2.04748	4.08289	2.04748	4.13
Active profile diameter, inches	3.7984	1.8969	3.7984	1.8969	3.7984	1.8969	3.7984	1.8969	3.75
Addendum factor	1.0	1.0	1.0	1.0	1.0	1.0	1.0	1.0	1.0
Dedendum factor	1.25	1.25	1.25	1.25	1.40	1.40	1.40	1.40	1.20
Whole depth factor	2.25	2.25	2.25	2.25	2.40	2.40	2.40	2.40	2.20
Outside diameter, inches	4.333	2.167	4.333	2.167	4.333	2.167	4.333	2.167	4.33
Root diameter, inches	3.583	1.792	3.583	1.792	3.533	1.767	3.533	1.767	3.60
Minimum fillet radius, inches	0.050	0.025	0.080	0.040	0.050	0.025	0.080	0.040	0.05
Maximum possible fillet radius, inches	0.1008	0.0506	0.1008	0.0506	0.1008	0.0506	0.1008	0.0506	0.08
Minimum fillet radius**, percent	50	50	80	80	50	50	80	80	60
Fillet type	← Full Ground →				← Protuberant →				←
Tooth thickness, inches	0.2618 0.2598	0.1309 0.1289	0.2618 0.2598	0.1309 0.1289	0.2618 0.2598	0.1309 0.1289	0.2618 0.2598	0.1309 0.1289	0.26 0.25
Face width, inches (±0.002)	0.50	0.25	0.50	0.25	0.50	0.25	0.50	0.25	0.50
Contact ratio	1.5403	1.4780	1.5403	1.4780	1.5403	1.4780	1.5403	1.4780	1.38

*HPSTC—high point of single tooth contact.
**Percent of maximum possible.

A

	8	9	10	11	12	13	14	15	16
78	EX-78779	EX-78780	EX-78781	EX-78782	EX-78783	EX-78784	EX-78785	EX-78786	EX-78787
	24	24	24	24	24	24	24	24	24
	20	25	25	25	25	25	25	25	25
	12	6	12	6	12	6	12	6	12
	2.0	4.0	2.0	4.0	2.0	4.0	2.0	4.0	2.0
	1.8794	3.6252	1.8126	3.6252	1.8126	3.6252	1.8126	3.6252	1.8126
	2.04748	4.1324	2.0729	4.1324	2.0729	4.1324	2.0729	4.1324	2.0729
	1.8969	3.7571	1.8759	3.7571	1.8759	3.7571	1.8759	3.7571	1.8759
	1.0	1.0	1.0	1.0	1.0	1.0	1.0	1.0	1.0
	1.40	1.20	1.20	1.20	1.20	1.35	1.35	1.35	1.35
	2.40	2.20	2.20	2.20	2.20	2.35	2.35	2.35	2.35
	2.167	4.333	2.167	4.333	2.167	4.333	2.167	4.333	2.167
	1.767	3.600	1.800	3.600	1.800	3.550	1.775	3.550	1.775
	0.040	0.050	0.025	0.067	0.033	0.050	0.025	0.067	0.033
	0.0506	0.0836	0.0418	0.0836	0.0418	0.0836	0.0417	0.0836	0.0417
	80	60	60	80	80	60	60	80	80
	→	← Full Ground			→	← Protuberant			→
	0.1309	0.2618	0.1309	0.2618	0.1309	0.2618	0.1309	0.2618	0.1309
	0.1289	0.2598	0.1289	0.2598	0.1289	0.2598	0.1289	0.2598	0.1289
	0.25	0.50	0.25	0.50	0.25	0.50	0.25	0.50	0.25
	1.4780	1.3823	1.3230	1.3823	1.3230	1.3823	1.3240	1.3823	1.3240

6

Face widths of 0.500 inch for the 6-pitch gears and 0.250 inch for the 12-pitch gears were selected to provide slightly larger axial width than tooth thickness at the weakest section in bending. The face widths maintain proportional similarity between the two gear pitches. Carburized case depths were also varied to maintain proportional similarity.

Two root fillet configurations are in general use in aircraft gearing—full form ground and protuberance hobbed. Since almost all aircraft engine gears have ground involute profile surfaces, the root fillet radii can be ground during the same operation, thus producing a "full form" ground gear. The ground root area is subject to grinding burns, excessive case removal, and/or high residual stresses if the grinding procedures are not carefully specified and controlled. Ground root fillets may be produced by formed wheels with true radii or specially shaped fillets, or by generation which produces trochoidal fillets.

Hobbing the gear with a special hob that has protrusions at the tips results in a controlled amount of undercut in the root area, thus producing a protuberance gear. Involute grinding can be accomplished after hardening without grinding the root fillet radii. The full residual stress developed by case hardening is retained. The root surface finish will be as hobbed unless a grinding operation is incorporated.

A trochoidal fillet is produced by a protuberant hob or shaper cutter. (The undercut could be broached into the gear tooth.)

The protuberance cut gears are necessarily slightly thinner at the weakest section and have smaller root diameters as compared with full form ground gears; thus, the bending stress is increased. The material strength should also be greater. The resulting fatigue life, however, is not predictable because of the many factors involved which can not be accurately assessed.

A generated ground fillet was used for the full form gears to maintain similarity with the protuberant fillet configuration. All gears were shot peened in the root. The fillet type designation part of the designed experiment, therefore, included changes in tooth thickness, root diameter, case depth, and surface treatment. Figure 6 shows two typical fatigue test gears.

MANUFACTURE OF FATIGUE TEST GEARS

Fatigue test gear manufacturing was controlled to minimize variation within and between each of the 16 groups. Significant efforts were made to maintain constant metallurgical microstructure and surface treatment as well as geometry. Specific items of control were as follows.

- All material was from a single heat (Carpenter Steel Company heat number 61629). The material was forged from 6-inch round corner squares to 2.875- and 5.125-inch bar stock form. The raw material record is given in Table V.
- All heat treat operations were performed at the same time except carburizing (due to two different case depths required) and stress relief after grinding (due to time limits).
- Copper plating prior to hardening and stripping of copper plate after hardening were each accomplished simultaneously on all parts.
- Shot blasting and peening were accomplished simultaneously on all gears of each group.

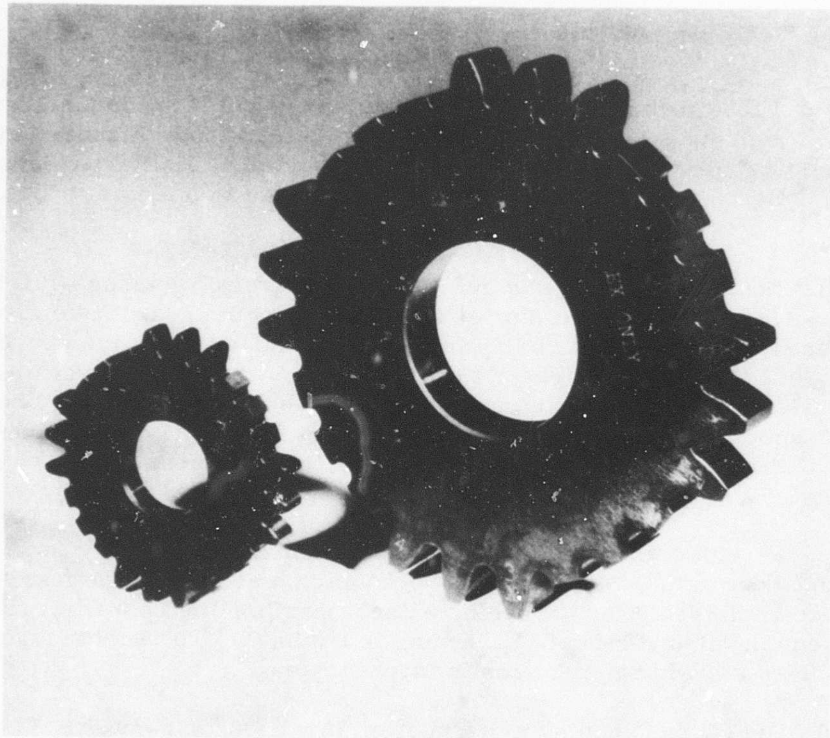

Figure 6. Typical Fatigue Test Gears.

- Gear tooth hobbing and grinding were accomplished by using an arbor that stacked all gears of each group. Each gear was honed separately.
- All test gears were black-oxide coated simultaneously (except for several sets which were processed early to permit initiation of testing).
- The high point of concentricity of all gears in each set was matched at each gear grinding operation, and gears were carefully aligned to obtain uniformity of stock removal.

TABLE V
RAW MATERIAL RECORD

Allison Purchase Order Numbers J8-05266 and J8-05265	
STEEL SUPPLIER DATA—CARPENTER STEEL COMPANY	
Material specification—AMS-6265	
Heat number—61629	
Material size—6-inch round corner squares	
Grain size—5	
Jominy hardenability—Top of ingot	R_c38 at surface
	R_c38 at 6/16 inch
Bottom of ingot	R_c39 at surface
	R_c38 at 6/16 inch

TABLE V (CONT)
RAW MATERIAL RECORD

Hardness—Brinell 269
Jernkontoret (J. K.) rating

Inclusion Type	A		B		C		D	
Inclusion Size	Thin	Thick	Thin	Thick	Thin	Thick	Thin	Thick
Top	1	0	1	0	0	0	1	0
Bottom	1	0	1	0	0	0	1	1

Chemical analysis

C	Mn	P	S	Si	Cr	Ni	Mo
0.11	0.66	0.004	0.004	0.30	1.33	3.39	0.14

Steel forger—Indianapolis Drop Forging Company Incorporated
Forged size—Two pieces 5.125 inches in diameter and 36 inches long
Two pieces 2.875 incnes in diameter and 36 inches long

ALLISON METALLURGICAL INSPECTION RECORD

Coarse etch—okay
Magnaflux step-down bars—okay
Chemical analysis

C	Mn	P	S	Si	Cr	Ni	Mo
0.10	0.67	—	—	0.29	1.29	3.41	0.12

Tensile tests

Material from 2.875-inch-diameter bar stock heat treated to Allison specification (EPS 200) as follows: 1475°F. for 1 hour, oil quenched; 325°F. for 1 hour, air cooled; Rockwell "C" hardness of 38.0 to 38.5. Tests were conducted at room temperature.

Specimen number	Yield strength 0.2% offset (p.s.i.)	Tensile strength (p.s.i.)	Elongation in 1 inch (percent)	Reduction of area (percent)
A	140,200	181,100	18.2	70.2
B	141,500	180,300	18.2	68.8
C	142,600	179,000	18.0	68.0

Izod impact tests

The heat treated material tests were conducted at room temperature.

Specimen number	Impact energy (foot-pounds)	Reference
D	74.0	Russel, J. E., and Chesters, W.T., "Significance of the Izod Test with Regard to Gear Design and Performance," Engineering, Volume 176, 1953, pp. 166-169.
E	75.0	
F	74.0	

Many in-process and finished part measurements were made to h... define stock removal and to record the final geometry of each part. Tables VI and VII list the protuberant cut gear measurements and analysis. Tables VIII and IX provide comparable data for the ground fillet gears.

The root diameter, dimension over pins, root radius, and protuberance undercut depth are the critical dimensions for the fatigue specimens.

Most of the gears had some, usually slight, dimensional deviation. All the gears of each group were well within the dimensional tolerance limits. Thus, repeatabilily of fatigue test data within any group should be excellent due to the stack machining techniques employed. Some variation from the designed experiment, however, may occur between groups. These variations could be eliminated by basing bending stress calculations on actual rather than print dimensions.

Sample routing sheets for a full ground (EX-78772) and a protuberant cut gear (EX-78776) are given in Appendix II.

Table X lists the fatigue test gear hob dimensions necessary to define the gear tooth root fillet shape. The dimensions given must be modified by the finish stock allowance to obtain an accurate finished gear configuration. The full ground root fillet configuration hobs are listed to permit analysis of the finish stock allowance in the root fillet area rather than for bending stress determination.

TEST RIG DESIGN AND PROCEDURE

The test rig was designed for single tooth fatigue testing of either the 2- or 4-inch-pitch-diameter gear. Single tooth testing was selected over a dynamic four-square gear test to permit accurate control of test variables. Adjacent teeth on the test gear were removed to ensure single tooth contact.

Two design concepts were considered for the fatigue testing device—a hydraulic servovalve system where a measured torque is applied on the test gear to produce the desired tooth load and an electromagnetic shaker for use as the input loading device. The two concepts were evaluated on the basis of available equipment, usage experience, and inherent advantages and disadvantages. Design studies showed that the electromagnetic shaker was preferred, provided that a high frequency of operation could be achieved at the specified test loads. Additional considerations were accurate tooth load measurements and good dynamic stability.

To achieve the desired operational requirements, a fatigue test rig was designed with inherent high axial and radial stiffness of all load transmitting and reacting components and with a load cell at the point of tooth loading. The fatigue rig was coupled to an electromagnetic shaker. Operation at or near a system resonance of approximately 200 c.p.s. was realized. The principle of operation of the fatigue test rig is shown schematically in Figure 7.

The shaker driving force was applied directly to a mass which, in turn, loaded the gear tooth through a load cell. The mass was supported flexibly in the direction of loading and was stabilized in all radial directions by two disk-type flexible plates.

TABLE VI
TABULATION OF PROTUBERANT FILLET GEAR MEASUREMENTS*

	Root Fillet Radius			Root Diameter				
Part Number	Print Minimum	After Hob	After Solution Machining	Print (± 0.002)	After Hob	After Solution Machining	Print	[illegible]
EX-78776	0.050	0.060 to 0.065	0.065 to 0.070	3.533	3.535	3.5227 to 3.5241	4.3953 to 4.3999	4.
EX-78777	0.025	0.030	0.030 to 0.032	1.767	1.775	1.7679 to 1.7688	2.1953 to 2.2000	2.
EX-78778	0.080	0.085	0.090	3.533	3.536	3.5248 to 3.5275	4.3953 to 4.3999	4.
EX-78779	0.040	0.042	0.044	1.767	1.7745	1.7672 to 1.7682	2.1953 to 2.2000	2.
EX-78784	0.050	0.056	0.065	3.550	3.551	3.5412 to 3.5424	4.3973 to 4.4012	4.
EX-78785	0.025	0.026 to 0.032	0.028 to 0.036	1.775	1.7815	1.7755 to 1.7764	2.1967 to 2.2006	2
EX-78786	0.067	0.068 to 0.070	0.070 to 0.075	3.550	3.555	3.5436 to 3.5448	4.3973 to 4.4012	4
EX-78787	0.033	0.032	0.034 to 0.036	1.775	1.784	1.7775 to 1.7778	2.1967 to 2.2006	2

* All dimensions in inches

A

Dimension Over Pins					
Print	After Hob	After Heat Treat	After Solution Machining	After Final Grind	Minimum Finishing Stock After Hob Operation
4.3953 to 4.3999	4.4353	4.4338 to 4.4345	4.4201 to 4.4239	4.3963 to 4.3965	0.0354
2.1953 to 2.2000	2.2362	2.2300 to 2.2305	2.2246 to 2.2257	2.1958 to 2.1968	0.0362
4.3953 to 4.3999	4.4352	4.4339 to 4.4344	4.4205 to 4.4255	4.3903 to 4.3906	0.0353
2.1953 to 2.2000	2.2355	2.2347 to 2.2353	2.2247 to 2.2257	2.1961 to 2.1963	0.0355
4.3973 to 4.4012	4.431	4.4290 to 4.4298	4.4183 to 4.4205	4.3973 to 4.3980	0.0298
2.1967 to 2.2006	2.2306	2.2296 to 2.2305	2.2208 to 2.2222	2.1972 to 2.1978	0.0300
4.3973 to 4.4012	4.4316	4.4298 to 4.4300	4.4183 to 4.4202	4.3982 to 4.3983	0.0304
2.1967 to 2.2006	2.2312	2.2302 to 2.3209	2.2222 to 2.2230	2.1945 to 2.1949	0.0306

TABLE VII
ANALYSIS OF PROTUBERANT FILLET GEAR MEASUREMENTS*

	Root Diameter			Dimension Over P				
Part Number	Maximum Change, Hob to Solution Machining	Maximum Variation Between Gears After Solution Machining	Finishing Stock After Hob Operation	Maximum Change, Hob to Heat Treat	Maximum Variation Between Gears After Heat Treat	Change Between Minimum Heat Treat and Minimum Solution Machining	Maximum Variation Between Gears After Solution Machining	Maxi Cha Hob Solu Mach
EX-78776	0.0123	0.0014	0.002	0.0015	0.0007	0.0137	0.0038	0.0
EX-78777	0.0071	0.0009	0.008	0.0062***	0.0005	0.0054	0.0011	0.
EX-78778	0.0118	0.0027	0.003	0.0013	0.0005	0.0134	0.0050	0.
EX-78779	0.0073	0.0010	0.0075	0.0008	0.0006	0.0100	0.0010	0.
EX-78784	0.0098	0.0012	0.001	0.0020	0.0008	0.0107	0.0022	0.
EX-78785	0.0060	0.0009	0.0065	0.0010	0.0009	0.0088	0.0014	0.
EX-78786	0.0119	0.0012	0.005	0.0018	0.0002	0.0115	0.0019	0.
EX-78787	0.0065	0.0003	0.009	0.0010	0.0007	0.0080	0.0008	0.
Average †	0.0115	0.0016	0.0024	0.0017	0.0006	0.0123	0.0032	0.
Average ‡	0.0067	0.0008	0.0078	0.0010	0.0007	0.0081	0.0011	0.

* All dimensions in inches.

** Dimension over pins calculated for 0.000 to 0.004 backlash with mating gear on standard centers. Therefore, dimension over pins tolerances equivalent to 0.002 change in tooth thickness or 0.001 stock allowance per surf The 0.0039 tolerance for 25-degree pressure angle gears and 0.0300 average finishing stock after hob are equ to 0.0077 per surface. The 0.0047 tolerance for 20-degree pressure angle gears and 0.0355 finishing stock af hob are equivalent to 0.0076 per surface.

*** Questionable reading—deleted from averages.

Dimension Over Pins						
Change Between [illegible]imum Heat [illegible]reat and [illegible]inimum Solution [illegible]achining	Maximum Variation Between Gears After Solution Machining	Maximum Change Hob to Solution Machining	Change Between Minimum Solution Machining and Final Grind	Minimum Finishing Stock After Hob Operation **	Maximum Variation Between Gears After Final Grind	Maximum Change, Hob to Final Grind
0.0137	0.0038	0.0152	0.0238	0.0354	0.0002	0.0390
0.0054	0.0011	0.0116	0.0288	0.0362	0.0010	0.0404
0.0134	0.0050	0.0147	0.0302	0.0353	0.0003	0.0449
0.0100	0.0010	0.0108	0.0286	0.0355	0.0002	0.0394
0.0107	0.0022	0.0127	0.0210	0.0298	0.0007	0.0337
0.0088	0.0014	0.0098	0.0236	0.0300	0.0006	0.0334
0.0115	0.0019	0.0133	0.0201	0.0304	0.0001	0.0334
0.0080	0.0008	0.0090	0.0277	0.0306	0.0004	0.0367
0.0123	0.0032	0.0140	0.0265	—	0.0003	0.0378
0.0081	0.0011	0.0103	0.0272	--	0.0006	0.0375

[illegible]ar on standard centers. Therefore,
[illegible]s or 0.001 stock allowance per surface.
[illegible]ge finishing stock after hob are equivalent
[illegible] gears and 0.0355 finishing stock after

† For large-diameter gears.

‡ For small-diameter gears.

B

TABLE VIII
TABULATION OF GROUND FILLET GEAR MEASUREMENTS*

	Root Fillet Radius			Root Diameter			
Part Number	Print Minimum	After Hob	After Final Grind	Print (± 0.002)	After Hob	After Final Grind	Pri
EX-78772	0.050	0.075	0.065	3.5830	3.5916	3.5800 to 3.5806 (3.5830)**	4.399 4.3
EX-78773	0.025	0.040	0.040	1.7920	1.808	1.7836 to 1.7850 (1.7903)**	2.195 2.2
EX-78774	0.080	0.085	0.070	3.5830	3.594	3.5863 to 3.5882 (3.5820)**	4.399 4.3
EX-78775	0.040	0.036 to 0.038	0.034	1.7920	1.809	1.7950 to 1.7955	2.195 2.2
EX-78780	0.050	0.065 to 0.070	0.055 to 0.060	3.600	3.6152	3.5998 to 3.6010	4.397 4.4
EX-78781	0.025	0.026	0.026 to 0.028	1.800	1.815	1.8093 to 1.8105	2.196 2.2
EX-78782	0.067	0.070	0.070	3.600	3.614	3.600 to 3.604 (3.605)**	4.397 4.4
EX-78783	0.033	0.032 to 0.036	0.034 to 0.036	1.800	1.815	1.805 (1.803)**	2.196 2.2

* All dimensions in inches.

** Setup part not included.

'S*

	Root Diameter		Dimension Over Pins			
rint	After Hob	After Final Grind	Print	After Hob	After Heat Treat	After Finish Grind and Hone
999 to 3953	3.5916	3.5800 to 3.5806 (3.5830)**	4.3999 to 4.3953	4.4354	4.4345 to 4.4350	4.3961 to 4.3971 (4.39[illegible])**
953 to 2000	1.808	1.7836 to 1.7850 (1.7903)**	2.1953 to 2.2000	2.2344	2.2335 to 2.2342	2.1920 to 2.1922 (2.1942)**
999 to 3953	3.594	3.5863 to 3.5882 (3.5820)**	4.3999 to 4.3953	4.4352 to 4.4354	4.4340 to 4.4347	4.3990 to 4.3990 (4.3941)**
953 to .2000	1.809	1.7950 to 1.7955	2.1953 to 2.2000	2.2355	2.2345 to 2.2355	2.1912 to 2.1928 (2.1895)**
973 to .4012	3.6152	3.5998 to 3.6010	4.3973 to 4.4012	4.4293 to 4.4298	4.4275 to 4.4282	4.3997 to 4.4005
.967 to .2006	1.815	1.8093 to 1.8105	2.1967 to 2.2006	2.2312 to 2.2313	2.2305 to 2.2307	2.1961 to 2.1976
973 to .4012	3.614	3.600 to 3.604 (3.605)**	4.3973 to 4.4012	4.4319	4.4292 to 4.4297	4.3976 to 4.3981 (4.3967)**
.967 to .2006	1.815	1.805 (1.803)**	2.1967 to 2.2006	2.2305	2.2295 to 2.2300	2.1965 to 2.1972 (2.1947)**

8

TABLE IX
ANALYSIS OF GROUND FILLET GEAR MEASUREMENTS*

	Root Diameter					
Part Number	Maximum Change, Hob to Final Grind	Maximum Variation Between Gears after Final Grind	Grind Stock After Hob Operation (±0. 002)	Maximum Change, Hob to Heat Treat	Maximum Variation Between Gears After Heat Treat	Maximum Change, Minimum Heat Treat to Minimum Hone
EX-78772	0. 0116	0. 0006	0. 0086	0. 0009	0. 0005	0. 0384
EX-78773	0. 012	0. 000	0. 016	0. 0009	0. 0007	0. 0415
EX-78774	0. 0077	0. 0019	0. 011	0. 0012	0. 0007	0. 0370
EX-78775	0. 014	0. 0005	0. 017	0. 0010	0. 0010	0. 0433
EX-78780	0. 0154	0. 0012	0. 0152	0. 0018	0. 0007	0. 0278
EX-78781	0. 0057	0. 0012	0. 015	0. 0007	0. 0002	0. 0344
EX-78782	0. 014	0. 0040	0. 014	0. 0027	0. 0005	0. 0316
EX-78783	0. 010	0. 000	0. 015	0. 0010	0. 0005	0. 033
† Average	0. 0122	0. 0019	0. 0122	0. 0017	0. 0006	0. 0337
‡ Average	0. 0104	0. 0009	0. 016	0. 0009	0. 0006	0. 0381

* All dimensions in inches.

** Dimension over pins calculated for 0. 000 to 0. 004 backlash with mating gear on standard centers. pins tolerances equivalent to 0. 002 change in tooth thickness or 0. 001 stock allowance per surface. 25-degree pressure angle gears and 0. 0300 average finishing stock after hob are equivalent to 0. 00 tolerance for 20-degree pressure angle gears and 0. 0355 finishing stock after hob are equivalent to

† For large-diameter gears.

‡ For small-diameter gears.

A

ENTS*

D		Dimension Over Pins						
Max Var... Bet... G... After Grind ...	...mum ...ge, to Treat	Maximum Variation Between Gears After Heat Treat	Maximum Change, Minimum Heat Treat to Minimum Hone	Maximum Variation Between Gears After Final Grind and Hone	Maximum Change, Hob to Final Grind and Hone	Maximum Finishing Stock After Hob Operation **	Pressure Angle (Degrees)	
0.	09	0.0005	0.0384	0.0010	0.0393	0.0355	20	
0.	09	0.0007	0.0415	0.0002	0.0424	0.0344	20	
0.	12	0.0007	0.0370	0.0018	0.0384	0.0353	20	
0.	10	0.0010	0.0433	0.0016	0.0443	0.0355	20	
0.	18	0.0007	0.0278	0.0008	0.0296	0.0281	25	
0.	07	0.0002	0.0344	0.0015	0.0351	0.0306	25	
0.	27	0.0005	0.0316	0.0005	0.0343	0.0307	25	
0.	10	0.0005	0.033	0.0007	0.0340	0.0299	25	
0.	17	0.0006	0.0337	0.0010	0.0354	—	—	
0.	09	0.0006	0.0381	0.0010	0.0389	—	—	

. Theref... with mating gear on standard centers. Therefore, dimension over
e. The ... s or 0.001 stock allowance per surface. The 0.0039 tolerance for
0077 per ... ng stock after hob are equivalent to 0.0077 per surface. The 0.0047
to 0.007... nishing stock after hob are equivalent to 0.0076 per surface.

TABLE X
HOB DIMENSIONS

Gear Configuration	Gear Part Number	Hob Tooth Thickness HTT (inches)	Hob Addendum HADD (inches)	Hob Lead, HLEAD (inches)	Hob Pressure Angle, HPAR (degrees)	Hob Tip Radius, HTIPR (inch
1	EX-78772	0.2468	0.2005	0.52436	20	0.055 to 0.050
2	EX-78773	0.1159	0.0962	0.26194	20	0.025 to 0.030
3	EX-78774	0.2468	0.2005	0.52436	20	0.072 full
4	EX-78775	0.1159	0.0962	0.26194	20	0.033 full
5	EX-78776	0.2032	0.1717	0.50888	14.5	0.050 to 0.055
6	EX-78777	0.0943	0.0842	0.25421	14.5	0.025
7	EX-78778	0.2032	0.1717	0.50888	14.5	0.082 full
8	EX-78779	0.0943	0.0842	0.25421	14.5	0.039 full
9	EX-78780	0.2468	0.1920	0.52435	25	0.045 to 0.040
10	EX-78781	0.1159	0.0920	0.26194	25	0.024 full
11	EX-78782	0.2468	0.1920	0.52435	25	0.053 full
12	EX-78783	0.1159	0.0920	0.26194	25	0.024 full
13	EX-78784	0.1799	0.1509	0.50564	20	0.050 to 0.055
14	EX-78785	0.0654 *	0.0500 *	0.24632	15.5	0.025 to 0.030
15	EX-78786	0.1449 *	0.1030 *	0.49301	15.5	0.067 full
16	EX-78787	0.0654 *	0.0500 *	0.24632	15.5	0.032 full

* Theoretical

A

ob Pressure Angle, PAR (degrees)	Hob Tip Radius, HTIPR (inches)	Hob Protuberance, HPW (inches)	Hob Part Number	Tooth Thickness per Side (inches)	Root Diameter per Side (inches)
20	0.055 to 0.050	0	SPT-2603	0.008	0.008
20	0.025 to 0.030	0	SPT-2608	0.008	0.008
20	0.072 full	0	SPT-2602	0.008	0.008
20	0.033 full	0	SPT-2607	0.008	0.008
14.5	0.050 to 0.055	0.007 to 0.008	SPT-2604	0.008	0.003
14.5	0.025	0.0055 to 0.0060	SPT-2611	0.008	0.003
14.5	0.082 full	0.006 to 0.007	SPT-2605	0.008	0.003
14.5	0.039 full	0.0050 to 0.0055	SPT-2609	0.008	0.003
25	0.045 to 0.040	0	SPT-2594	0.008	0.008
25	0.024 full	0	SPT-2597	0.008	0.008
25	0.053 full	0	SPT-2595	0.008	0.008
25	0.024 full	0	SPT-2598	0.008	0.008
20	0.050 to 0.055	0.007 to 0.008	SPT-2593	0.008	0.003
15.5	0.025 to 0.030	0.007 to 0.008	SPT-2600	0.008	0.003
15.5	0.067 full	0.007 to 0.008	SPT-2591	0.008	0.003
15.5	0.032 full	0.007 to 0.006	SPT-2599	0.008	0.003

B

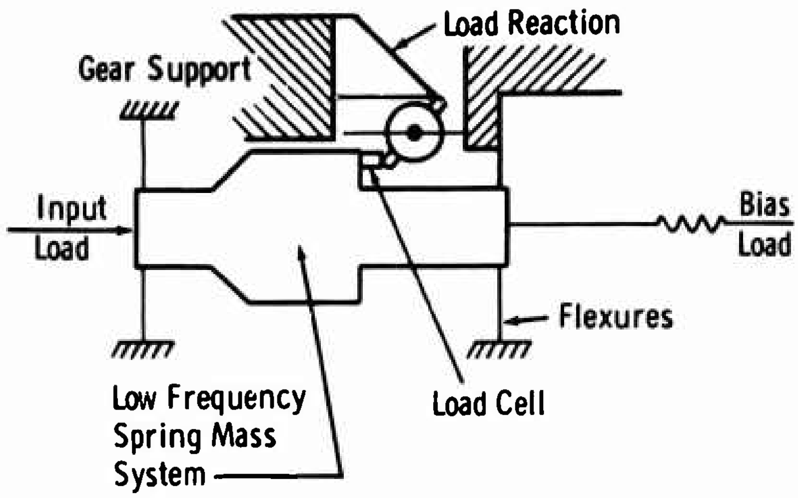

Figure 7. Principle of Operation of Fatigue Test Rig.

The required static preload was provided by compressing a relatively low spring rate coil spring. Inertia loading of the tooth, using the moving mass, made possible considerable force amplification at and near the system axial resonance. The forced dynamic load was about the mean value which, in this case, was the static preload. Figure 8 shows the test rig in its final configuration. Figure 9 shows the rig coupled to the shaker.

The load cell incorporated at the point of tooth loading to provide accurate control of both static and dynamic tooth loading during fatigue testing was an Allison designed strain gage type cell. Figure 10 shows the load cell instrumented with axial and circumferential strain gages, and Figure 11 shows the load cell in its final assembly. The strain gage hookup was a four-active-arm bridge. The bridge signal output was directly proportional to the change in applied thrust, independent of load cell bending and temperature change, and $2(1 + \mu)$ times as large as the corresponding output of a single strain gage. The symbol μ is Poisson's ratio.

The automatic control system of the electromagnetic shaker was not used. Excellent control stability was realized by manual control.

A series of check-out procedures was performed prior to dynamic testing. The following paragraphs present the check-out procedures in the sequence in which they were performed.

- <u>Radial Spring Rate of Fatigue Rig</u>

  The fatigue rig was installed in the electromagnetic shaker and instrumented with dial indicators as shown in Figure 12. With gear EX-78784 installed and statically loaded by means of the bias spring loading device, the radial deflections were measured. The radial spring rate of the system as determined by test was 5,900,000 pounds/inch. This high radial spring rate verified the design objective of high system stiffness to ensure accurate load application at the high point of single tooth contact and good alignment of all moving parts during operation.

- **Dimensional Check-Out**

  Measurements were made to verify that contact between the load member tip and the gear tooth occurred at the high point of single tooth contact. The measurements verified tip spacing to the center of the pilot shaft to be as designed, and to ensure tip contact at the high point of single tooth contact during fatigue. Figures 13 and 14 show typical dimensions for the 6- and 12-pitch gears.

- **Tooth Load Distribution**

  Gear EX-78784 was designated as the check-out gear. The gear was instrumented with strain gages and a thermocouple, as shown in Figure 15. The instrumented gear was installed in the fatigue test rig, and a static load was applied in 1000-pound increments to 3000 pounds. The strain read-out of the two gages on face A was compared for indication of nonuniform loading or misalignment. The gages indicated uniform loading and good alignment. Accurate location of the strain gages was verified by inserting a small piece of shim stock, 0.003 inch thick, between the load member tip and the gear tooth. The shim stock was inserted an equal distance on both sides of the gear tooth, and differential strain was compared. The differential strain was of equal value, verifying good strain gage location.

- **Dynamic Resonance Frequency**

  To determine the system operating frequency, a frequency scan was made versus shaker driver current. With the check-out gear installed and preloaded to 1000 pounds, the frequency scan was made from 50 to 500 c.p.s., plotting driver current while dynamically applying ±800 pounds of load to the gear tooth. The frequency scan indicated that the system resonance frequency was 240 c.p.s. with a reduction of 20:1 in driver coil current at resonance. Figure 16 shows the relative response.

- **Dynamic Separation**

  To ensure continued contact between the gear tooth and the load member tip and to determine differential load margin, the output signal of a dynamic gage on face B was displayed on an oscilloscope. By varying the dynamic load about a constant preload, the signal wave shape was analyzed. Figure 17 presents the pictorial wave shape analysis. The analysis shows that a minimum of 20 pounds differential is required to maintain contact between the tooth and load tip.

- **Load Cell Calibration**

  To eliminate inaccuracies in the loading, a precise calibration was made on the load cell. The load cell was tested in a Baldwin press as shown in Figures 18 and 19. The load was applied in 500-pound increments to 5000 pounds maximum; the output of the strain gage bridge was recorded. Each load cell was tested five times for repeatability. Figure 20 shows typical calibration data. The calibration of the load cell repeated within one percent in the new condition and within two percent after usage.

To allow the load member tip to contact the gear test tooth at the high point of single tooth contact, a number of teeth were removed as shown in Figure 21. Figure 21 shows load sides A and B. Teeth 1, 2, 3, and 4 are the test teeth, and teeth 1X, 2X, 3X, and 4X are the load reaction teeth.

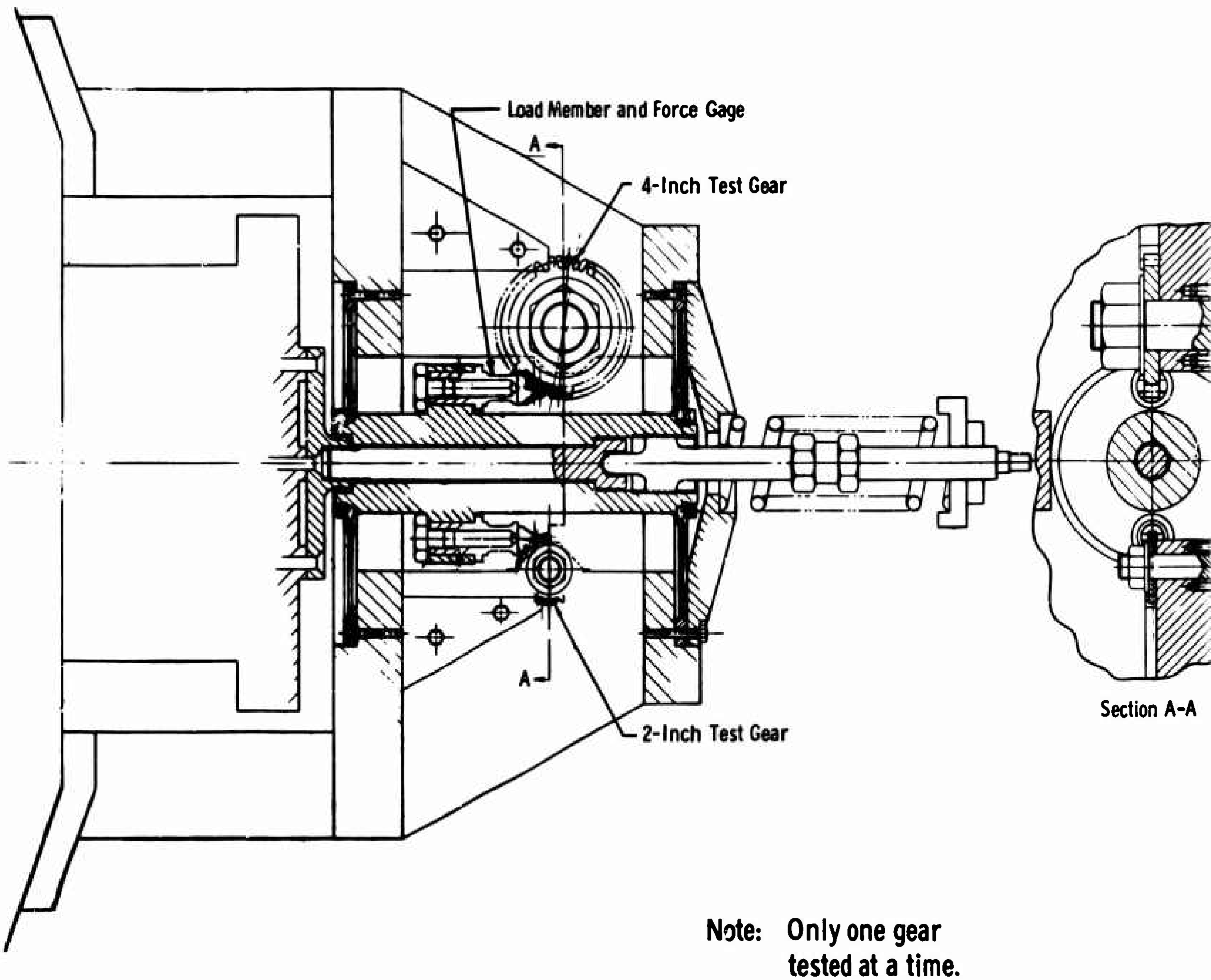

Figure 8. Fatigue Test Rig Schematic.

A

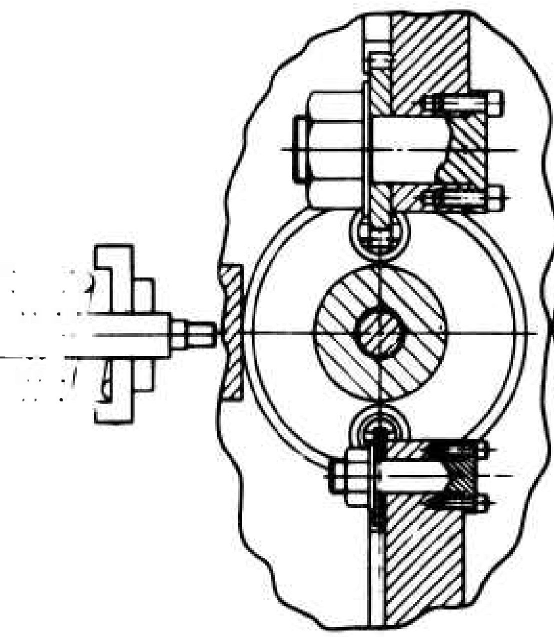

Section A-A

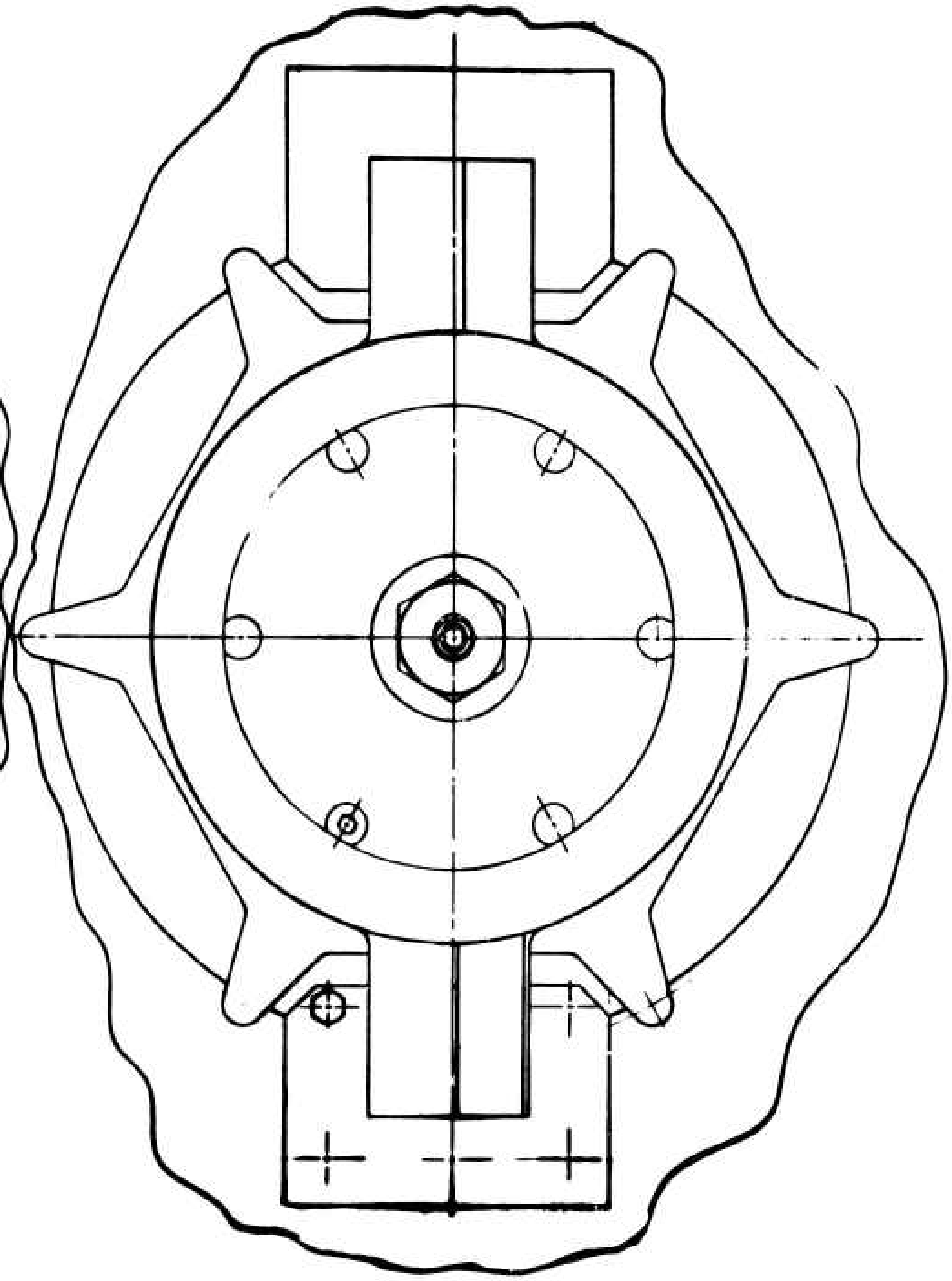

ar
me.

b

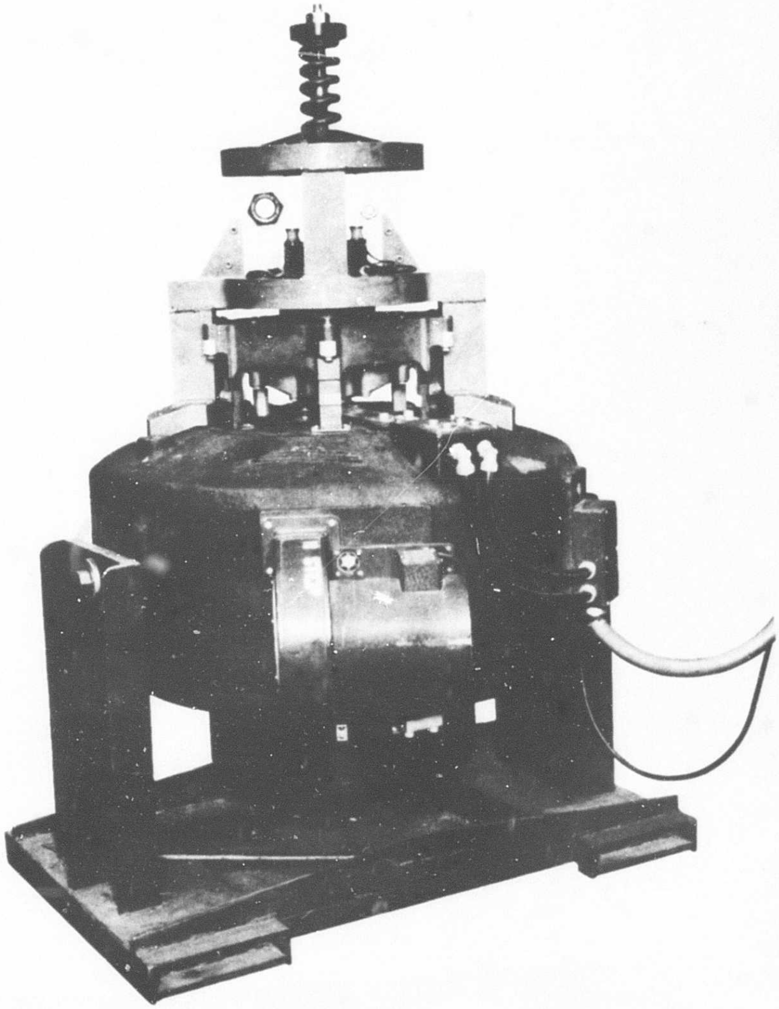

Figure 9. Fatigue Test Setup.

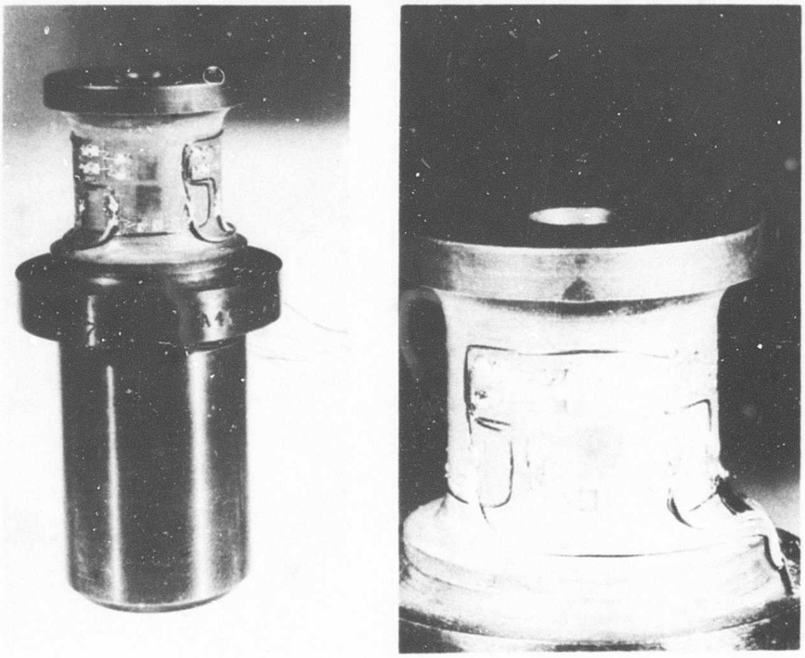

Figure 10. Load Cell Showing Instrumentation.

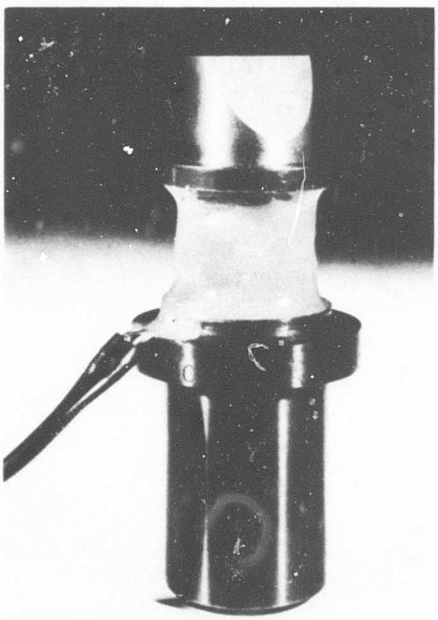

Figure 11. Assembled Load Cell.

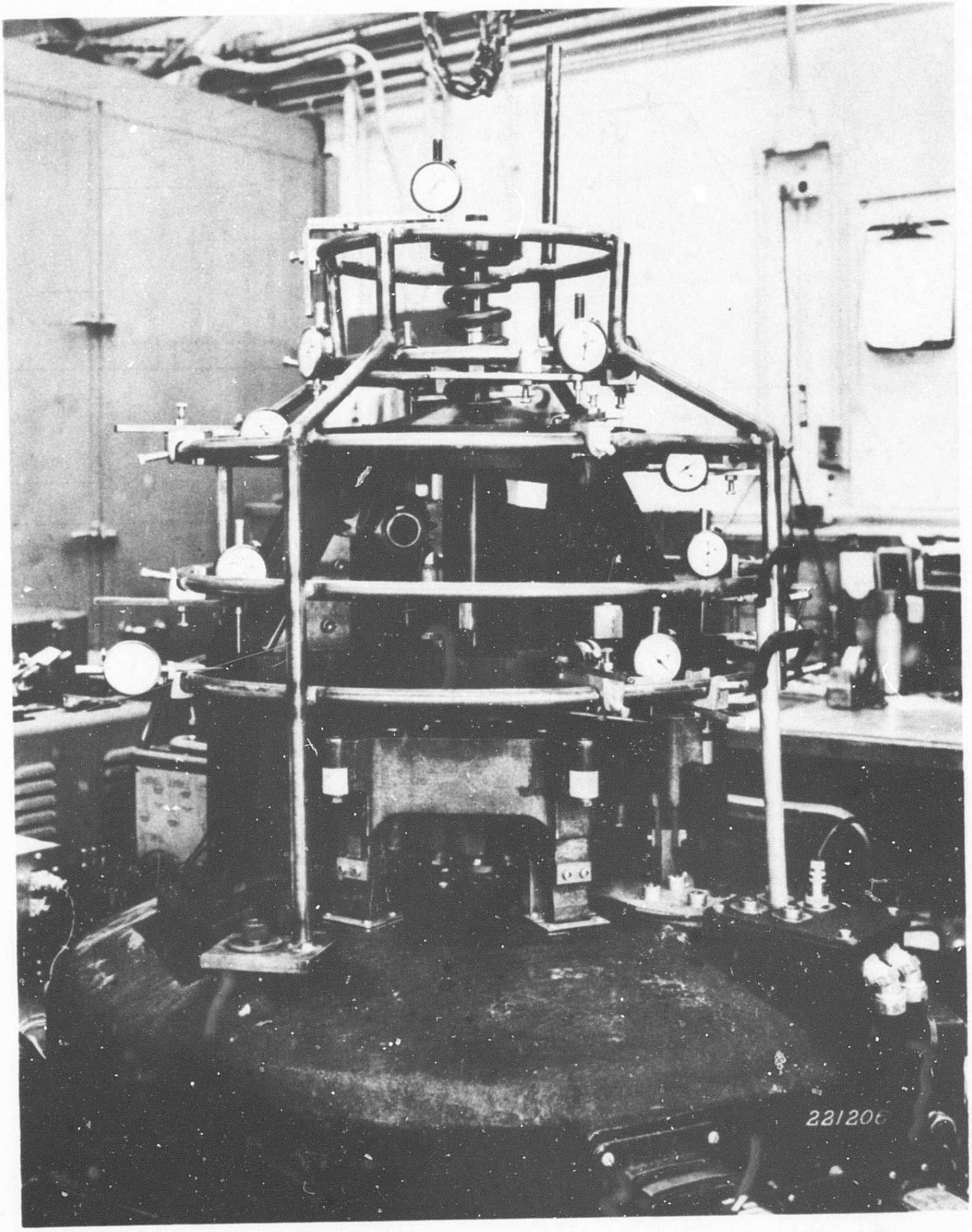

Figure 12. Instrumented Fatigue Test Rig.

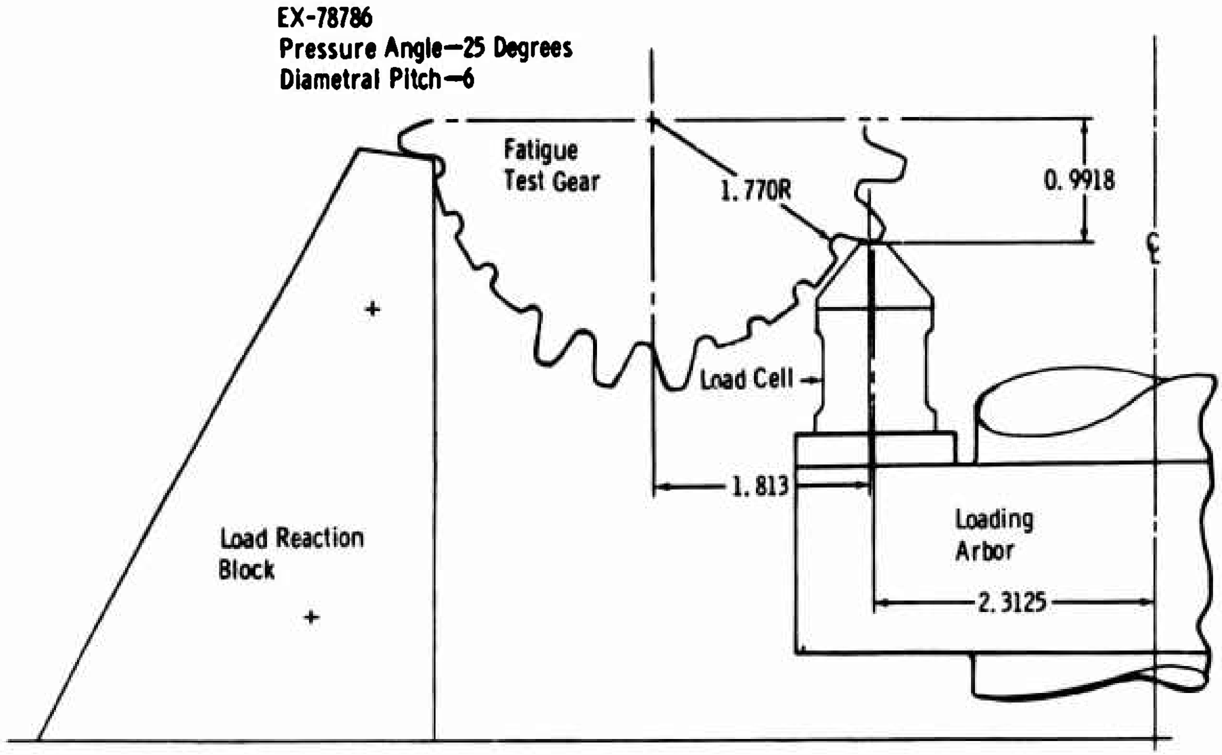

Figure 13. Typical Dimensions of 6-Pitch Gear Test Setup.

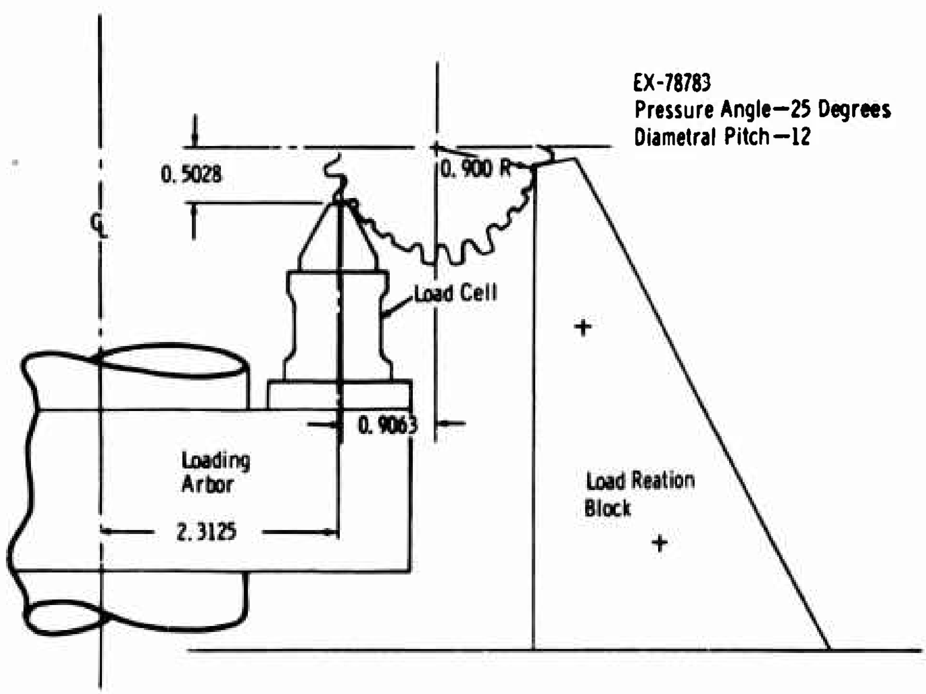

Figure 14. Typical Dimensions of 12-Pitch Gear Test Setup.

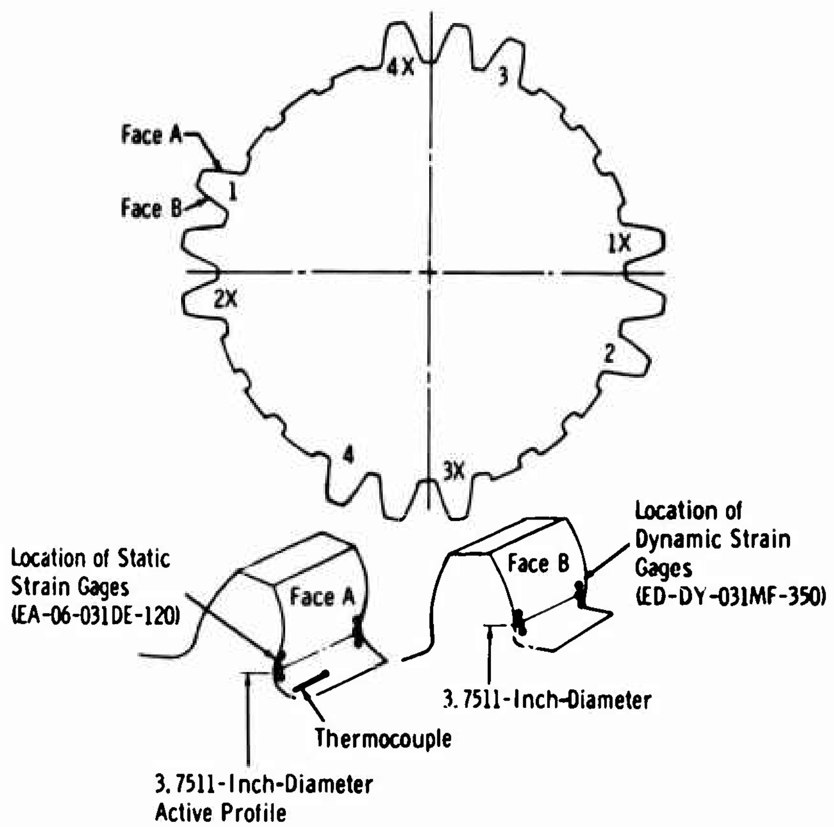

Figure 15. Schematic of Check-Out Gear Instrumentation.

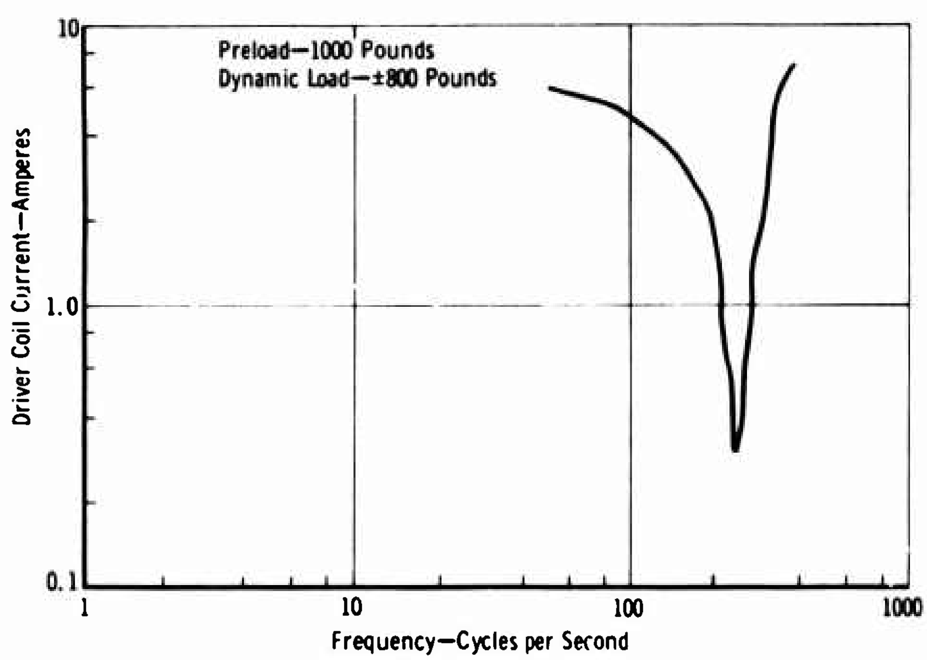

Figure 16. Test System Resonant Frequency.

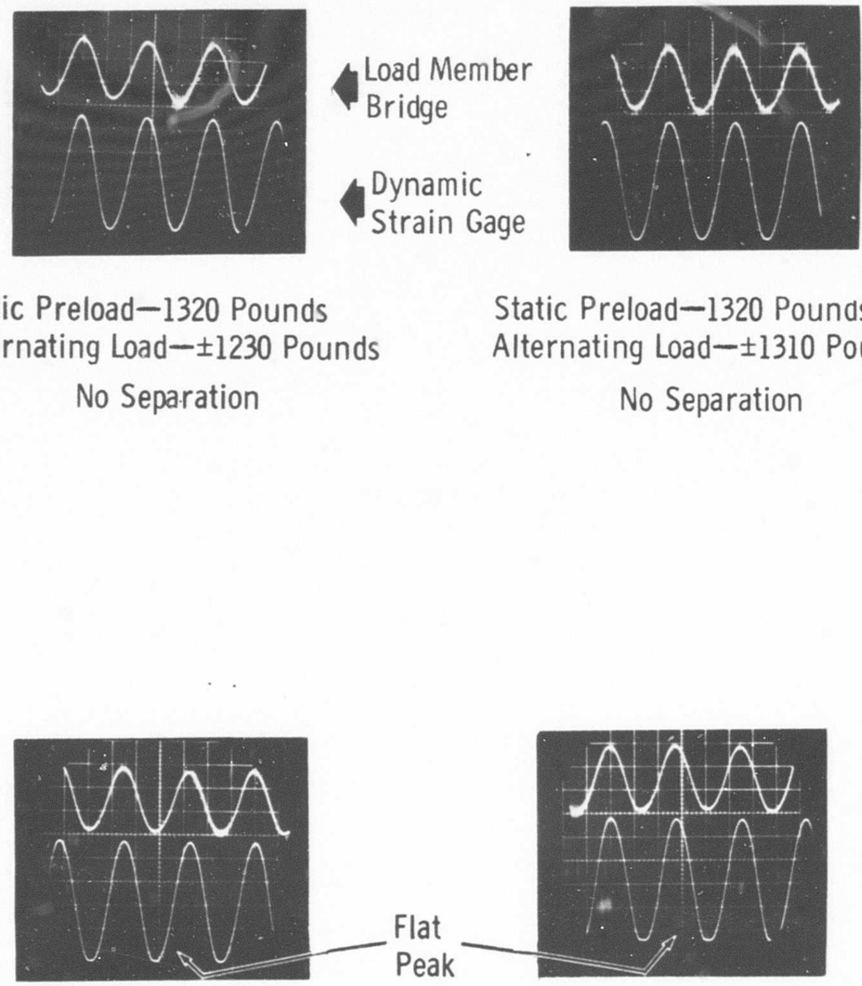

Static Preload—1320 Pounds
Alternating Load—±1230 Pounds
No Separation

Static Preload—1320 Pounds
Alternating Load—±1310 Pounds
No Separation

Static Preload—1320 Pounds
Alternating Load—±1345 Pounds
Separation

Static Preload—1320 Pounds
Alternating Load—±1380 Pounds
Separation

Figure 17. Dynamic Strain Gage Signal Showing Tooth-to-Load Tip Contact.

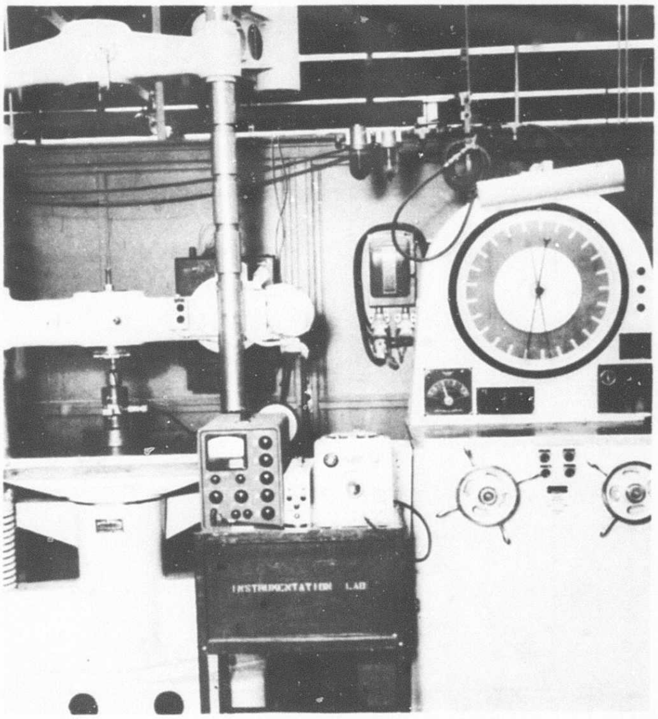

Figure 18. Load Cell Test Setup.

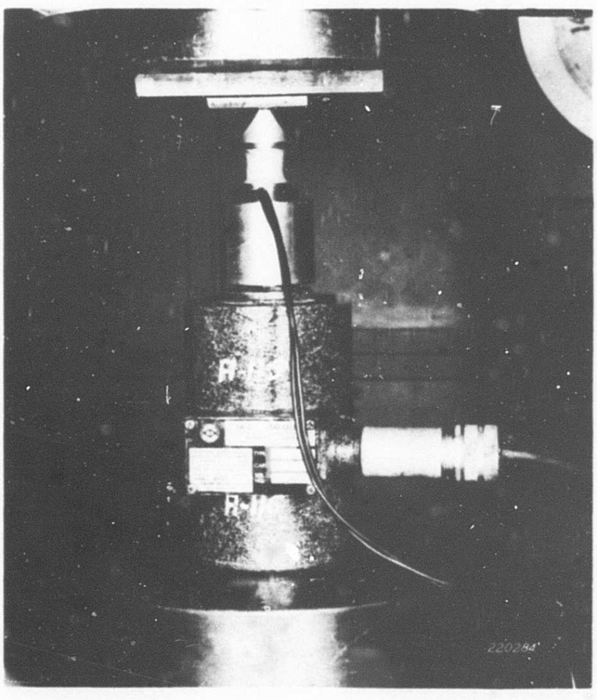

Figure 19. Close-up of Load Cell Test Setup.

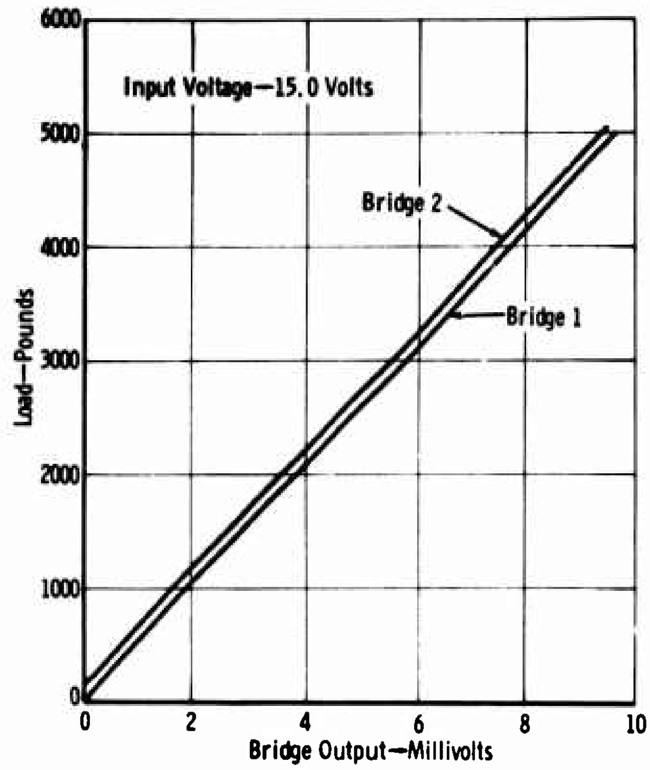

Figure 20. Typical Load Cell Calibration Curve.

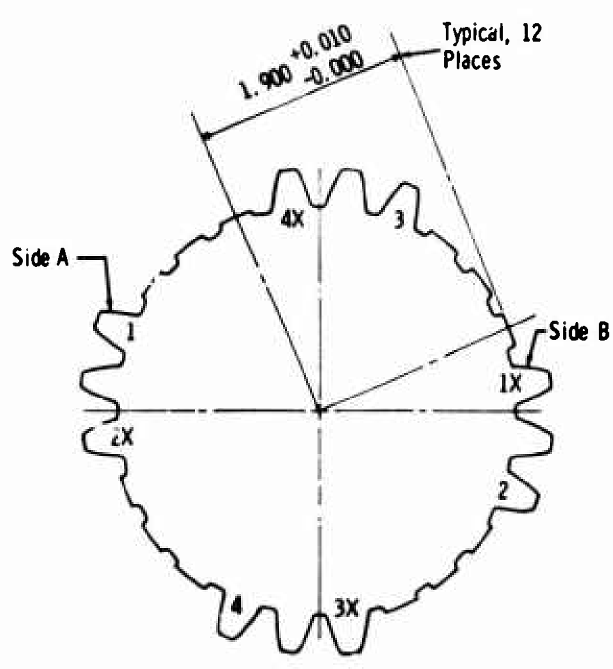

Figure 21. Test Gear Showing Teeth Removed.

The test procedure required that the test tooth, once positioned, be preloaded with a bias load which was equal to one-half of the total fatigue load. Once the preload was obtained and verified by the load cell, an alternating load was applied about a mean which was the preload. The tentative plan was that three gear teeth be tested for each combination of variables until fatigue failure occurred or 10^7 cycles were accumulated.

During testing, the dynamic load at the load cell (signal from strain gage bridge) was monitored and recorded on a strip chart recorder. A typical strip chart recording is shown in Figure 22.

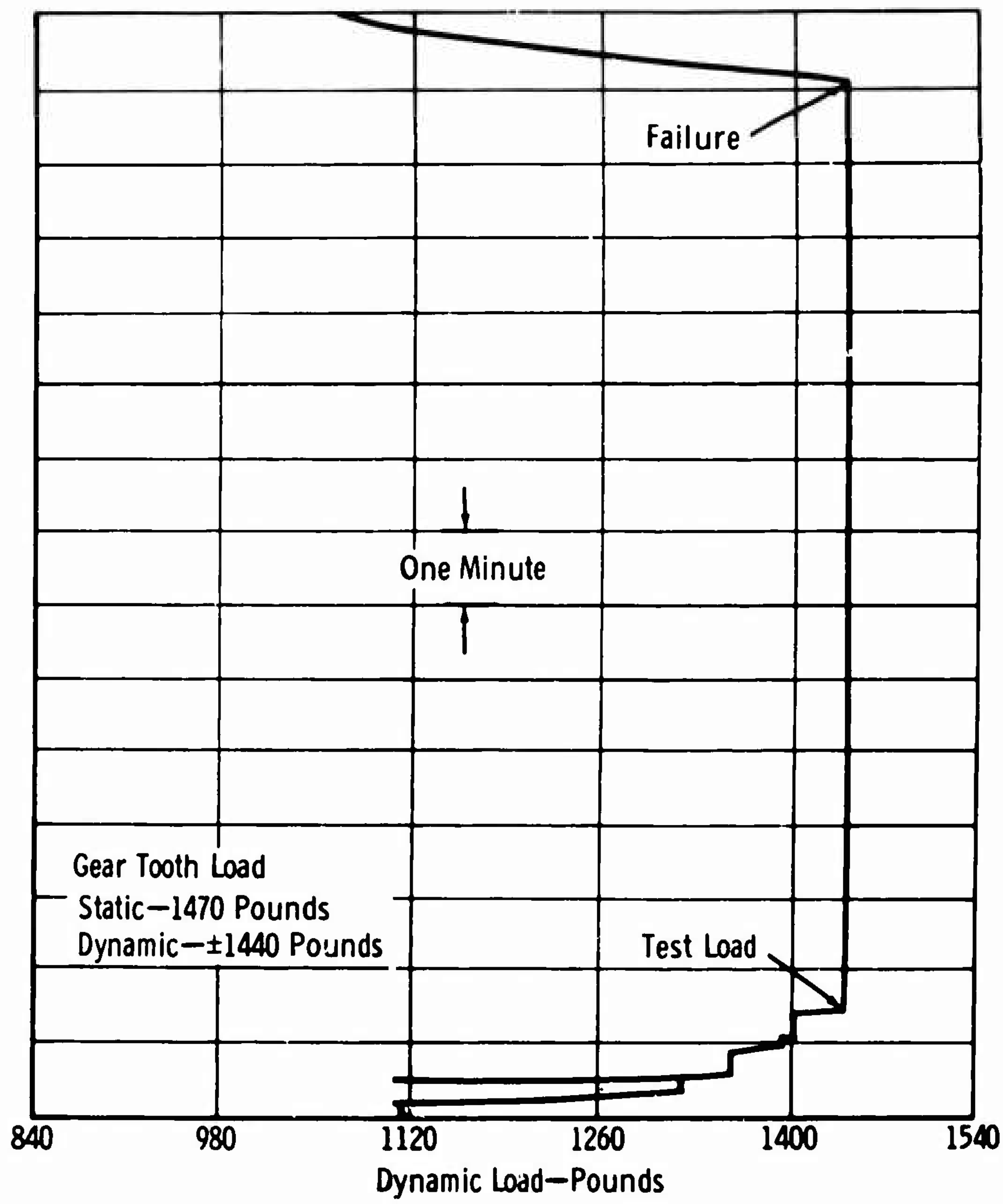

Figure 22. Typical Strip Chart Recording of Test Gear Dynamic Load.

RESULTS

FATIGUE TESTS

The fatigue test program was based on a designed experiment for evaluation of four geometric variables—diametral pitch, pressure angle, root fillet size, and root fillet configuration. Two levels of each variable were employed requiring 16 different gear configurations. See Table IV. Initially, three teeth from each gear configuration were to be tested at four stress levels. Failures were required to permit test evaluation on the finite portion of the S/N curve. Early test experience with the small 12 diametral pitch gears indicated only a 30-percent spread between the desired minimum and maximum stress levels. The maximum stress was determined by the short test time (3 to 5 minutes) and high stresses that could cause plastic yielding and thus result in a different mode of failure. The minimum stress was determined by a high percent of runouts to 10,000,000 cycles without failure. It was decided, therefore, to obtain four failures at three stress levels to permit a 10-percent difference between levels.

Table XI lists the fatigue test data—load, cycles to failure, and configuration—for the 214 gear teeth tested. Of this total, 173 failed; the remaining gear tooth tests were terminated at 2×10^6 or 10^7 cycles.

Fatigue test data for each configuration are plotted as S/N curves based on unit load in Figures 23 through 38. Unit load is defined as the equivalent load in pounds on a tooth having a diametral pitch of 1 and a face width of 1 inch. The mean curve drawn through the data was calculated by a procedure explained in detail in Appendix III. Proportionality factors can be used to relate applied load (test rig load), unit load, Lewis stress, Dolan-Broghamer stress, AGMA stress, Heywood stress, and Kelley-Pedersen stress for any single gear configuration. Therefore, S/N curves of the test data based on any of these stress calculation methods would produce the same fit of the mean curve to the data points. S/N curves based on AGMA calculated stress are presented in Appendix IV.

A series of reworks was initiated during the test program to modify or perfect parts related to the fatigue rig. The areas involved are discussed in the following paragraphs.

Cooling Air

As a result of the high fatigue loads required for the gears having a diametral pitch of 6, it became necessary to provide cooling air to the fatigue tooth at the tension fillet and lubrication between the tooth and load cell tip. The need for cooling air at the compression fillet became apparent when two gears cracked from the tooth root to the gear center. Metallurgical analysis indicated that high localized temperatures existed during the final phase of tooth fatigue. Additional cooling air eliminated this problem. All but three teeth on the large gears were tested with the additional cooling air. It is believed that the test results for these three teeth were not seriously biased.

Tip

The initial design specified that the contact surfaces of the tips be coated with plasma spray tungsten carbide. The process was to provide a surface which would offer resistance to wear, scuffing, and distortion. However, after limited usage, the coating cracked and cavitated. The first rework, nitriding the contact surface, was an improvement under low-load conditions, but the surface distorted under high loads. The second

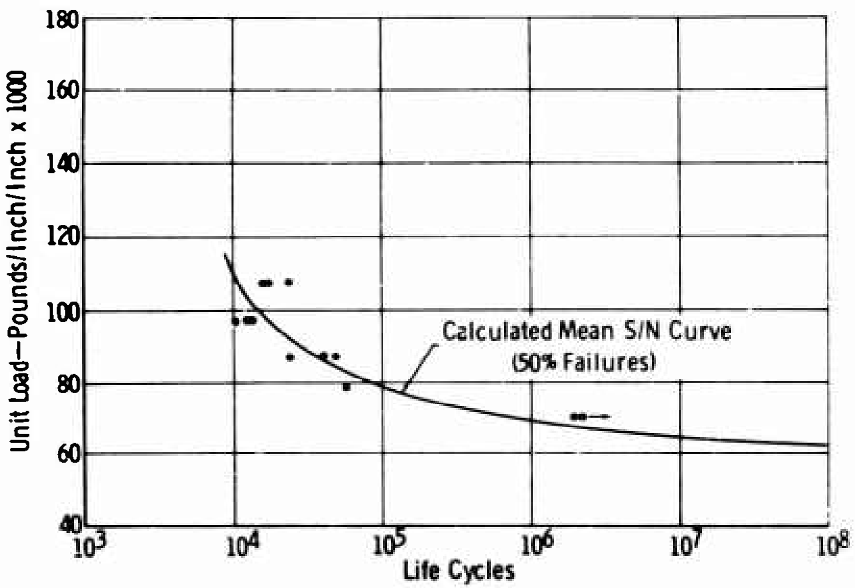

Figure 23. Fatigue Test Results—EX-78772.

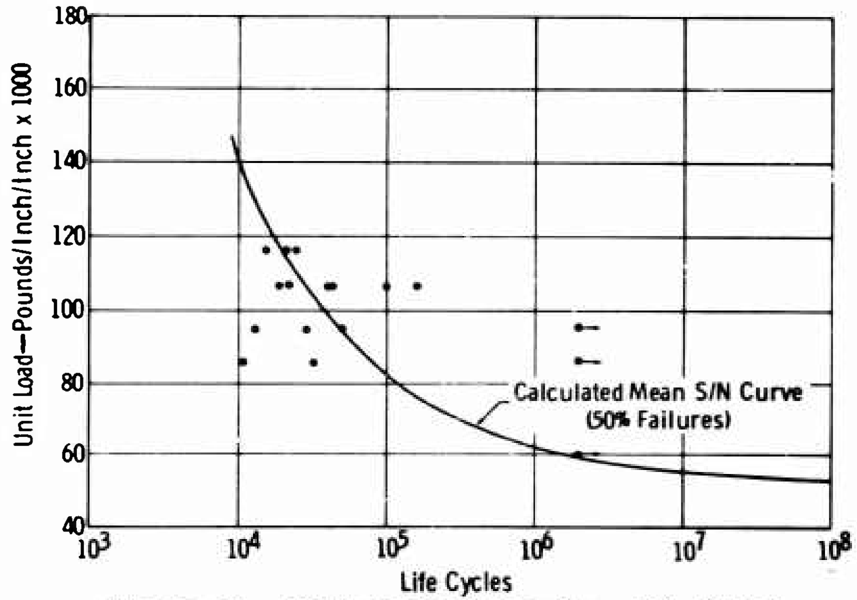

Figure 24. Fatigue Test Results—EX-78773.

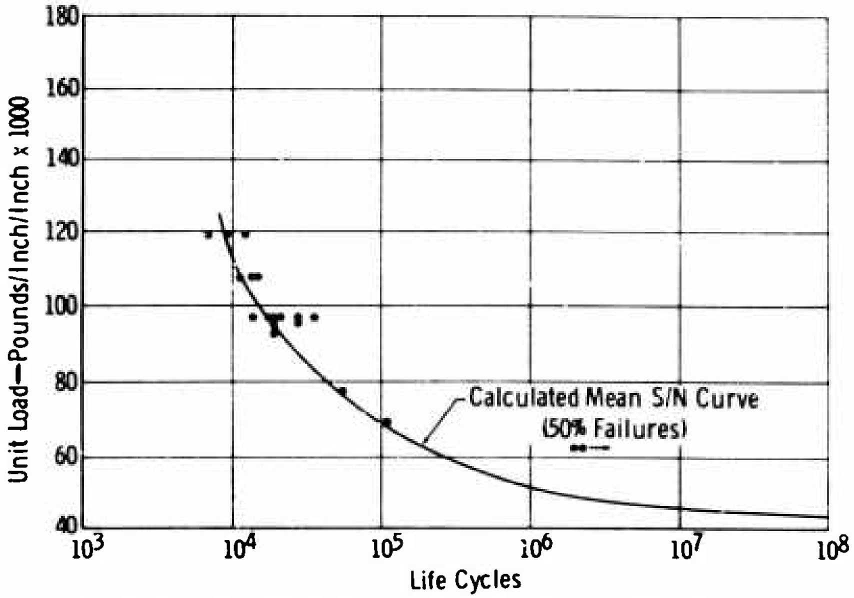

Figure 25. Fatigue Test Results—EX-78774.

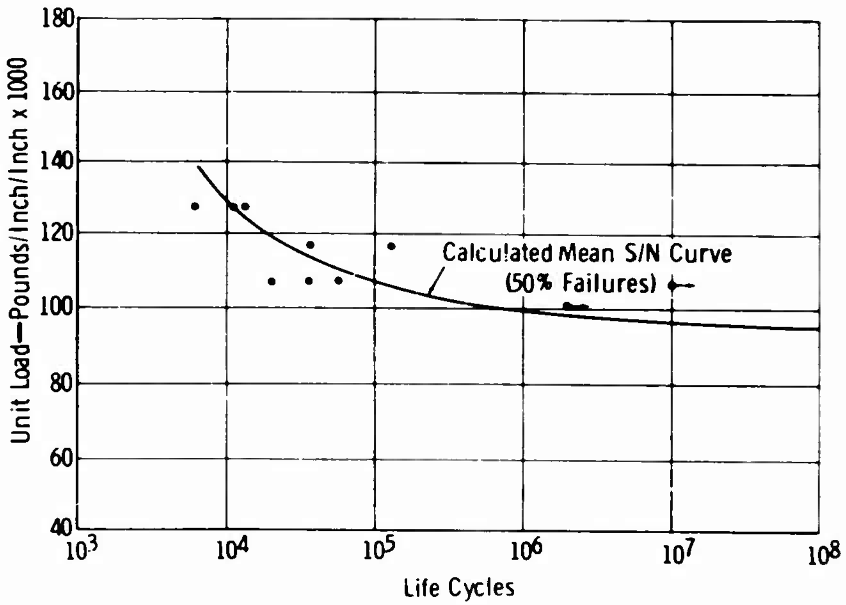

Figure 26. Fatigue Test Results—EX-78775.

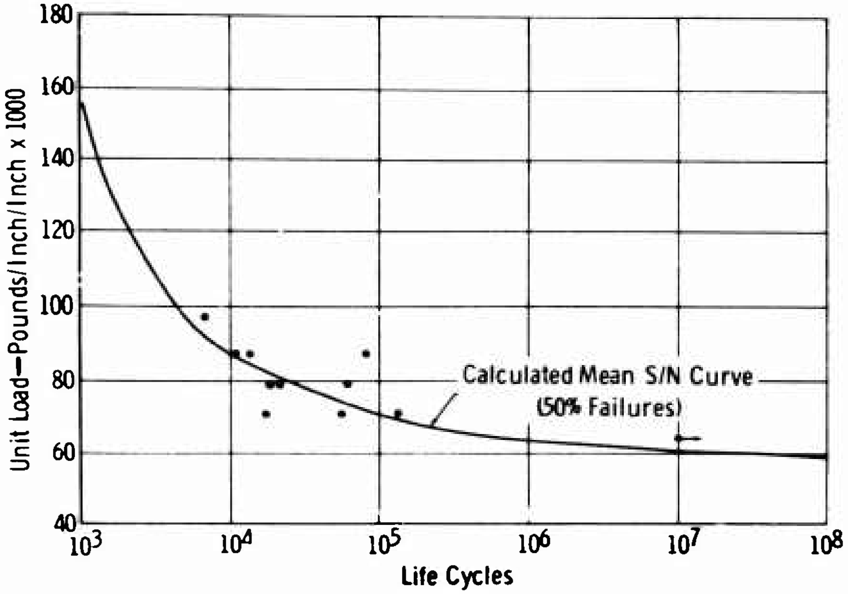

Figure 27. Fatigue Test Results—EX-78776.

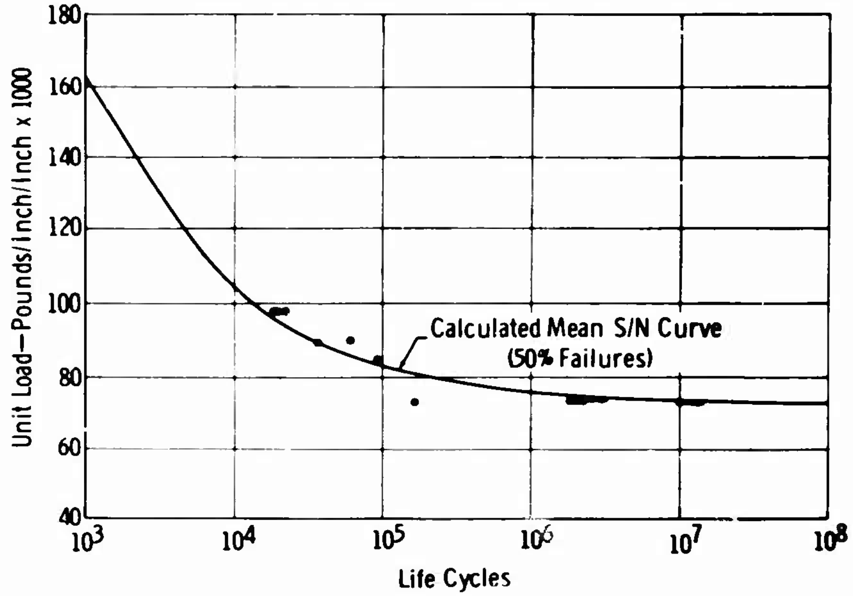

Figure 28. Fatigue Test Results—EX-78777.

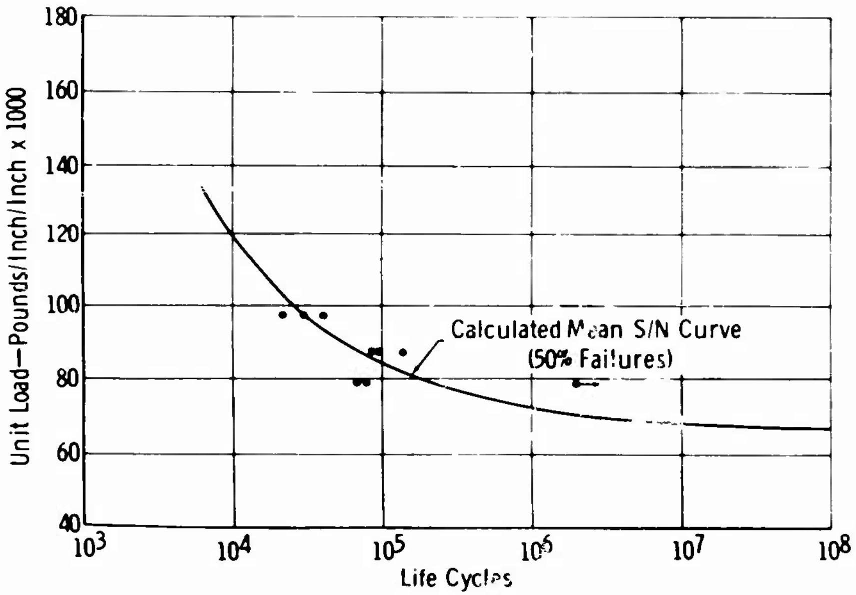

Figure 29. Fatigue Test Results—EX-78778.

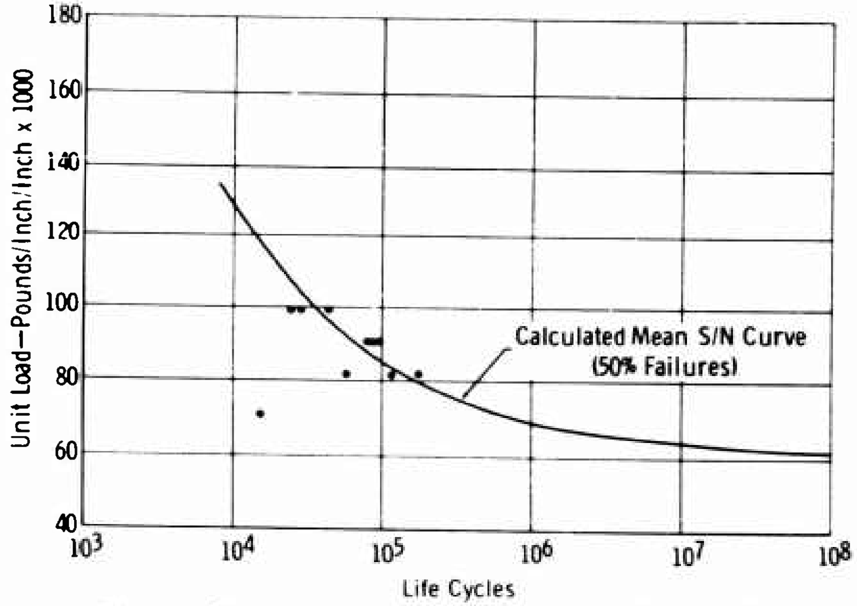

Figure 30. Fatigue Test Results—EX-78779.

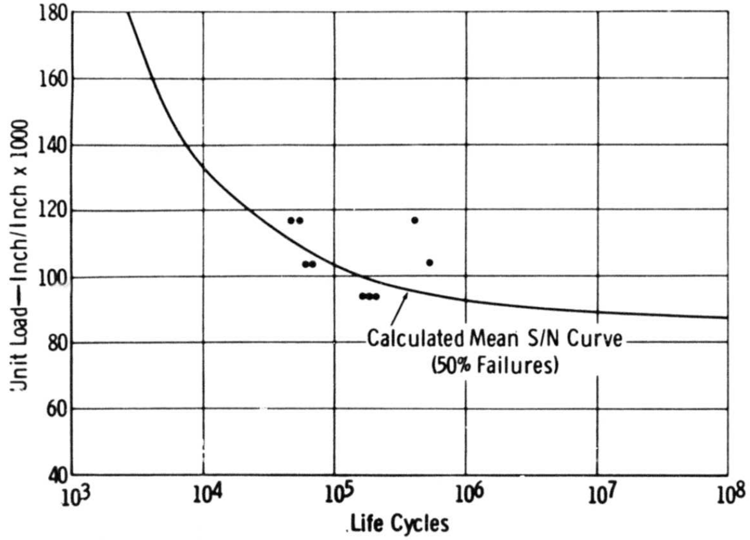

Figure 31. Fatigue Test Results—EX-78780.

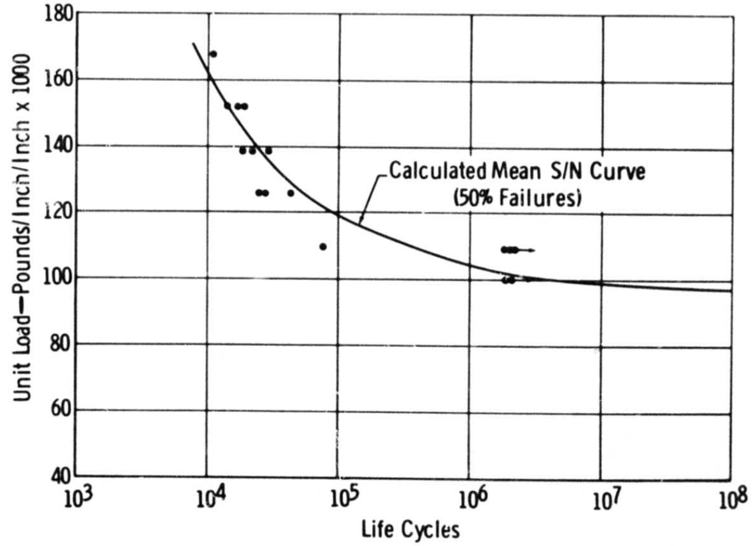

Figure 32. Fatigue Test Results—EX-78781.

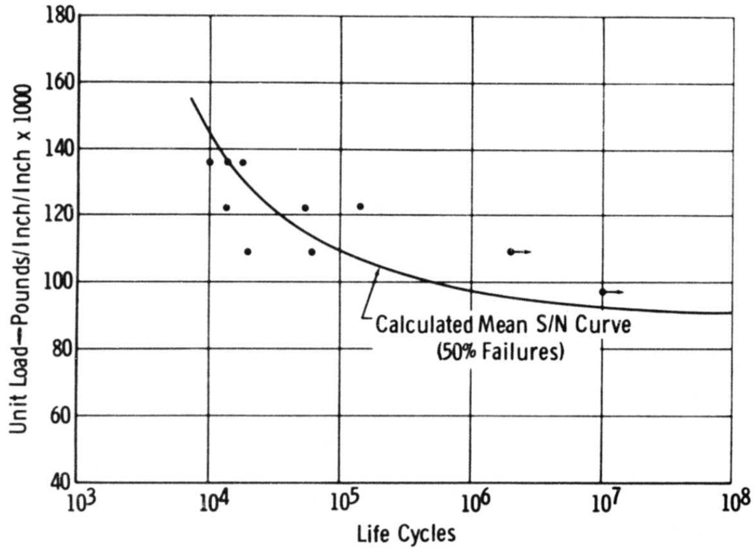

Figure 33. Fatigue Test Results—EX-78782.

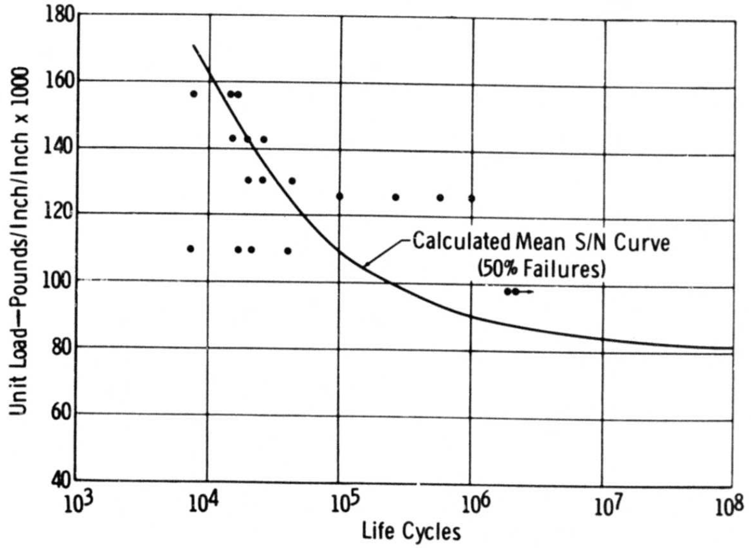

Figure 34. Fatigue Test Results—EX-78783.

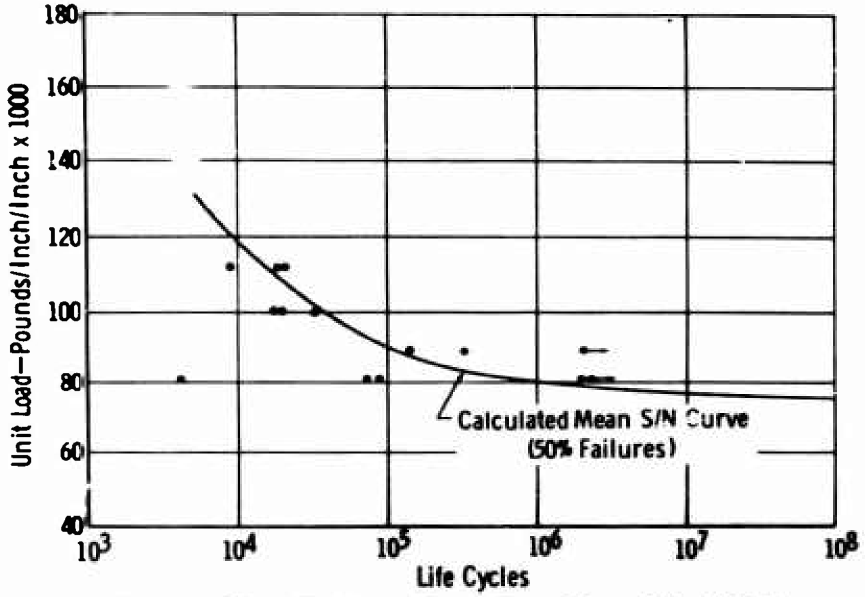

Figure 35. Fatigue Test Results—EX-78784.

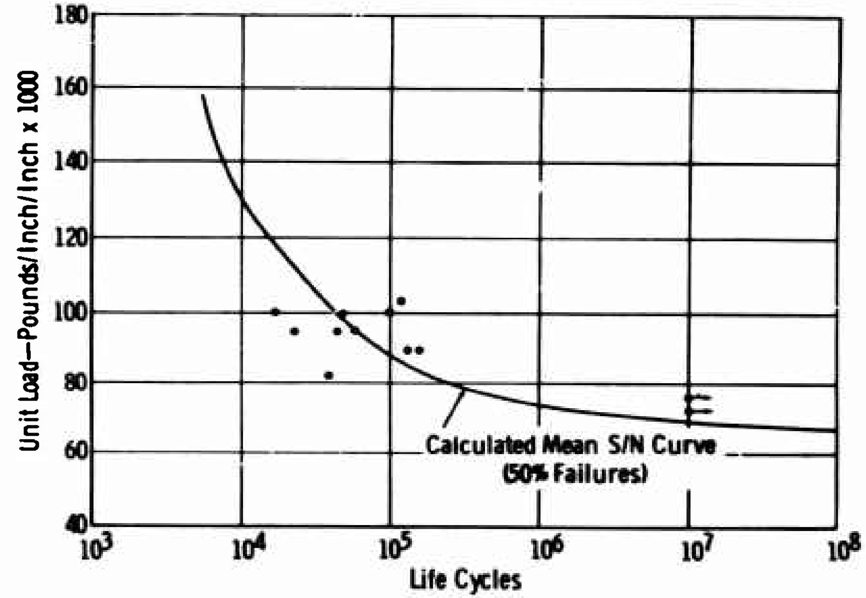

Figure 36. Fatigue Test Results—EX-78785.

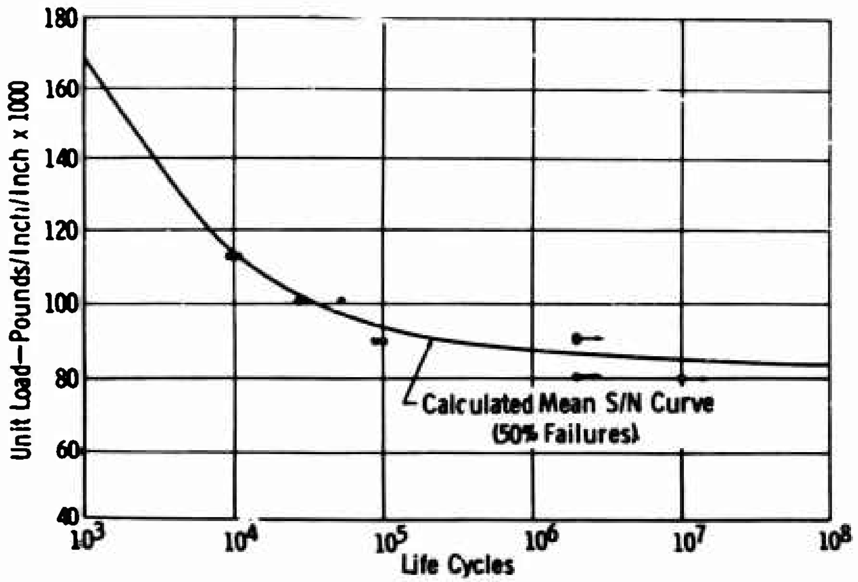

Figure 37. Fatigue Test Results—EX-78786.

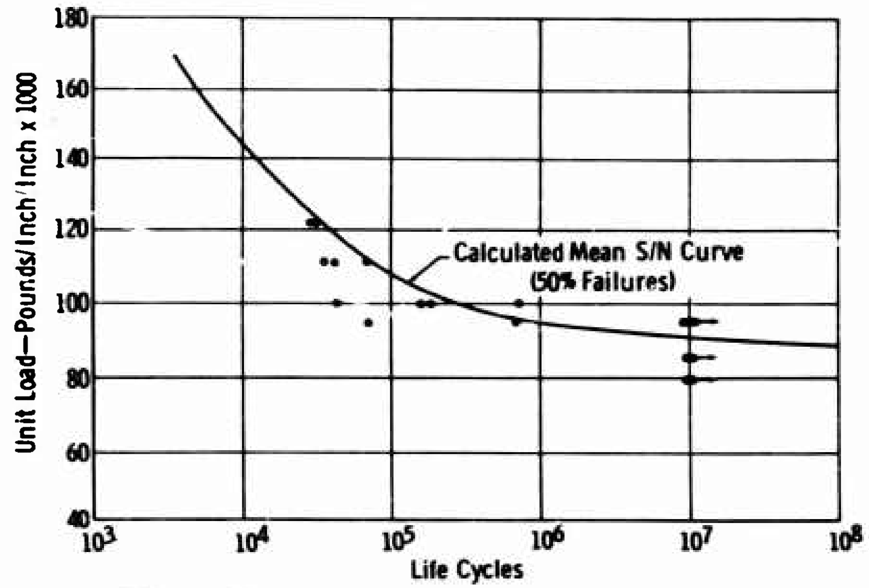

Figure 38. Fatigue Test Results—EX-78787.

TABLE XI
GEAR TEETH FATIGUE TEST DATA

Part Number	Serial Number	Tooth Number	Load (pounds) Static	Dynamic	Total	Cycles to Failure	Test Frequency (c. p. s.)	Y Corr S/N Side
EX-78772	CX 9092	1	5340	5300	10, 640	Void Data	—	0. 3657
		2	4810	4770	9, 580	$1\ 585 \times 10^4$	220	0. 3657
		3	4810	4770	9, 580	1.715×10^4	220	0. 3637
		4	4810	4770	9, 580	2.38×10^4	220	0. 3597
	CX 9091	1	4430	4230	8, 660	1.06×10^4	220	0. 3697
		2	4430	4230	8, 660	1.32×10^4	220	0. 3577
		3	4430	4230	8, 660	1.3×10^4	220	0. 3677
		4	3995	3795	7, 790	2.38×10^4	220	—
	CX 9090	1	3600	3400	7, 000	5.8×10^4	220	—
		2	3995	3795	7, 790	4.8×10^4	220	—
		3	3995	3795	7, 790	4.0×10^4	220	—
EX-78774	CX 9067	1	5900	Void Data High Dynamic Load			220	0. 3547
		2	5390	5190	10, 580	1.188×10^4	220	0. 3607
		3	5390	5190	10, 580	8.9×10^3	220	0. 3617
		4	5390	5190	10, 580	6.6×10^3	220	0. 3557
	CX 9068	1	4860	4660	9, 520	1.076×10^4	220	0. 3576
		2	4860	4660	9, 520	1.32×10^4	220	0. 3576
		3	4860	4660	9, 520	1.32×10^4	220	0. 3546
		4	4385	4185	8, 570	3.43×10^4	220	0. 3586
	CX 9064	1	4385	4185	8, 570	1.32×10^4	220	0. 3536
		2	4385	4185	8, 570	1.98×10^4	220	0. 3616
		3	4385	4185	8, 570	2.64×10^4	220	0. 3536
		4	4385	4185	8, 570	1.85×10^4	220	0. 3536
	CX 9065	1	4385	4185	8, 570	1.7×10^4	220	0. 3586
		2	4385	4185	8, 570	1.85×10^4	220	0. 3606
		3	4385	4185	8, 570	2.64×10^4	220	0. 3496
		4	4385	4185	8, 570	1.85×10^4	220	0. 3526
EX-78776	CX 9010	1	4340	4300	8, 640	6.6×10^3	220	0. 3793
		2	3910	3870	7, 780	7.92×10^4	220	—
		3	3910	3870	7, 780	1.32×10^4	220	—
		4	3910	3870	7, 780	1.04×10^4	220	0. 3933
	CX 9008	1	3600	3400	7, 000	1.78×10^4	220	—
		2	3600	3400	7, 000	5.94×10^4	220	0. 3873
		3	3600	3400	7, 000	206×10^4	220	—
		4	3250	3050	6, 300	6.6×10^4	220	0. 3903
	CX 9009	1	2950	2750	5, 700	$10^7 \rightarrow$	220	—
		2	3250	3050	6, 300	Void Data	—	0. 3883
		3	3250	3050	6, 300	Void Data	—	—
		4	3250	3050	6, 300	1.3×10^5	220	—
	CX 9007	1	3250	3050	6, 300	5.3×10^4	220	—
EX-78778	CX 9054	1	4400	4200	8, 600	2.9×10^4	220	0. 3637
		2	4400	4200	8, 600	3.96×10^4	220	0. 3757

A

Cycles to Failure	Test Frequency (c. p. s.)	Fatigue Crack Dimensions			
		Y Corrected (inches)		Z (degrees)	
		S/N Side	Opposite Side	S/N Side	Opposite Side
oid Data	—	0. 3657	0. 3657	33	36
. 585X10^4	220	0. 3657	0. 3657	31	34
. 715X10^4	220	0. 3637	0. 3647	27	31
. 38X10^4	220	0. 3597	0. 3647	30	31
. 06X10^4	220	0. 3697	0. 3697	32	35
. 32X10^4	220	0. 3577	0. 3657	30	37
. 3X10^4	220	0. 3677	0. 3587	35	30
. 38X10^4	220	—	—	32	—
. 8X10^4	220	—	—	—	—
. 8X10^4	220	—	—	—	—
. 0X10^4	220	—	—	—	—
Load	220	0. 3547	0. 3637	26	36
. 188X10^4	220	0. 3607	0. 3717	32	35
. 9X10^3	220	0. 3617	0. 3637	30	32
. 6X10^3	220	0. 3557	0. 3617	29	29
. 076X10^4	220	0. 3576	—	32	—
. 32X10^4	220	0. 3576	0. 3596	31	32
. 32X10^4	220	0. 3546	0. 3516	31	35
. 43X10^4	220	0. 3586	0. 3586	25	32
. 32X10^4	220	0. 3536	0. 3536	28	33
1. 98X10^4	220	0. 3616	0. 3526	28	34
2. 64X10^4	220	0. 3536	0. 3576	33	32
1. 85X10^4	220	0. 3536	0. 3576	28	33
1. 7X10^4	220	0. 3586	0. 3656	29	28
1. 85X10^4	220	0. 3606	0. 3646	30	31
2. 64X10^4	220	0. 3496	0. 3616	32	29
1. 85X10^4	220	0. 3526	0. 3536	31	29
5. 6X10^3	220	0. 3793	0. 3823	26	30
7. 92X10^4	220	—	—	—	—
1. 32X10^4	220	—	—	31	—
1. 04X10^4	220	0. 3933	0. 3973	31	31
1. 78X10^4	220	—	—	28	27
5. 94X10^4	220	0. 3873	0. 3913	28	29
206X10^4	220	—	—	—	—
6. 6X10^4	220	0. 3903	0. 3923	28	28
10^7 →	220	—	—	—	—
Void Data	—	0. 3883	0. 3913	21	15
Void Data	—	—	—	—	—
1. 3X10^5	220	—	—	—	—
5. 3X10^4	220	—	—	—	—
2. 9X10^4	220	0. 3637	0. 3667	28	28
3. 96X10^4	220	0. 3757	0. 3847	29	28

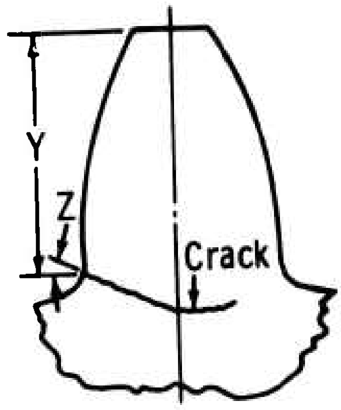

B

TABLE XI (CONT)

Part Number	Serial Number	Tooth Number	Load (pounds)			Cycles to Failure	Test Frequency (c. p. s.)
			Static	Dynamic	Total		
		3	4400	4200	8,600	2.1×10^{4}	220
		4	3970	3770	7,740	9.23×10^{4}	220
	CX 9057	1	3970	3770	7,740	8.71×10^{4}	220
		2	3970	3770	7,740	1.346×10^{5}	220
		3	3583	3383	6,965	Void Data →	—
		4	3583	3383	6,965	2.0×10^{6} →	220
	CX 9056	1	3583	3383	6,965	7.65×10^{4}	220
		2	3583	3383	6,965	6.6×10^{4}	220
EX-78780	CX 9097	1	4900	4700	9,600	5.28×10^{5}	220
		2	4900	4700	9,600	6.6×10^{4}	220
		3	4900	4700	9,600	5.94×10^{4}	220
		4	5500	5300	10,800	4.62×10^{4}	220
	CX 9098	1	5500	5300	10,800	4.125×10^{4}	220
	CX 9095	1	5500	5300	10,800	4.62×10^{4}	220
		2	4420	4220	8,640	2.0×10^{5}	220
		3	4420	4220	8,640	1.85×10^{5}	220
		4	4420	4220	8,640	1.85×10^{5}	220
	CX 9096	1	6040	5840	11,880	1.32×10^{4}	220
		2	6040	5840	11,880	6.6×10^{3}	220
		3	6040	5840	11,880	6.6×10^{3}	220
EX-78782	CX 9113	1	6360	6160	12,520	9.5×10^{3}	220
		2	6360	6160	12,520	Void Data	—
		3	5730	5530	11,260	5.38×10^{4}	220
		4	5730	5530	11,260	1.42×10^{5}	220
	CX 9112	1	5110	4910	10,020	1.19×10^{5}	220
		2	5110	4910	10,020	5.93×10^{4}	220
		3	5110	4910	10,020	2.0×10^{6} →	220
		4	4600	4400	9,000	10^{7} →	220
	CX 9111	1	5730	5530	11,260	1.32×10^{4}	220
		2	6360	6160	12,520	1.32×10^{4}	220
		3	6360	6160	12,520	1.76×10^{4}	220
EX-78784	CX 9072	1	5250	5050	10,300	1.8×10^{4}	220
		2	5250	5050	10,300	1.8×10^{4}	220
		3	5250	5050	10,300	8.6×10^{3}	220
		4	4220	4020	8,240	1.345×10^{5}	220
	CX 9070	1	4220	4020	8,240	2.0×10^{6} →	220
		2	4220	4020	8,240	3.313×10^{5}	220
		3	3800	3600	7,400	2.0×10^{6} →	220
		4	3800	3600	7,400	2.0×10^{6} →	220
	CX 9073	1	3800	3600	7,400	3.96×10^{3}	220

A

... pounds) ... mic	Total	Cycles to Failure	Test Frequency (c.p.s.)	Fatigue Crack Dimensions: Y Corrected (inches) S/N Side	Y Corrected (inches) Opposite Side	Z (degrees) S/N Side	Z (degrees) Opposite Side
	8,600	2.1×10^4	220	—	—	—	28
	7,740	9.23×10^4	220	0.3637	0.3657	30	27
	7,740	8.71×10^4	220	0.3737	0.3767	27	30
	7,740	1.346×10^5	220	0.3587	0.3647	27	29
	6,965	Void Data →	—	—	—	—	—
	6,965	2.0×10^6 →	220	—	—	—	—
	6,965	7.65×10^4	220	—	—	—	—
	6,965	6.6×10^4	220	—	—	—	—
	9,600	5.28×10^5	220	—	—	42	45
	9,600	6.6×10^4	220	—	—	—	—
	9,600	5.94×10^4	220	—	—	—	—
	10,800	4.62×10^4	220	0.3717	0.3717	38	43
	10,800	4.125×10^4	220	—	—	—	—
	10,800	4.62×10^4	220	—	—	—	—
	8,640	2.0×10^5	220	—	—	—	—
	8,640	1.85×10^5	220	—	—	—	—
	8,640	1.85×10^5	220	—	—	—	—
	11,880	1.32×10^4	220	—	—	—	—
	11,880	6.6×10^3	220	—	—	—	—
	11,880	6.6×10^3	220	—	—	—	—
	12,520	9.5×10^3	220	0.3599	0.3699	—	—
	12,520	Void Data	—	0.3719	0.3679	—	—
	11,260	5.38×10^4	220	0.3669	0.3659	—	—
	11,260	1.42×10^5	220	—	—	—	—
	10,020	1.19×10^5	220	—	—	—	—
	10,020	5.93×10^4	220	0.3628	0.3688	39	41
	10,020	2.0×10^6 →	220	—	—	—	—
	9,000	10^7 →	220	—	—	—	—
	11,260	1.32×10^4	220	—	—	—	—
	12,520	1.32×10^4	220	—	—	—	—
	12,520	1.76×10^4	220	—	—	—	—
	10,300	1.8×10^4	220	0.3731	0.3921	34	32
	10,300	1.8×10^4	220	0.3911	0.3941	31	30
	10,300	8.6×10^3	220	0.3901	0.3941	35	36
	8,240	1.345×10^5	220	0.3961	0.3981	31	39
	8,240	2.0×10^6 →	220	—	—	—	—
	8,240	3.313×10^5	220	0.3869	0.3919	34	34
	7,400	2.0×10^6 →	220	—	—	—	—
	7,400	2.0×10^6 →	220	—	—	—	—
	7,400	3.96×10^3	220	0.3881	0.3951	35	42

B

TABLE XI (CONT)

Part Number	Serial Number	Tooth Number	Load (pounds) Static	Dynamic	Total	Cycles to Failure	Test Frequency (c. p. s.)	Y Corr[illegible] S/N Side
		2	3800	3600	7,400	8.58×10^4	220	0.3821
		3	3800	3600	7,400	7.1×10^4	220	—
		4	4735	4535	9,270	1.76×10^4	220	0.3881
	CX 9071	1	4735	4535	9,270	3.16×10^4	220	—
		2	4735	4535	9,270	Void Data	—	—
		3	4735	4535	9,270	1.85×10^4	220	—
EX-78786	CX 9013	1	5295	5095	10,390	1.057×10^4	220	0.3842
		2	5295	5095	10,390	9.23×10^3	220	0.3862
		3	5295	5095	10,390	9.9×10^3	220	0.3872
		4	4260	4060	8,320	9.77×10^4	220	—
	CX 9014	1	4260	4060	8,320	$2\times10^6 \rightarrow$	220	—
		2	4260	4060	8,320	$2\times10^6 \rightarrow$	220	—
		3	3830	3660	7,490	$2\times10^6 \rightarrow$	220	—
		4	3830	3660	7,490	$2\times10^6 \rightarrow 10^7 \rightarrow$	220	—
	CX 9015	1	4775	4575	9,350	2.64×10^4	220	—
		2	4775	4575	9,350	2.64×10^4	220	—
		3	4775	4575	9,350	5.28×10^4	220	—
		4	4260	4060	8,320	9.2×10^4	220	0.3822
EX-78773	CX 9076	1	678	658	1,335	$2.0\times10^6 \rightarrow$	240	—
		2	1198	1178	2,375	1.0×10^5	240	—
		3	1198	1178	2,375	1.58×10^5	240	—
		4	1198	1178	2,375	4.32×10^4	240	—
	CX 9077	1	1303	1283	2,585	2.1×10^4	50	0.1830
		2	1303	1283	2,585	2.4×10^4	50	0.1860
		3	1303	1283	2,585	1.5×10^4	50	0.1830
		4	1073	1053	2,125	$2.0\times10^6 \rightarrow$	240	0.1870
	CX 9075	1	1073	1053	2,125	1.29×10^4	240	0.1849
		2	1073	1053	2,125	5.04×10^4	240	—
		3	1073	1053	2,125	2.88×10^4	240	—
		4	1198	1178	2,375	3.96×10^4	240	—
	CX 9074	1	1198	1178	2,375	2.11×10^4	240	0.1829
		2	1198	1178	2,375	1.85×10^4	240	—
		3	966	946	1,912	1.05×10^5	240	—
		4	966	946	1,912	$2\times10^6 \rightarrow$	240	—
	CX 9078	1	966	946	1,912	3.16×10^4	240	0.1829
EX-78775	CX 9099	1	1135	1115	2,250	$2.0\times10^6 \rightarrow$	240	—
		2	1198	1178	2,375	$2.0\times10^7 \rightarrow$	240	—
		3	1303	1283	2,585	1.296×10^5	240	—
		4	1303	1283	2,585	3.6×10^4	240	0.1675

A

l (pounds)		Cycles to Failure	Test Frequency (c. p. s.)	Fatigue Crack Dimensions			
				Y Corrected (inches)		Z (degrees)	
ynamic	Total			S/N Side	Opposite Side	S/N Side	Opposite Side
600	7,400	8.58×10^4	220	0.3821	0.3891	34	36
600	7,400	7.1×10^4	220	—	—	—	—
535	9,270	1.76×10^4	220	0.3881	0.3911	36	38
535	9,270	3.16×10^4	220	—	—	—	—
535	9,270	Void Data	—	—	—	—	—
535	9,270	1.85×10^4	220	—	—	—	—
095	10,390	1.057×10^4	220	0.3842	0.3882	36	35
095	10,390	9.23×10^3	220	0.3862	0.3872	33	33
095	10,390	9.9×10^3	220	0.3872	0.3932	33	32
060	8,320	9.77×10^4	220	—	—	—	—
060	8,320	$2\times10^6 \rightarrow$	220	—	—	—	—
060	8,320	$2\times10^6 \rightarrow$	220	—	—	—	—
660	7,490	$2\times10^6 \rightarrow$	220	—	—	—	—
660	7,490	$2\times10^6 \rightarrow 10^7 \rightarrow$	220	—	—	—	—
575	9,350	2.64×10^4	220	—	—	30	—
575	9,350	2.64×10^4	220	—	—	—	—
575	9,350	5.28×10^4	220	—	—	—	—
060	8,320	9.2×10^4	220	0.3822	0.3852	30	36
658	1,335	$2.0\times10^6 \rightarrow$	240	—	—	—	—
178	2,375	1.0×10^5	240	—	—	—	—
178	2,375	1.58×10^5	240	—	—	—	—
178	2,375	4.32×10^4	240	—	—	—	—
283	2,585	2.1×10^4	50	0.1830	0.1880	31	38
283	2,585	2.4×10^4	50	0.1860	0.1830	31	36
283	2,585	1.5×10^4	50	0.1830	0.1830	30	35
053	2,125	$2.0\times10^6 \rightarrow$	240	0.1870	0.1800	33	26
053	2,125	1.29×10^4	240	0.1849	0.1859	28	37
053	2,125	5.04×10^4	240	—	—	—	—
053	2,125	2.88×10^4	240	—	—	—	—
178	2,375	3.96×10^4	240	—	—	—	—
178	2,375	2.11×10^4	240	0.1829	0.1849	29	32
178	2,375	1.85×10^4	240	—	—	—	—
946	1,912	1.05×10^5	240	—	—	—	—
946	1,912	$2\times10^6 \rightarrow$	240	—	—	—	—
946	1,912	3.16×10^4	240	0.1829	0.1809	30	31
115	2,250	$2.0\times10^6 \rightarrow$	240	—	—	—	—
178	2,375	$2.0\times10^7 \rightarrow$	240	—	—	—	—
283	2,585	1.296×10^5	240	—	—	—	—
283	2,585	3.6×10^4	240	0.1675	0.1715	—	—

B

TABLE XI (CONT)

Part Number	Serial Number	Tooth Number	Load (pounds)			Cycles to Failure	Test Frequency (c.p.s.)
			Static	Dynamic	Total		
	CX 9033	1	1460	1440	2,900	2.4×10^4	50
		2	1605	1585	3,190	1.8×10^4	50
		3	1605	1585	3,190	2.1×10^4	50
		4	1765	1745	3,510	1.65×10^4	50
	CX 9034	1	1160	1140	2,300	$2\times10^6 \rightarrow$	240
		2	1160	1140	2,300	$2\times10^6 \rightarrow$	240
		3	1330	1310	2,640	$2\times10^6 \rightarrow$	240
		4	1330	1310	2,640	$2\times10^6 \rightarrow$	240
EX-78783	CX 9025	1	1160	1140	2,300	$2\times10^6 \rightarrow$	240
		2	1160	1140	2,300	$2\times10^6 \rightarrow$	240
		3	1330	1310	2,640	1.73×10^5	240
		4	1330	1310	2,640	4.03×10^5	240
	CX 9026	1	1460	1440	2,900	$2.0\times10^6 \rightarrow$	240
		2	1460	1440	2,900	1.008×10^5	240
		3	1510	1490	3,000	2.52×10^4	50
		4	1510	1490	3,000	1.98×10^4	50
	CX 9027	1	1510	1490	3,000	4.32×10^4	50
		2	1660	1640	3,300	1.95×10^4	50
		3	1660	1640	3,300	1.5×10^4	50
		4	1660	1640	3,300	2.55×10^4	50
	CX 9028	1	1810	1790	3,600	1.44×10^4	50
		2	1810	1790	3,600	1.53×10^4	50
		3	1810	1790	3,600	7.5×10^3	50
	CX 9029	1	1460	1440	2,900	2.68×10^5	240
		2	1460	1440	2,900	5.76×10^5	240
		3	1330	1310	2,640	7.2×10^3	50
		4	1330	1310	2,640	2.1×10^4	50
EX-78785	CX 9035	1	1200	1160	2,360	1.15×10^5	240
		2	950	928	1,878	3.6×10^4	240
		3	850	800	1,650	$10^7 \rightarrow$	240
		4	890	860	1.750	$10^7 \rightarrow$	240
	CX 9037	1	1100	1080	2,180	4.32×10^4	50
		2	1100	1080	2,180	5.04×10^4	50
		3	1040	1020	2,060	1.29×10^5	50
		4	1040	1020	2,060	1.512×10^5	50
	CX 9038	1	1160	1140	2,300	9.37×10^4	50
		2	1160	1140	2,300	4.5×10^4	50
		3	1160	1140	2,300	1.62×10^4	50
		4	1100	1080	2,180	2.16×10^4	50

A

Y S/N	Load (pounds) Dynamic	Total	Cycles to Failure	Test Frequency (c.p.s.)	Fatigue Crack Dimensions: Y Corrected (inches) S/N Side	Y Corrected (inches) Opposite Side	Z (degrees) S/N Side	Z (degrees) Opposite Side
0.	1440	2,900	2.4×10^4	50	0.1769	0.1769	31	33
0.	1585	3,190	1.8×10^4	50	0.1789	0.1769	34	34
0.	1585	3,190	2.1×10^4	50	0.1789	0.1789	32	37
0.	1745	3,510	1.65×10^4	50	0.1759	0.1759	31	36
	1140	2,300	2×10^6 →	240	—	—	—	—
	1140	2,300	2×10^6 →	240	—	—	—	—
	1310	2,640	2×10^6 →	240	—	—	—	—
	1310	2,640	2×10^6 →	240	—	—	—	—
	1140	2,300	2×10^6 →	240	—	—	—	—
	1140	2,300	2×10^6 →	240	—	—	—	—
	1310	2,640	1.73×10^5	240	—	—	—	—
	1310	2,640	4.03×10^5	240	—	—	—	—
	1440	2,900	2.0×10^6 →	240	—	—	—	—
	1440	2,900	1.008×10^5	240	—	—	—	—
0.	1490	3,000	2.52×10^4	50	0.1807	0.1857	32	41
0.	1490	3,000	1.98×10^4	50	0.1847	0.1847	36	37
	1490	3,000	4.32×10^4	50	—	—	—	—
0.	1640	3,300	1.95×10^4	50	0.1867	0.1827	35	36
0.	1640	3,300	1.5×10^4	50	0.1787	0.1807	34	36
	1640	3,300	2.55×10^4	50	—	—	—	—
	1790	3,600	1.44×10^4	50	—	—	—	—
	1790	3,600	1.53×10^4	50	—	—	—	—
	1790	3,600	7.5×10^3	50	—	—	—	—
0.	1440	2,900	2.68×10^5	240	0.1720	0.1740	31	33
	1440	2,900	5.76×10^5	240	—	—	—	—
	1310	2,640	7.2×10^3	50	—	—	—	—
	1310	2,640	2.1×10^4	50	—	—	—	—
0.	1160	2,360	1.15×10^5	240	0.1891	0.1871	28	31
	928	1,878	3.6×10^4	240	—	—	—	—
	800	1,650	10^7 →	240	—	—	—	—
	860	1.750	10^7 →	240	—	—	—	—
	1080	2,180	4.32×10^4	50	—	—	—	—
	1080	2,180	5.04×10^4	50	—	—	—	—
	1020	2,060	1.29×10^5	50	—	—	—	—
	1020	2,060	1.512×10^5	50	—	—	—	—
0.	1140	2,300	9.37×10^4	50	0.1901	0.1921	26	32
	1140	2,300	4.5×10^4	50	—	—	—	—
	1140	2,300	1.62×10^4	50	—	—	—	—
	1080	2,180	2.16×10^4	50	—	—	—	—

TABLE XI (CONT)

Part Number	Serial Number	Tooth Number	Load (pounds) Static	Dynamic	Total	Cycles to Failure	Test Frequency (c. p. s.)	Y S/N
EX-78787	CX 9114	1	1160	1140	2,300	4.32×10^4	240	
		2	1160	1140	2,300	1.87×10^5	240	
		3	1160	1140	2,300	7.2×10^5	240	
	CX 9115	1	1100	1080	2,180	$10^7 \rightarrow$	240	
		2	1100	1080	2,180	6.91×10^5	240	
		3	1100	1080	2,180	$10^7 \rightarrow$	240	
		4	1100	1080	2,180	$10^7 \rightarrow$	240	
	CX 9116	1	1285	1265	2,550	6.9×10^4	50	0. 1
		2	1285	1265	2,550	4.2×10^4	50	0. 1
		3	1285	1265	2,550	3.6×10^4	50	
		4	1415	1395	2,810	2.85×10^4	50	
	CX 9117	1	935	915	1,850	$10^7 \rightarrow$	240	
		2	935	915	1,850	$10^7 \rightarrow$	240	
		3	980	970	1,950	$10^7 \rightarrow$	240	
		4	980	970	1,950	$10^7 \rightarrow$	240	
	CX 9118	1	1415	1395	2,810	3×10^4	50	0. 1
		2	1415	1395	2,810	2.94×10^5	50	

A

...unds) ...amic	Total	Cycles to Failure	Test Frequency (c. p. s.)	Fatigue Crack Dimensions: Y Corrected (inches) S/N Side	Y Corrected (inches) Opposite Side	Z (degrees) S/N Side	Z (degrees) Opposite Side
	2, 300	4.32×10^4	240	—	—	26	27
	2, 300	1.87×10^5	240	—	—	—	—
	2, 300	7.2×10^5	240	—	—	—	—
	2, 180	10^7 →	240	—	—	—	—
	2, 180	6.91×10^5	240	—	—	—	—
	2, 180	10^7 →	240	—	—	—	—
	2, 180	10^7 →	240	—	—	—	—
	2, 550	6.9×10^4	50	0. 1890	0. 1920	27	32
	2, 550	4.2×10^4	50	0. 1890	0. 1930	27	32
	2, 550	3.6×10^4	50	—	—	—	—
	2, 810	2.85×10^4	50	—	—	—	—
	1, 850	10^7 →	240	—	—	—	—
	1, 850	10^7 →	240	—	—	—	—
	1, 950	10^7 →	240	—	—	—	—
	1, 950	10^7 →	240	—	—	—	—
	2, 810	3×10^4	50	0. 1843	0. 1893	25	34
	2, 810	2.94×10^5	50	—	—	—	—

B

rework involved fabricating tips with carburized surfaces. The carburized surfaces did not distort under high load; thus, carburizing appeared to be a desirable process for this type of testing. It is believed that the difficulties encountered did not affect the data because each condition was recognized early and was corrected.

Another difficulty involved tip rotation under high loads during the fatigue test of the 4.0-inch-pitch-diameter gears. By rotating, the load point was changed; thus, one data point was affected and was discarded. To prevent rotation, a small piece of shim stock was spot-welded to the outside diameter of the tip and load cell, locking the two together and preventing rotation.

Gage Locating Block

Interference between the gage locating block and the stub tooth was discovered early in the program. This interference would have prevented true angular positioning of the gear tooth on the contact surface of the tip, thus defining a load point other than the high point of single tooth contact. The gage blocks were reworked for clearance; no data points were affected.

Bias Spring

The original bias spring had a spring rate of 2000 pounds per inch, which was not sufficient to preload the 4.0-inch-pitch-diameter gears. Therefore, springs with a spring rate of 20,000 pounds per inch were purchased to satisfy the preload requirements.

Load Cell

It was discovered during the rework of the tips that the squareness and flatness of the tip surface mating with the load cell affected load cell calibration. The rework that most effectively corrected this difficulty was lapping of the two surfaces. Once good surface contact was established, the difficulty was eliminated. A number of data points (32 total) were affected by this condition. A series of tests was conducted where this condition existed; the test was duplicated. This yielded a correction factor which was applied to the affected data points. It is believed that the data were corrected with sufficient accuracy to avoid distortion of the final evaluation.

Test Frequency

The gears having a diametral pitch of 12 were tested at two frequencies—50 and 240 c.p.s. The frequency of 240 c.p.s. was at system resonance. The 50-c.p.s. frequency was selected for use at the higher test loads to provide increased duration of fatigue test time. The time required to establish the test rig load was thereby maintained small when compared with the fatigue time at load. The literature indicates that less than a 2-percent difference in fatigue life would be expected from this change in frequency (reference 20). A similar nonresonance operating procedure was not possible with the gears having a diametral pitch of 6 without overloading the shaker. Quicker establishment of the load on the larger gears was possible without overloading, so there was no strong requirement for a drop in test frequency.

FAILED GEAR TOOTH CRACK MEASUREMENTS

A comparison was made of the calculated location of the weakest section of each

tooth and the actual location. To do this, the crack in each failed tooth was measured and recorded. See Table XI. The bar charts in Figures 39 and 40 summarize the results of this investigation. For each configuration, the location of the crack at the tooth surface was measured from the outside diameter and center line of the tooth, within an estimated 0.002 inch. The average dimension corrected for outside diameter variations is plotted for comparison with the theoretical locations as determined by both Lewis and Kelley-Pedersen construction. The charts indicate that for all configurations, Kelley-Pedersen construction locates the weakest section of the tooth closer to the actual measured location than does Lewis construction. The gears having a diametral pitch of 12 show the measured location to be, on the average, 0.015 inch closer to the root than the Lewis theoretical locations. In the gears having a diametral pitch of 6, the deviation is proportional or 0.030 inch closer to the root than the calculated Lewis location. For a graphical presentation of these data, a typical tooth profile trace of each configuration was made. Two such traces are shown in Figures 41 and 42. The weakest section is shown on each trace as calculated by Lewis and Kelley-Pedersen and as measured.

It would be natural to conclude from the examination of these results alone that the Kelley-Pedersen construction provides a more accurate means to locate the true weakest section of the tooth. However, fatigue test data have already shown that the AGMA stress formula using the Lewis tooth form factor most nearly approximates the endurance characteristics of the gear material. The reason for this paradox may be the change of tooth geometry as the tooth deflects under load. Another possibility is the Kelley-Pedersen stress formula, which was derived from a photoelastic study. It may be assumed that the method derived for locating the weakest section is accurate, as the experimental data show. However, the stress concentration factor employed may require modification to obtain a stress value comparable to the true stress in the material. Unfortunately, further pursuit of this phase of the investigation was not possible within the scope of this program; it should be considered, however, in future studies.

Crack measurements were obtained on twelve EX-78774 gears (configuration 3). These data were statistically analyzed to calculate a standard deviation of 0.48×10^{-4} and a variance of 0.234×10^{-4} from the 0.3581 corrected average "Y" value for this configuration. These data tend to indicate the consistency of fatigue test gear manufacturing and test.

METALLURGICAL INVESTIGATIONS

Metallurgical examinations of failed test gears were conducted to determine mode of failure, origin of failure, microstructure, case depth, hardness gradient, and material cleanliness.

Six gears were submitted for metallurgical investigation as follows:

Part Number	Serial Number
EX-78773	CX 9077
EX-78775	CX 9100
EX-78777	CX 9059
EX-78779	CX 9104
EX-78782	CX 9113
EX-78784	CX 9069

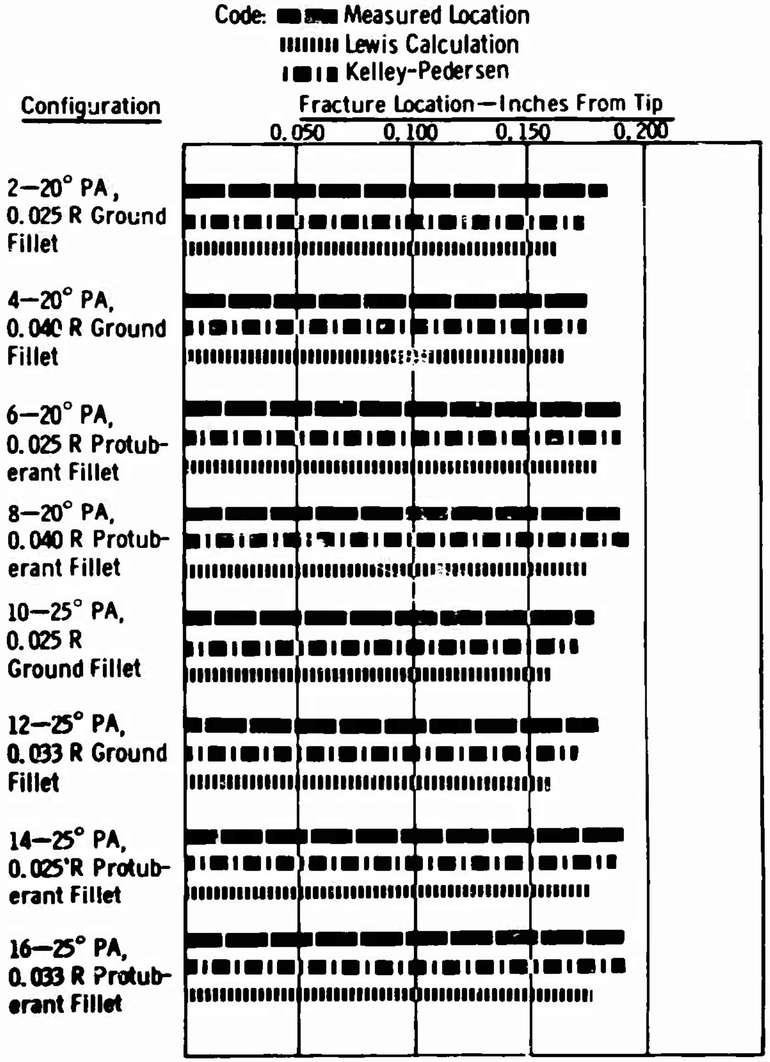

Figure 39. Location of Fracture Compared With Calculated Location of Weakest Section From Gear Outside Diameter (Diametral Pitch = 6).

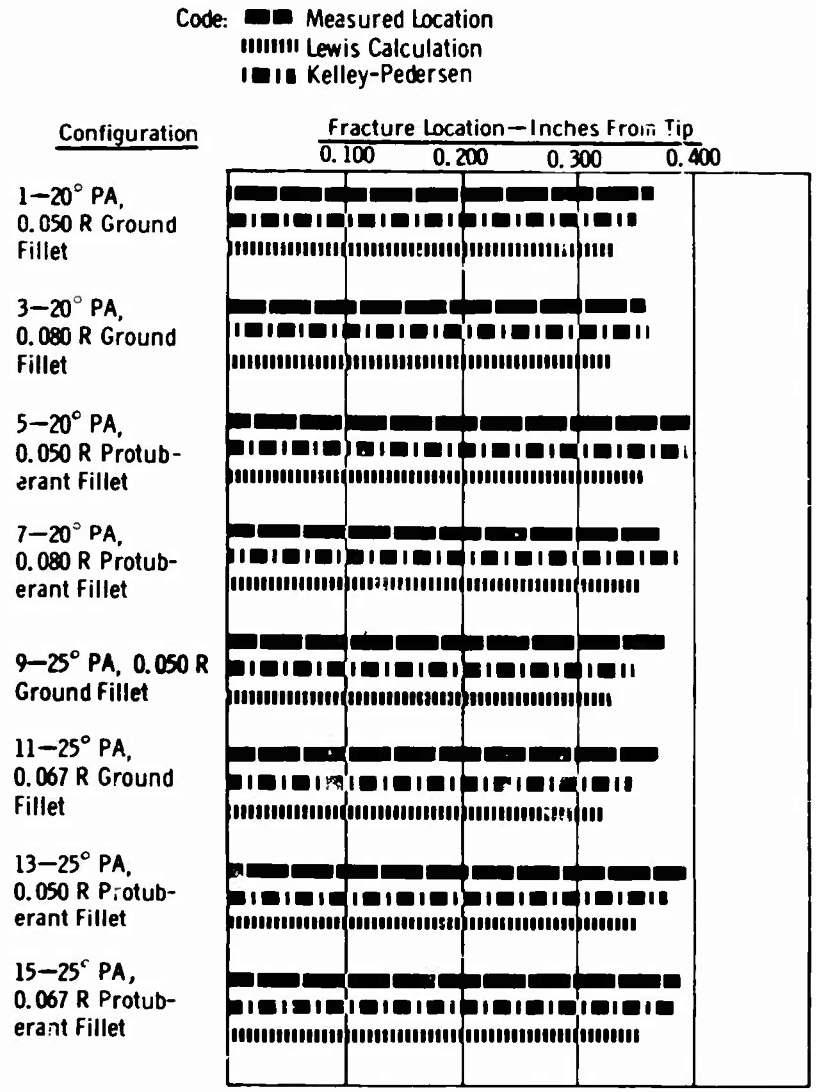

Figure 40. Location of Fracture Compared With Calculated Location of Weakest Section From Gear Outside Diameter (Diametral Pitch = 12).

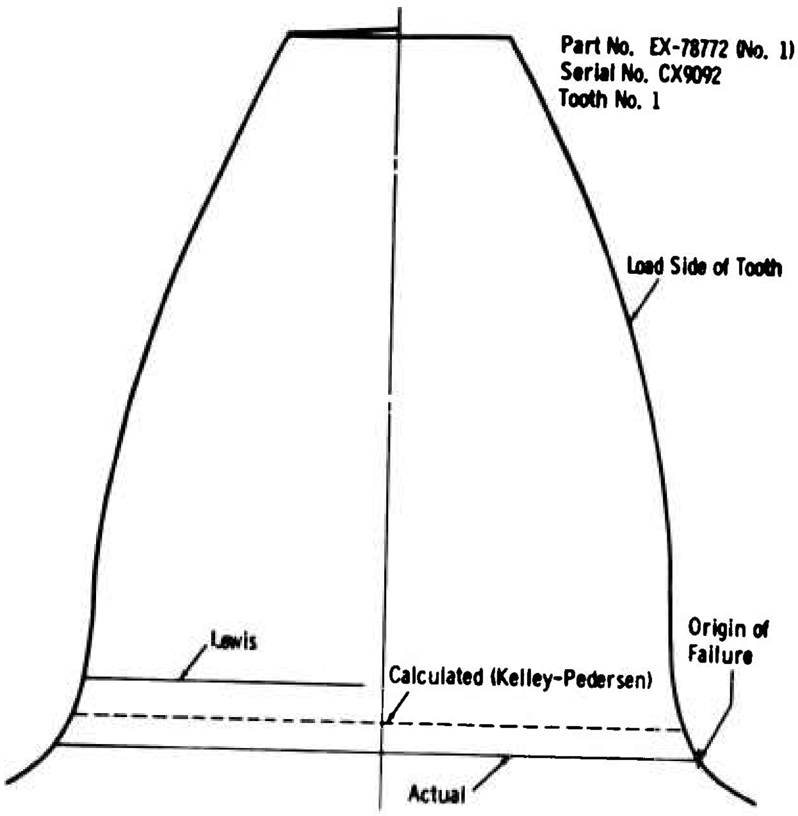

Figure 41. Typical Tooth Profile Trace—EX-78772.

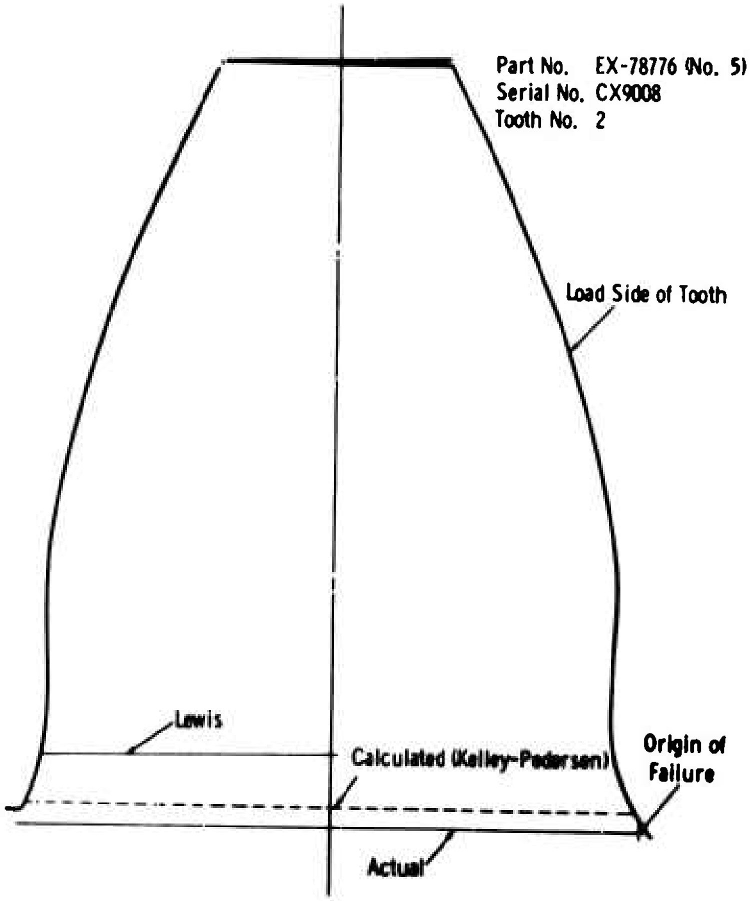

Figure 42. Typical Tooth Profile Trace—EX-78776.

The following metallurgical conclusions were made.

- Failure of the tested teeth occurred in fatigue.
- The fatigue failures of the tested gear teeth originated in the carburized case of the root radius below the loaded involute.
- Electron fractographs were used to determine the precise origin of failure. The failures appeared to be predominantly multiple.
- The microstructure of the carburized case of the various gears was typical of spheroidized carbides in a martensitic matrix with no indication of carbide network in the areas of failure in the root radii. The core microstructures were of tempered martensite.
- The effective case depth, measured to the R_c 50 level, was indicated to be approximately 0.030 inch on test gears (EX-78773 and EX-78775); approximately 0.040 inch on test gears EX-78777, EX-78779, and EX-78782; and approximately 0.050 inch on test gear EX-78784.
- The test gear material was clean and free from inclusions.
- The material conformed to the compositional requirements of AMS-6265.

Electron fractographs of the failure surfaces of the four failed teeth of test gear EX-78784, serial number CX 9069, confirmed a fatigue failure mode on each surface, as shown in Figures 43, 44, 45, and 46. Visual examination of the failure surfaces of the failed teeth of all submitted gears revealed similar straight-line failures, some of which displayed occasional arrest lines of progressing, typical of fatigue, originating in the root radii. Visual examination of test gear EX-78782, serial number CX 9113, revealed an additional fatigue failure progressing radially from below the root on the nonloaded side of a failed tooth to the center of the gear. (This isolated failure, discussed in the subsection titled Fatigue Tests, was due to localized temperature and was subsequently corrected by cooling the gear.) Microexamination of transverse sections through the failure surfaces of failed teeth from each of the submitted gears revealed straight-line failures typical of fatigue. These failures originated in the carburized case structure in the root radius below the loaded involute, as shown in Figures 47 through 52. The failures, typically, had multiple origins, indicating equalized loading in clean material. Unetched, polished specimens revealed good material quality. The microstructures were of spheroidized carbides in a martensitic matrix with no carbide network in the case and tempered martensite in the core. A typical core microstructure of tempered martensite is shown in Figure 53. Effective case depth measured to the R_c 50 level varied approximately 0.030 inch on part numbers EX-78773 and EX-78775; approximately 0.040 inch on part numbers EX-78777, EX-78779, and EX-78782; and approximately 0.050 inch on part number EX-78784. Case hardness of the various test gears was R_c 61 to 62 at 0.002 inch below the surface with a diminishing gradient as shown in Table XII. Spectrographic analysis indicated conformance of the material in the test gears to the compositional requirements of AMS-6265. Photographs indicating case depths around root fillet contour are shown in Figures 54 through 59.

Fluorescent penetrant inspection of the test gears indicated that all failures of the teeth occurred in the root radii, as indicated in Figures 60 through 65. Fluorescent penetrant inspection of test gear part number EX-78782, serial number CX 9113, revealed an additional radial crack, as shown in Figure 64. Visual examination of the surfaces of failure revealed flat fractures with multiple origins of failure, but only occasional arrest lines indicative of fatigue, as shown in Figures 66 through 70. Visual examination of the failure surface of the radial failure in test gear part number EX-78782, serial number CX 9113, revealed a smooth failure with arrest lines of progression, typical of fatigue, originating below the root radius on the unloaded side of a failed tooth and progressing to the hub, as shown in Figure 71.

Magnification: 2,500×

Magnification: 10,000×

EX-78784, Serial Number CX 9069

Figure 43. Fractographs of Surface of Failure of Gear Tooth Number 1 Showing Failure Contour Typical of Fatigue.

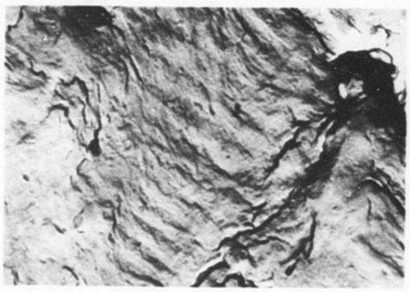

Magnification: 2,500×

Magnification: 10,000×

EX-78784, Serial Number CX 9069

Figure 44. Fractographs of Surface of Failure of Gear Tooth Number 2 Showing Failure Contour Typical of Fatigue.

Magnification: 2,500X

Magnification: 10,000X

EX-78784, Serial Number CX 9069

Figure 45. Fractographs of Surface of Failure of Gear Tooth Number 3 Showing Failure Topography Typical of Fatigue.

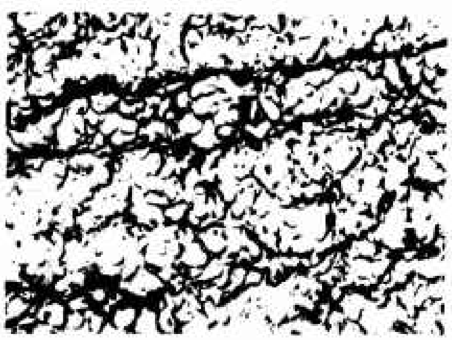

Magnification: 2,500X

Magnification: 10,000X

EX-78784, Serial Number CX 9069

Figure 46. Fractographs of Surface of Failure of Gear Tooth Number 4 Showing Failure Topography Typical of Fatigue.

Magnification: 100×
Etchant: Vilella's Reagent
EX-78773, Serial Number CX 9077

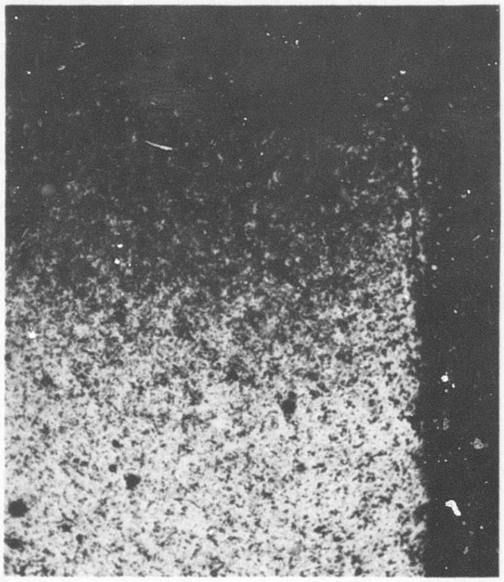

Figure 47. Photomicrograph of Transverse Section Through Failure Surface of Failed Tooth Showing Straight-Line Failure Typical of Fatigue Originating in the Carburized Case Hardened Root Radius.

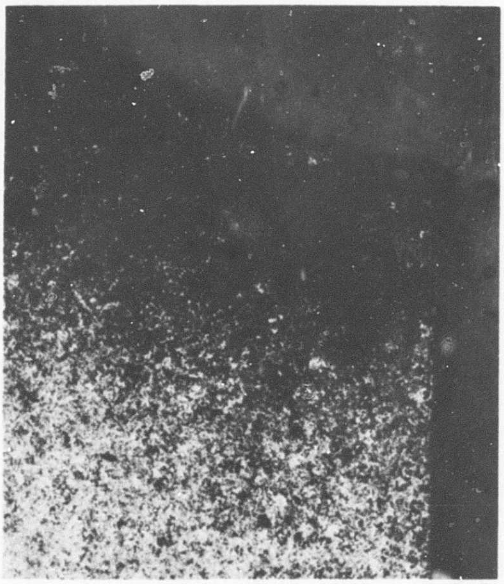

Magnification: 100×
Etchant: Villella's Reagent
EX-78775, Serial Number CX 9100

Figure 48. Photomicrograph of Transverse Section Through Failure Surface of Failed Tooth Showing Straight-Line Failure Surface Typical of Fatigue Originating in the Case Hardened Root Radius.

Magnification: 100×
Etchant: Vilella's Reagent
EX-78777, Serial Number CX 9059

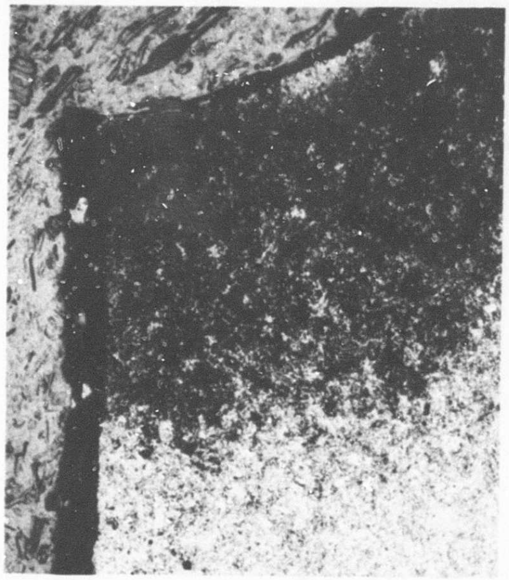

Figure 49. Photomicrograph of Transverse Section Through Failure Surface of Failed Tooth Showing Straight-Line Failure Surface Typical of Fatigue Originating in Carburized Case in the Root Radius.

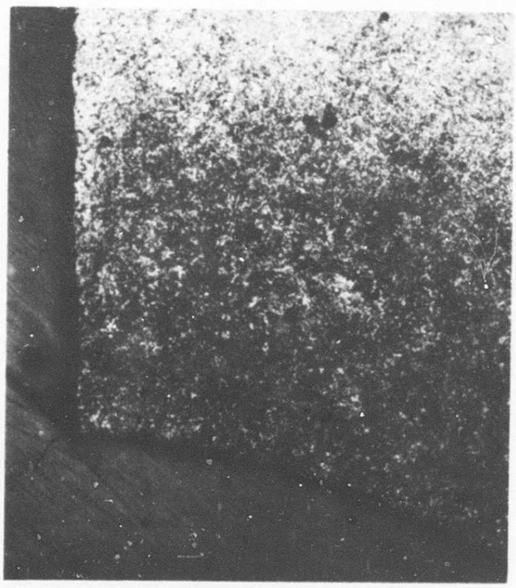

Magnification: 100×
Etchant: Vilella's Reagent
EX-78779, Serial Number CX 7104

Figure 50. Photomicrograph of Transverse Section Through Failure Surface of Failed Tooth Showing Straight-Line Failure Surface Typical of Fatigue Originating in the Case Hardened Root Radius.

Magnification: 100X
Etchant: Villella's Reagent
EX-78782, Serial Number CX 9113

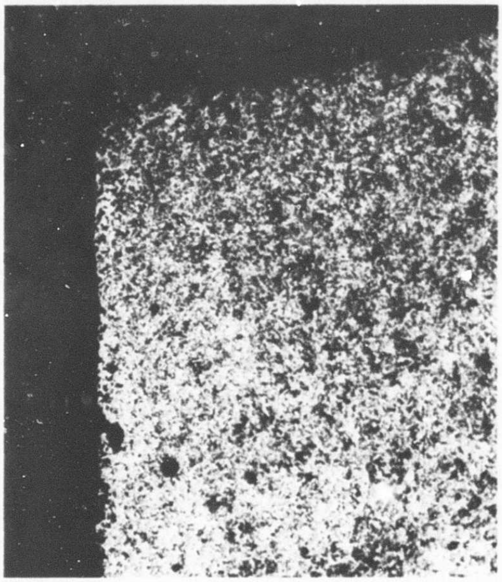

Figure 51. Photomicrograph of Transverse Section Through Failed Tooth Showing Straight-Line Failure Typical of Fatigue Through a Carburized Case on Martensitic Microstructure.

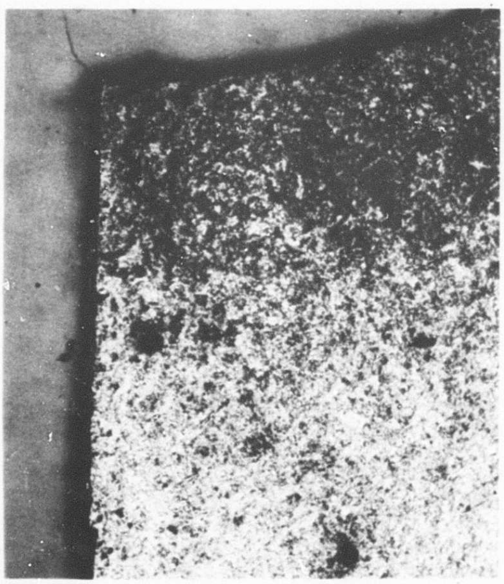

Magnification: 100X
Etchant: Vilella's Reagent
EX-78784, Serial Number CX 9069

Figure 52. Photomicrograph of Transverse Section Through Failure Surface of Failed Tooth Showing a Straight-Line Failure Surface Typical of Fatigue Through Case Hardened Microstructure.

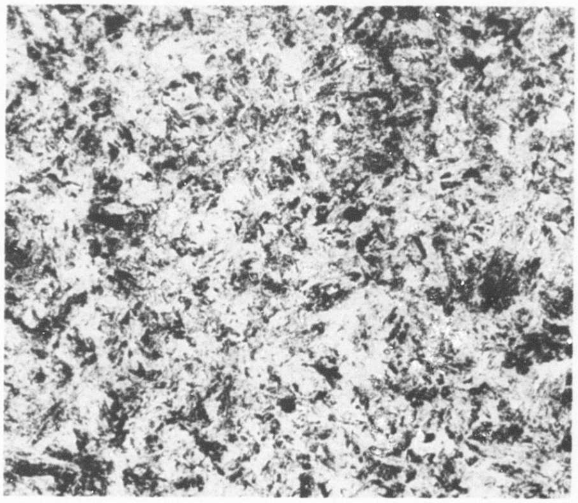

Magnification: 250X
Etchant: Vilella's Reagent
EX-78777, Serial Number CX 9059

Figure 53. Photomicrograph of Transverse Section Through Test Gear Showing Typical Core Structure of Tempered Martensite.

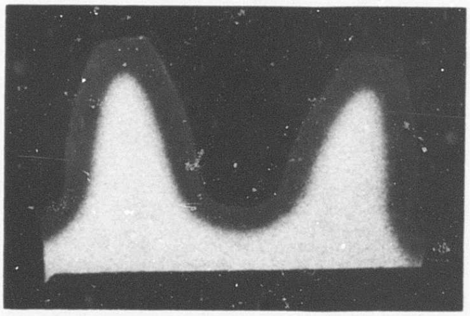

Figure 54. Photograph of Section Through Test Gear Showing Case Depth Around Root Fillet Contour.

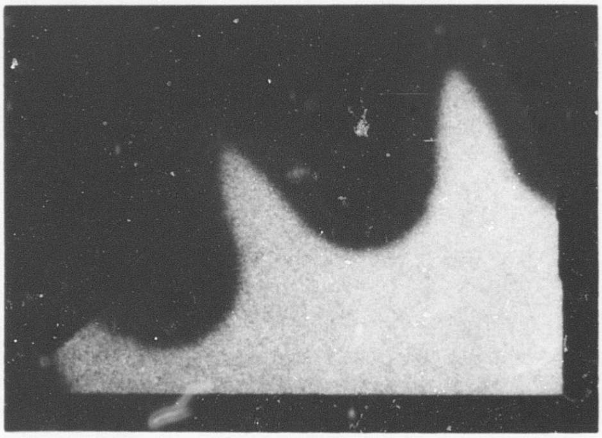

Magnification: 6X EX-78775, Serial Number CX 9100

Figure 55. Photograph of Section Through Test Gear Showing Case Depth Around Root Fillet Contour.

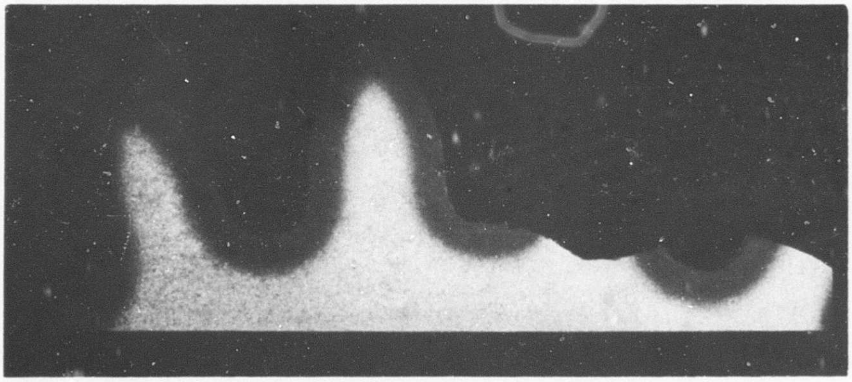

Magnification: 6X EX-78777, Serial Number CX 9059

Figure 56. Photograph of Section Through Test Gear Showing Case Depth Around Root Fillet Contour.

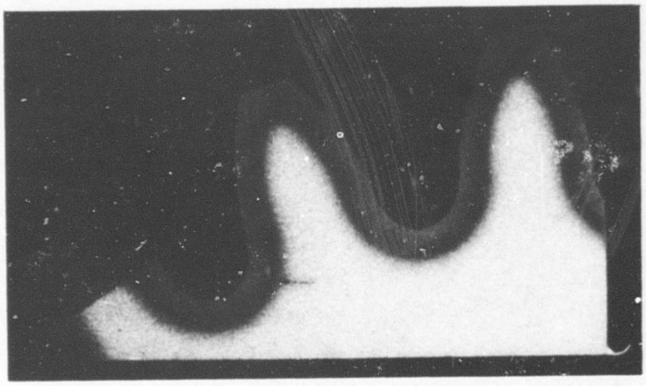

Magnification: 6X EX-78779, Serial Number CX 9104

Figure 57. Photograph of Section Through Test Gear Showing Carburized Case Depth Around Root Fillet Contour.

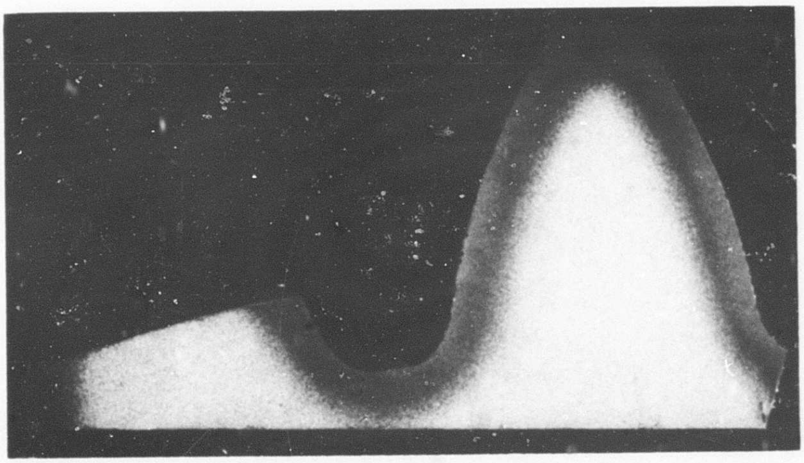

Magnification: 6X EX-78782, Serial Number CX 9113

Figure 58. Photograph of Section Through Test Gear Showing Carburized Case Depth Around Root Fillet Contour.

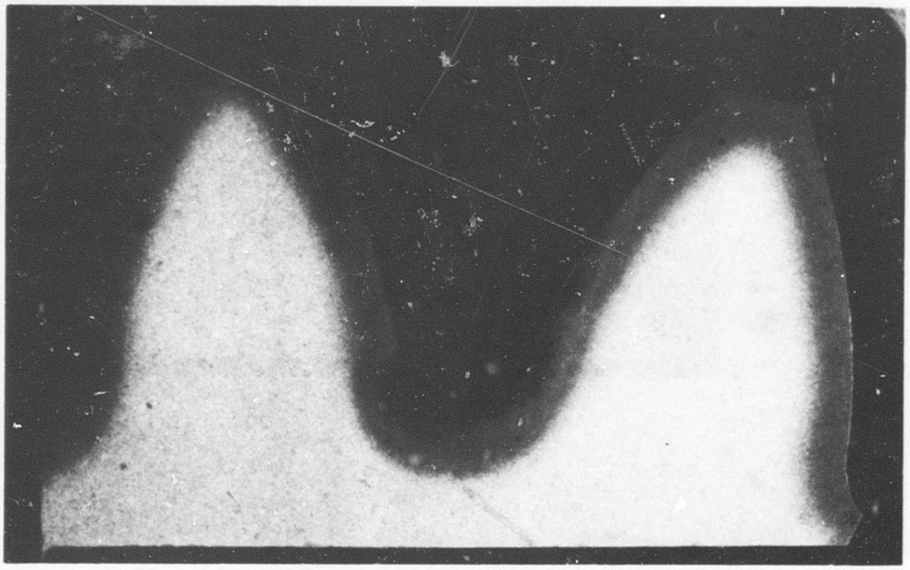

Magnification: 6X EX-78784, Serial Number CX 9069

Figure 59. Photograph of Section Through Test Gear Showing Carburized Case Depth Around Root Fillet Contour.

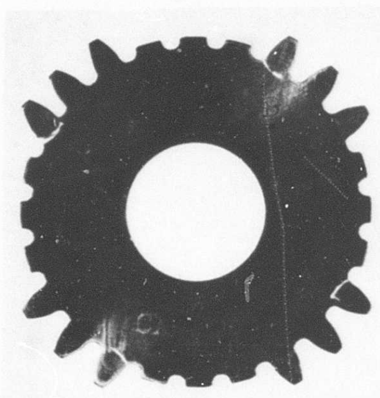

Magnification: 1X
EX-78775, Serial Number CX 9077

Figure 60. Blacklight Photograph of Test Gear Showing Cracks Indicated by Fluorescent Penetrant Inspection in Root Radii of Tested Teeth.

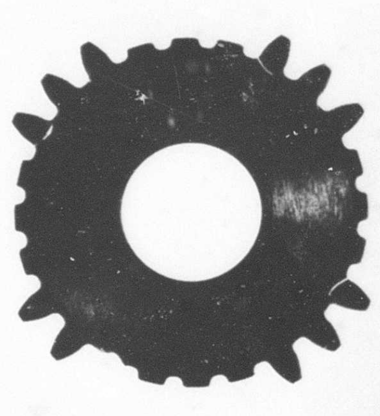

Magnification: 1X
EX-78775, Serial Number CX 9100

Figure 61. Blacklight Photograph of Test Gear Showing Cracks Indicated by Fluorescent Penetrant Inspection in Root Radii of Failed Teeth.

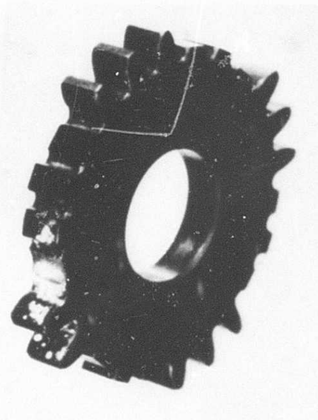

Magnification: 1X
EX-78777, Serial Number CX 9059

Figure 62. Blacklight Photograph of Test Gear Showing Cracks Indicated by Fluorescent Penetrant Inspection in Center Root Radius Adjacent to Failed Tooth.

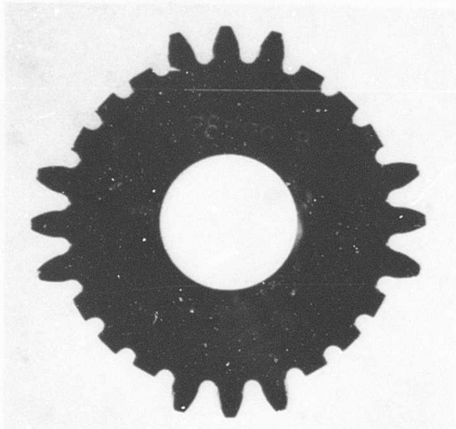

Magnification: 1X
EX-78779, Serial Number CX 9104

Figure 63. Blacklight Photograph of Test Gear Showing Cracks Indicated by Fluorescent Penetrant Inspection in Root Radii of Failed Teeth.

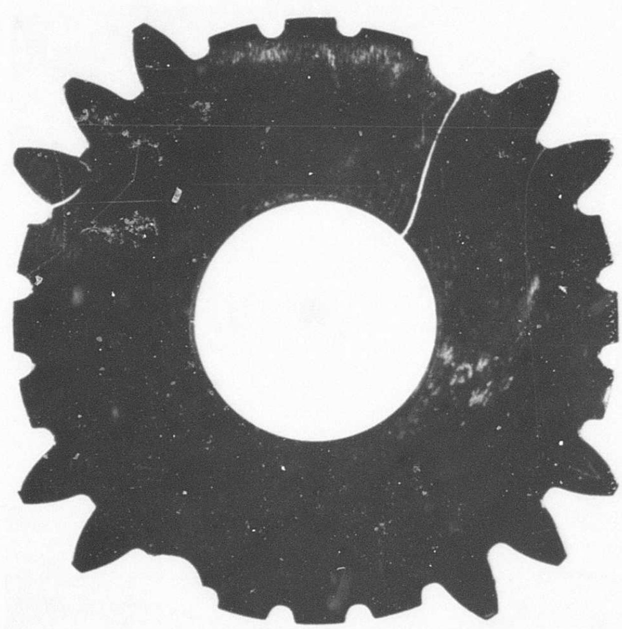

Magnification: 1X
EX-78782,
Serial Number CX 9113

Figure 64. Blacklight Photograph of Test Gear Showing Radial Crack and Failed Teeth.

Magnification: 1X
EX-78784,
Serial Number CX 9069

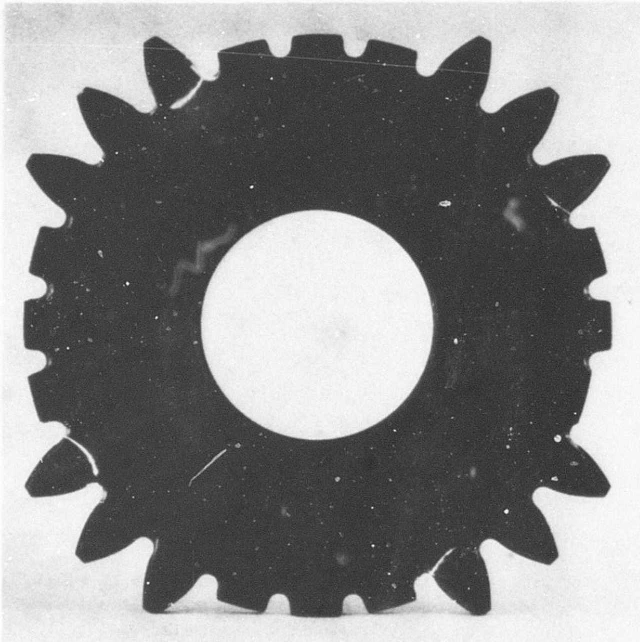

Figure 65. Blacklight Photograph of Test Gear Showing Cracks Indicated by Fluorescent Penetrant Inspection in Root Radii of Teeth 1, 2, 3, and 4.

Magnification: 9X
EX-78773, Serial Number CX 9077

Figure 66. Photomicrograph of Surface of Failure of Tooth From Test Gear.

Magnification: 9×
EX-78775, Serial Number CX 9100

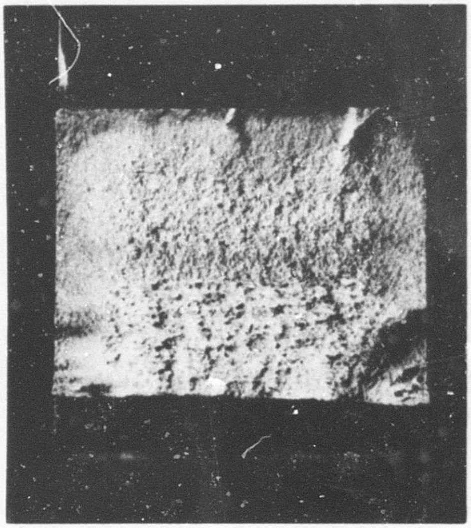

Figure 67. Photomicrograph of Surface of Failure of Failed Tooth From Test Gear Showing Flat Failure in Root Radii of Teeth.

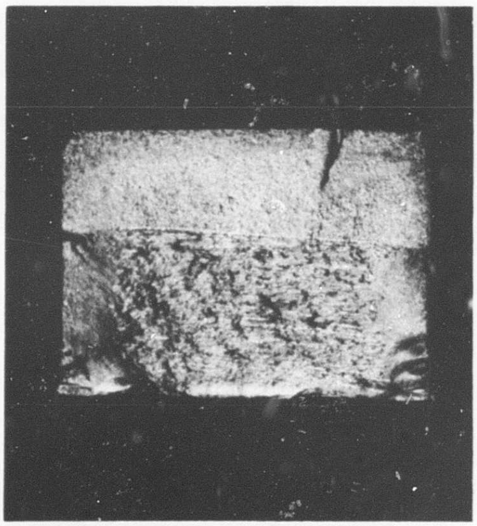

Magnification: 9×
EX-78779, Serial Number CX 9104

Figure 68. Photomicrograph of Surface of Failure of Tooth From Test Gear.

Magnification: 9X EX-78782, Serial Number CX 9113

Figure 69. Photomicrograph of Surface of Failure of Tooth 1 of Test Gear Showing Multiple Origins of Failure in Root of Loaded Involute – No Typical Arrest Lines of Fatigue Progression.

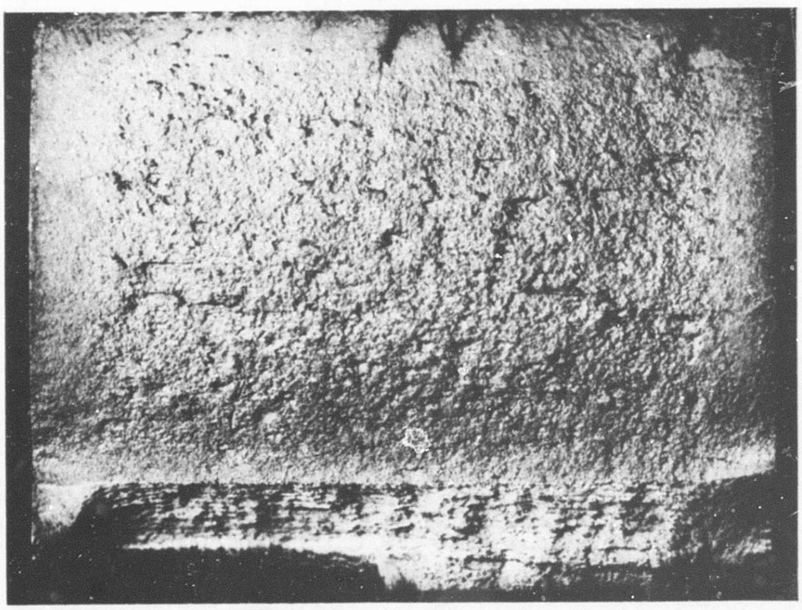

Magnification: 9X EX-78782, Serial Number CX9113

Figure 70. Photomicrograph of Surface of Failure of Tooth 3 of Test Gear Showing Multiple Origins of Failure and No Distinct Arrest Lines Typical of Fatigue Progression.

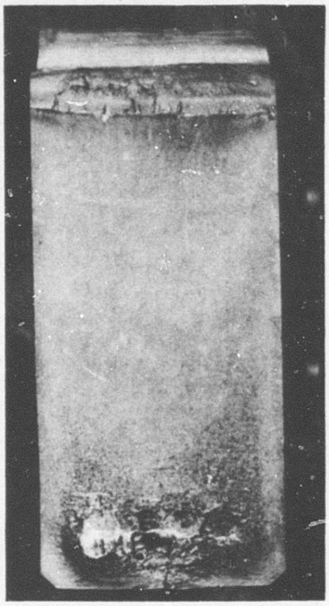

Magnification: 5X
EX-78782
Serial Number CX 9113

Figure 71. Photomicrograph of Radial Surface of Failure of Test Gear Showing Marks of Fatigue Progression From Below the Root to the Hub.

TABLE XII
RECORD OF HARDNESS GRADIENT TESTS OF TEST GEARS

Depth Below Carburized Surface (inch)	R_c Readings					
	EX-78773 CX 9077	EX-78775 CX 9100	EX-78777 CX 9059	EX-78779 CX 9104	EX-78782 CX 9113	EX-78784 CX 9069
0.002	61	62	61	62	61	61
0.005	61	61	60	61	61	61
0.010	60	60	58	59	60	62
0.015	56	58	57	55	57	62
0.020	55	58	57	54	57	57
0.025	55	54	55	54	55	57
0.030	51*	51*	53	55	53	56
0.035	46	46	51	55	51	56
0.040	42	46	51*	53*	48*	55
0.045	40	44	47	47	46	52
0.050	42	45	46	48	46	52*
0.055	42	43	45	46	44	48
0.060	41	43	45	45	43	45
0.065	41	41	42	44	44	46
0.070	41	41	42	43	43	45
0.075	—	—	—	42	42	45
0.080	—	—	—	—	42	45
0.085	—	—	—	—	—	43
0.090	—	—	—	—	—	43

* Approximate effective case depth.
All hardness readings were taken at the root radii adjacent to the failure surface.

R. R. MOORE TESTS

R. R. Moore test specimens were manufactured from the same heat of material as the **test gears. Manufacturing followed** heat treating and grinding routings used for the **gears as closely as feasible. The** process routing for the specimens is presented in **Table XIII. The test results are given** in Table XIV.

TABLE XIII
SPECIMEN PROCESS ROUTING PROCEDURE

1. Carburize and anneal per EPS* 202 to an effective case depth of 0.035 inch as determined by the fracture specimen.
2. Harden and temper per EPS 202 and PCI** 8000 and stabilize per EPS 202.

   Core Hardness—R_c 40
   Case Hardness—$R_{15/N}$ 90 (R_c 60)

3. Grit blast with 80-grit shot.
4. Remove 0.010 to 0.016 inch from outside diameter by grinding.
5. Stress relieve per EPS 202 and PCI 8000.
6. Nital etch per EIS† 1510.
7. Shot peen per EPS 12140 followed by EPS 12176.
8. Stress relieve per EPS 202 and PCI 8000.
9. Coat with black oxide per AMS-2485.

* Allison Engineering Processing Specification.
** Allison Process Control Instruction.
† Allison Engineering Inspection Specification.

EXPERIMENTAL INVESTIGATIONS

In this phase of the program, photostress and strain gage measurements were used to investigate the location and magnitude of the maximum bending stress.

By cementing a sheet of special plastic* to the gear face (actual fatigue test gear) and trimming to the contour of the test tooth, it was possible to obtain indications of stress distribution, stress values along the tooth contour, and maximum stress locations. A large field reflection polariscope (LF/Z meter) and a telemicroscope were used to study in some detail the point of high stress.

To complement the photostress analysis, strain gages were installed in the root of the gear tooth at the theoretical point of maximum stress as shown in Figure 72. The gear was mounted to the fatigue test rig and loaded by means of the bias spring.

The protuberance hobbed gear, part number EX-78776 (with a 20-degree pressure angle and a minimum fillet radius), was selected for stress analysis.

The plastic sheet manufacturer supplied the calibration of the optical strain constant of 1080 microinches per inch per fringe or tint-of-passage (sharp line between red and blue).

---

*Special birefringent material, plastic sheet type S, 0.120 inch thick, Model Number X-10062, Instruments Division of The Budd Company, Phoenixville, Pennsylvania

TABLE XIV
R. R. MOORE TEST RESULTS

Specimen Number	Stress (p.s.i.)	Test Cycles* ($\times 10^3$)	Surface Finish (microinches)	Failure Origin	Failure Location
18	130,000	106,584	23 to 27	Terminated	—
17	135,000	105,951	25 to 28	Terminated	—
2	140,000	101,234	30 to 35	Terminated	—
6	140,000	102,384	25 to 30	Terminated	—
15	140,000	111,435	20 to 25	Terminated	—
14	150,000	74	25 to 30	Surface	Off center ***
1	150,000	138	32 to 37	Surface	Slightly off center †
4	150,000	50,683	30 to 35	Subsurface **	Center ‡
13	150,000	90,852	28 to 32	Surface	Slightly off center
11	150,000	103,034	8 to 13	Terminated	—
10	160,000	44	25 to 28	Surface	Center
7	160,000	134	12 to 20	Surface	Off center
5	160,000	3,317	25 to 30	Surface	Center
3	160,000	6,061	30 to 35	Surface	Center
16	170,000	74	25 to 30	Surface	Slightly off center
9	170,000	114	20 to 25	Surface	Center
8	170,000	187	10 to 15	Surface	Center
12	170,000	228	28 to 32	Surface	Center

* Arithmetic average.
** Within effective case.
‡ Center is midpoint of specimen.
† Slightly off center is 1/16 to 1/4 inch from midpoint.
*** Off center is 1/4 to 1/2 inch from midpoint.

The photostress gear was statically loaded in 1000-pound increments. Readings were taken at each 1000-pound step, and photographs were taken at zero and 4000 pounds. This load limit was chosen as the stopping point because the concentration of strain was so confined and was beyond the reading capacity of the LF/Z meter.

The greatest stress concentration, as measured by the LF/Z meter, occurred at the calculated point for the placement of the strain gages. The strain rate was 1080 microinches per inch (32,400 p.s.i.) per 1000 pounds of load by photostress and 1140 microinches per inch (34,200 p.s.i.) by strain gage. Figure 73 illustrates the stress distribution for the 4000-pound load point. Since monochromatic light was not used, both isoclinic lines (lines of stress direction) and tints-of-passage are seen as the darker lines and cannot be defined without the aid of the color photographs.

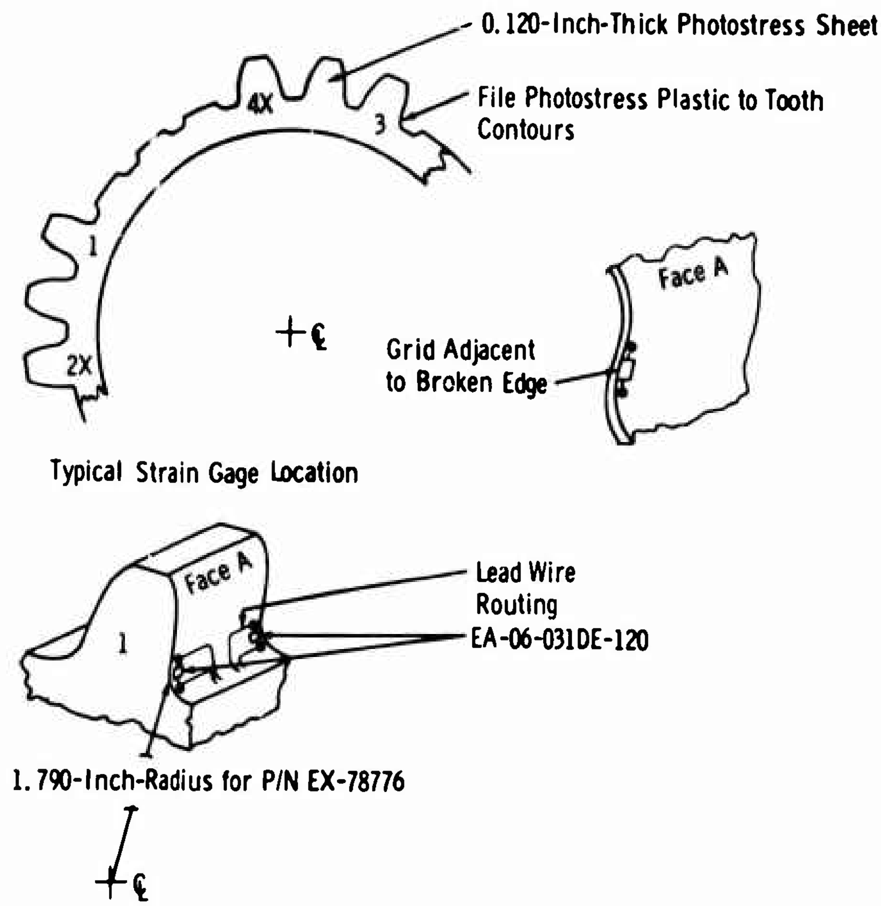

Figure 72. Schematic of Instrumentation on Photostress Gear.

To permit comparison of calculated stresses with actual measured stresses, one tooth from each of the eight 4-inch-pitch-diameter gears was instrumented with strain gages. Static strain versus load at the high point of single tooth contact was obtained. Each gear was instrumented with strain gages as shown in Figure 74. The radial location of the gages was at the expected crack point based on crack measurements from the gears (diametral pitch = 12) that were available at the time.

The gears were tested on the fatigue test rig using the same procedure for installation as used for fatigue and photostress tests. The results of the data are shown in Figures 75 and 76. The gages were located on the tension side except for one on the compression side of one gear.

DYNAMIC TESTS

The effect of speed on bending stress can be categorized as follows.

- Centrifugal stress, a steady-state stress at any particular speed caused by internal forces. As noted in Figure 77, this effect consists of tensile stresses in the tooth and hoop stresses in the gear rim.
- Dynamic stress, a cyclic stress with a constant peak magnitude at any particular speed caused by tooth load, imperfect tooth meshing, load sharing, and other geometrical and manufacturing properties of the gear. It is cyclic since it occurs only when the tooth is under load, e.g., in mesh with a mating gear. This is shown graphically in Figure 78.

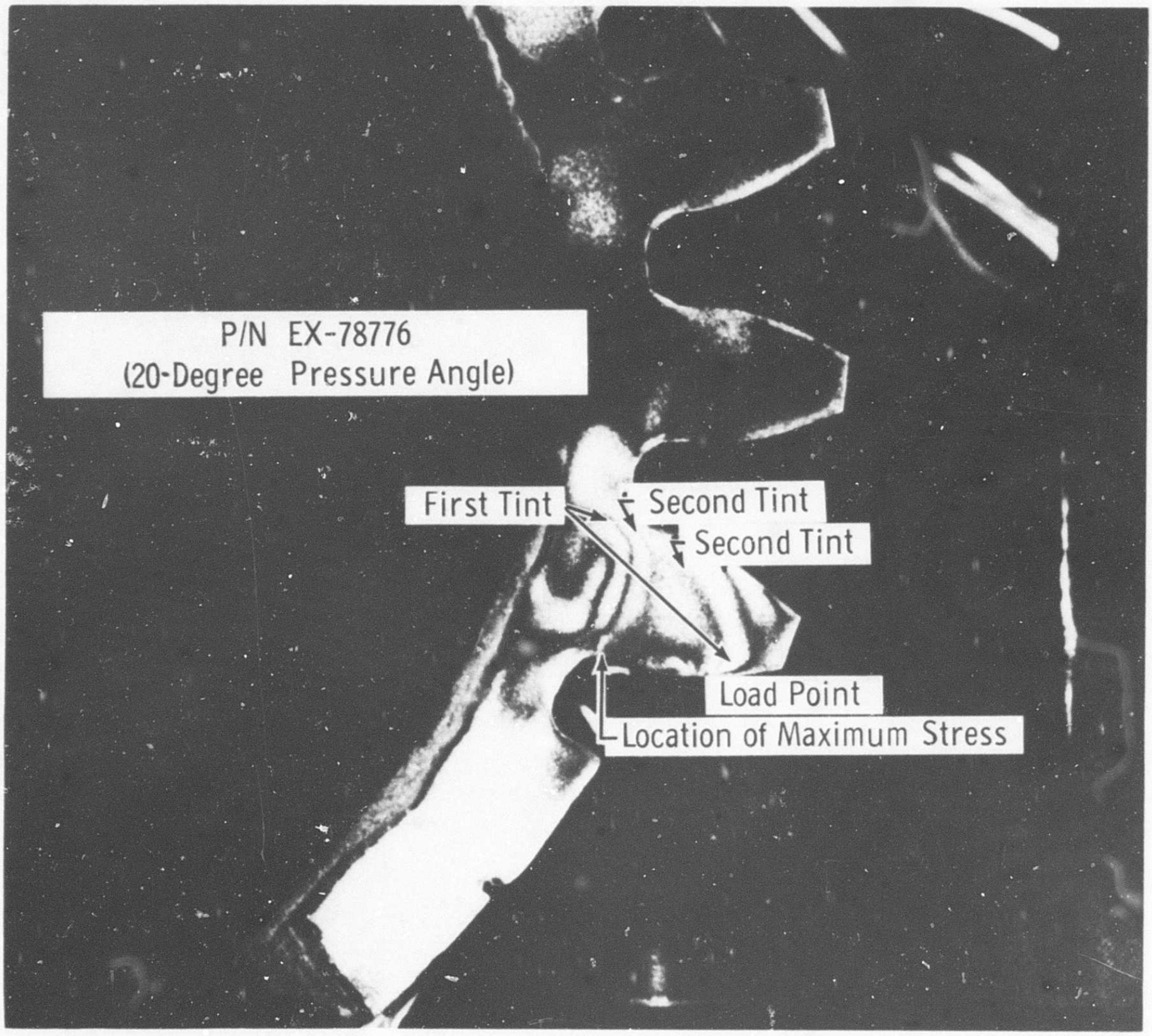

Figure 73. Gear Tooth Showing Photostress Pattern at 4000-Pound Load.

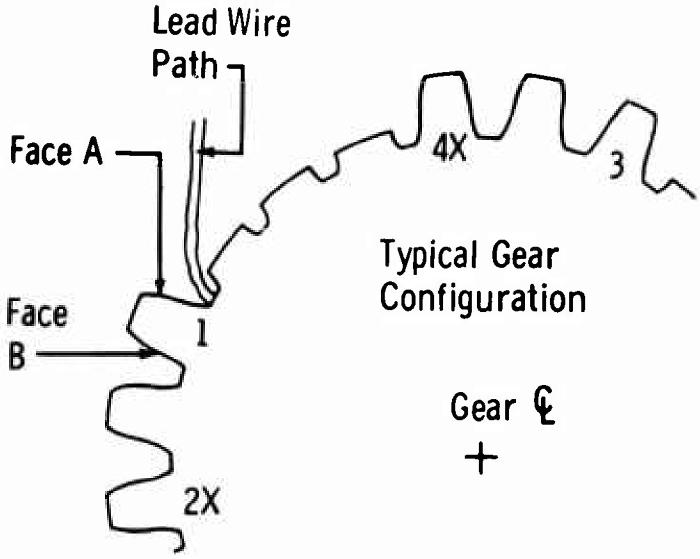

Strain Gage Mounting Procedure

1. Vapor blast to remove black oxide.
2. Wipe with W. T. Bean neutralizer.
3. Attach strain gage with Eastman No. 910 contact cement.
4. Protect gage with Dow Corning silicon wax fluid F145.
5. Attach 4-foot-long lead wires.

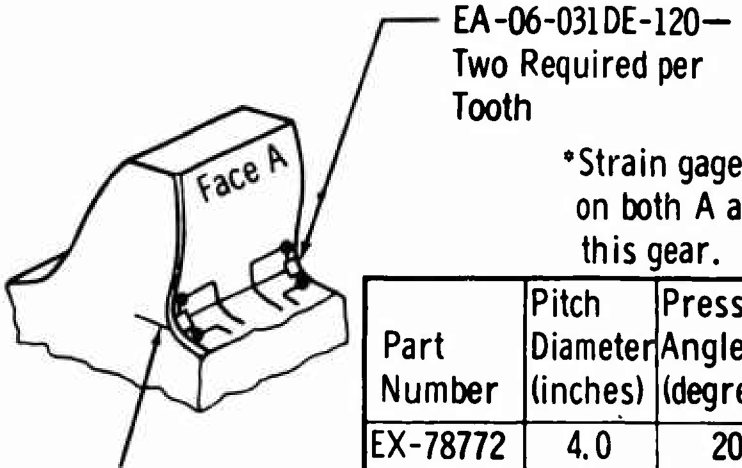

Lay out scribe marks as shown on both sides. Then draw line between scribe marks. Locate strain gage grid on scribe line adjacent to edge break on face A.

*Strain gages to be installed on both A and B faces on this gear.

Part Number	Pitch Diameter (inches)	Pressure Angle (degrees)	Serial Number	Tooth Number	Radius, R
EX-78772	4.0	20	CX9090	4	1.7959
EX-78774	4.0	20	CX9066	1	1.8023
EX-78776	4.0	20	CX9007	2	1.7713
EX-78778	4.0	20	CX9056	3	1.7781
EX-78780*	4.0	25	CX9096	4	1.7804
EX-78782	4.0	25	CX9111	4	1.8058
EX-78784	4.0	25	CX9071	4	1.7741
EX-78786	4.0	25	CX9012	1	1.7751

Figure 74. Schematic of Strain Gage Instrumentation for 4-Inch-Pitch-Diameter Gear.

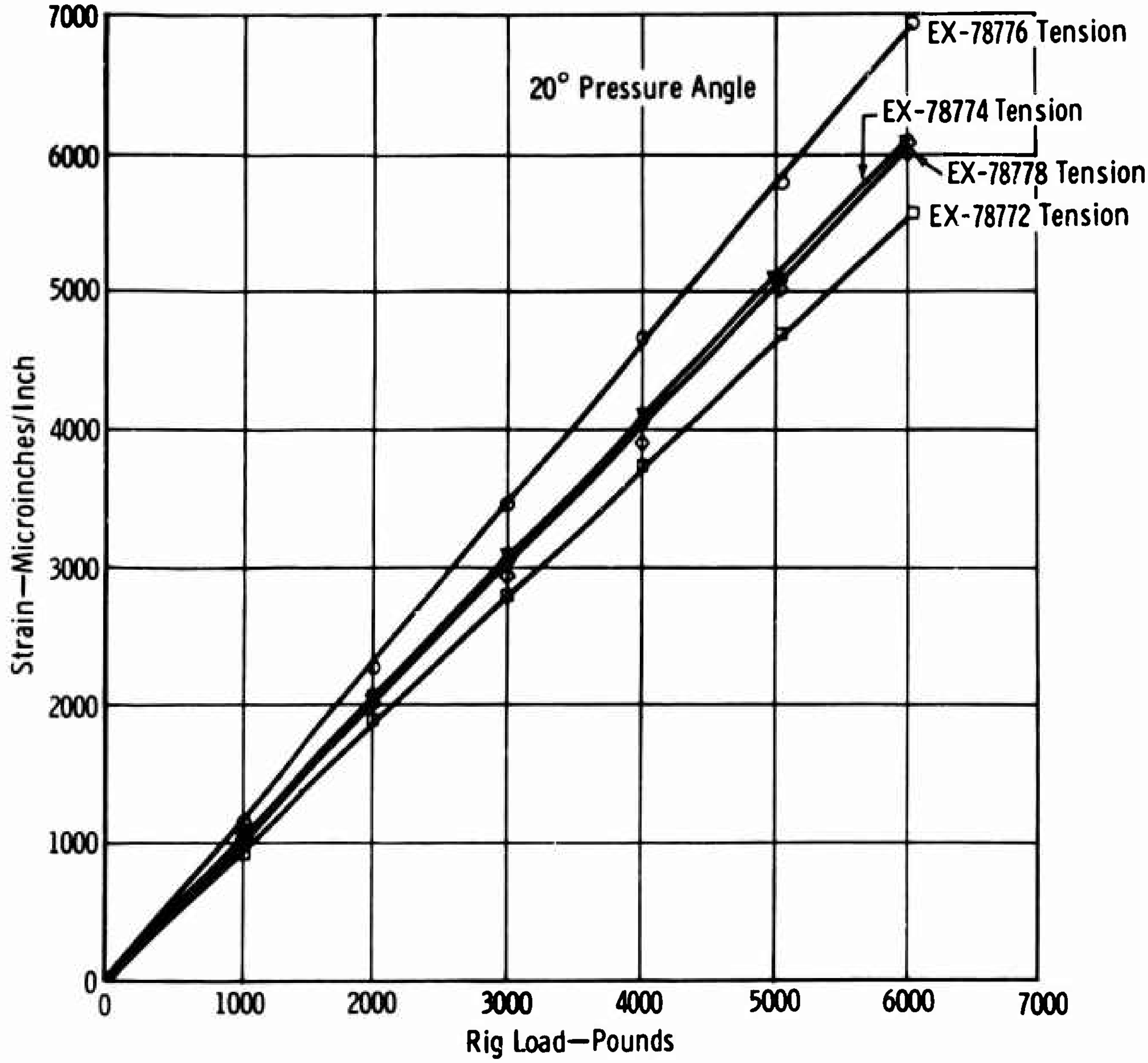

Figure 75. Calibration Curve for Gear Test Rig – 20-Degree Pressure Angle.

As shown in Figure 78, doubling the speed not only increases the frequency of the dynamic stress, but also raises the centrifugal stress level and the amplitude of the dynamic stress.

To better understand the effects of speed on gear tooth bending stress, a gear was instrumented and strain data were recorded during actual running conditions. Data were recorded to 26,500 feet per minute pitch-line velocity. The gear tested was the propeller brake outer member (part number 6829395) in a 501-D13 turboprop engine gearbox. The instrumentation consisted of strain gages located on the tooth as shown in Figure 79. One tooth had gages located on the tension side and another tooth, 180 degrees, had gages on the compression side. Two gages were located in the root and two at the point of expected maximum stress in the root fillet.

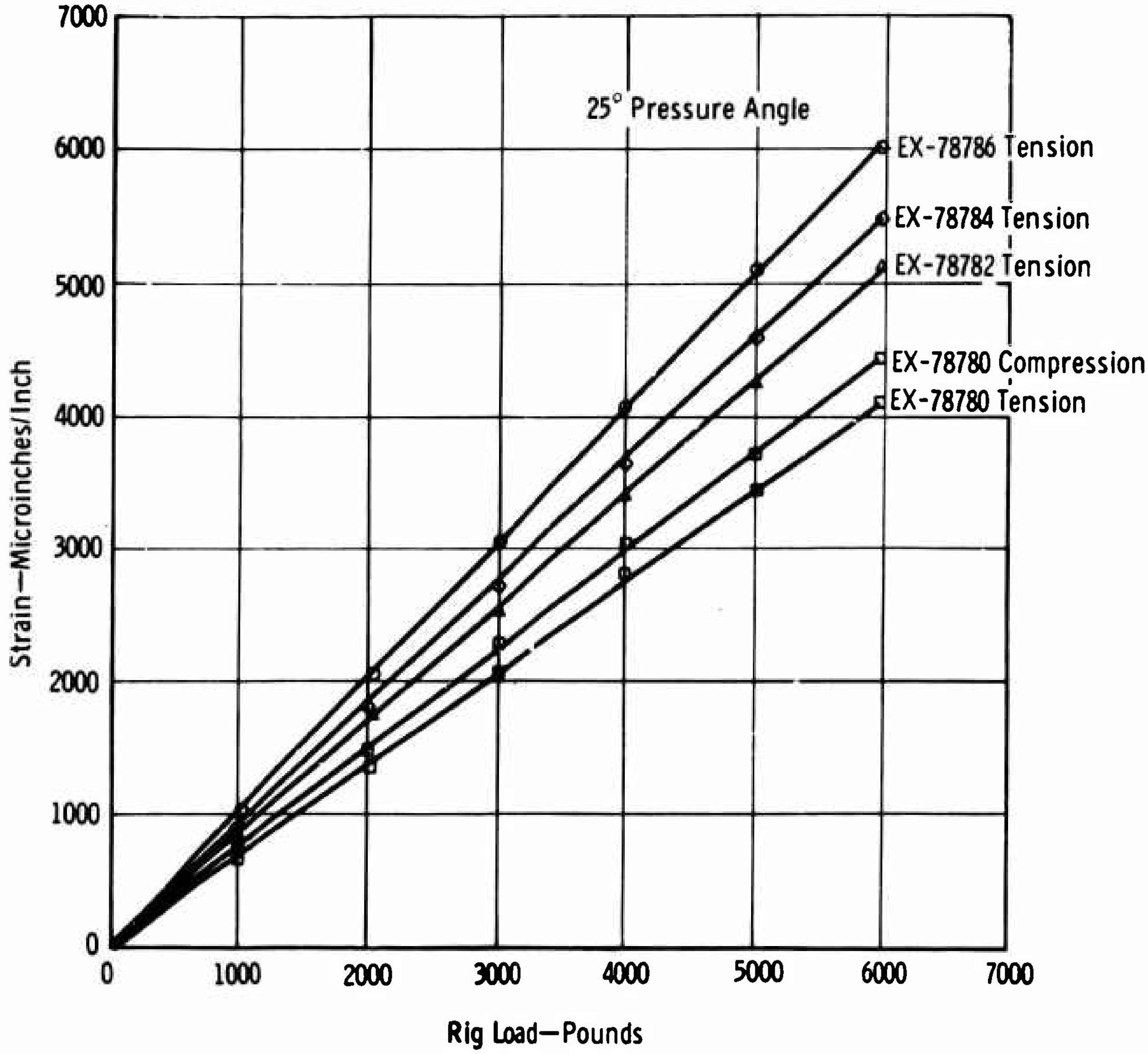

Figure 76. Calibration Curve for Gear Test Rig— 25-Degree Pressure Angle.

By means of electronic test data recording, the centrifugal stress and the dynamic stress were separated. This was possible since centrifugal stress is a steady-state stress and dynamic stress is a cyclic stress. The centrifugal stress was obtained by taking strain gage readings under zero-load conditions at various speeds. The dynamic stress was taken under loaded conditions and was the peak strain reading above the centrifugal base line.

The gear train used is shown schematically in Figure 80. The power input was through the main accessory drive gear which mated with the test gear. The load was applied by means of a water brake attached to the alternator drive. To calibrate the strain gages, torque was applied in a static condition. The instrumented tooth was rolled through the highest load point for maximum stress calibration. This setup is shown in Figure 81. The test gear and mating gear meet AGMA class 10 to 12 tolerances. The gear geometry and tolerances are shown in Figure 82.

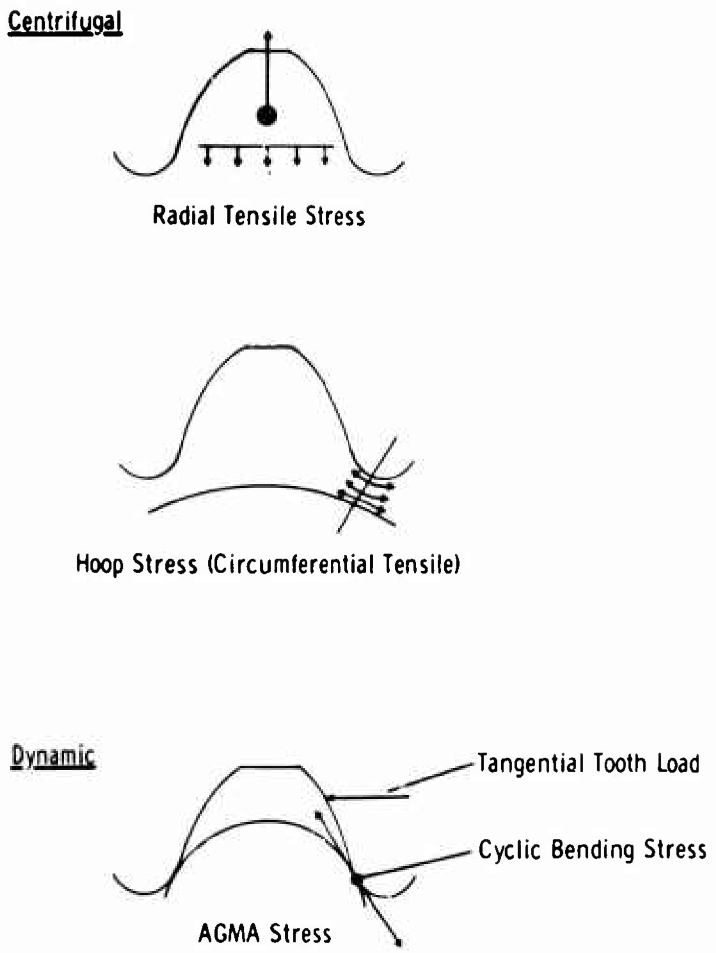

Figure 77. Gear Tooth Bending Stress Schematic.

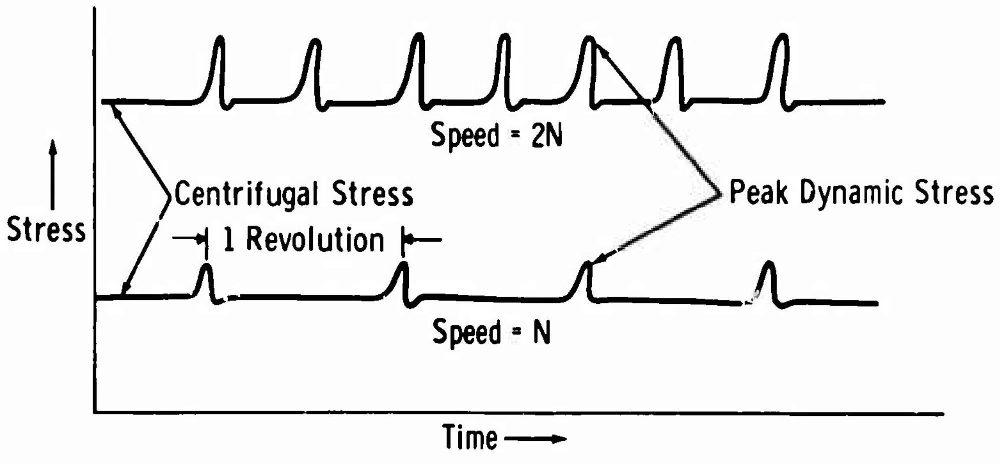

Figure 78. Diagram Showing Effect of Speed on Gear Tooth Stresses.

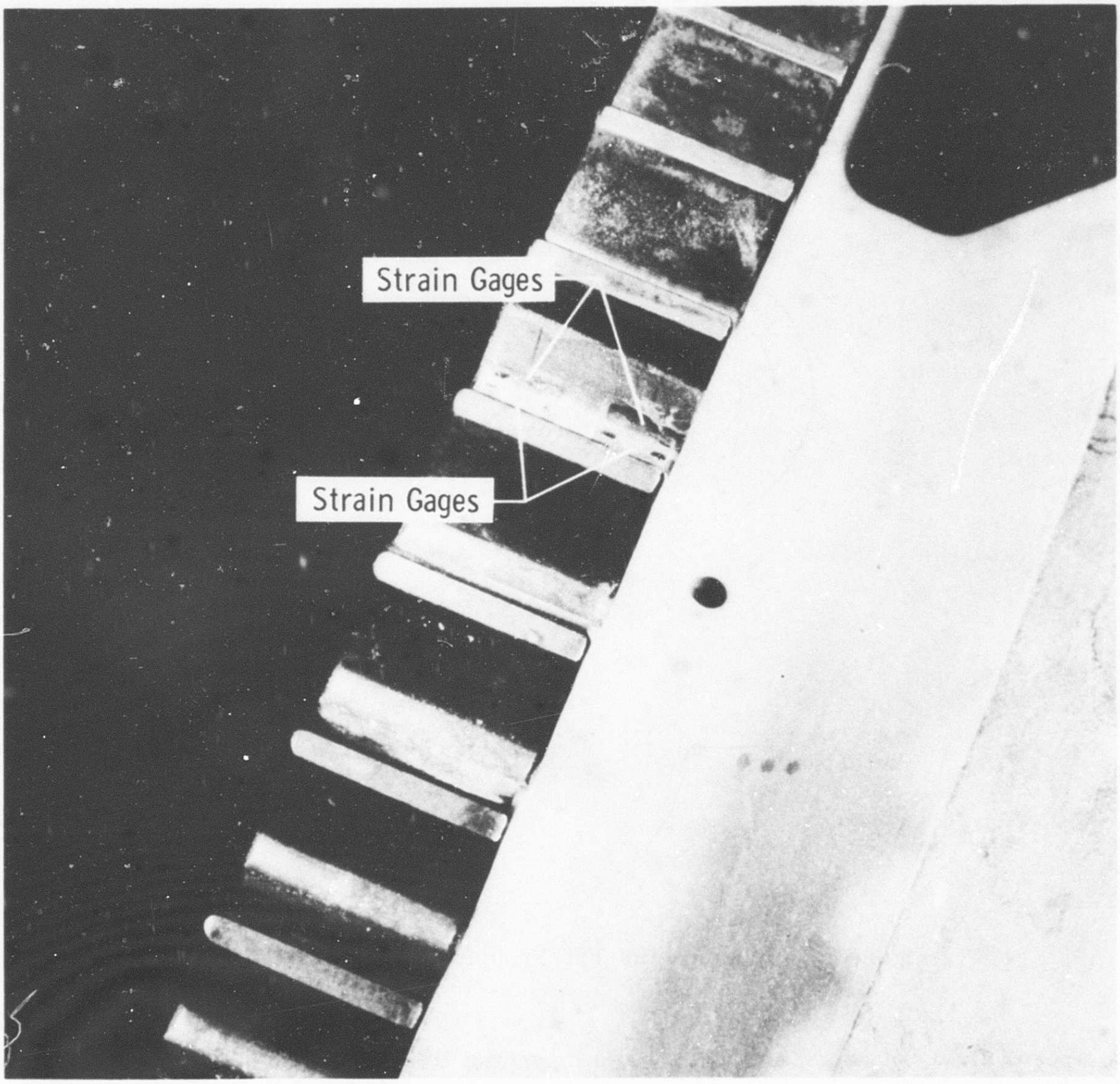

Figure 79. Dynamic Test Gear Strain Gage Instrumentation.

To isolate the stresses due to speed effects in the tooth root, the instrumented gear was first tested at zero load in the reduction gearbox. Using a three-wire strain gage hookup and allowing gearbox oil temperatures to stabilize, strain due to centrifugal loads was recorded. Testing was conducted at essentially zero tangential loads for speeds varying from 10,000 to 15,000 r.p.m. Figure 83 shows the centrifugal strain (tension) on the gear tooth.

The gear was then loaded by means of a water brake to obtain stress versus speed data. The strain gage instrumentation was routed through a slip-ring assembly, and the gage signal was recorded by a 16-channel Miller oscilloscope recorder. The gear was tested

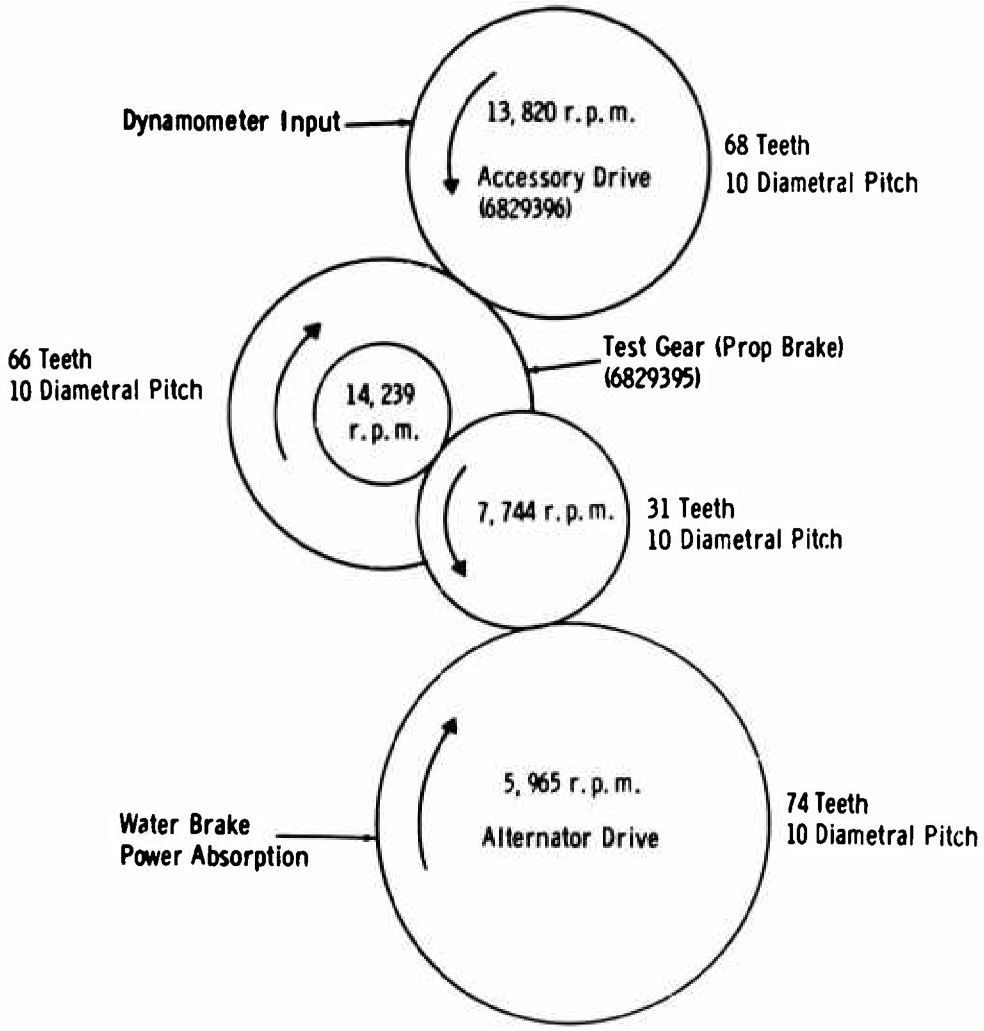

Figure 80. Schematic of T56 Propeller Brake Gear Train.

at speeds of 10, 000 to 15, 530 r. p. m. and tangential loads of 350 to 950 pounds. Figure 84 shows data from four strain gages. The data shown represent the average strain range at the speed at which the gear was tested. Of the eight gages installed, only these four survived the testing schedule.

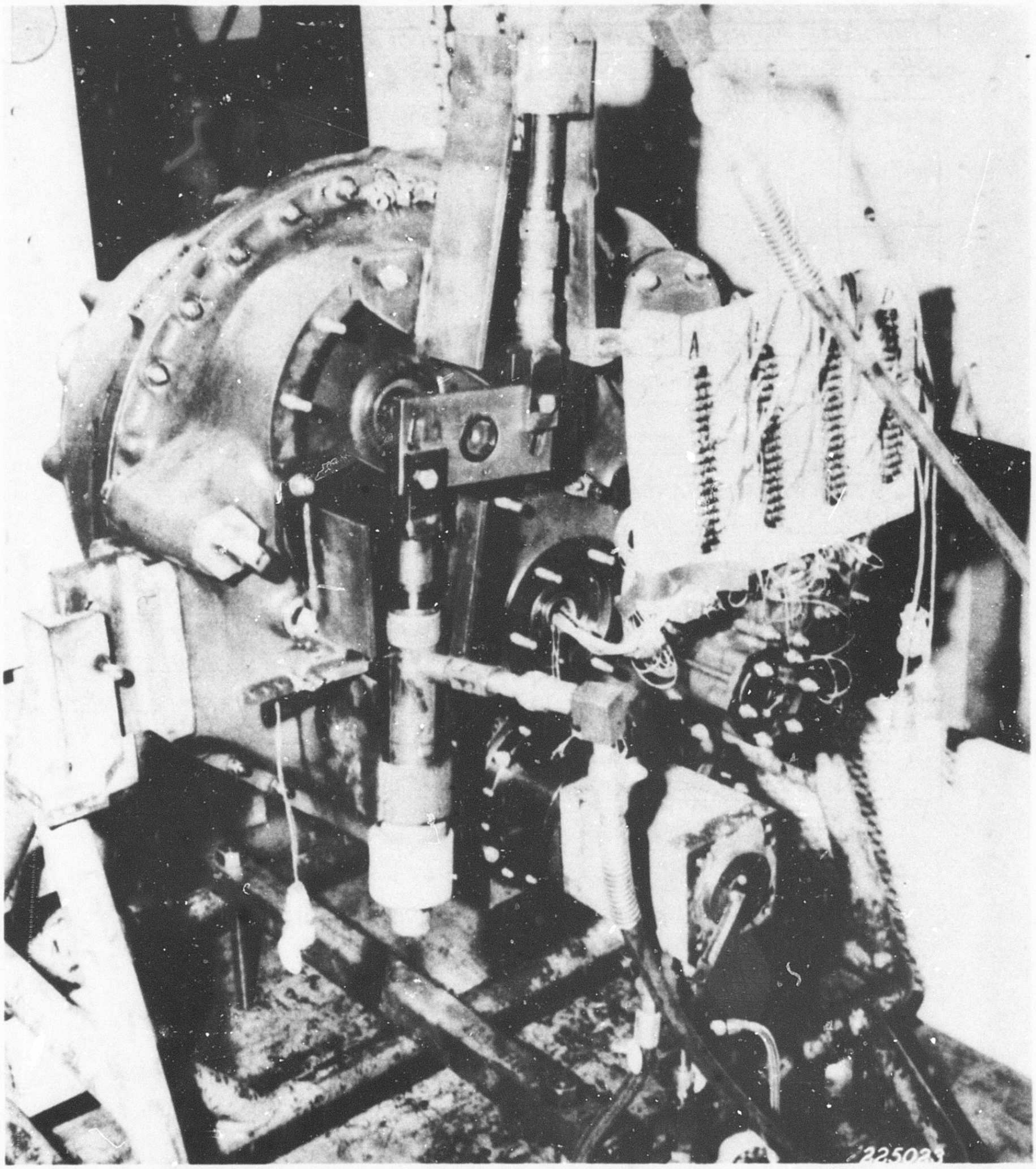

Figure 81. T56 Gearbox Used for Dynamic Gear Test.

Propeller Brake Outer Gear 6829395
(dynamic test gear)

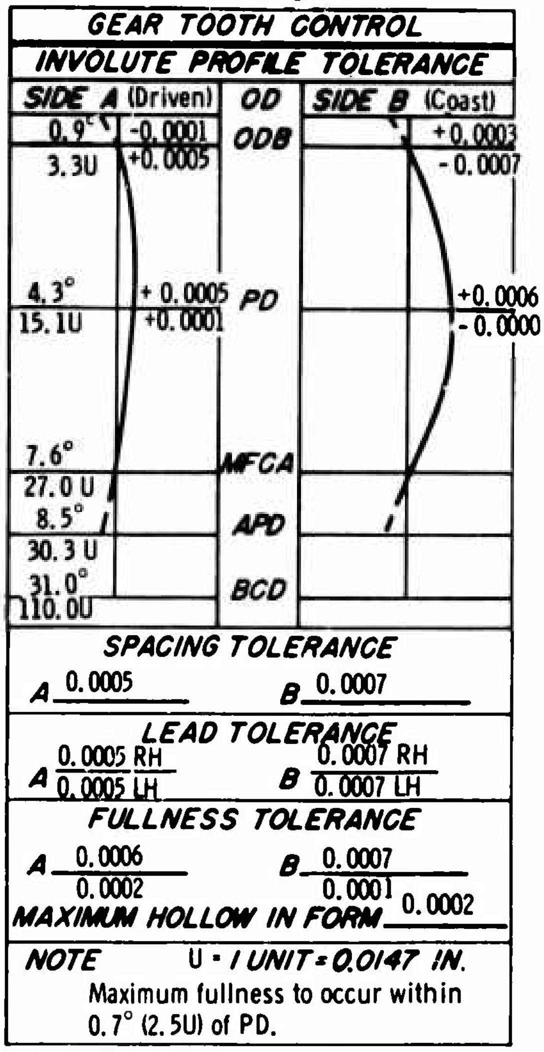

10 pitch
66 teeth
25° Pressure Angle

Distance over two 0.1728-dia pins

6.8370 $^{+0.0000}_{-0.0041}$

PD run-out, 0.002

Face width, 0.375
Arc tooth thickness at PD

0.1541 $^{+0.0000}_{-0.0020}$

Base circle diameter—5.9816

Accessory Drive Gear 6829396 (drivin_ _ ar)

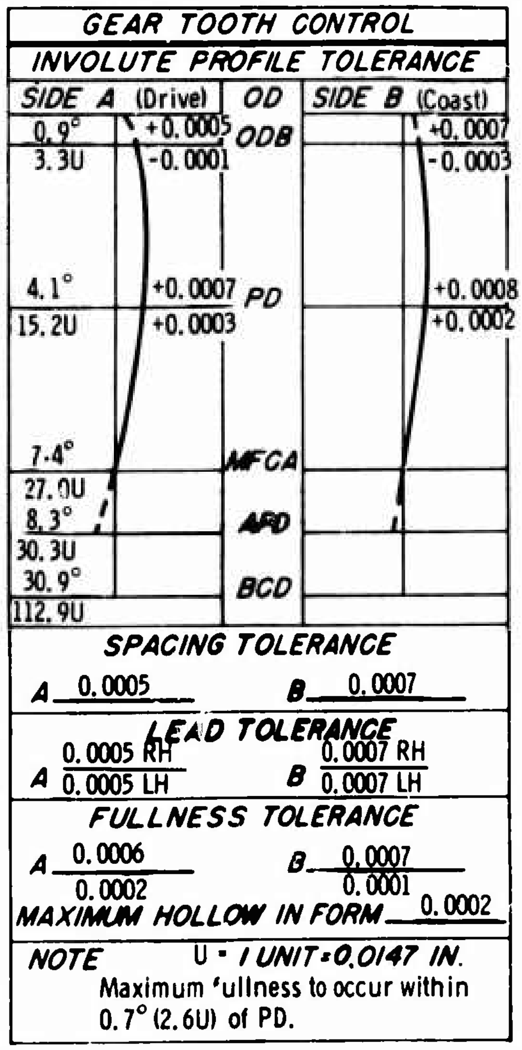

10 pitch
68 teeth
25° Pressure Angle

Distance over two 0.1728-dia pins

7.0370 $^{+0.0000}_{-0.0041}$

PD run-out, 0.002

Face width, 0.628
Arc tooth thickness at PD

0.1541 $^{+0.0000}_{-0.0020}$

Base circle diameter—6.1629

0.006 to 0.010 backlash with mating gear on STD centers

Figure 82. Dynamic Test Gear and Driving Gear Geometry and Tolerances.

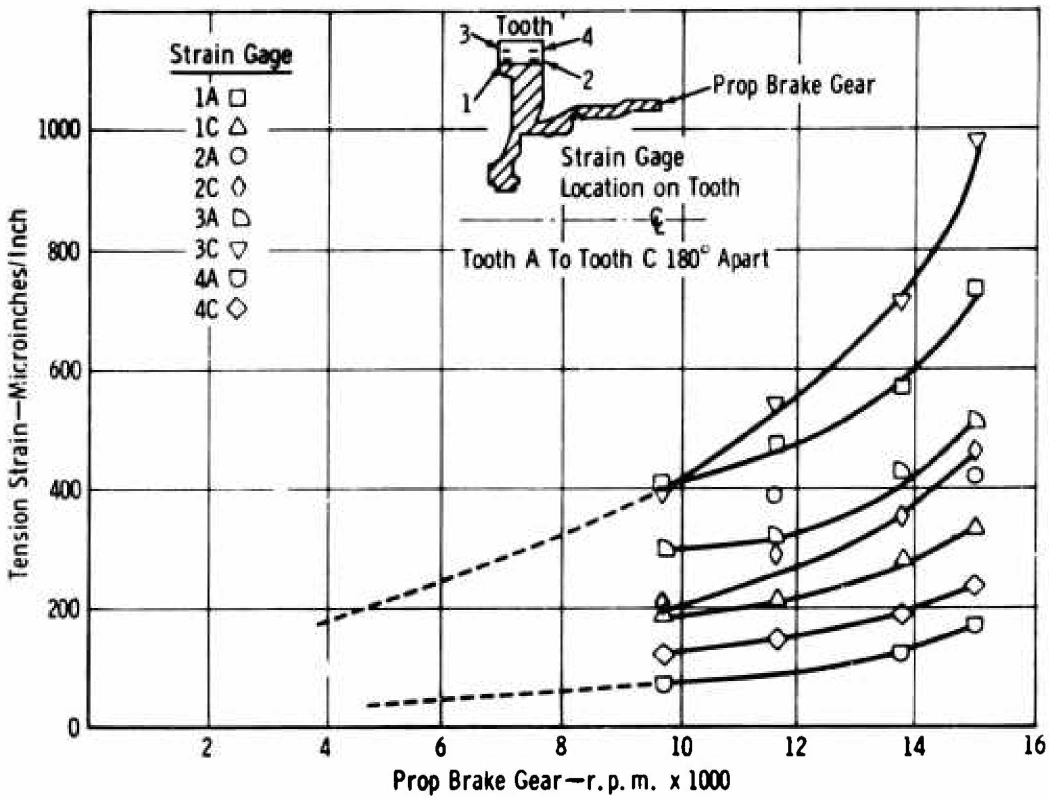

Figure 83. Effect of Speed on Gear Tooth at No-Load Condition.

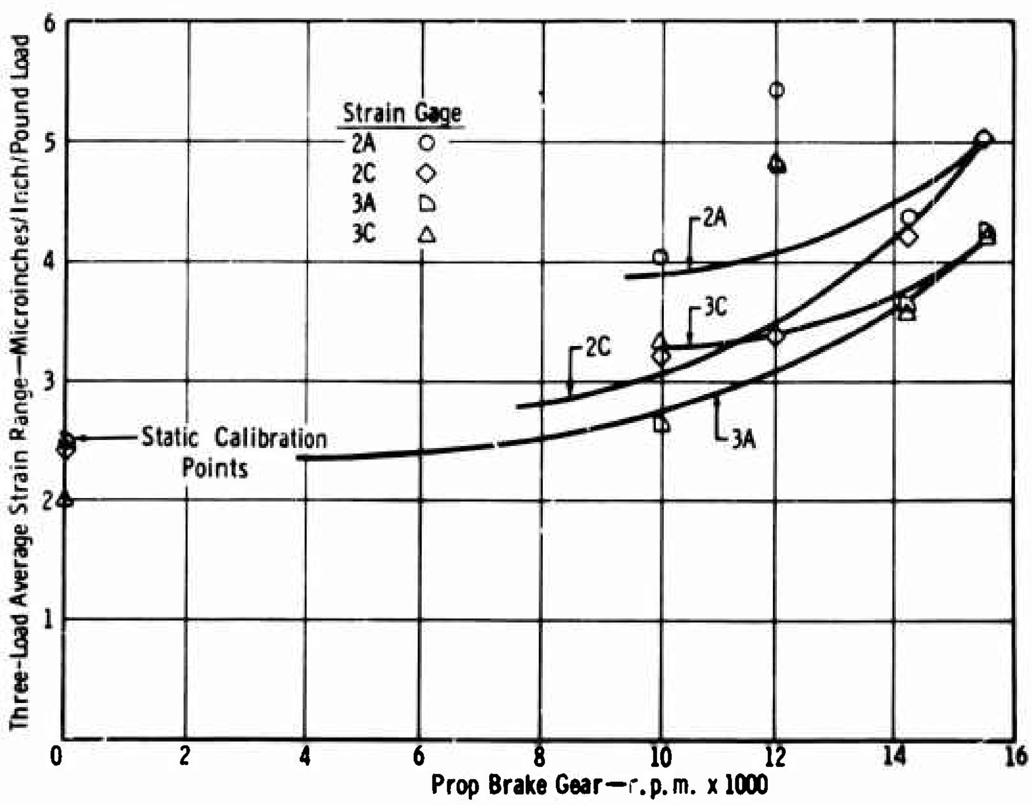

Figure 84. Effect of Speed on Loaded Gear Tooth.

BLANK PAGE

DISCUSSION OF RESULTS

EVALUATION PROCEDURE

The test results were evaluated by the following steps:

1. Determine predictive ability of the five calculation methods.
2. Compare strain gage and photostress data with calculated stress.
3. Determine significance of geometric variables based on most predictive calculation methods.
4. Determine basic material strength and design value.
5. Compare test data and design value to the literature.
6. Analyze centrifugal and dynamic load effects.
7. Establish computer program.

PREDICTIVE ABILITY OF CALCULATION METHODS

The predictive ability of the five methods studied for calculating bending stress was evaluated by use of the mean endurance limits fitted through the fatigue test gear data points. Proportionality factors were used to convert the unit load endurance limits for each gear configuration to endurance limit values based on each of the stress calculation methods. These endurance limit values are listed in Table XV and are ranked in descending order. Average, range, and variation in endurance strength for each calculation method are also given. The AGMA method produced the smallest variation which is considered to be one of the best criteria for evaluation of the various calculation methods. Also, the test rig (applied load) ranked all the larger (6-diametral-pitch) gears first as would be expected. However, the Heywood and Kelley-Pedersen method also ranked all but one of the large gears first, indicating that these calculation methods may not adequately compensate for changes in diametral pitch.

Further analyses were made by comparing the rank given to each test gear configuration by each calculation method with the test rig load endurance limit ranking. Since a high stress should result in a low life, the calculated stress rankings were inverted. The results of this comparison are given in Table XVI. The AGMA formula predicted the greatest number of correct rank positions (6 out of 16) and also had the best average prediction accuracy (within 1.25 rank positions).

The endurance limit for fatigue test gear configuration number 3 appears to be abnormally low. See Table XV. It was therefore deleted from critical calculations (range and variation) but not from averages. This configuration (part number EX-78774) did have dimensional discrepancies (0.070-inch root fillet radius instead of 0.080-inch minimum print requirement). This should have lowered the life to approach that of configuration number 1, which is the same except for 0.050-inch minimum root fillet radius. The life was actually only two-thirds of that of configuration number 1. The test data had very low fatigue life scatter, which may be indicative of a severe stress concentration. Since the low endurance life was not determined until late in the program, no metallurgical investigations of this gear were accomplished.

Continued analysis of the fatigue test results based on individual measured physical dimensions rather than part number drawing dimensions could appreciably increase the confidence level of the results. The test results of one gear have been corrected to a 10-percent lower stress level to adjust for a 0.010-inch oversize root diameter. Thus, correction of all data to compensate for individual sizes within the ± 0.002-inch root diameter drawing tolerance would adjust relative calculated stresses by approximately 4 percent. Similar changes could be made for individually measured tooth thicknesses and fillet radii. The protuberant hobbed configurations could be revised, based on measured hob dimensions.

To accomplish the individual analysis described for each fatigue test tooth would require conversion of the present computer program to permit operation on the smaller IBM 1130 rather than on the IBM 7094. The program would also require revision to eliminate unnecessary output and thus would avoid overloading the smaller computer. Also, the input would have to be modified to use the measured dimensions directly. Table XVII lists the critical root diameter, root fillet radius, and over-pin dimensions for each gear.

Each fatigue test gear tooth was examined to determine and record the edge break condition in the failure region. See Table XVII. These edge breaks were not as consistent as desired due to the difficulty of controlling a hand operation. Direct comparison of edge break and fatigue life failed to indicate any general influence of edge break on the test results.

STRAIN GAGE DATA

Evaluation of the static strain gage measurements confirmed the validity of the AGMA method of calculating bending strength. Table XVIII shows the measured strain gage data in terms of strain rate for each configuration tested. The remaining columns show a comparison of the various methods of calculating bending strength in terms of strain rate. The percent deviation shows the magnitude of difference between the measured and calculated strain for each configuration. The AGMA method produces a minimum difference for each configuration. The last column shows the stress concentration factor calculated from the difference between the Lewis calculated and the measured data.

To further indicate the degree of correlation, Figure 85 shows stress versus load for the measured data and the AGMA calculation. The percent deviation of the calculated stress from the measured stress is shown in Figure 86. The present AGMA method gave the smallest deviation from the measured stress.

Since none of the formulas considered fillet configuration, the data were split into two groups—full form ground and protuberance hobbed. Although Figure 86 shows that the averages for the two groups differed, statistical "t" tests indicated that these differences could have occurred by chance alone. (See Appendix III for description of "t" tests.) The comparisons were based on four data points in each set. Real differences would have to be very large to be detectable in such small samples. The results were therefore not inconsistent with the analysis of endurance limits which showed that, based on about 200 points, the fillet configuration does produce different endurance limits based on AGMA stresses. Even with this small sample, the results, while not conclusive, have the same sense as the more comprehensive analysis; i.e., protuberance hobbed fillet should produce a higher endurance limit when stresses are calculated with the AGMA formula.

TABLE XV
RANKED ENDURANCE LIMITS FOR VARIOUS STRESS CALCULATION METHODS

Configuration Number	Endurance Load (p. s. i.)	Lewis Configuration Number	Lewis Endurance Limit (p. s. i.)	Heywood Configuration Number	Heywood Endurance Limit (p. s. i.)	Kelley-Peders Configuration Number	Kelley-Peders End Limi
10	96, 429	16	154, 560	5	164, 050	9	162
4	94, 968	6	143, 040	9	162, 182	13	149
11	90, 107	15	138, 530	13	150, 419	5	145
16	88, 149	13	123, 070	15	148, 948	11	143
9	86, 978	10	122, 610	11	148, 539	15	142
15	83, 507	4	122, 250	7	137, 582	1	133
12	80, 647	7	118, 660	1	134, 517	7	113
13	74, 698	5	116, 430	6	107, 429	6	91
6	72, 192	14	116, 360	10	94, 267	10	89
14	65, 807	9	115, 035	4	87, 820	4	88
7	65, 698	11	115, 000	16	82, 852	16	75
2	64, 400	8	110, 210	3	74, 769	12	64
1	61, 901	12	100, 080	2	74, 000	3	74
8	60, 622	1	90, 562	12	70, 617	2	74
5	59, 165	2	88, 754	14	69, 581	14	65
3*	42, 689	3*	58, 292	8	67, 914	8	52
Average	74, 247		114, 590		110, 970		104
Range	59, 165 to 96, 429		90, 562 to 154, 560		67, 914 to 164, 050		52 162
Variation = $\frac{\text{maximum}}{\text{minimum}}$ range = 1. 63			1. 71		2. 42		3.

Note: Configuration number 3 was deleted from range and variation calculation when it was lowest value.

A

Kelley-Pedersen		Dolan-Broghamer		AGMA		Test Rig Load	
Configuration Number	Endurance Limit (p. s. i.)	Configuration Number	Endurance Limit (p. s. i.)	Configuration Number	Endurance Limit (p. s. i.)	Configuration Number	Endurance Limit (p. s. i.)
[illegible]	162,389	6	204,030	6	223,400	11	8,210
[illegible]	149,504	16	196,380	16	218,700	9	7,997
[illegible]	145,707	4	180,960	4	203,100	15	7,678
[illegible]	143,768	15	179,020	15	199,600	13	6,868
[illegible]	142,965	10	168,430	10	191,300	7	5,826
[illegible]	133,006	5	166,800	7	182,600	1	5,490
[illegible]	113,718	7	166,360	5	182,300	5	5,247
6	91,292	13	161,410	13	180,000	3	3,786
[illegible]	89,268	9	159,035	9	179,900	10	2,217
4	88,111	11	156,200	11	177,100	4	2,106
[illegible]	75,368	8	153,370	8	168,600	16	2,026
12	64,428	14	148,230	14	165,000	12	1,854
3	74,405	1	139,480	1	154,900	6	1,601
[illegible]	74,200	2	136,300	12	153,800	14	1,513
[illegible]	65,731	12	135,160	2	152,200	2	1,429
[illegible]	52,957	3*	86,559	3*	96,600	8	1,344
	104,180		158,600		176,820		4,075
	52,957 to 162,389		136,300 to 204,030		153,800 to 223,400		1,344 to 8,210
	3.07		1.50		1.45		6.11

B

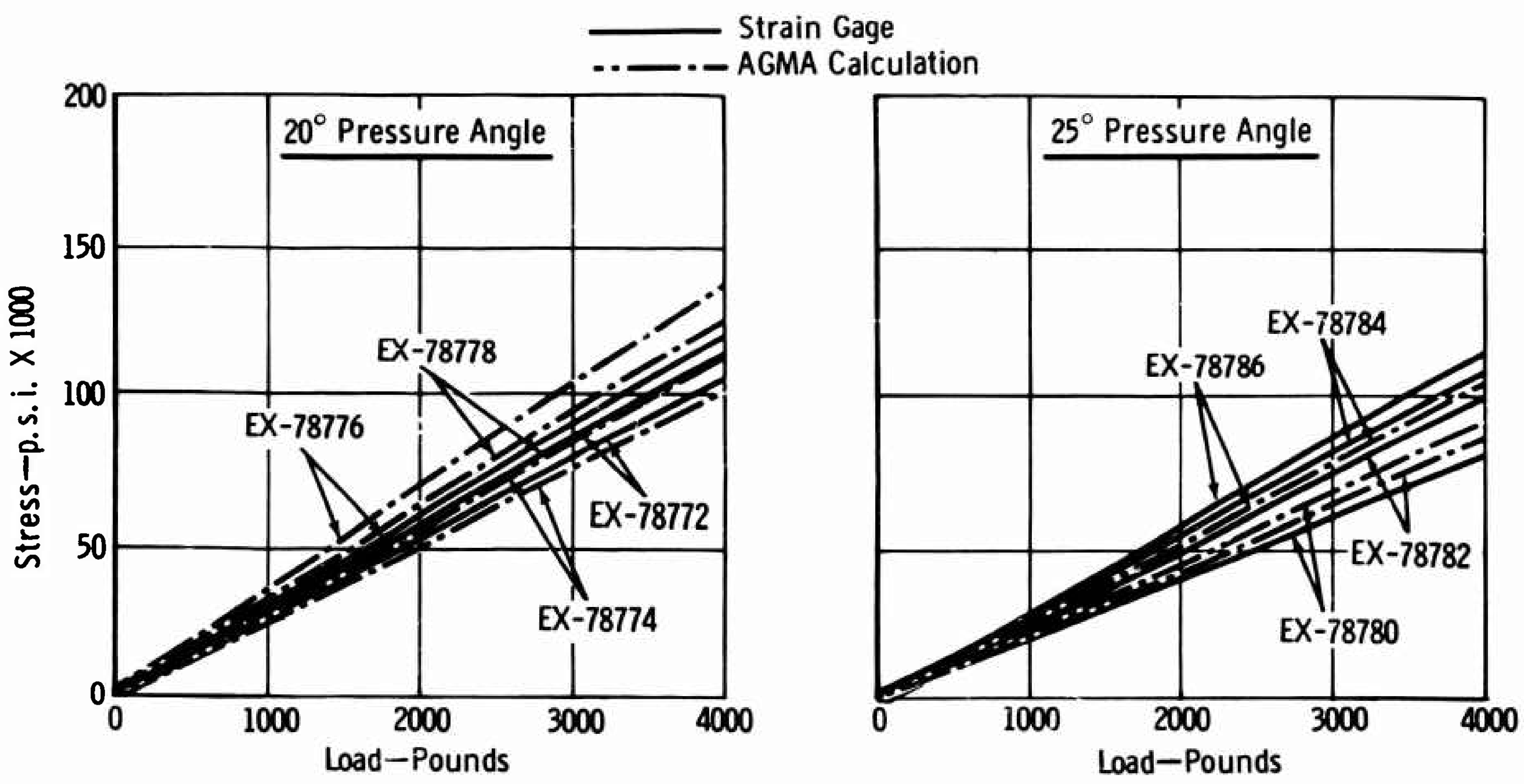

Figure 85. Calculated Stress for Gear Tooth Load.

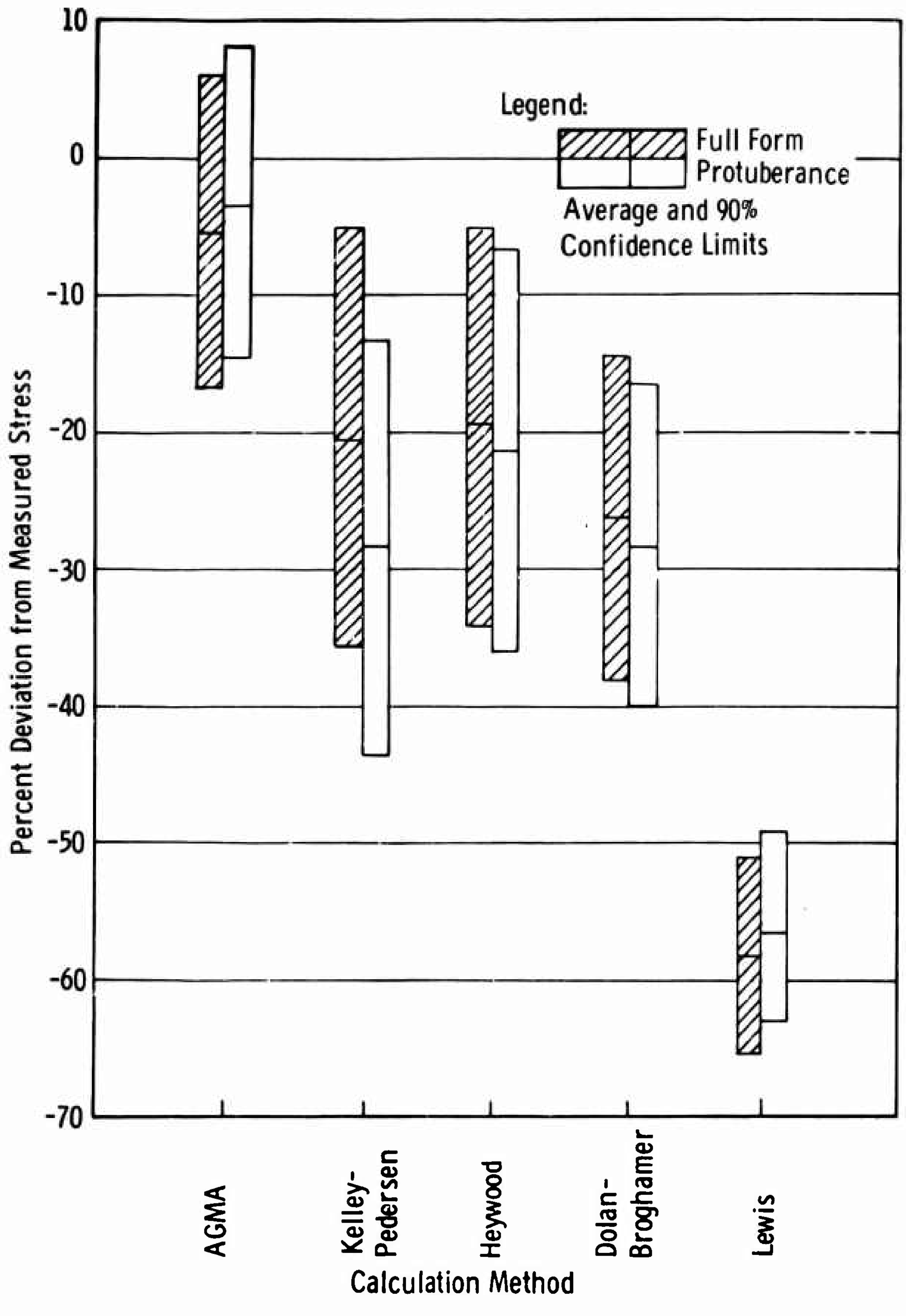

Figure 86. Comparison of Methods for Calculating Gear Stress.

TABLE XVI
GEAR CONFIGURATION RANKING COMPARISON

Test Rig Load Ranking	Lewis		Heywood		Kelley-Pedersen		Dolan-Broghamer		AGMA	
	Rank	Difference	Rank	Difference	Rank	Difference	Rank	Difference	Rank	Difference
11	11	0	11	0	11	0	11	0	11	0
9	9	0	15	1	15	1	15	1	9	0
15	15	0	3	5	7	2	9	1	15	0
13	3	4	9	2	3	4	13	0	13	0
7	13	1	13	1	9	3	3	3	3	3
1	1	0	7	1	13	2	1	0	1	0
5	7	2	1	1	1	1	7	2	7	2
3	5	1	5	1	5	1	5	1	5	1
10	12	3	12	3	12	3	12	3	12	3
4	10	1	16	1	16	1	10	1	10	1
16	16	0	4	1	8	5	16	0	16	0
12	14	2	10	3	10	3	14	2	14	2
6	4	3	14	1	4	3	4	3	4	3
14	2	1	8	2	14	0	2	1	2	1
2	8	1	2	0	2	0	8	1	8	1
8	6	3	6	3	6	3	6	3	6	3
Correct Rankings	5		2		3		4		6	
Prediction Accuracy		1.375		1.625		2.000		1.375		1.25

Note: Numbers in difference columns indicate difference in rank position from test rig load ranking.

TABLE XVII
FATIGUE TEST GEAR MEASURED DIMENSIONS

Part Number	Serial Number	Dimension Over Pins	Root Diameter (inches)	Minimum Root Radius (inch)	Tooth Edge Break (inch)* 1	2	3	4
EX-78772	CX 9089	4.3926	3.5806	0.065	—	—	—	—
	CX 9090	4.3938	3.5800	0.065	0.020 CUS	0.020 CUD	0.020 CUD	0.020 CUD
	CX 9091	4.3947	3.5800	0.065	0.020 CE	0.015 CE	0.015 CE	0.015 CE
	CX 9092	4.3950	3.5802	0.065	0.010 CUS	0.020 CUS	0.010 CUS	0.020 CUD
	CX 9093	4.3950	3.5830	0.065	—	—	—	—
EX-78773	CX 9074	2.1920	1.7835	0.040	0.005 CE	0.005 CE	0.005 CE	0.005 CE
	CX 9075	2.1921	1.7838	0.040	0.005 CE	0.005 CE	0.005 CE	0.005 CE
	CX 9076	2.1942	1.7903	0.038	0.005 RE	0.005 RE	0.005 RE	0.005 RE
	CX 9077	2.1920	1.7838	0.040	—	—	—	—
	CX 9078	2.1922	1.7836	0.040	0.005 CE	—	—	—
EX-78774	CX 9064	4.3981	3.5875	0.070	0.030 CE	0.020 CE	0.020 CE	0.020 CE
	CX 9065	4.3976	3.5867	0.070	0.020 CUS	0.030 CE	0.020 CUS	0.030 CUS
	CX 9066	4.3981	3.5863	0.070	—	—	—	—
	CX 9067	4.3947	3.5820	0.070	—	0.030 CE	0.030 CE	0.030 CE
	CX 9068	4.3984	3.5882	0.070	0.030 CE	0.020 CUS	0.020 CUD	0.020 CUS
EX-78775	CX 9099	2.1912	1.7955	0.034	S	S	S	S
	CX 9100	2.1930	1.7955	0.034	—	—	—	—
	CX 9101	2.1918	1.7955	0.035	—	—	—	—
	CX 9102	2.1926	1.7955	0.035	S	0.005 RE	S	S
	CX 9103	2.1897	1.7955	0.024	—	—	—	—
EX-78776	CX 9007	4.3965	3.5252	0.068	0.030 CUS	--	—	—
	CX 9008	4.3964	3.5231	0.068	0.030 CUS	0.030 RE	0.030 CUS	0.030 CUS
	CX 9009	4.3963	3.5237	0.068	0.015 CE	—	—	0.015 CUD
	CX 9010	4.3963	3.5241	0.068	S	0.010 CUS	0.010 CUS	0.015 CUS
	CX 9011	4.3964	3.5227	0.068	—	—	—	—

TABLE XVII (CONT)

Part Number	Serial Number	Dimension Over Pins	Root Diameter (inches)	Minimum Root Radius (inch)	Tooth Edge Break (inch)* 1	2	3	4
EX-78777	CX 9059	2.1967	1.767	0.030	—	—	—	—
	CX 9060	2.1967	1.768	0.030	—	—	—	—
	CX 9061	2.1967	1.767	0.032	0.020 CE	0.020 CE	0.020 CE	0.020 CE
	CX 9062	2.1967	1.769	0.032	0.020 CE	0.020 CE	0.020 CE	0.020 CE
	CX 9063	2.1967	1.767	0.032	0.020 CE	0.020 CE	0.020 CE	0.020 CE
EX-78778	CX 9054	4.3904	3.5267	0.090	0.030 CUD	0.030 CUD	0.030 CUD	0.030 CE
	CX 9055	4.3905	3.5267	0.090	—	—	—	—
	CX 9056	4.3903	3.5266	0.090	0.010 CE	0.020 CE	0.020 CE	0.020 CUS
	CX 9057	4.3905	3.5275	0.090	0.030 CE	0.030 CE	0.030 CUD	0.030 CUS
	CX 9058	4.3906	3.5281	0.090	—	—	—	—
EX-78779	CX 9104	2.1961	1.7678	0.044	—	—	—	—
	CX 9105	2.1961	1.7672	0.044	0.020 CE	0.020 CE	0.020 CE	0.020 CUD
	CX 9106	2.1961	1.7679	0.044	0.020 CE	0.020 CE	0.020 CE	0.020 CE
	CX 9107	2.1963	1.7682	0.044	—	—	—	—
	CX 9108	2.1963	1.7680	0.044	0.020 CE	—	—	—
EX-78780	CX 9094	4.3979	3.6000	0.055	—	—	—	—
	CX 9095	4.3978	3.5999	0.055	0.020 CE	0.020 CE	0.020 CE	0.020 CE
	CX 9096	4.3978	3.5995	0.055	0.030 CE	0.030 CE	0.030 CE	0.030 CE
	CX 9097	4.3980	3.6005	0.055	0.020 RE	0.020 RE	0.020 RE	0.020 RE
	CX 9098	4.3985	3.5998	0.055	—	—	—	—
EX-78781	CX 9030	2.1968	1.8097	0.028	0.010 CUD	0.010 CE	0.005 CE	0.020 CE
	CX 9031	2.1967	1.8095	0.028	0.010 CE	0.020 CE	0.010 CE	0.010 CE
	CX 9032	2.1976	1.8105	0.026	0.005 CE	0.005 CE	0.005 CE	0.005 CE
	CX 9033	2.1961	1.8093	0.026	0.005 CE	0.005 CE	0.005 CE	0.005 CE
	CX 9034	2.1969	1.8096	0.028	0.010 CE	0.005 CE	0.005 CE	0.005 CUD
EX-78782	CX 9109	4.3967	3.6050	0.070	—	—	—	—
	CX 9110	4.3976	3.6035	0.070	—	—	—	—
	CX 9111	4.3976	3.6040	0.070	0.010 CUD	0.020 CE	0.020 CE	0.020 CUD
	CX 9112	4.3978	3.6040	0.070	0.015 CE	0.010 CE	0.010 CE	0.005 CE
	CX 9113	4.3981	3.6035	0.070	—	—	—	—

TABLE XVII (CONT)

Part Number	Serial Number	Dimension Over Pins	Root Diameter (inches)	Minimum Root Radius (inch)	Tooth Edge Break (inch)* 1	2	3	4
EX-78783	CX 9025	2.1965	1.805	0.036	0.020 CE	0.020 CE	0.020 CE	0.020 CE
	CX 9026	2.1972	1.805	0.036	0.020 CE	0.020 CE	0.020 CE	0.020 CE
	CX 9027	2.1967	1.805	0.036	0.020 CE	0.020 CE	0.020 CE	0.020 CE
	CX 9028	2.1947	1.803	0.034	0.020 CE	0.020 CE	0.020 CE	0.020 CE
	CX 9029	2.1968	1.805	0.036	0.020 CE	0.020 CUD	0.020 CUD	0.020 CE
EX-78784	CX 9069	4.3980	3.5424	0.065	—	—	—	—
	CX 9070	4.3974	3.5415	0.065	0.030 CUD	0.030 CUD	0.030 CUS	0.020 CUS
	CX 9071	4.3975	3.5413	0.065	0.030 CE	0.020 CUD	0.030 CUD	0.020 CUD
	CX 9072	4.3975	3.5418	0.065	0.020 CUD	0.020 CUD	0.020 CUD	0.030 CUD
	CX 9073	4.3973	3.5412	0.065	0.005 CE	0.005 CE	0.005 CE	0.005 CE
EX-78785	CX 9035	2.1975	1.775	0.033	0.020 CE	0.020 CE	0.020 CE	0.020 CE
	CX 9036	2.1976	1.776	0.033	—	—	—	—
	CX 9037	2.1972	1.775	0.033	0.020 CE	0.020 CE	0.020 CE	0.020 CE
	CX 9038	2.1978	1.776	0.033	0.010 CUD	0.005 CUS	0.010 CUS	0.010 CUD
	CX 9039	2.1974	1.776	0.033	—	—	—	—
EX-78786	CX 9012	4.3982	3.5436	0.073	—	—	—	—
	CX 9013	4.3983	3.5445	0.073	0.050 CE	0.050 CE	0.040 CE	0.040 CE
	CX 9014	4.3983	3.5440	0.073	0.030 CE	0.020 CUD	0.020 CE	0.030 CE
	CX 9015	4.3983	3.5448	0.073	0.030 CE	0.030 CE	0.030 CE	0.030 CUD
	CX 9016	4.3982	3.5447	0.073	—	—	—	—
EX-78787	CX 9114	2.1947	1.7785	0.036	0.020 CE	0.020 CE	0.020 CE	0.020 CE
	CX 9115	2.194[illegible]	1.7785	0.034	0.020 CE	0.020 CE	0.020 CE	0.020 CE
	CX 9116	2.1945	1.7785	0.034	0.020 CE	0.020 CE	0.020 CE	0.020 CE
	CX 9117	2.1949	1.7785	0.034	0.020 CE	0.020 CE	0.020 CE	0.020 CE
	CX 9118	2.1946	1.7785	0.036	0.020 CE	0.020 CE	0.020 CE	0.020 CE

*Note—Edge Break Code:
C—edge break approximates chamfer
R—edge break approximates radius
E—even blend from flank to root
UD—uneven but rounded blend from flank to root
US—uneven blend leaving sharp edge at weakest section
S—sharp

TABLE XVIII
MEASURED STRESS OF FATIGUE TEST GEARS COMPARED
WITH CALCULATED STRESS

Fatigue Test Gear	Pitch	Pressure Angle (degrees)	Fillet Radius (inch)	Fillet Configuration	Measured Strain Gage Strain Rate*	AGMA Strain Rate*	Percent Deviation	Kelley-Pedersen Strain Rate*	Perc Deviat
EX-78772	6	20	0.050	Full form	927	941	+ 1.5	810	-12.
EX-78774	6	20	0.080	Full form	1010	850	-15.8	655	-35.
EX-78776	6	20	0.050	Protuberance	1150	1157	+ 0.6	923	-19.
EX-78778	6	20	0.080	Protuberance	1008	1042	+ 3.4	652	-35.
EX-78780	6	25	0.050	Full form	691	750	+ 8.5	677	- 2.
EX-78782	6	25	0.067	Full form	856	718	-16.1	584	-31.
EX-78784	6	25	0.050	Protuberance	900	873	- 3.0	723	-19.
EX-78786	6	25	0.067	Protuberance	1017	867	-14.5	621	-39.

*Strain Rate— [illegible] hes/inch/1000 pounds

A

...ersen ...te*	Percent Deviation	Heywood Strain Rate*	Percent Deviation	Dolan-Broghamer Strain Rate*	Percent Deviation	Lewis Strain Rate*	Percent Deviation	Stress Concentration Factor (Lewis)
	-12.6	817	-11.9	756	-18.5	423	-54.5	2.19
	-35.1	659	-34.8	645	-36.1	367	-63.6	2.75
	-19.7	1040	- 9.6	945	-17.8	591	-48.6	1.95
	-35.4	787	-21.9	760	-22.6	466	-53.8	2.16
	- 2.2	675	- 2.3	585	-15.4	328	-52.5	2.10
	-31.8	602	-29.7	555	-35.2	314	-63.3	2.72
	-19.7	730	-18.9	622	-30.8	367	-59.2	2.45
	-39.0	646	-36.5	585	-42.5	349	-65.6	2.91

8

In summary, the bar chart in Figure 87 shows the average degree of correlation for the various methods of calculation versus the measured data. It is apparent that the AGMA method offers the greatest degree of correlation.

PHOTOSTRESS DATA

As described in the section titled Results, the photostress investigations showed the stress location and stress distribution to be in agreement with the theoretical location.

EFFECT OF GEOMETRIC VARIABLES OF GEAR FATIGUE TEST

The following studies of the data evaluate the four variables of the gear fatigue test. Despite the high precision achieved in the manufacture of test gears, the scatter in fatigue life was high. Many run-outs (termination of test before failure) occurred, although the planned stress levels were altered in an attempt to fail teeth with 10^7 cycles. It was decided, therefore, to base the analysis on the endurance limit produced by each of the 16 configurations of gear teeth by developing a mathematical model for the S/N curve. The derivation of the analytical model is included in Appendix V. This method was used to determine the characteristic and fit of the S/N curve for all the fatigue test points, stress curves, and R. R. Moore curves. S/N curves were fitted to the gear tooth fatigue data with respect to basic applied load, AGMA calculated stress, and Kelley-Pedersen calculated stress. The basic applied load (test rig load) was used as a positive baseline since it is unaffected by any calculations. The AGMA calculated stress was of prime interest, since it was determined to be the best predictive calculation method. The Kelley-Pedersen method was used as a second stress method to provide direct comparison for the AGMA method. The endurance limits obtained from the S/N curves were used to evaluate each of the four geometric variables and their interactions—i.e., diametral pitch, pressure angle, fillet size, and fillet configuration.

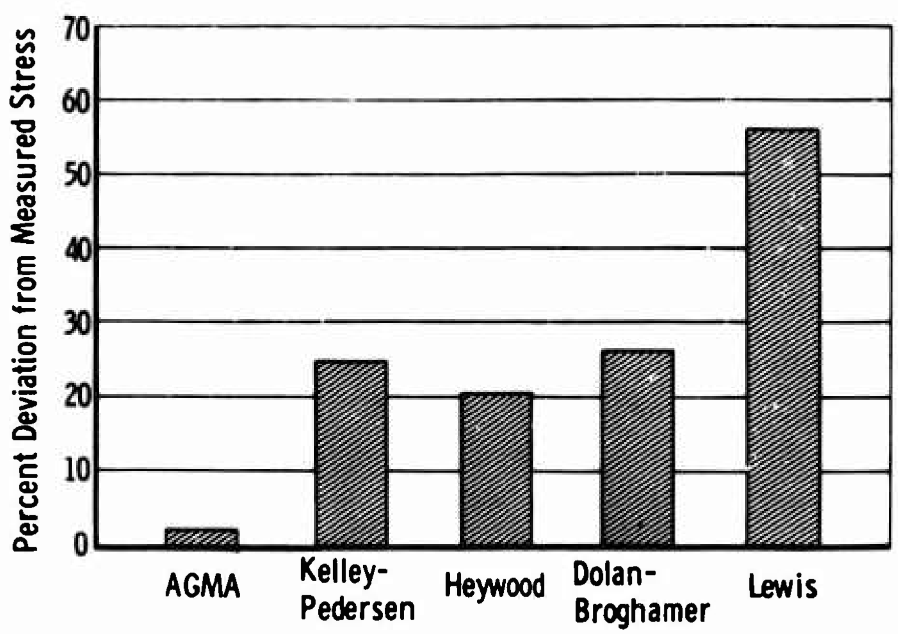

Figure 87. Comparison of Calculated and Measured Stresses.

A summary of significant test results is given in the following paragraphs. The preselected significance level was $\alpha = 0.05$, which corresponds to a statistical "t" value of 2.0. This level indicates that the result would occur 95 out of 100 times. A discussion of the statistical test of significance is included in Appendix III.

Diametral Pitch

As would be expected, due to the different face width and pitch, a significant effect was found for diametral pitch (6 and 12) based on applied load. It would be expected that stress calculations would adequately consider these geometric variables. It was found that the AGMA stress calculation did adequately predict a stress level. The Kelley-Pedersen method reduced the significance value but was still very significant. Table XIX summarizes these data (the load values have been corrected for diametral pitch and load for comparison).

TABLE XIX
EFFECT OF DIAMETRAL PITCH ON GEAR FATIGUE DATA

Diametral Pitch	Load (pounds)	Corrected Load (pounds)*	AGMA Stress (p.s.i.)	Kelley-Pedersen Stress (p.s.i.)
6	6674	6807**	175,500	138,750
12	1795	6820	184,600	75,500

*Corrected 12 pitch as follows for comparison with 6 pitch on a load basis:

Pitch	6	12	Correction
Pitch	6	12	2.00 x load
Face Width (inch)	0.500	0.250	2.00 x load
			Total = 4.0 x Load
Y (average)	0.513	0.486	0.95 x 4.0 x load = 3.8 x load

3.8 x 1795 = 6820 pounds

**Per reference 37, a 2-percent size effect might be expected for the range of face widths tested; therefore, 1.02 x 6674 = 6807 pounds.

Pressure Angle

A significant effect was found due to the change in 20- and 25-degree pressure angle gears based on applied load. Also, it would be expected that the stress calculation should adequately predict this geometric effect. The study indicated that the AGMA and Kelley-Pedersen calculation methods adequately predicted the stress level. Table XX summarizes these data (the load values have been corrected for pressure angle for comparison).

TABLE XX
EFFECT OF PRESSURE ANGLE ON GEAR FATIGUE DATA

Pressure Angle (degrees)	Load (pounds)	Corrected Load (pounds)*	AGMA Stress (p.s.i.)	Kelley-Pedersen Stress (p.s.i.)
20	3802	5027	176,500	104,480
25	4328	4328	183,600	105,700

*Correction for pressure angle was made by averaging Y values for 20- and 25-degree pressure angle gears.
20-degree average Y = 0.4302
25-degree average Y = 0.5688
$3802 \times \frac{0.5688}{0.4302} = 5027$ pounds

Fillet Size

For the practical range of fillet sizes tested, no significant difference was found on the basis of applied load or AGMA calculations. A significant difference was found, however, on the basis of the Kelley-Pedersen calculated stress. These data are summarized as follows:

	Load (pounds)	AGMA Stress (p. s. i.)	Kelley-Pedersen Stress (p. s. i.)
Small Fillet	3915	179,000	111,960
Large Fillet	4246	181,500	98,540

Fillet Configuration

For the fillet configurations tested—full form and protuberance hobbed—no significant difference was found on the basis of applied load or the Kelley-Pedersen method. A significant difference was found, however, on the basis of calculated AGMA stress. These data are summarized as follows:

	Load (pounds)	AGMA Stress (p. s. i.)	Kelley-Pedersen Stress (p. s. i.)
Full form	4234	169,300	106,100
Protuberance	3908	193,000	104,100

The average endurance limit for each variable and the corresponding statistical "t" value for the tests of significance are presented in Table XXI. Several interactions were found, as indicated in the table.

It is apparent that the AGMA formula adequately predicts gear tooth bending stress with but two exceptions: fillet configuration and the interaction of pressure angle, fillet radius, and fillet configuration. No exact reason for these differences can be shown. The difference may be due to any of the changes previously listed between the two fillet configurations such as residual stress, case depth, surface finish, etc. In view of the interaction obtained and its relative value, the difference may be due to the accumulation of errors in extrapolation of the stress concentration factor.

The significant differences between levels for each factor are apparent. Changing the value assigned to any significant geometric factor produces a change in the endurance limit. This limit is larger than can be explained by the inherent variability associated with fatigue testing. For example, diametral pitch was significant in terms of basic load, as was expected. The reduction in endurance limit in going from a diametral pitch of 6 to 12 was 4879 pounds. The fillet configuration was not significant in terms of basic load; the difference between endurance limits for the full form and the protuberance configuration was only 326 pounds.

The interpretation of significant interactions is more difficult. In general, it can be stated that the change in endurance limits caused by changing one factor is dependent on the value assigned to the interacting factor. An example is provided by the significant AB interaction associated with applied load. See Table XXI. At the 20-degree pressure angle, the endurance limit is reduced from 5780 to 1610 pounds in going from a diametral pitch value of 6 to 12; at the 25-degree pressure angle, the endurance limit

TABLE XXI
ANALYSIS OF GEOMETRIC VARIABLES AND INTERACTIONS

	Basic Applied Load (pounds)			AGMA Stress (p. s. i. × 1000)			Kelley-Pedersen Stress (p. s. i. × 1000)		
	Low	High	t*	Low	High	t*	Low	High	t*
A—Diametral Pitch	6674	1795	**24.27	175,500	184,600	1.15	138,750	75,500	**13.8
B—Pressure Angle	3802	4328	** 2.62	176,500	183,600	0.89	104,480	105,700	0.3
C—Fillet Size	3915	4246	1.65	179,000	181,500	0.31	111,960	98,540	** 2.9
D—Fillet Configuration	4234	3908	1.62	168,300	193,000	**2.98	106,100	104,100	0.4
AB Interaction	3620	4660	** 5.17	176,100	185,500	1.18	97,800	114,300	** 3.6
AC Interaction	3975	4187	1.05	180,500	180,200	0.03	106,040	104,300	0.4
AD Interaction	4286	3878	** 2.03	182,900	178,200	0.53	105,910	104,390	0.3
BC Interaction	3765	4430	** 3.31	182,800	177,600	0.65	102,360	108,200	1.3
BD Interaction	4195	4003	0.96	179,100	181,700	0.20	105,900	104,320	0.3
CD Interaction	4024	4139	0.57	183,400	177,400	0.76	103,750	106,490	0.6
ABC Interaction	4006	4181	0.87	180,000	180,600	0.08	103,000	107,910	1.7
ABD Interaction	3999	4154	0.77	183,900	177,200	0.84	104,950	105,330	0.1
ACD Interaction	4106	4057	0.24	179,900	180,800	0.11	105,560	104,700	0.2
BCD Interaction	4307	3828	** 2.38	193,900	165,000	**3.64	112,160	97,220	** 3.3

*t = statistical "t" test of significant value.
**Denotes significance at α = 0.05.

is reduced from 7650 to 1930 pounds for the same change in diametral pitch. This example is shown graphically in Figure 88. The interaction is indicated by the convergence of the lines; i. e., the difference in endurance limits between a 20- and a 25-degree pressure angle is not the same at the two values of diametral pitch. The information used is presented in Tables XXII, XXIII, and XXIV for the basic applied load and the AGMA and Kelley-Pedersen calculated stress.

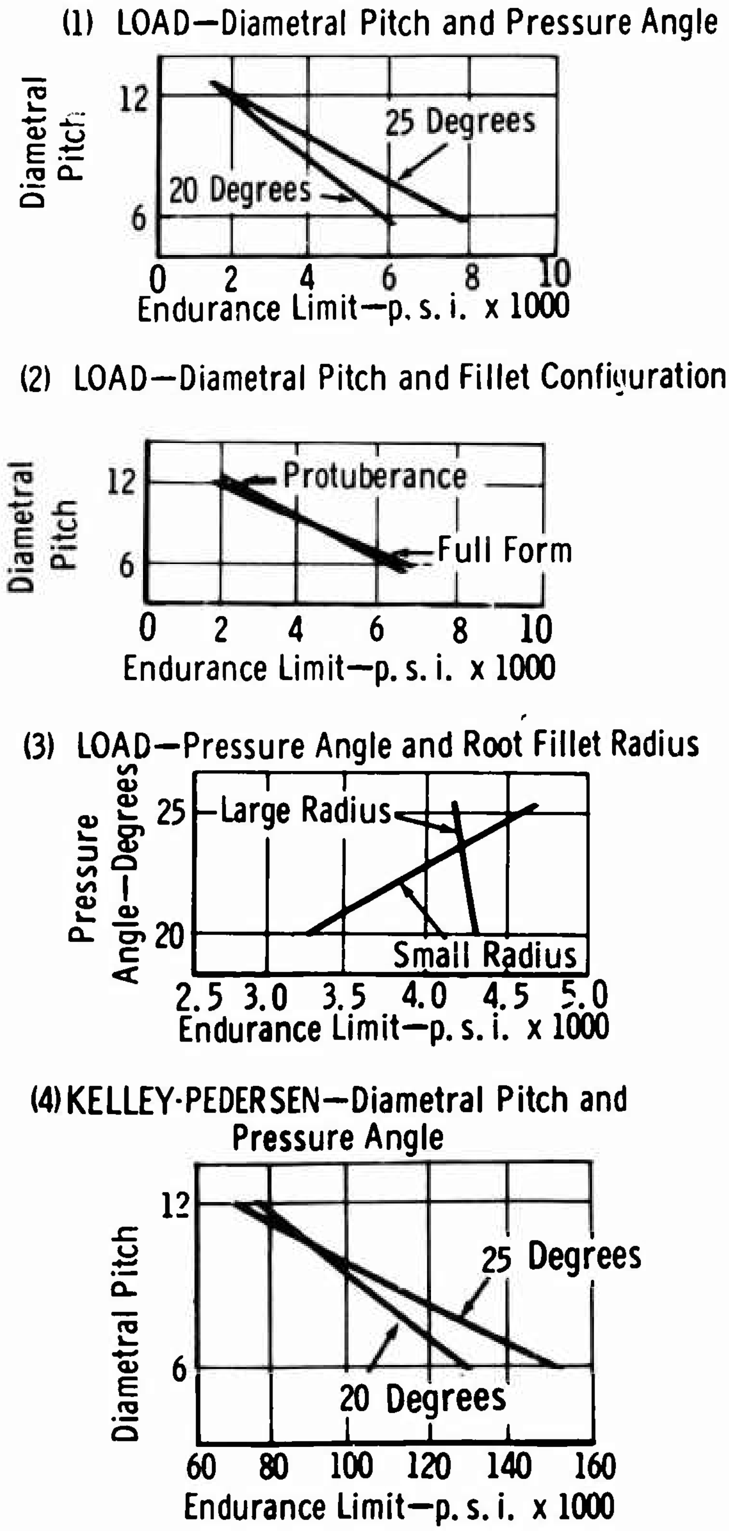

Figure 88. Significant Two-Factor Interactions.

TABLE XXII

ENDURANCE LIMITS BASED ON BASIC GEAR TOOTH LOADING

Root Radius	Fillet Configuration		Diametral Pitch 6, Pressure Angle (degrees) 20	Diametral Pitch 6, Pressure Angle (degrees) 25	Diametral Pitch 12, Pressure Angle (degrees) 20	Diametral Pitch 12, Pressure Angle (degrees) 25
Small	Full Form	1*	1 = EX-78772	9 = EX-78780	2 = EX-78773	10 = EX-78781
		2**	12	12	14	16
		3†	5.490×10^3	7.995×10^3	1.429×10^3	2.217×10^3
		4‡	3.080×10^5	3.476×10^5	0.3543×10^5	0.0749×10^5
	Protub-erance	1	5 = EX-78776	13 = EX-78784	6 = EX-78777	14 = EX-78785
		2	11	13	13	12
		3	5.247×10^3	6.867×10^3	1.601×10^3	1.513×10^3
		4	1.805×10^5	1.170×10^5	0.0207×10^5	0.5195×10^5
Large	Full Form	1	3 = EX-78774	11 = EX-78782	4 = EX-78775	12 = EX-78783
		2	19	10	10	19
		3	6.238×10^3	8.210×10^3	2.105×10^3	1.854×10^3
		4	0.4042×10^5	5.832×10^5	0.1131×10^5	1.134×10^5
	Protub-erance	1	7 = EX-78778	15 = EX-78786	8 = EX-78779	16 = EX-78787
		2	9	12	9	18
		3	5.827×10^3	7.678×10^3	1.344×10^3	2.026×10^3
		4	4.934×10^5	0.0727×10^5	0.3142×10^5	0.0461×10^5

*1—Configuration number and part number.

**2—Sample size (data points) used to compute endurance limit.

†3—Endurance limit, pounds.

‡4—Variance of endurance limit, pounds.

TABLE XXIII
ENDURANCE LIMITS BASED ON AGMA CALCULATED STRESS

Root Radius	Fillet Configuration		Diametral Pitch 6, Pressure Angle (degrees) 20	Diametral Pitch 6, Pressure Angle (degrees) 25	Diametral Pitch 12, Pressure Angle (degrees) 20	Diametral Pitch 12, Pressure Angle (degrees) 25
Small	Full Form	1*	1 = EX-78772	9 = EX-78780	2 = EX-78773	10 = EX-78781
		2**	12	12	14	16
		3†	1.549×10^5	1.798×10^5	1.524×10^5	1.913×10^5
		4‡	2.3966×10^8	1.7827×10^8	4.252×10^8	0.535×10^8
	Protub-erance	1	5 = EX-78776	13 = EX-78784	6 = EX-78777	14 = EX-78785
		2	11	13	13	12
		3	1.823×10^5	1.800×10^5	2.234×10^5	1.650×10^5
		4	2.1788×10^8	0.8038×10^8	0.3870×10^8	6.1814×10^8
Large	Full Form	1	3 = EX-78774	11 = EX-78782	4 = EX-78775	12 = EX-78783
		2	19	10	10	19
		3	1.592×10^5	1.771×10^5	2.031×10^5	1.538×10^5
		4	0.8754×10^8	2.7160×10^8	0.9998×10^8	7.8283×10^8
	Protub-erance	1	7 = EX-78778	15 = EX-78786	8 = EX-78779	16 = EX-78787
		2	9	12	9	18
		3	1.826×10^5	1.996×10^5	1.686×10^5	2.187×10^5
		4	4.6733×10^8	0.0491×10^8	4.9309×10^8	0.5281×10^8

*1—Configuration number and part number.
**2—Sample size (data points) used to compute endurance limit.
†3—Endurance limit, p.s.i.
‡4—Variance of endurance limit, p.s.i.

TABLE XXIV

ENDURANCE LIMITS BASED ON KELLEY-PEDERSEN CALCULATED STRESS

Root Radius	Fillet Configuration		Diametral Pitch 6, Pressure Angle (degrees) 20	Diametral Pitch 6, Pressure Angle (degrees) 25	Diametral Pitch 12, Pressure Angle (degrees) 20	Diametral Pitch 12, Pressure Angle (degrees) 25
Small	Full Form	1*	1 = EX-78772	9 = EX-78780	2 = EX-78773	10 = EX-78781
		2**	12	12	14	16
		3†	133.03×10^3	162.34×10^3	74.11×10^3	89.29×10^3
		4‡	17.67×10^7	14.52×10^8	8.31×10^7	1.17×10^7
	Protub-erance	1	5 = EX-78776	13 = EX-78784	6 = EX-78777	14 = EX-78785
		2	11	13	13	12
		3	145.68×10^3	149.47×10^3	91.31×10^3	65.73×10^3
		4	13.92×10^7	5.54×10^7	0.65×10^7	9.81×10^7
Large	Full Form	1	3 = EX-78774	11 = EX-78782	4 = EX-78775	12 = EX-78783
		2	19	10	10	19
		3	122.62×10^3	143.76×10^3	88.10×10^3	64.44×10^3
		4	4.712×10^7	17.90×10^7	1.88×10^7	13.74×10^7
	Protub-erance	1	7 = EX-78778	15 = EX-78786	8 = EX-78779	16 = EX-78787
		2	9	12	9	18
		3	113.72×10^3	143.01×10^3	52.97×10^3	75.35×10^3
		4	18.12×10^7	0.25×10^7	4.86×10^7	0.63×10^7

*1—Configuration number and part number.

**2—Sample size (data points) used to compute endurance limit.

†3—Endurance limit, p. s. i.

‡4—Variance of endurance limit, p. s. i.

The endurance limit for test gear configuration number 1 (EX-78774) was increased from a computed 96, 600-p. s. i. AGMA stress value to 159, 200 p. s. i. It was necessary to neutralize this low value to prevent bias to the designed experiment. The new value was determined by proportioning the configuration number 1 endurance limit based on fillet size. Fillet size is the only difference between configurations 1 and 3. The basic applied load and Kelley-Pedersen endurance limit for configuration 3 were similarly proportioned.

BASIC MATERIAL STRENGTH

An ideal bending stress calculation would permit direct correlation of tooth strength with the basic material strength. R. R. Moore rotating beam fatigue test data were compared with fatigue test gear data to determine the degree of correlation.

The R. R. Moore S/N curve shown in Figure 89 presents the basic bending strength of the carburized AMS-6265 material of the test gears. R. R. Moore rotating beam specimens are related to gears as described in the following paragraphs.

Type of Loading

The R. R. Moore test bar rotates while supporting a bending load. This results in complete reversal of the bending load on the test bar once each revolution. The relationship of fatigue data for the two types of loading is indicated in the modified Goodman diagram in Figure 90. Metallurgical investigations showed that the fatigue failures for the R. R. Moore samples and the test gears started on the carburized case surface. The modified Goodman diagram, therefore, is based on the case material properties. The ultimate strength level for the case was calculated by increasing the measured ultimate strength of the core material by the ratio of the case hardness and the core hardness at the surface:

$$180,000 \times \frac{58}{38} = 274,000 \text{ p. s. i.}$$

Points A and B in Figure 89 are located on the S/N curve to establish 10^8 and 10^5 cycle lines. These points are then plotted on the modified Goodman diagram, Figure 90, at the zero mean stress ordinate. Since the gear tooth load was in one direction only, the one-direction line was drawn at a slope of 2. A slope of 2 is used since the mean stress is one-half of the maximum stress for one-direction loading as shown in the following sketch. The intersection of the one-direction line and the cycle lines,

points C and D, establish points for an R. R. Moore S/N data curve modified for the fatigue test gear mode of loading. The modified S/N curve is shown in Figure 89. This modification is not required for use with idler gear applications where the gear tooth is subjected to complete reversal of loading.

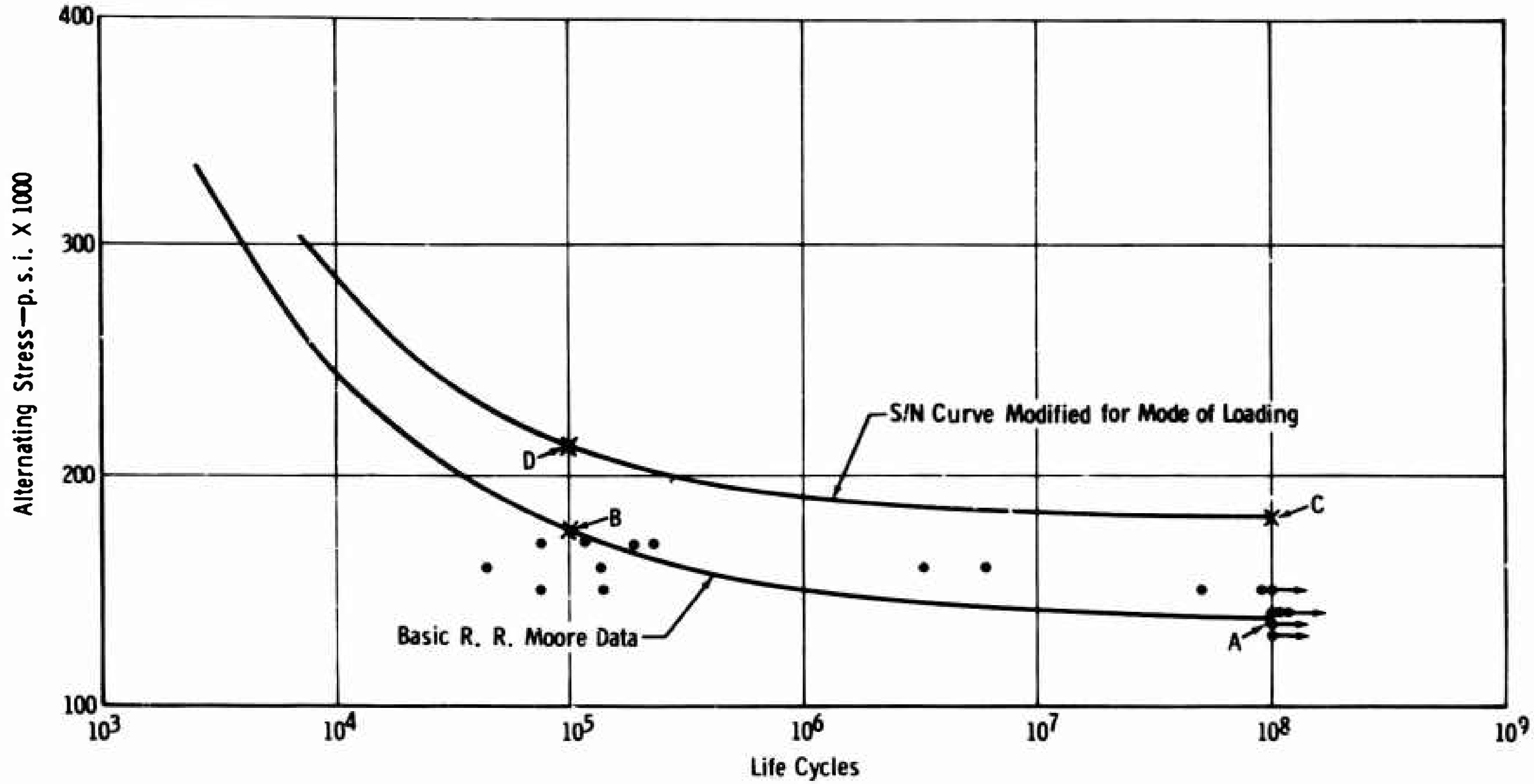

Figure 89. R. R. Moore Fatigue Test Data.

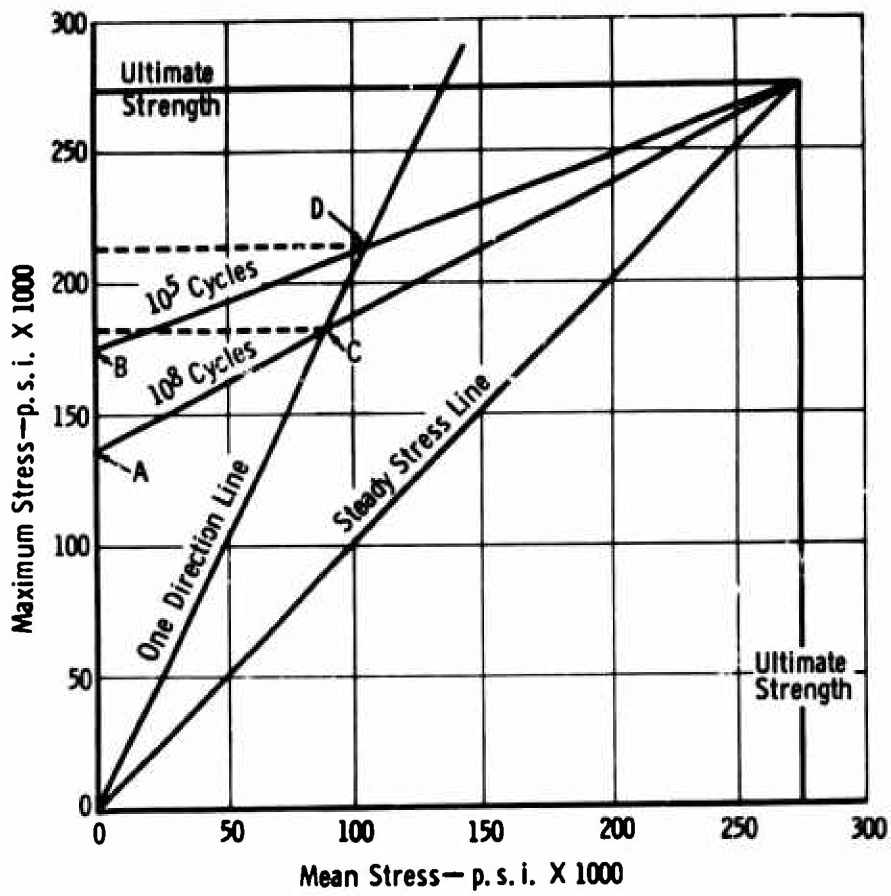

Figure 90. Modified Goodman Diagram.

Size Effect

R. R. Moore standard specimens are 0.250-inch-diameter bars. Generally, for bending, the endurance strength tends to decrease as size increases. To relate the size effect factor to carburized gears, it is recommended that the factor be "one." The literature indicates that the decrease of endurance strength for size is approximately 2 percent for carburized material; however, this effect has not been completely tested.

Surface Effect

Usually R. R. Moore specimens are polished. For this analysis, however, the R. R. Moore specimens were ground to the same surface finish as the gear roots; thus, the surface effect factor is "one." R. R. Moore data from polished samples must be reduced 10 percent.

Stress Concentration

R. R. Moore specimens are considered to have no stress concentration. Most current gear tooth bending stress calculation methods incorporate a stress concentration term based on tooth geometry. Therefore, no further consideration of stress concentration is required.

Reliability

Both R. R. Moore and fatigue test data have been analyzed based on mean endurance strength (50 percent failures) for comparison. Depending on the application, any confidence level may be selected for the gear design.

Surface Treatment

The R. R. Moore samples in this program were carburized, shot peened, and black oxided to the same specifications as the gears. Thus, the surface treatment factor is "one."

All of the aforementioned factors except stress concentration, size effect, and mode of loading are considered as one for this analysis. Thus, the modified R. R. Moore data as plotted on the S/N curve of Figure 89 are comparable (within 2 percent) to a calculated stress that incorporates a stress concentration factor.

Figures 91, 92, 93, and 94 show the fatigue test data with respect to size and pressure angle plotted against AGMA stress. Superimposed on these curves is the endurance strength line from the modified R. R. Moore data developed previously. It is considered significant that close correlation is indicated for the AGMA method and the basic R. R. Moore data. A further comparison is made in Figures 95 and 96 by superimposing the R. R. Moore S/N curve on the protuberance hobbed and the full form ground data. A final comparison is made by averaging the fatigue test gear data and comparing with the R. R. Moore S/N curve. Figure 97 shows this comparison. It is apparent that extremely close correlation was demonstrated between the overall AGMA stress calculation for the gear fatigue tests and the basic strength as determined by the R. R. Moore data.

The endurance strengths previously listed in Tables XXII, XXIII, and XXIV are plotted in Figure 98 and are compared to the basic R. R. Moore data. It is apparent that the Lewis, Heywood, and Kelley-Pedersen methods do not approach the basic material strength. The Dolan-Broghamer and AGMA methods, which are very similar, do bracket the basic material strength line.

DEVELOPMENT OF DESIGN VALUE

The S/N curve of Figure 97 was obtained from an average of all the fatigue test data. It represents a mean or 50-percent failure estimate of the test data. For design purposes, a much lower failure probability would normally be required. An endurance limit consistent with such a higher reliability was obtained as follows. If some of the differences among the derived endurance limits are attributed to geometric factors and combined into one group, a distributed quantity results. The group of endurance limits has an average value and some scatter or dispersion about this average. A meaningful statement of the form of this distribution is not possible because there are only 16 points. However, a plot of these points on normal probability paper (Figure 99), using the mean rank procedure, indicates that an assumption of normalcy is reasonable. Assuming normalcy, a lower tolerance value can be calculated for the endurance limit. The average, $\bar{X}$, and standard deviations of the distribution were calculated after deleting the endurance limit derived from configuration 3. The K factor for a one-sided tolerance limit was obtained from tables which can be found in standard statistical texts. This K factor for a proportion P = 0.99 and a probability of 0.80 is 3.212. The 1-percent endurance limit is then $\bar{X}$ - K_{σ} or 182,000 - 3.212 (24,900) = 102,000 p.s.i. The

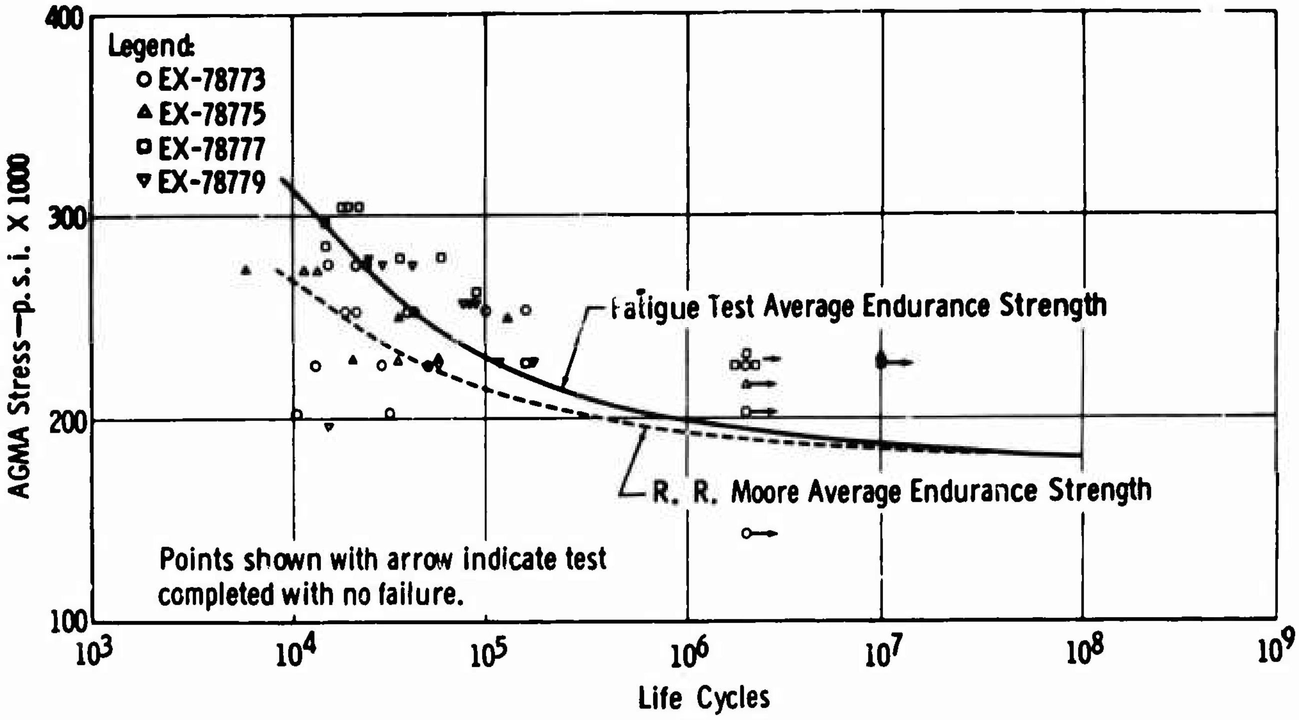

Figure 91. AGMA Stress Fatigue Test Data
(Diametral Pitch = 12; Pitch Diameter = 2 Inches; Pressure Angle = 20 Degrees).

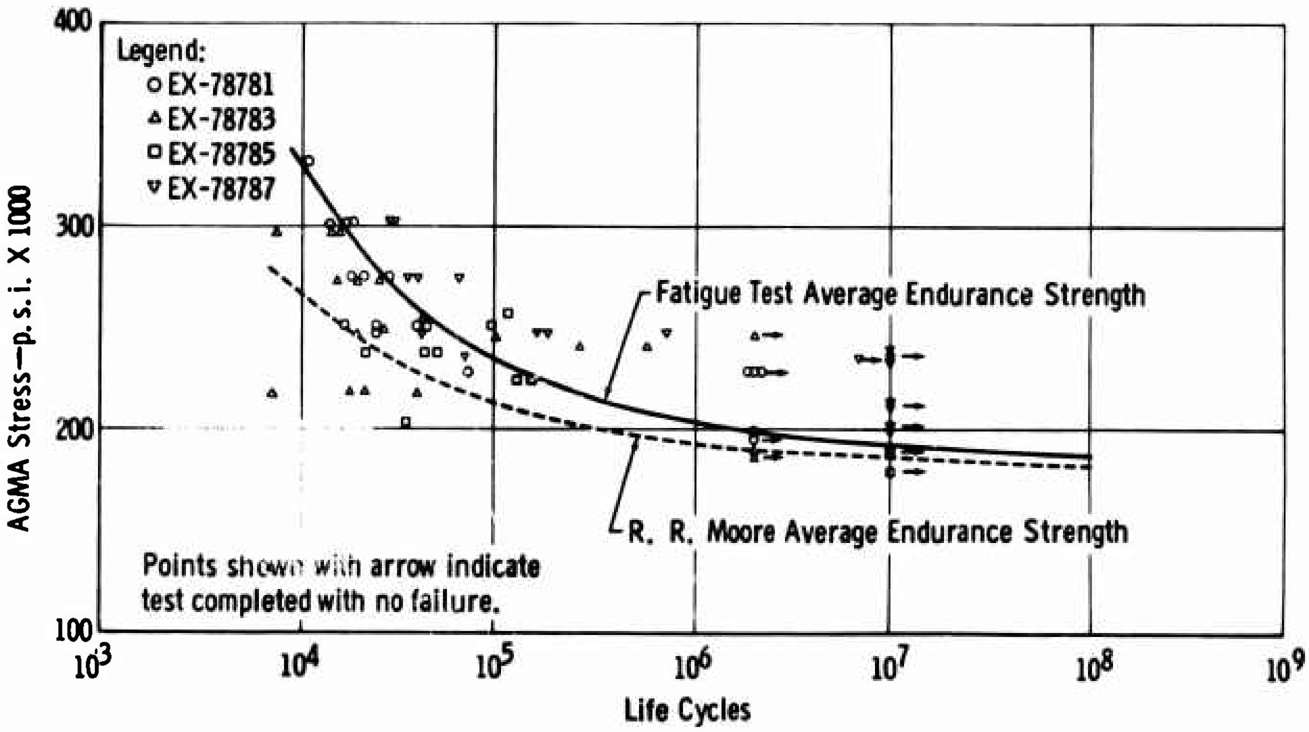

Figure 92. AGMA Stress Fatigue Test Data
(Diametral Pitch = 12; Pitch Diameter = 2 Inches; Pressure Angle = 25 Degrees).

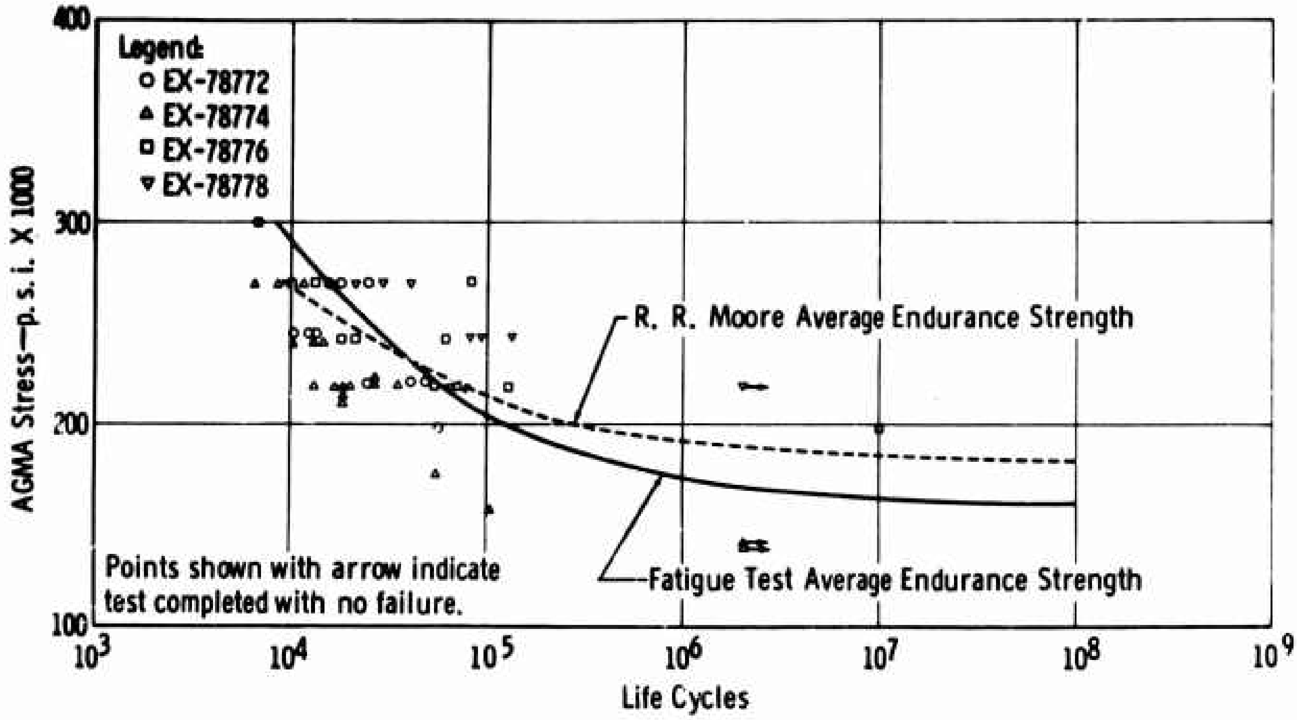

Figure 93. AGMA Stress Fatigue Test Data
(Diametral Pitch = 6; Pitch Diameter = 4 Inches; Pressure Angle = 20 Degrees).

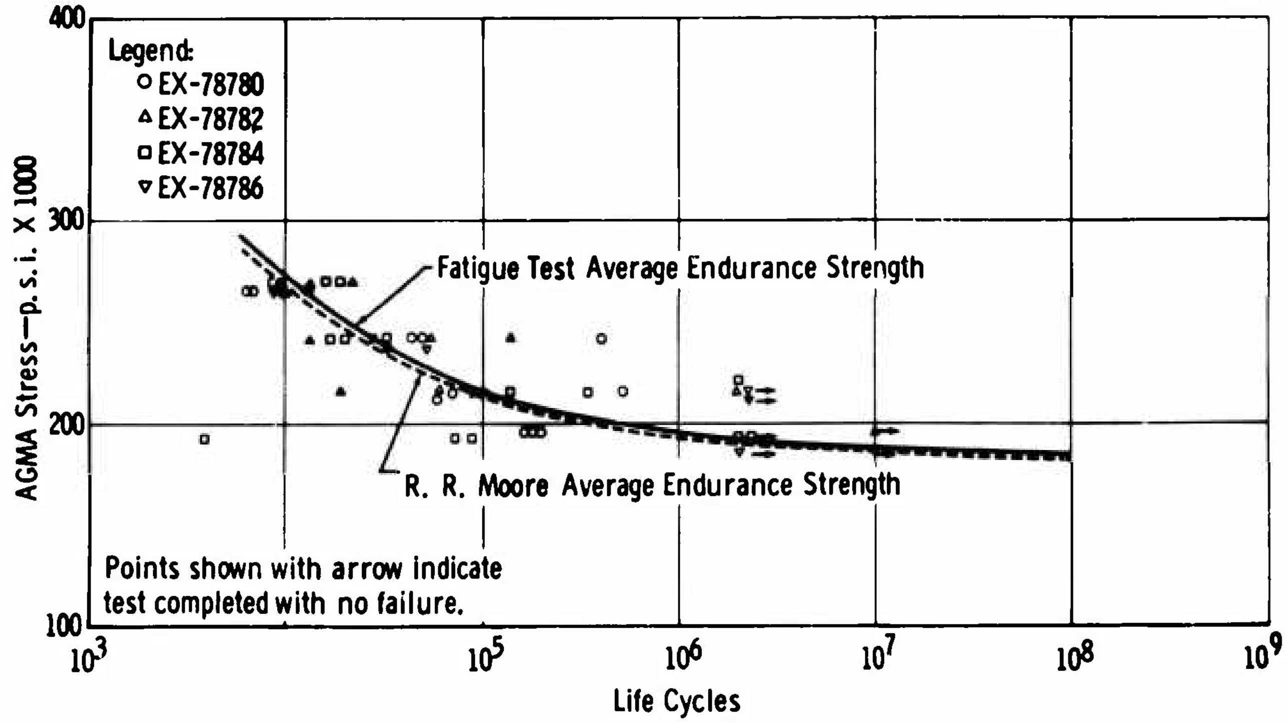

Figure 94. AGMA Stress Fatigue Test Data
(Diametral Pitch = 6; Pitch Diameter = 4 Inches; Pressure Angle = 25 Degrees).

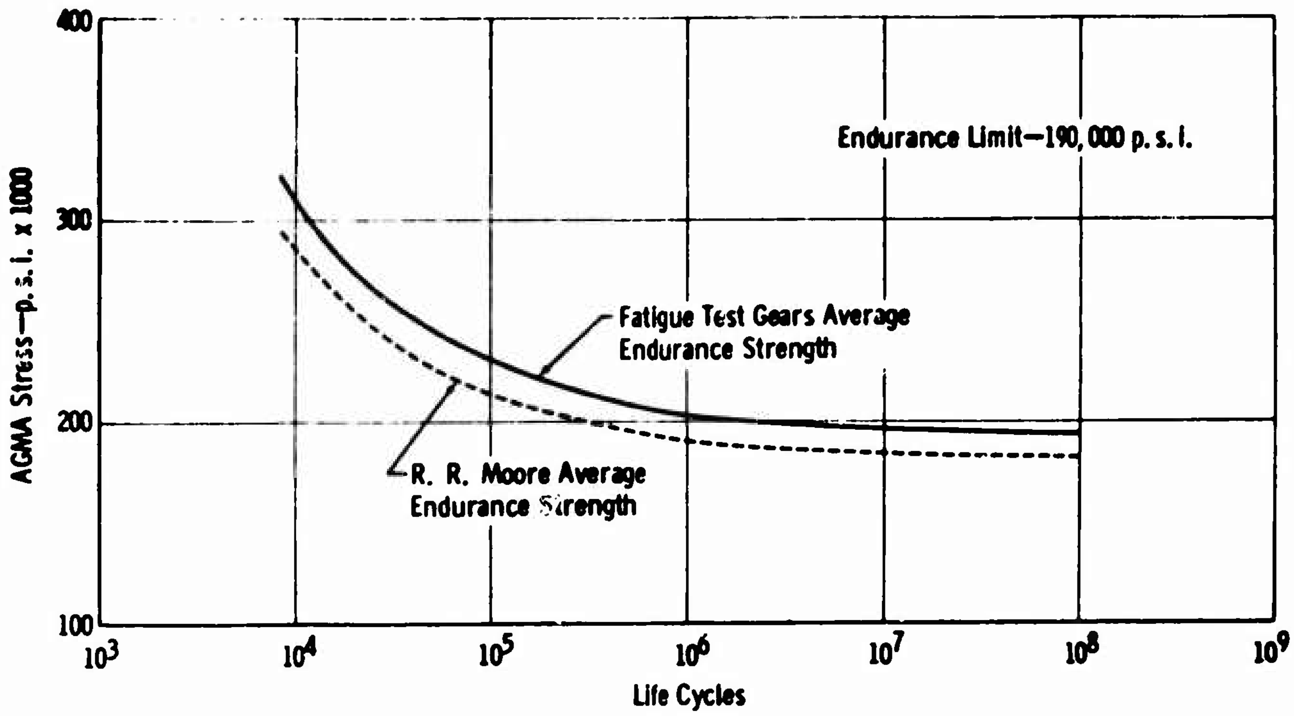

Figure 95. S/N Diagram for Protuberant Fillet.

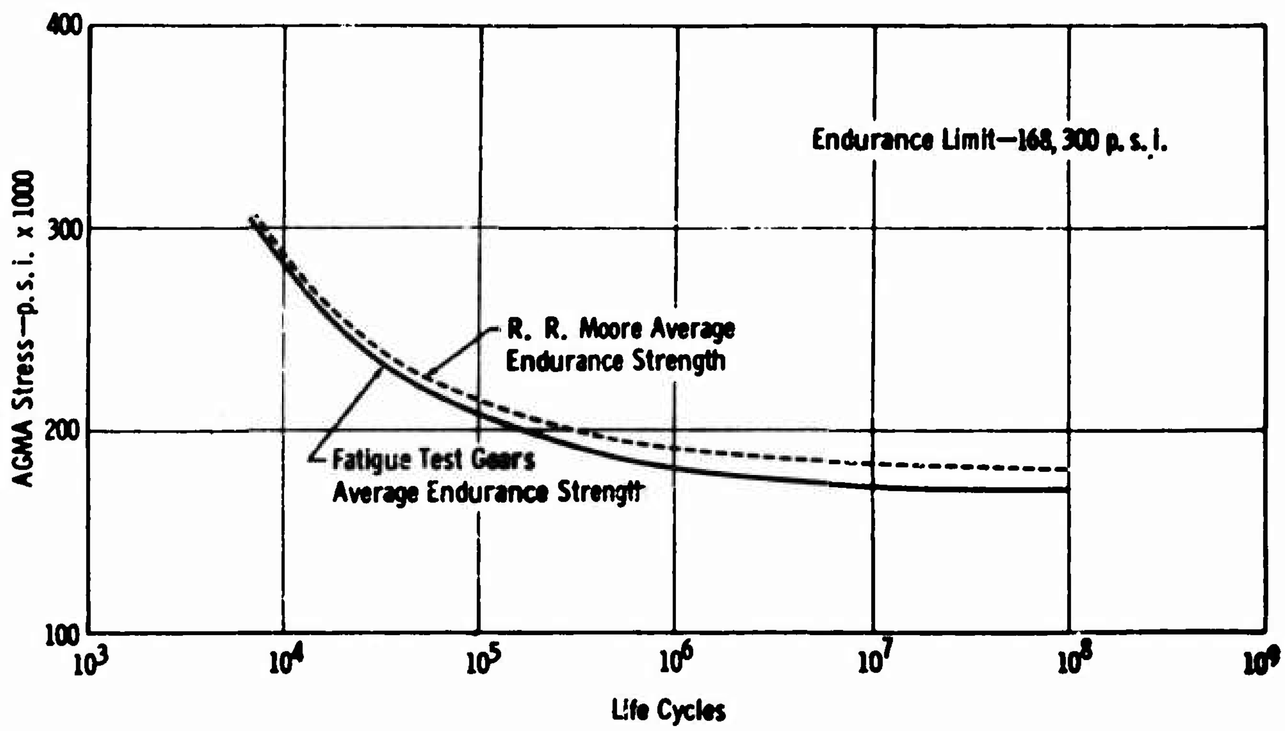

Figure 96. S/N Diagram for Full Form Ground Fillet.

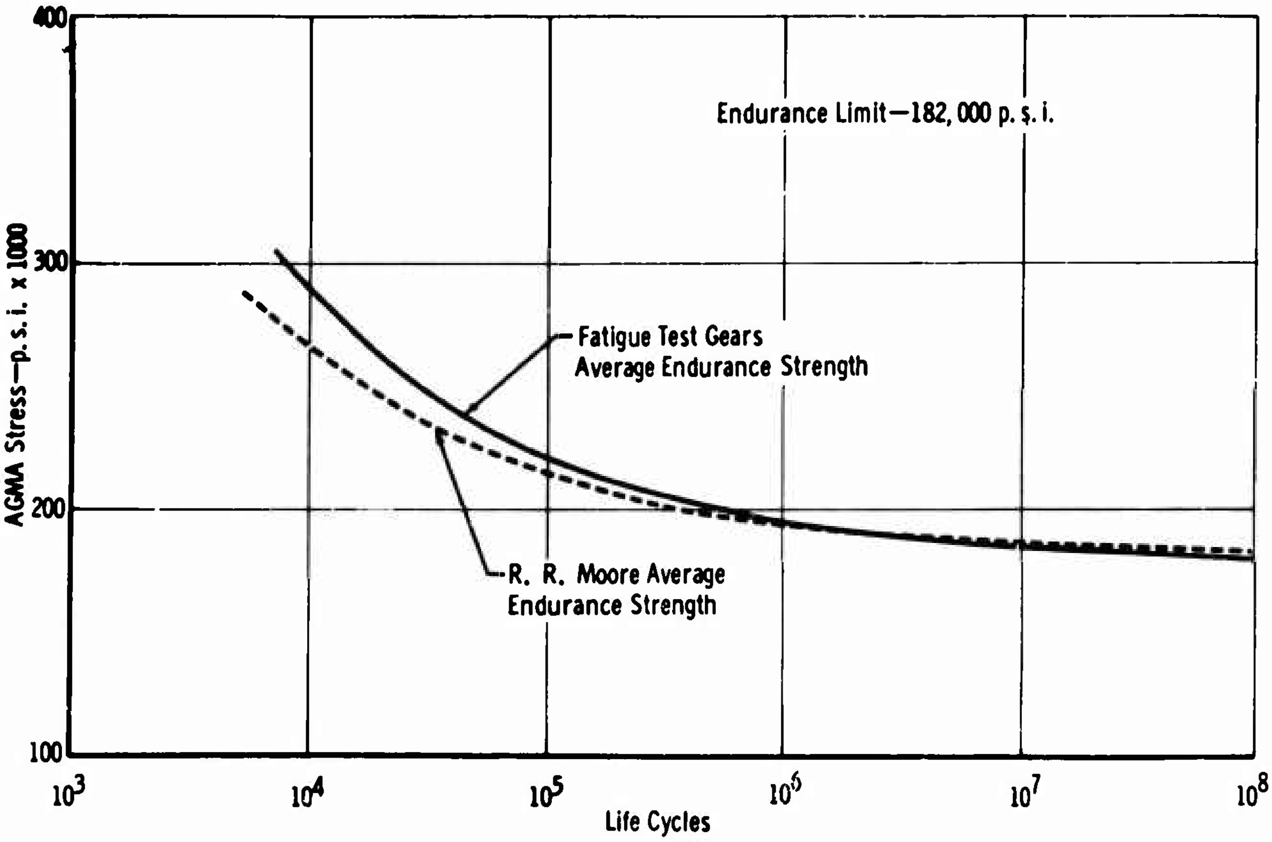

Figure 97. Average Fatigue Endurance Strengths Compared With R. R. Moore Data.

probability statement then is: "There is 95 percent probability (confidence) that at least 99 percent of the endurance limits of gears will be greater than 102,000 p.s.i.". Thus, a fatigue reliability factor of approximately 182,000/102,000 = 1.78 is indicated.

The S/N curve representing the overall average and a tolerance representing 1-percent failure are shown in Figure 100. Using the 1-percent line as a design value, it is estimated that 1 percent of the gear teeth will experience failure in bending. This statement is only an approximation, being restricted by the range of variables investigated, the significant effect of some of the geometric factors, and the limited knowledge of relating failure analysis of a single tooth to the probability of failure of one or more teeth on a gear.

LITERATURE COMPARISON

A comparison of the data with the literature indicates good correlation. Figures 101 through 104 show a comparison of the fatigue test points with the data published in reference 54. The data in the paper have been reduced to AGMA stress for comparison with the fatigue test data. In general the scatter is similar, with some fatigue points showing early failures.

Additional comparison was made with AGMA Proposed Standard 411.02, which specifies allowable endurance life values with load and stress distribution factors. This comparison is shown in Figure 105. Table XXV summarizes these data for AGMA, R. R. Moore, and the fatigue test gears. There is close correlation of the gear test data

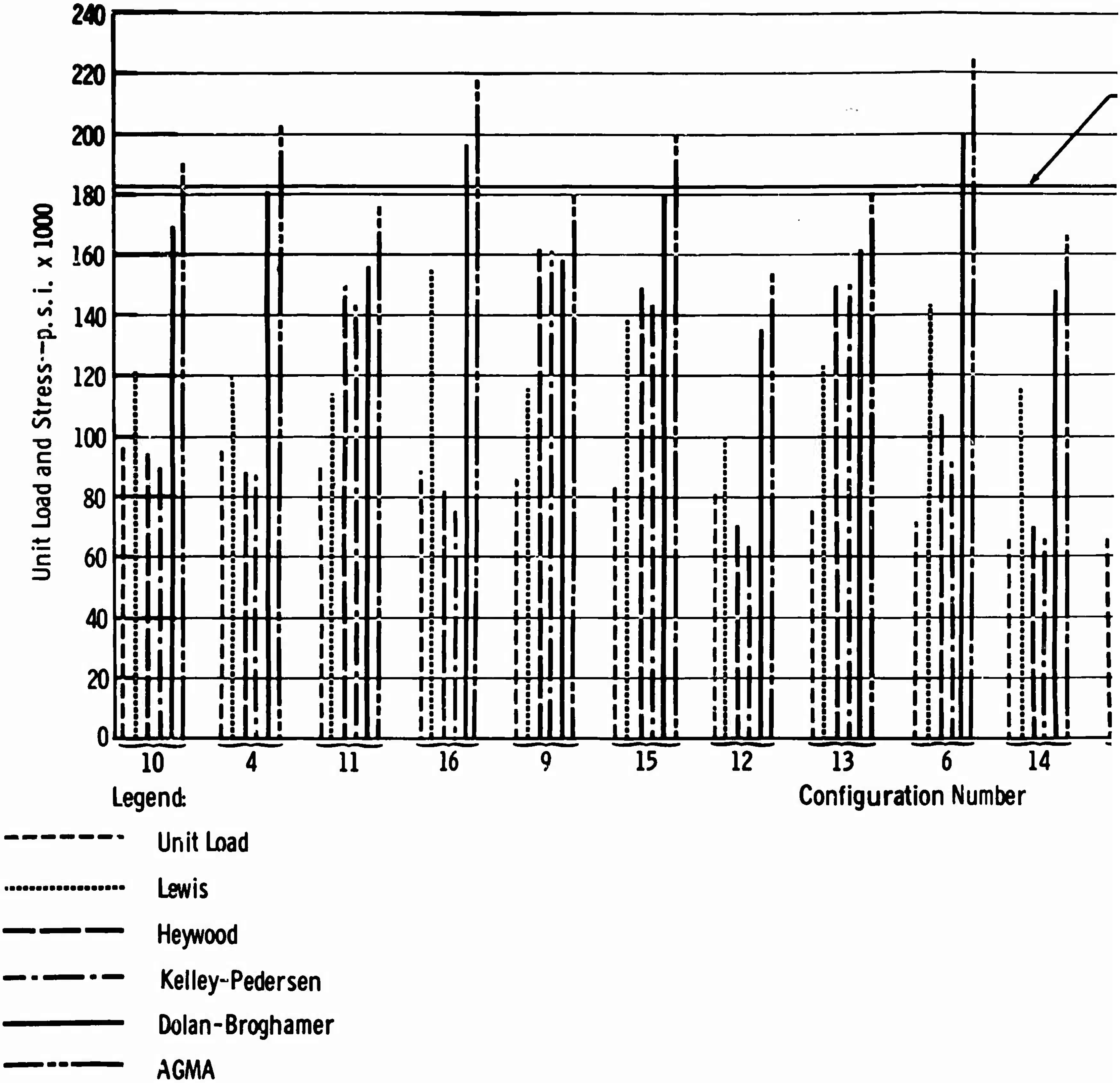

Figure 98. Methods of Calculating Stress for Endurance Strength Based on Fatigue Test Gears Compared With R. R. Moore Endurance Strength.

A

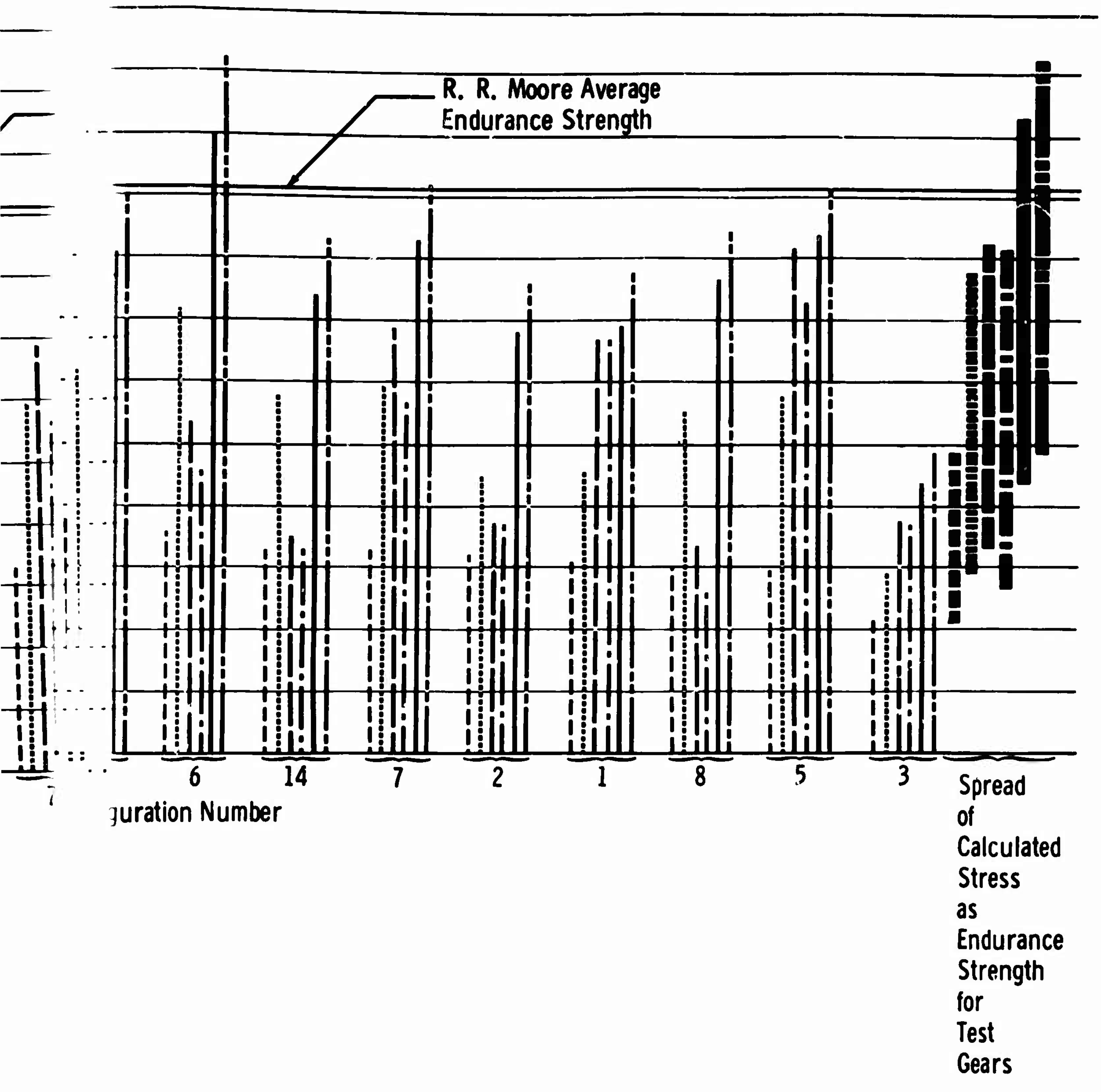
R. R. Moore Average
Endurance Strength
6
14
7
2
1
8
5
3
Spread of Calculated Stress as Endurance Strength for Test Gears
guration Number

B

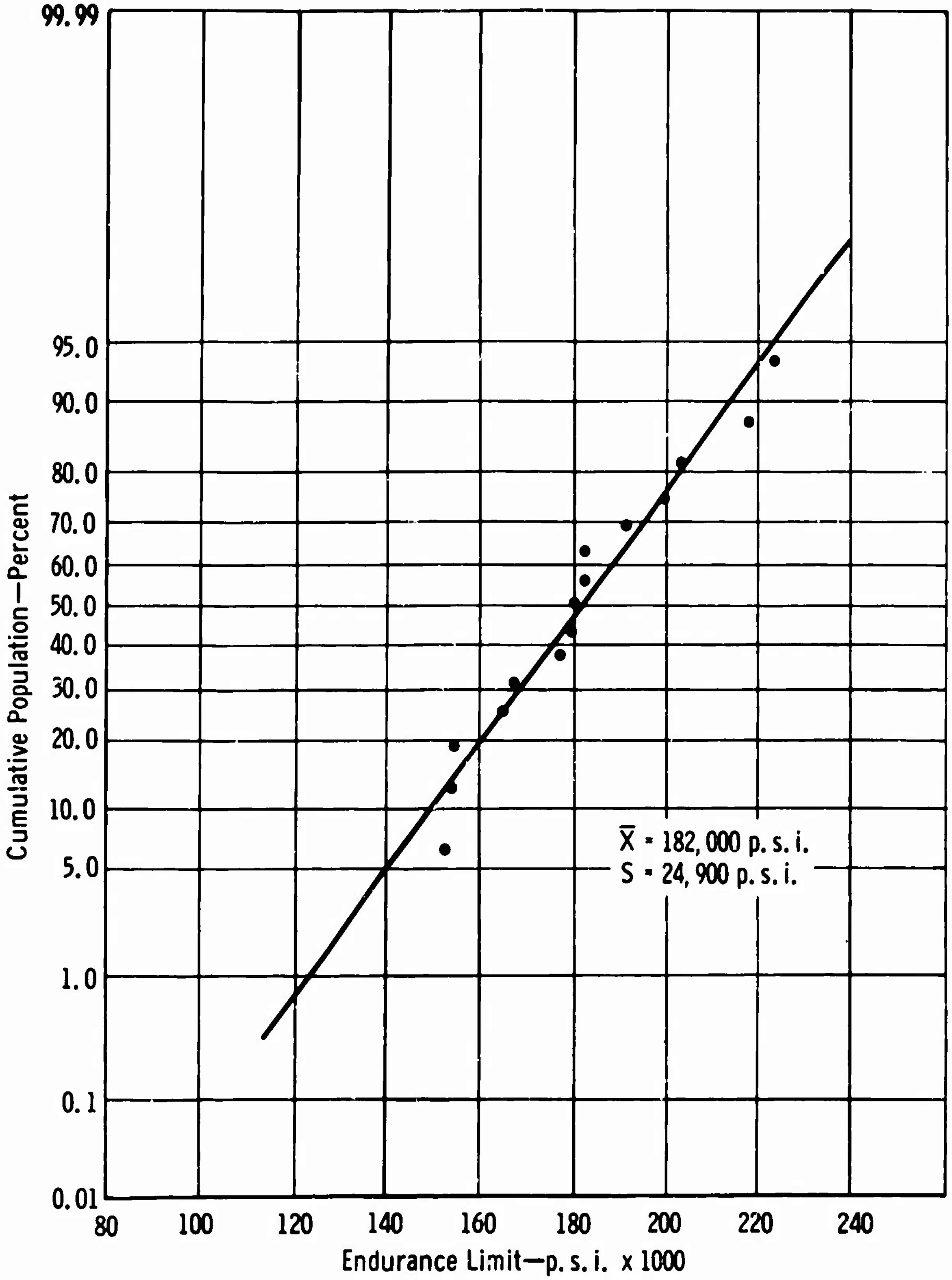

Figure 99. Distribution of Endurance Limits.

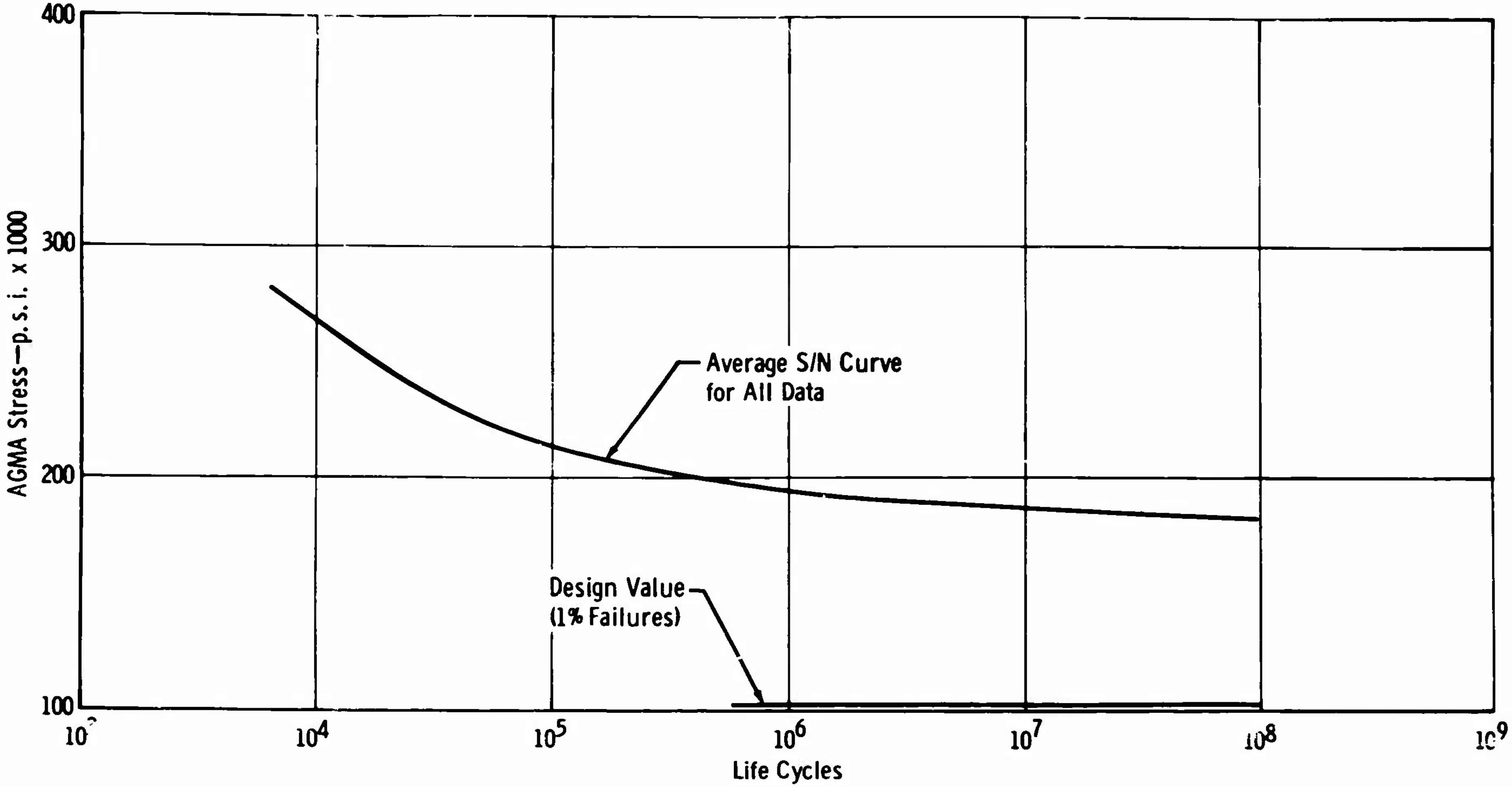

Figure 100. AGMA Average S/N Curve and Design Value.

endurance strengths for 10^7 cycle life with the basic R. R. Moore data. The selection of the load and stress distribution factors for the fatigue test gears was based on the dynamic tests (Figure 109) for a gear at 16,000 feet/minute pitch-line velocity. It is obvious that selection of the various load and stress distribution factors may change the calculated stress appreciably.

EVALUATION OF DYNAMIC EFFECTS

Centrifugal Stress

Centrifugal stress consists of two major parts—hoop stress and centrifugal force stress. The hoop stress is a circumferential tensile stress at the root diameter caused by the tendency of the rim to expand from centrifugal force. The centrifugal force stress is a radial tensile stress caused by the centrifugal force exerted by the gear tooth.

The measured centrifugal stress was found to be much higher than the calculated stress caused by centrifugal forces on the gear teeth. However, the measured stress was found to coincide closely with the calculated hoop stress. This was true for both the root and the active profile positions. This suggested that the hoop stress spread onto the active profile of the gear tooth. Figure 106 shows a comparison of calculated centrifugal force stress, calculated hoop stress, and measured centrifugal stress. The measured stress was found to be 75 percent of the calculated hoop stress.

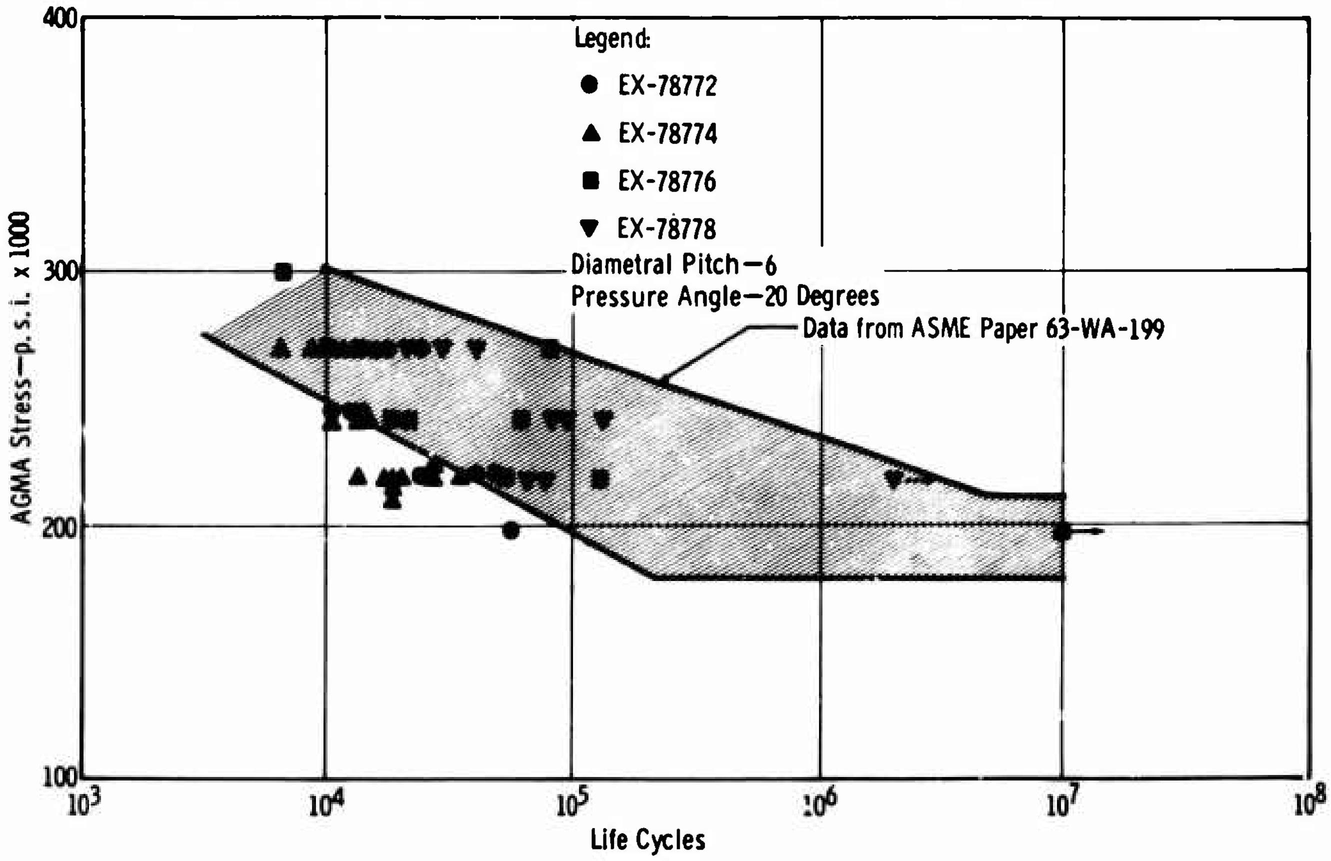

Figure 101. Comparison of Test Data With ASME Paper 63-WA-199 (Reference 54).

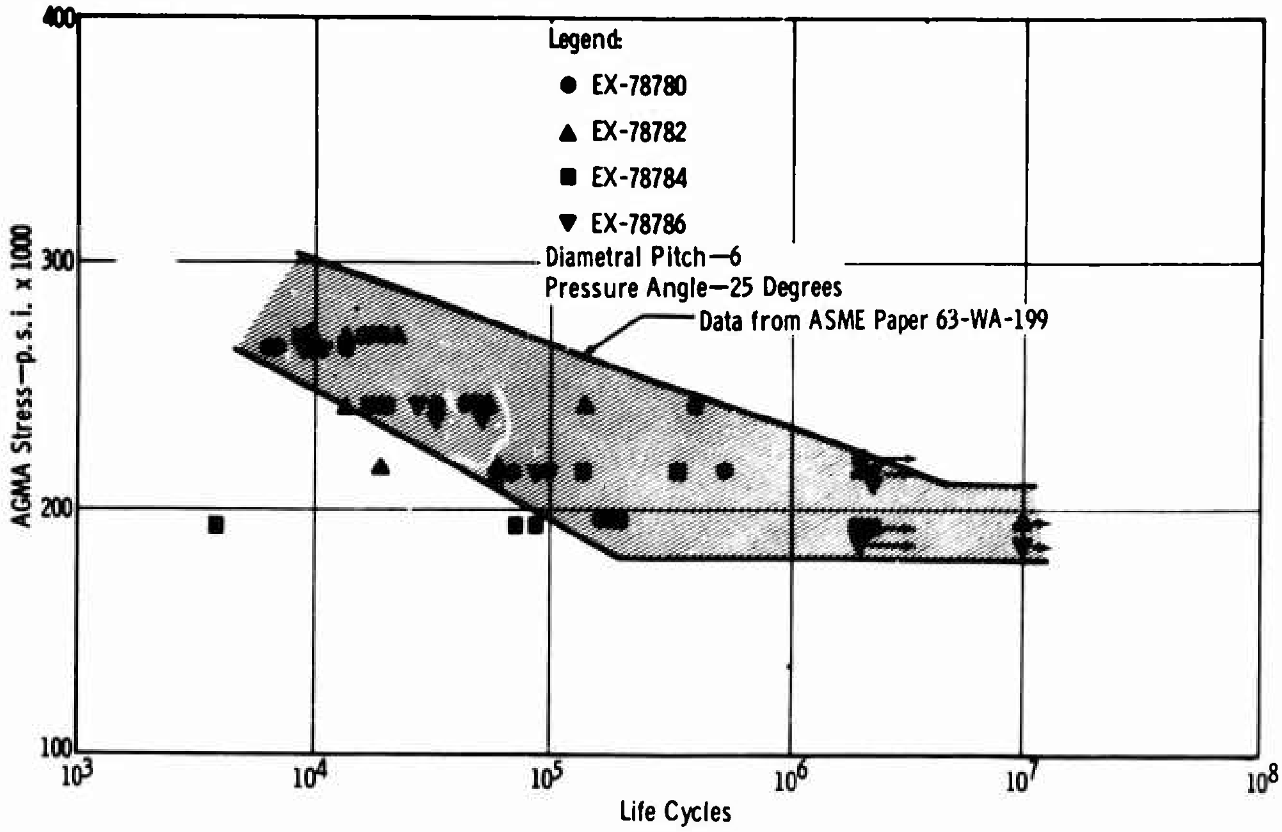

Figure 102. Comparison of Test Data With ASME Paper 63-WA-199 (Reference 54).

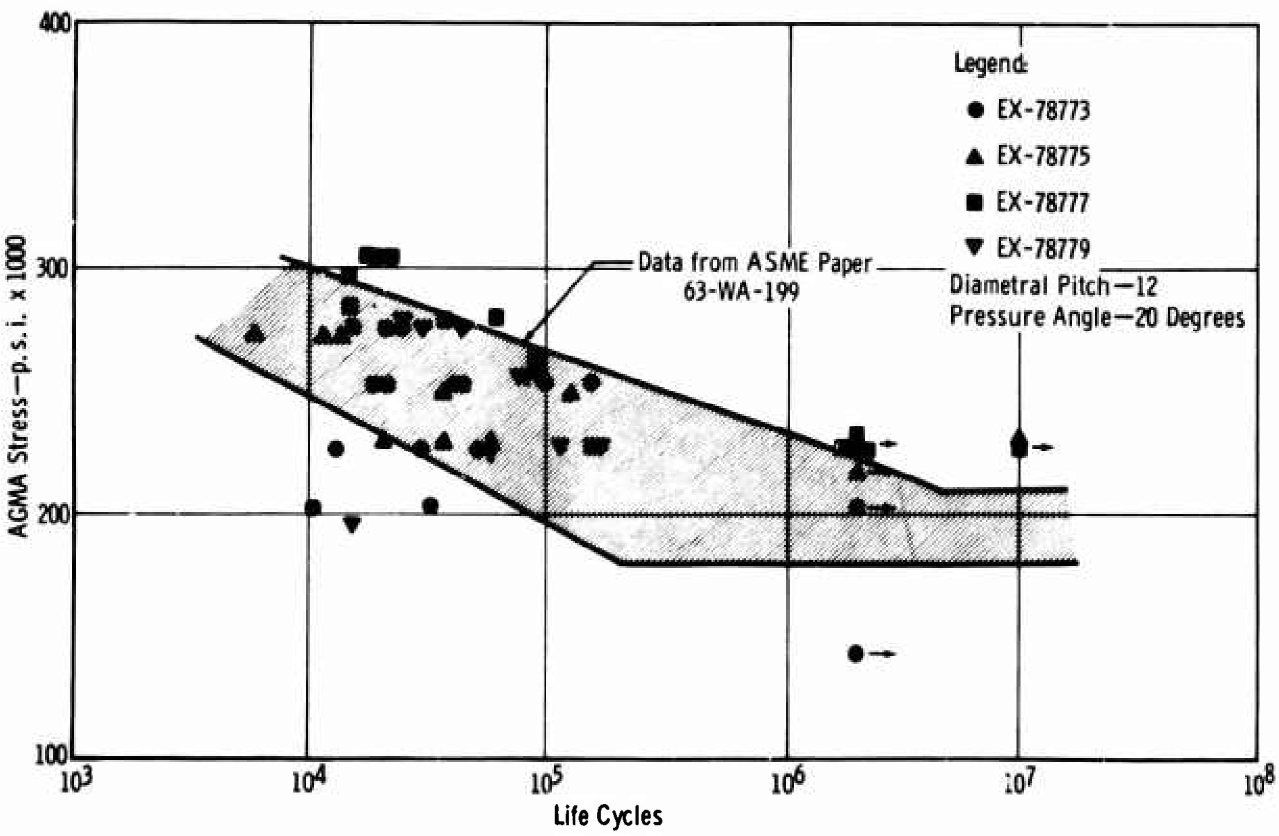

Figure 103. Comparison of Test Data With ASME Paper 63-WA-199 (Reference 54).

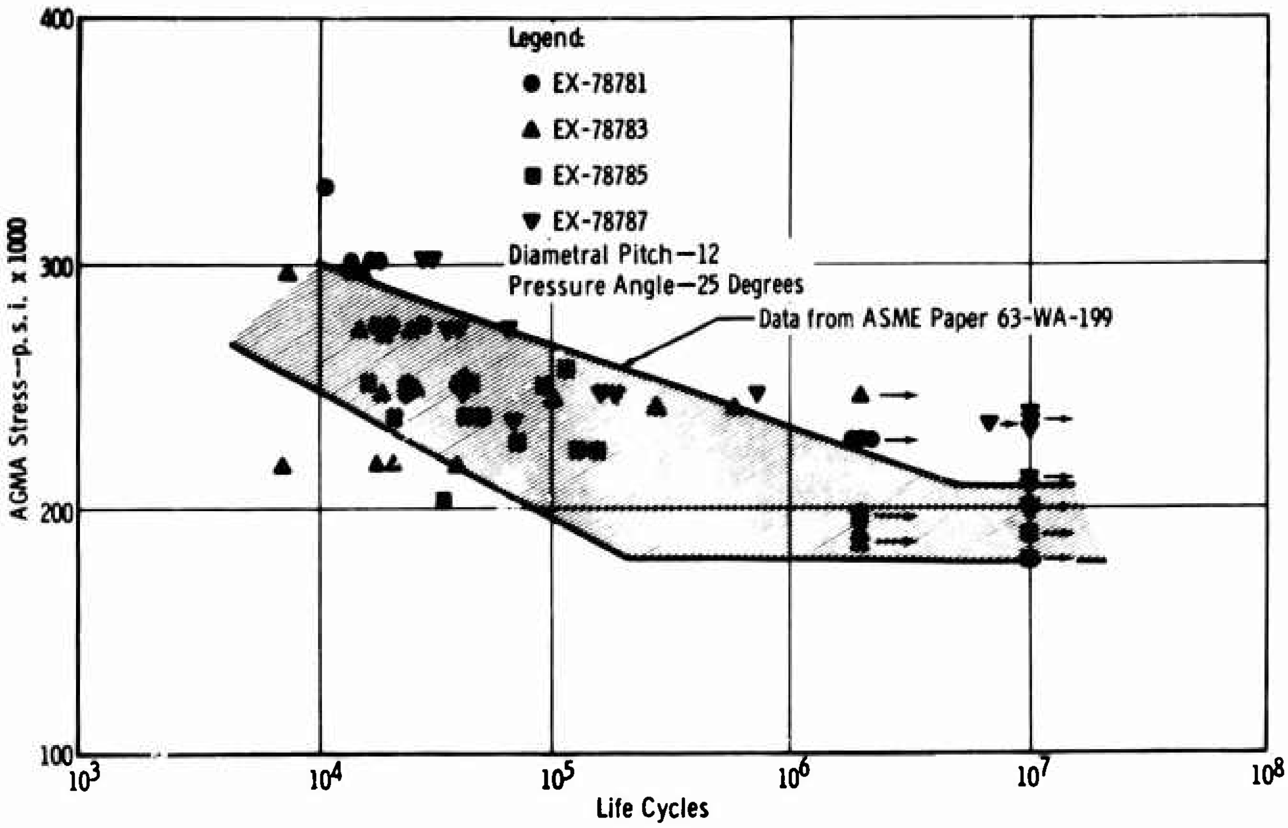

Figure 104. Comparison of Test Data With ASME Paper 63-WA-199 (Reference 54).

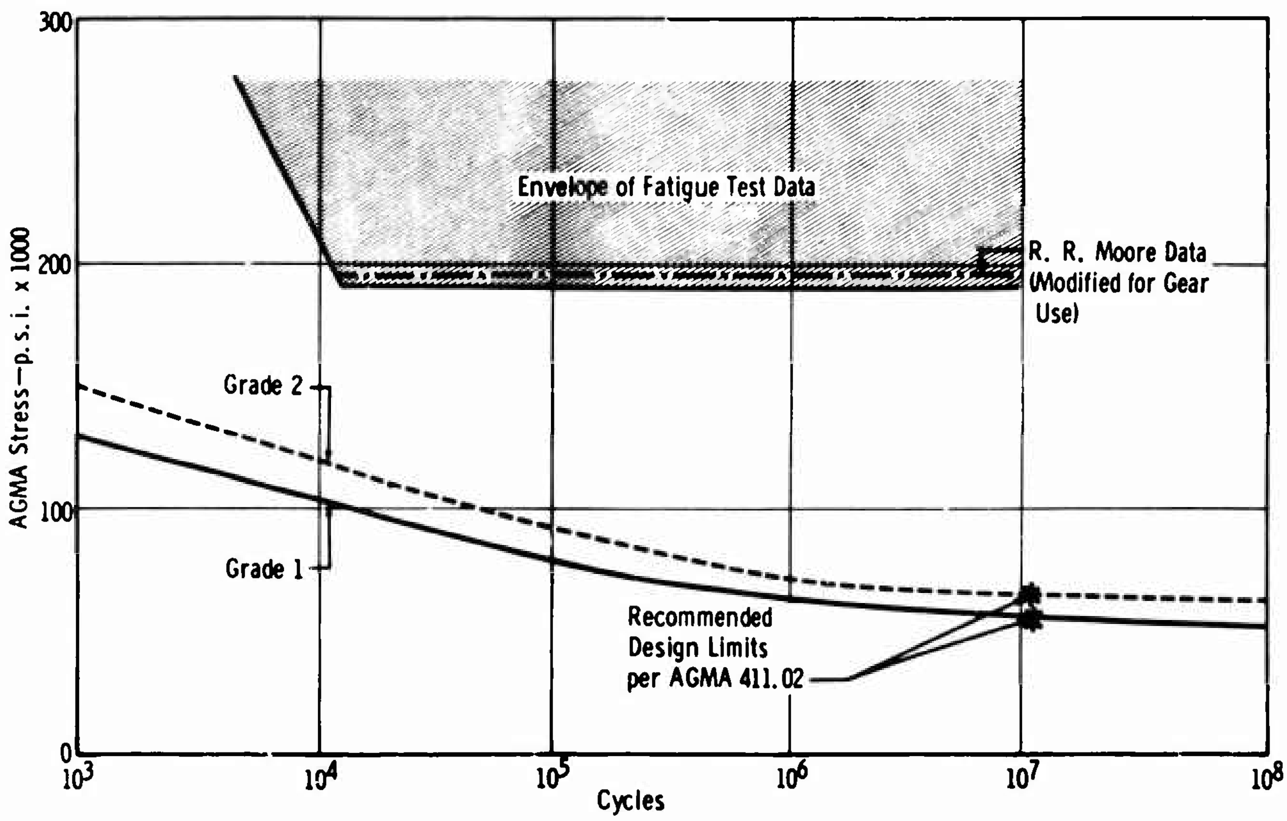

Figure 105. Comparison of Test Data With AGMA Standard 411.02 Design Limits.

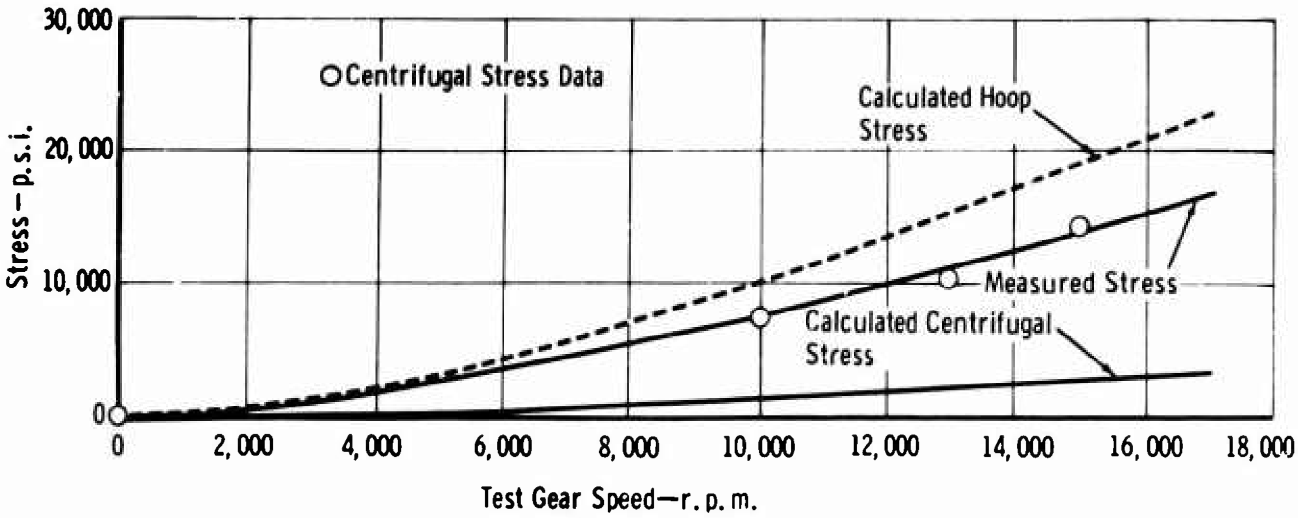

Figure 106. Comparison of Calculated and Measured Gear Stresses.

No detailed study was made of the possible effect of various gear tooth geometries and/or rim proportions on centrifugal stress at the weakest section. The similarity of the hoop stress and centrifugal force formula, both of which vary with the square of the speed, and the similarity of normal gear tooth geometry (unit diametral pitch rule) suggest that the observed proportional values should remain essentially constant. Design use of the calculated hoop stress should therefore be conservative.

Hoop stress, S_h, can be calculated by the following equation:

$$S_h = P \frac{V^2}{g}$$

where

V = velocity at rim, inches/second
P = material density, pounds/cubic inch
g = gravitational acceleration constant, 386 inches/second squared

Since the stress was desired at the root diameter, the equation may be expressed as:

$$S_h = \frac{N}{60g} P D_r = 0.000136 \, PND_r$$

where

N = rotational speed, r.p.m.
D_r = root diameter, inches
P = material density, pounds/cubic inch

Since the centrifugal stress is at a constant level (at constant speed), use of a modified Goodman diagram was required to permit combining with the alternating bending stress from the normal tooth load. See Figure 107. The S/N curve developed from the fatigue test program (Figure 97) was used at the zero centrifugal stress ordinate to construct the modified Goodman diagram. The Goodman diagram may be used to determine the endurance strength required for the bending stress calculation given a desired life, speed, and gear size.

TABLE XXV
COMPARISON OF FATIGUE TEST DATA

	Load		Stress Distribution					
	K_o (Overload)	K_v (Dynamic)	K_s (Size)	K_m (Distribution)	J (Geometry)	Centrifugal Factor	Endurance Strength from Test Data (p. s. i.)	Allowable Stress for 10^7 Cycle Life (p. s. i.)
AGMA (for typical aircraft)	Section 9* Table 4	Section 8* Figure 5	Section 7*	Section 6* Table 3	Section 5*	—	—	65, 000 Grade 2**
	1. 0	1. 0	1. 0	1. 0	0. 33	—	—	55, 000 Grade 1**
ASME 63-WA-199 (reference 54)	1. 0	1. 0	1. 0	1. 0	0. 33	—	180, 000	60, 000
R. R. Moore***	1. 0	1. 0	1. 0	1. 0	1. 0	—	195, 000	—
Fatigue Tests	1. 0	1. 0	1. 0	1. 0	0. 425	—	182, 000	102, 000 (1% Failures)
Dynamic Tests	1. 0	1. 3†	1. 0	1. 0	0. 425‡	1. 1‡	182, 000	71, 000 (1% Failures)

*AGMA Standard 220. 02 (Appendix VI herein).
**AGMA Standard 411. 02.
***Corrected data presented in the subsection titled Basic Material Strength.
† Dynamic factor for 16, 000 feet/minute per Figure 109.
‡ Stress concentration factor—average of test gears based on Lewis and measured strain gage data = 2. 42.
‡ Centrifugal factor at 16, 000 feet/minute per Figure 106.

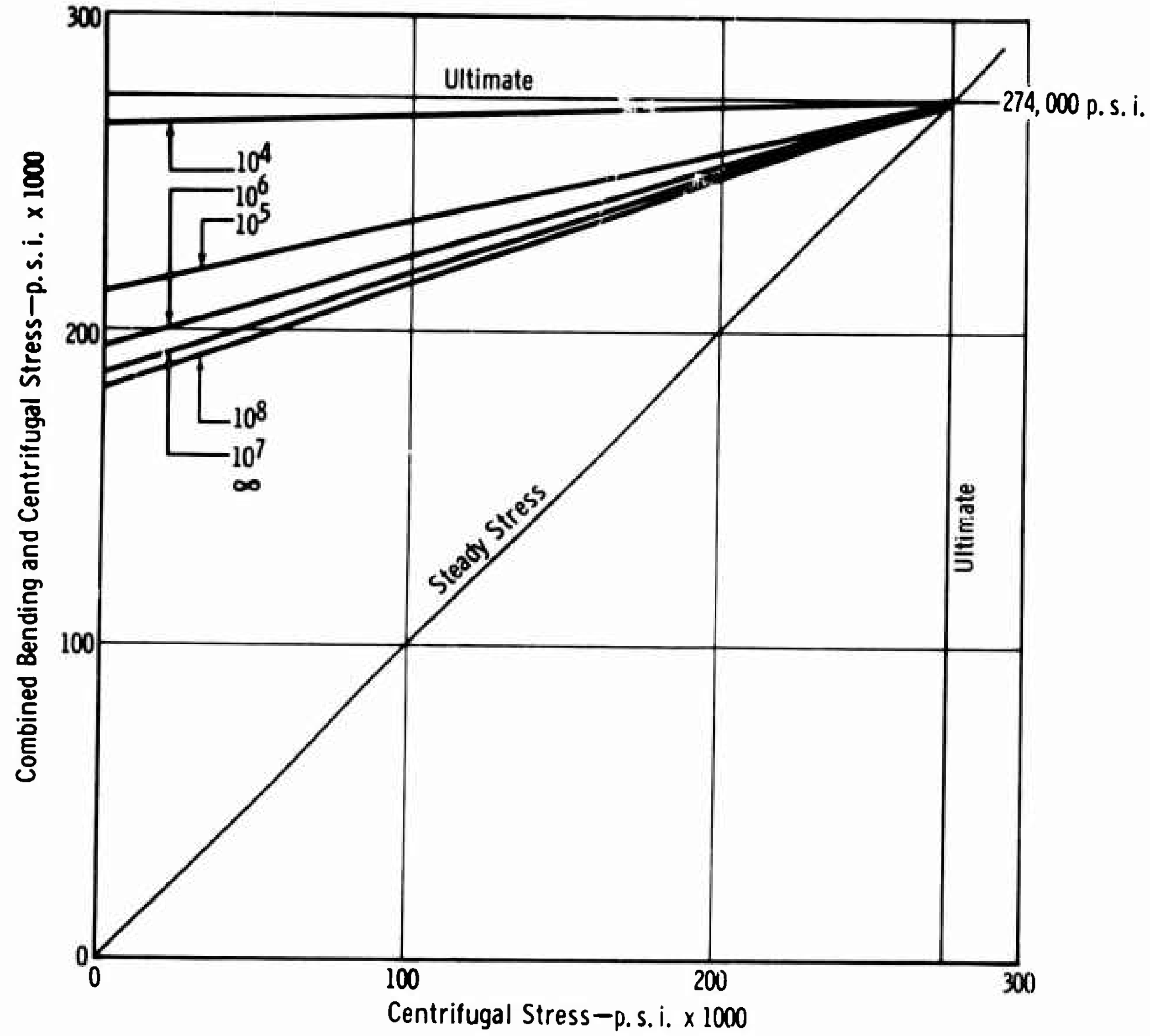

Figure 107. Modified Goodman **Diagram** Combining Centrifugal and Bending Stresses.

For example, the dynamic test gear when operating at 16,000 r.p.m. has a calculated hoop stress of 20,000 p.s.i. For 10^7 cycle life, a bending stress of 175,000 p.s.i. would be permitted based on the modified Goodman diagram. Based on direct addition of the centrifugal and bending stress (an improper procedure), the S/N curve would permit only 162,000-p.s.i. bending stress. Also, this gear, if designed for 10^7 cycle life without considering centrifugal stress, would actually have a mean life expectancy of slightly less than 10^5 cycles or only 1 percent of that anticipated. To calculate a more comprehensive gear tooth bending stress under high-speed operating conditions, the hoop stress must be combined with bending stress by use of the modified Goodman diagram.

Dynamic Stress

Figure 108 is a plot of the peak dynamic stress versus r.p.m. The strain readings were converted to stress and plotted against gear r.p.m. for three load conditions—380,

570, and 766 pounds (1000, 1400, and 2000 pounds/inch of face width). The curves represent the best fit square curve above the static base line; thus, the amount of increase above the static stress level is equal to the square of the ratio of the speed. The static stress level is the measured stress at zero r. p. m. for pure tangential load. It was felt that a square curve would be the most desirable, since the dynamic effect could be related to kinetic energy which involves velocity squared. Again, the measured dynamic stress does not include any constant centrifugal stress.

Figure 109 shows a dynamic stress correction factor derived from the curves in Figure 108.

Figure 110 is a comparison of the dynamic factor as previously described with the one given in AGMA Standards 220. 02 (Appendix VI). Curves 1, 2, and 3 represent various grades of gear quality with 1 being the highest quality gear. The propeller brake gear used in testing would be defined as a grade 1 gear. The two curves agree within 8 percent at 8000 feet/minute. Also, the AGMA data do not exceed 8000 feet/minute.

Although the dynamic data presented are very limited, they do indicate trends for high speed, lightweight gearing. It is recommended, therefore, that the curve of Figure 109 be used as a design factor for applications above 8000 feet/minute. Below this speed, a factor of one should be satisfactory for close-tolerance aircraft applications.

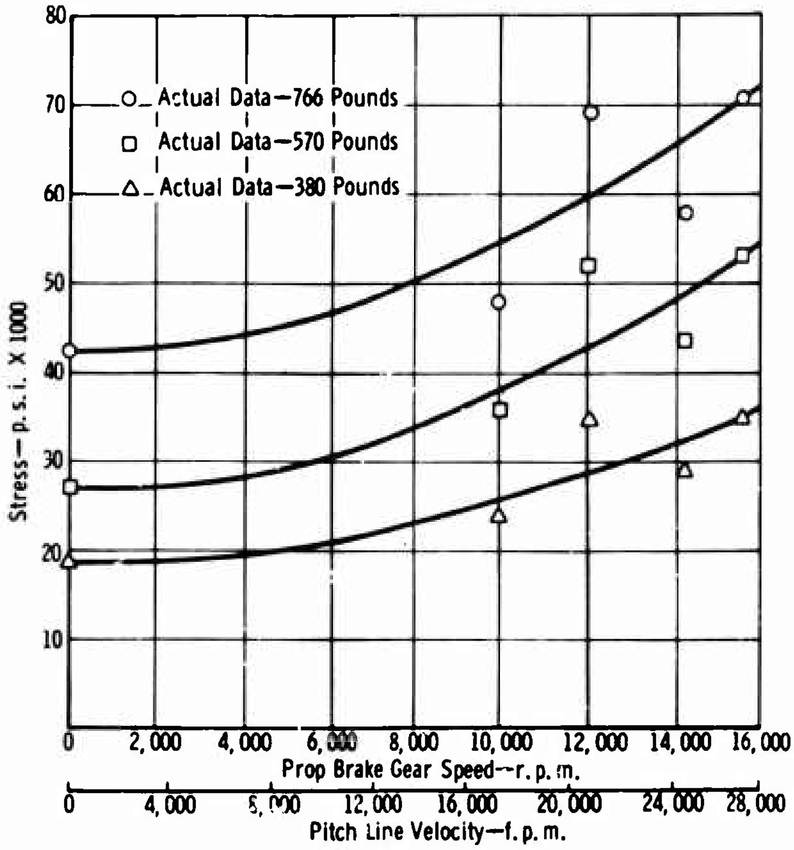

Figure 108. Graph Showing Peak Dynamic Stresses During Testing.

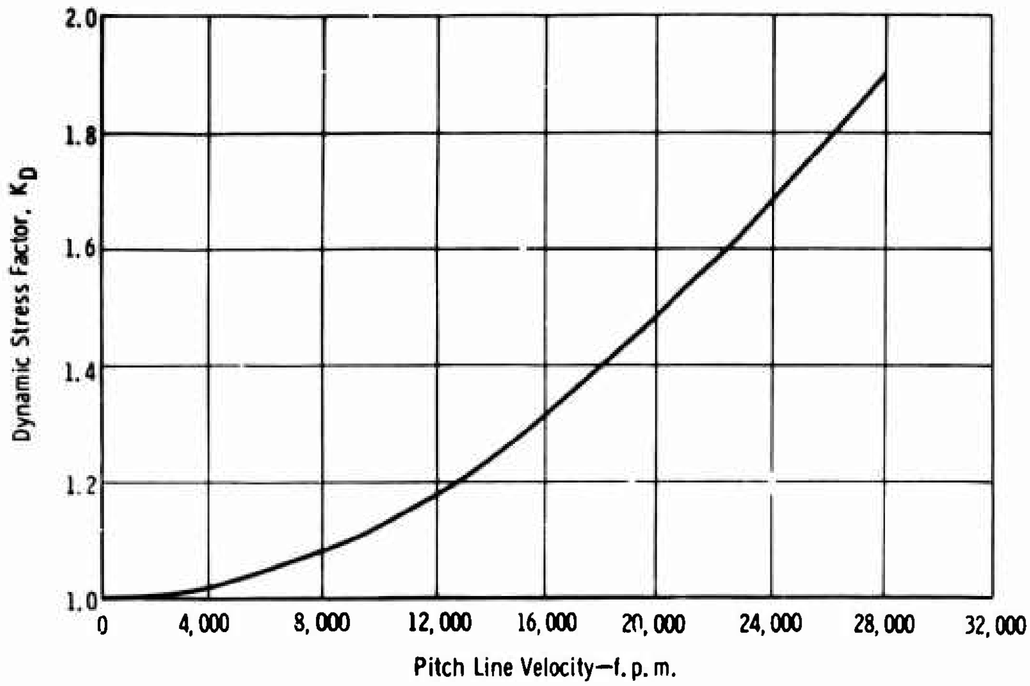

Figure 109. Dynamic Stress Factor as a Function of Pitch Line Velocity.

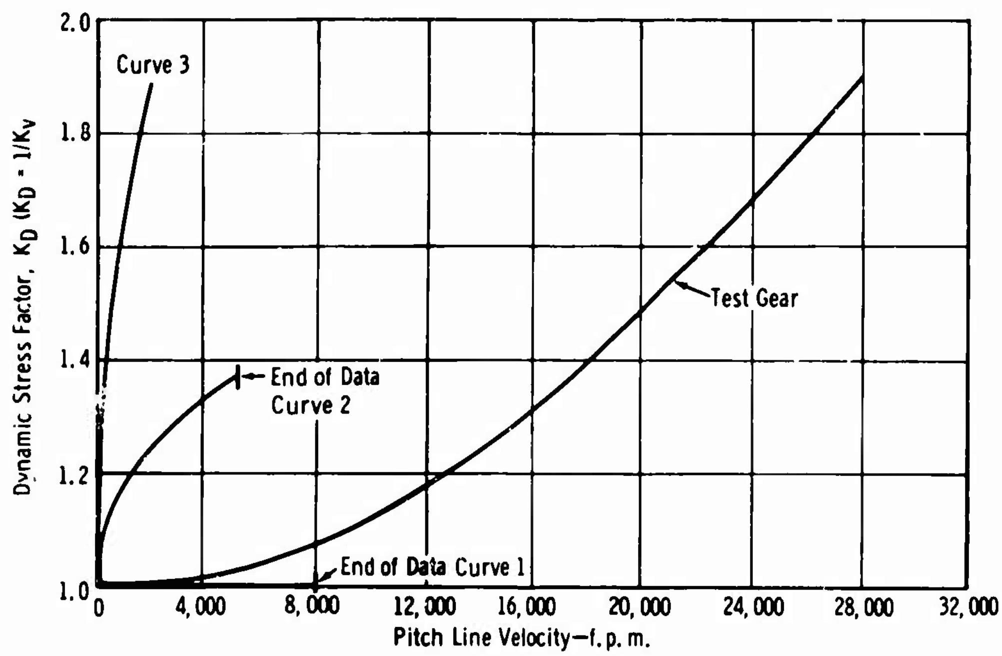

Figure 110. Comparison of Dynamic Stress Factors.

ESTABLISHMENT OF COMPUTER PROGRAM

Analysis of the fatigue test data indicates that the AGMA formula is the most accurate for predicting ranking, produces the least variation in calculated endurance limits, best matches experimentally measured stresses, and accommodates the geometric variables with the least difference of significant values. The AGMA formula was selected, therefore, for use in the computer program. The AGMA formula also is a well known method–it is required by some Government specifications (reference 47).

The Lewis gear tooth geometry form factor values (Y), as calculated by the computer, should be more accurate than values normally obtained by graphical layouts. The point of tangency between the inscribed parabola and the generated trochoidal root fillet as well as the trochoidal root fillet contour can be established with precision.

A dynamic factor is an input item of the computer program. The dynamic factor for a given application may be obtained from existing AGMA curves, the curve presented in Figure 109, literature sources, or from direct "in-house" measurements.

Hoop stress is calculated in the program and combined with the AGMA calculated bending stress based on the modified Goodman diagram. A mathematical expression for the combined stress is:

$$S_c = US - \frac{US\left[US - (S_h + S_t)\right]}{US - S_h}$$

where

S_c = combined stress, p. s. i.
S_h = hoop stress, p. s. i. (reference page 130)
S_t = tensile stress (AGMA), p. s. i. (reference page 10)
US = ultimate strength of the material, p. s. i.

Life cycles are then determined from the combined stress and the S/N curve based on R. R. Moore rotating beam tests of the gear material. The life may be modified further by the AGMA temperature factor and reliability factor (factor of safety) as indicated by the expression:

$$L \propto S_c K_T K_R$$

where

L = life in cycles
S_c = combined stress, p. s. i.
K_T = AGMA temperature factor (reference page 11)
K_R = AGMA factor of safety (reference page 11)

The term $\propto$ indicates the S/N curve stress-to-life cycle relationship.

Both AGMA bending stress and the combined bending and hoop stresses are printed out. Life is printed out if it is in the finite life area of the modified Goodman diagram; otherwise, an infinite life or an excessive stress note is printed.

Considerable effort was expended in graphical analysis of the Lewis gear tooth form factor Y and its relationship to the Dolan-Broghamer stress concentration factor K_f.

It is expected that strength and stress concentration factors should be geometrically related. Gear sets with the following range of parameters were computed and plotted:

- Pressure angle—14.5, 20, and 25 degrees
- Number of teeth in pinion—12 through 52
- Gear ratio—1.0 through 10.0
- Hob tip radius—100, 75, 50, and 25 percent of maximum possible
- Dedendum factor—1.157, 1.2, 1.3, and 1.4
- Tooth thickness at pitch diameter—100, 90, and 110 percent of half of the circular pitch

The parametric plots were not smooth, overlapping curves as expected. The original Dolan-Broghamer data (from reference 16) were therefore analyzed. Computer-determined dimensions (h, t, and θ_L) for the given gear teeth do not coincide with the dimensions for the plastic models as tabulated in reference 16. The computer values plot as smooth curves while the original data do not; this indicates that the error is most likely that which is inherent with the drafting layout procedure. Computed K_f values based on corrected geometry and observed stresses produce data which vary by ± 11 percent from that computed by the formula as indicated in Table XXVI.

Work to generate a formula to duplicate the corrected stress concentration factors obtained has not been completed.

The Dolan-Broghamer photoelastic data were obtained from models having pressure angles of 14.5 and 20 degrees, diametral pitch of 2, and a dedendum factor of 1.157. Graphical analyses should be used with the new stress concentration formula to determine the validity of the extrapolation if K_f values throughout the range of gear tooth geometric variables, as previously investigated. Similar analysis of additional photoelastic data (such as from Kelley-Pedersen work) would be valuable for correlation.

A new stress concentration factor, developed as described, would considerably enhance the correlation of the test data and would be a valuable modification to the AGMA formula and the computer program.

TABLE XXVI
COMPARISON OF STRESS CONCENTRATION FACTORS

Model Number	K_f (Dolan-Broghamer)	K_f (AGMA)	K_f (Calculated)	K_f(Calculated)/K_f(AGMA)
6-1	1.53	1.511591	1.500636	0.99272
6-2	1.65	1.647910	1.733851	1.05218
6-3	1.82	1.832482	1.876810	1.02417
6-4	2.18	2.097727	2.117530	1.00943
6-5	1.56	1.558408	1.638576	1.05146
6-6	1.68	1.694056	1.817664	1.07295
6-7	1.86	1.877288	1.959995	1.04405
6-8	2.10	2.141456	2.287704	1.06826
6-9	1.68	1.644061	1.826440	1.11088
6-10	1.76	1.783399	1.936391	1.08579
6-11	1.94	1.970920	2.057944	1.04414
6-12	2.21	2.241207	2.314211	1.03257

TABLE XXVI (CONT)

Model Number	K_f (Dolan-Broghamer)	K_f (AGMA)	K_f (Calculated)	K_f(Calculated)/K_f(AGMA)
7-1	1.57	1.588621	1.589230	1.00037
7-2	1.68	1.735900	1.746881	1.00633
7-3	1.93	1.936614	1.882616	0.97211
7-4	2.37	2.228237	2.168161	0.97307
7-5	1.69	1.664860	1.788942	1.07747
7-6	1.86	1.810860	1.843543	1.01800
7-7	2.04	2.008900	1.986026	0.98860
7-8	2.30	2.297209	2.124755	0.92495
7-9	1.74	1.750553	1.938912	1.10756
7-10	1.90	1.899773	2.085223	1.09758
7-11	2.10	2.101321	2.215057	1.05420
7-12	2.40	2.394263	2.368038	0.98905
8-1	1.62	1.629011	1.687625	1.03597
8-2	1.74	1.782054	1.782343	1.00011
8-3	1.94	1.991574	1.913581	0.96083
8-4	2.25	2.298240	2.063709	0.89796
8-5	1.74	1.724950	1.883809	1.09205
8-6	1.86	1.876333	1.956013	1.04247
8-7	2.06	2.082457	2.165639	1.03990
8-8	2.31	2.384652	2.271327	0.95244

Notes: K_f (Dolan-Broghamer) from reference 16 based on observed stress.

K_f (AGMA) computed by formula from corrected geometry.

K_f (Calculated) computed from corrected geometry and observed stress.

CONCLUSIONS

The following conclusions are made from this study.

- The investigation of four geometric variables indicated that the endurance strength was significantly affected by changes in pitch diameter and pressure angle. These effects were in some instances greater than those predicted by bending stress calculations. The effects of fillet size and fillet configuration—full form or protuberance—were not significant with respect to the endurance strength of the configurations tested. Stress calculations did not accurately consider the fillet configuration.
- A basic material strength curve for carburized AMS-6265 was established by R. R. Moore specimens. This strength curve correlated very closely with the AGMA method of calculating stress.
- By averaging all fatigue test data points, a design S/N curve was established. For design purposes, a 1-percent failure endurance strength of 102,000 p.s.i. was also established.
- Of the five strength formulas investigated, the AGMA bending strength formula provides the most accurate method for assessment of spur gear tooth bending strength.
- The limited dynamic testing conducted indicated that a dynamic factor for light-weight aircraft gears should be considered for applications with a pitch line velocity over 8000 feet/minute.
- A centrifugal speed factor is necessary for high pitch line velocity applications.
- A modification is required to the Dolan-Broghamer stress concentration factor used in the AGMA formula to consider tooth geometry more accurately.
- The AGMA formula modified to incorporate a centrifugal speed, a high speed dynamic factor, and to use R. R. Moore material strength data will produce an accurate estimate of gear tooth bending stress and life. The dynamic fluctuating stress calculated by the AGMA formula, $S_t = \frac{W_t K_o}{K_v} \frac{P_d}{F} \frac{K_s K_m}{J}$, is combined with the steady centrifugal hoop stress formula, $S_n = \rho \frac{V^2}{g}$, to produce a combined stress, S_c, as follows:

$$S_c = US - \frac{US\left[US - (S_h + S_t)\right]}{US - S_h}$$

The terms are defined on page 135. Life cycles may then be determined from an S/N curve based on R. R. Moore rotating beam tests of the gear material. The life may be modified further by the AGMA temperature and reliability factors as follows:

$$L \propto S_c K_T K_R$$

BIBLIOGRAPHY

1. Aida, T., and Ferauchi, Y., "On the Bending Stress of a Spur Gear," Japanese Society of Mechanical Engineers, Volume 5, Number 17, 1962, pp. 161-183.

2. Almen, J. O., and Straub, J. C., "Factors Influencing the Durability of Automobile Transmission Gears," Automotive Industries, 25 September and 9 October 1937.

3. Anderson, R. L., and Bancraft, T. A., Statistical Theory in Research, First Edition, McGraw-Hill Book Company, Inc., New York, 1952.

4. Attia, A. Y., "Dynamic Loading of Spur Gear Teeth," Transactions of the American Society of Mechanical Engineers—Journal of Engineering for Industry, February 1959, pp. 1-9.

5. Baud, R. V., and Hall, E., "Stress Cycles in Gear Teeth," Mechanical Engineering, Volume 53, Number 3, 1931, pp. 207-210.

6. Baud, R. V., and Peterson, R. E., "Load and Stress Cycles in Gear Teeth," Mechanical Engineering, Volume 51, Number 9, May 1929, pp. 653-662.

7. Black, P. H., An Investigation of Relative Stresses in Solid Spur Gears by the Photoelastic Method, Bulletin Series Number 288, University of Illinois Engineering Experiment Station, Urbana, Illinois, December 1936.

8. Borsoff, V. N., Accinelli, J. B., and Cattaneo, A. G., "Effect of Oil Viscosity on the Power Transmitting Capacity of Spur Gears," Transactions of American Society of Mechanical Engineers, Volume 73, 1951, pp. 687-696.

9. Botstiber, D. W., "Manufacturing Methods of Power Transmission Gears and Their Influence on Design Considerations," Mechanical Engineering, 1954, pp. 735-738.

10. Brugger, H., "Running Tests as a Basis for Selecting Heat-Treated Gears," Autobiltechnische Zeitschrift (ATZ), Volume 57, May 1955, pp. 127-132.

11. Buckingham, E., Analytical Mechanics of Gears, First Edition, Second Impression, McGraw-Hill Book Company Inc., New York, 1949.

12. Buckingham, E., Manual of Gear Design, Volumes 1, 2, and 3, Industrial Press, New York, 1955.

13. Buckingham, E., Spur Gears—Design, Operation, and Production, First Edition, Ninth Impression, McGraw-Hill Book Company Inc., New York, 1928.

14. Cochram, W. G., and Cox, G. M., Experimental Designs, Second Edition, John Wiley and Son, Inc., New York, 1960.

15. Davis, W. O., Gears for Small Mechanisms, N.A.G. Press Limited, London, England, 1953.

16. Dolan, T. J., and Broghamer, E. L., A Photoelastic Study of Stresses in Gear Tooth Fillets, Bulletin Series Number 335, University of Illinois Engineering Experiment Station, Urbana, Illinois, 1942.

17. Dolan, T. J., "Influence of Certain Variables on the Stresses in Gear Teeth," Journal of Applied Physics, Volume 12, August 1941, pp. 584-591.

18. Dudley, D. W., Gear Handbook, First Edition, McGraw-Hill Book Company Inc., New York, 1962.

19. Dudley, D. W., Practical Gear Design, First Edition, McGraw-Hill Book Company Inc., New York, 1954.

20. Forrest, P. G., Fatigue of Metals, Pergamon Press, Long Island City, New York, 1962.

21. Fosberry, R. A. C., and Mansion, H. D., Bending Fatigue Strength of Gear Teeth: A Comparison of Some Typical Gear Steels, The Motor Industries Research Association Report Number 1950/7, London, England, July 1950.

22. Fosberry, R. A. C., Bending Fatigue Strength of Gear Teeth: Preliminary Report, The Motor Industries Research Association Report Number 1949/7, London, England, December 1949.

23. Glaubitz, H., "The Influence of Fillet Radius on the Fatigue Strength of Spur Gears," The Engineers' Digest, Volume 19, Number 8, August 1958, pp. 342-345.

24. Grant, G. B., A Treatise on Gear Wheels, Twentieth Edition, Philadelphia Gear Works Incorporated, Philadelphia, Pennsylvania, 1899.

25. Grosser, C. E., "Involute Gear Geometry," Transactions of American Society of Mechanical Engineers, Volume 71, 1949, pp. 535-554.

26. Hald, A., Statistical Theory with Engineering Applications, First Edition, Third Printing, John Wiley and Sons Incorporated, New York, December 1957.

27. Halsey, F. A., "Some Special Forms of Computers," Transactions of American Society of Mechanical Engineers, Volume 18, 1897, pp. 70-74.

28. Heymans, P., and Kimball, A. L. "Distribution of Stresses in Electric-Railway Motor Pinions as Determined by the Photoelastic Method," Transactions of American Society of Mechanical Engineers, Volume 44, 1922, pp. 513-545.

29. Hicks, C. R., Fundamental Concepts in the Design of Experiments, First Edition, Holt, Rinehart and Winston, New York, 1965.

30. Johnson, S. J., Controlling Tooth Fillet Contours to Increase Finished Gear Strength, American Gear Manufacturers Association Paper 129.16, June 1965.

31. Jones, F. R., "Diagrams for Relative Strength of Gear Teeth," Transactions of American Society of Mechanical Engineers, Volume 18, 1897, pp. 766-794.

32. Kelley, B. W., and Pedersen, R., The Beam Strength of Modern Gear Tooth Design, Caterpillar Tractor Company, Society of Automotive Engineers Paper presented in October 1956.

33. Lewis, F. M., "Load Distribution of Reduction Gears," Transactions of American Society of Mechanical Engineers, Volume 67, 1945, pp. A87-A90.

34. Lewis, W., "Experiments on the Transmission of Power by Gearing," Transactions of American Society of Mechanical Engineers, Volume 7, 1886, pp. 273-310.

35. Lewis, W., "Gear Testing Machine," Transactions of American Society of Mechanical Engineers, Volume 36, 1914, pp. 231-237.

36. Lewis, W., "Interchangeable Involute Gearing," Transactions of American Society of Mechanical Engineers, Volume 32, 1910, pp. 823-851.

37. Lipson, C., and Juvinall, R. C., Handbook of Stress and Strength: Design and Material Applications, First Printing, The Macmillan Company, New York, 1963.

38. Love, R. J., and Campbell, J. G., Bending Strength of Gear Teeth: A Comparison of Some Carburizing Steels, The Motor Industries Research Association Report Number 1952/5, London, England, December 1952.

39. Love, R. J., Bending Fatigue Strength of Carburized Gears: A Comparison of Some Production Methods, The Motor Industries Research Association Report Number 1953/4, London, England, September 1953.

40. Love, R. J., White, D., and Allsopp, H. C., Bending Fatigue Strength of Some Induction Hardened, Pack Carburized and Gas Carburized Gears, The Motor Industry Research Association Report, London, England, September 1954.

41. Mansion, H. D., A Hydraulic Fatigue Testing Machine for Gear Teeth, The Motor Industry Research Association Report Number 1949/4, London, England, 1949.

42. Marx, G. H., and Cutter, L. E., "The Strength of Gear Teeth," Transactions of American Society of Mechanical Engineers, Volume 37, 1915, pp. 503-530.

43. Marx, G. H., "The Strength of Gear Teeth," Transactions of American Society of Mechanical Engineers, Volume 34, 1912, pp. 1323-1398.

44. Mayo, J. B., "A Strength of Gear Chart," Transaction of American Society of Mechanical Engineers, Volume 19, 1898, pp. 109-118.

45. Meier, D. R., and Rhoads, J. C., "Design and Application of Rail-Transportation Gearing," Transactions of American Society of Mechanical Engineers, Volume 68, 1946, pp. A127-A136.

46. Merritt, H. E., Gears, Third Edition, 1955 Printing, Sir Isaac Pitman and Sons Limited, London, England, 1942.

47. MIL-G-17859A (Ships), Military Specification—Gear Assembly, Propulsion (Naval Shipboard Use), January 1966.

48. **Natrella, M. G., Experimental Statistics (NBS Handbook 91), First Edition, U.S. Government Printing Office, Washington**, D. C., 1963.

49. **Nieman, G., and Glaubity, H.,** "Tooth Dedendum Strength of Straight Steel Spur **Gears," VDI-Zeitschrift, Volume** 92, Number 33, 1950, pp. 923-932.

50. **Poritsky, H., Sutton, A. D., and** Pernick, A., "Distribution of Tooth Load Along **a Pinion," Transactions** of American Society of Mechanical Engineers, Volume 67, **1945, pp. A78-A86.**

51. Proceedings of the International Conference on Gearing, Institute of Mechanical Engineers, London, England, 1958.

52. Reswick, J. B., "Dynamic Loads on Spur and Helical Gear Teeth," Transactions of American Society of Mechanical Engineers, Volume 77, 1955, pp. 635-644.

53. Roark, R. J., Formulas for Stress and Strain, Second Edition Seventh Impression, McGraw-Hill Book Company Inc., New York, 1943.

54. Seabrook, J. B., and Dudley, D. W., "Results of a Fifteen Year Program of Flexural Fatigue Testing of Gear Teeth," American Society of Mechanical Engineers, Paper Number 63-WA-199, 17 November 1963.

55. Semar, H. W., and McGinnis, [illegible], "Experimental Determination of Gear Tooth Stresses in Large Marine Gears," Transactions of the American Society of Mechanical Engineers, Volume 80, January 1958, pp. 195-201.

56. Small, N. C., "Bending of a Cantilever Plate Supported from an Elastic Half Space," Transactions of American Society of Mechanical Engineers, Volume 83, 1961, pp. 387-394.

57. Thum, A., and Richard, K., "Working Stresses and Working Strength of Spur Gears," The Engineers' Digest, Volume 14, Number 1, January 1953, pp. 9-12.

58. Timoshenko, S, and Baud, R. V., "The Strength of Gear Teeth," Mechanical Engineering, Volume 48, Number 11, May, 1926, pp. 1105-1109.

59. Tupline, W. A., Gear Design, American Edition, The Industrial Press, New York, 1962.

60. Ugodchikov, A. G., and Kuznetsov, A. M., "On Static Stress Calculation of Gear Wheel Teeth," Gorkiy, 1963, pp. 258-270. (Scientific and Technical Aerospace Reports, N64-28485—in Joint Publication Research Service, Washington, D.C., Engineering Journal No. 2.)

61. Wellauer, E. J., Dudley, D. W., and Coleman, W., Coordinated Rating for the Strength of Gear Teeth, American Gear Manufacturers Association Paper 229.03, June 1956.

62. "Working Pressure on Gear Teeth," Transactions of American Society of Mechanical Engineers, Volume 8, 1887, pp. 699-704.

DISTRIBUTION

US Army Materiel Command	4
US Army Aviation Materiel Command	6
Chief of R&D, DA	1
Director of Defense Research and Engineering	1
US Army R&D Group (Europe)	2
US Army Aviation Materiel Laboratories	28
Army Aeronautical Research Laboratory, Ames Research Center	1
US Army Test and Evaluation Command	1
US Army Combat Developments Command, Fort Belvoir	2
US Army Combat Developments Command Transportation Agency	1
US Army War College	1
US Army Command and General Staff College	1
US Army Aviation School	1
US Army Tank-Automotive Center	2
Air Force Flight Test Center, Edwards AFB	1
US Army Field Office, AFSC, Andrews AFB	1
Air Force Aero Propulsion Laboratory, Wright-Patterson AFB	1
Air Force Flight Dynamics Laboratory, Wright-Patterson AFB	1
Systems Engineering Group, Wright-Patterson AFB	4

Naval Air Systems Command, DN	15
Office of Naval Research	2
Naval Air Engineering Center, Philadelphia	1
Commandant of the Marine Corps	1
Marine Corps Liaison Officer, US Army Transportation School	1
Lewis Research Center, NASA	1
Manned Spacecraft Center, NASA	1
NASA Scientific and Technical Information Facility	2
NAFEC Library (FAA)	2
US Army Board for Aviation Accident Research	1
Federal Aviation Agency, Washington, D. C.	1
US Government Printing Office	1
Defense Documentation Center	20
US Army Research Office-Durham	1

APPENDIX I

FATIGUE TEST GEAR DRAWINGS

This appendix consists of the fatigue test gear drawings for the 16 configurations tested. These drawings are shown in Figures 111 through 126. The spur gear main accessory drive and propeller brake outer member are shown in Figures 127 and 128, respectively.

BLANK PAGE

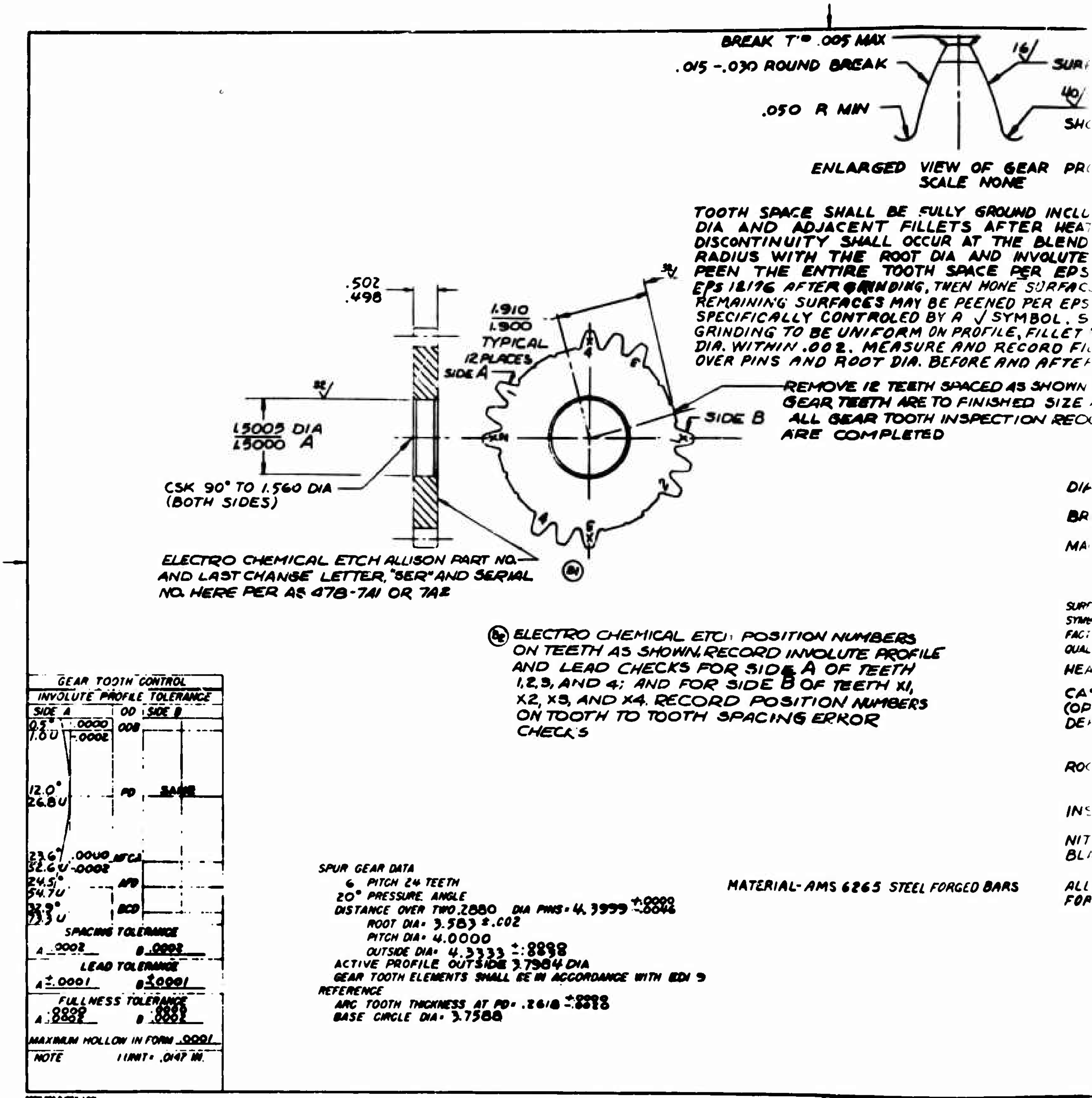

Figure 111. Fatigue Test Gear Configuration 1—EX-78772.

A

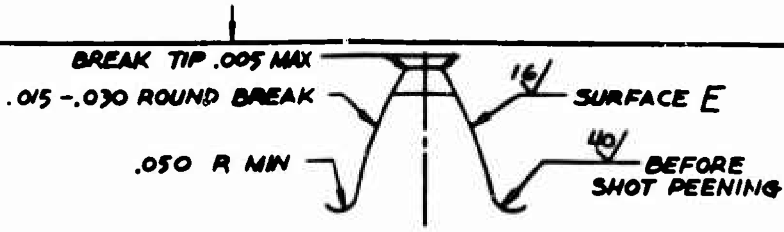

ENLARGED VIEW OF GEAR PROFILE
SCALE NONE

TOOTH SPACE SHALL BE FULLY GROUND INCLUDING ROOT DIA AND ADJACENT FILLETS AFTER HEAT TREAT. NO DISCONTINUITY SHALL OCCUR AT THE BLEND OF THE FILLET RADIUS WITH THE ROOT DIA AND INVOLUTE SURFACES. SHOT PEEN THE ENTIRE TOOTH SPACE PER EPS 12140 FOLLOWED BY EPS 12196 AFTER GRINDING, THEN HONE SURFACE E TO VALUE SHOWN. REMAINING SURFACES MAY BE PEENED PER EPS 12140 UNLESS SPECIFICALLY CONTROLED BY A √ SYMBOL. STOCK REMOVAL BY GRINDING TO BE UNIFORM ON PROFILE, FILLET RADIUS AND ROOT DIA. WITHIN .002. MEASURE AND RECORD FILLET RADIUS, DISTANCE OVER PINS AND ROOT DIA. BEFORE AND AFTER GRINDING.

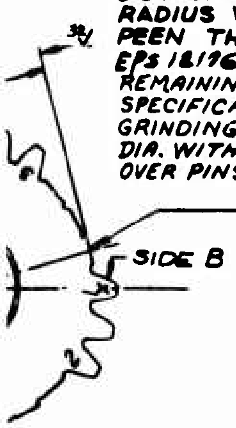

REMOVE 12 TEETH SPACED AS SHOWN AFTER GEAR TEETH ARE TO FINISHED SIZE AND ALL GEAR TOOTH INSPECTION REQUIREMENTS ARE COMPLETED

DIA A SHALL BE CONCENTRIC WITH ~~PD WITHIN~~ .002 TIR

BREAK SHARP EDGES .010 UOS

MACHINE ALL OVER.

SURFACE CHARACTERISTICS NOT CONTROLLED BY A √ SYMBOL SHALL BE COMMENSURATE WITH GOOD MANU-FACTURING PRACTICES WHICH PRODUCE ACCEPTABLE QUALITY LEVELS.

HEAT TREAT PER EPS 202

CASE HARDEN GEAR TEETH OUTSIDE 3.340 DIA (OPTIONAL TO CASE HARDEN ALL OVER) EFFECTIVE CASE DEPTHS AS FOLLOWS:
.035 -.045 BEFORE FINISHING
.030 -.045 AFTER FINISHING
ROCKWELL HARDNESS - CASE C58 MIN
CORE C34 MIN

INSPECT PER EIS 985 (MAGNETIC)

NITAL ETCH PER EIS 1510 THEN BLACK OXIDE PER AMS 2485

EMICAL ETCH POSITION NUMBERS
S SHOWN, RECORD INVOLUTE PROFILE
CHECKS FOR SIDE A OF TEETH
AND FOR SIDE B OF TEETH XI,
X4. RECORD POSITION NUMBERS
O TOOTH SPACING ERROR

MATERIAL - AMS 6265 STEEL FORGED BARS

ALL DIMENSIONS TO BE MET AFTER PROCESSING
FORGING SHALL CONFORM TO EDI 138 AND EIS 502

$^{+.0000}_{-.0046}$

WITH EDI 9

—EX-78772.

B

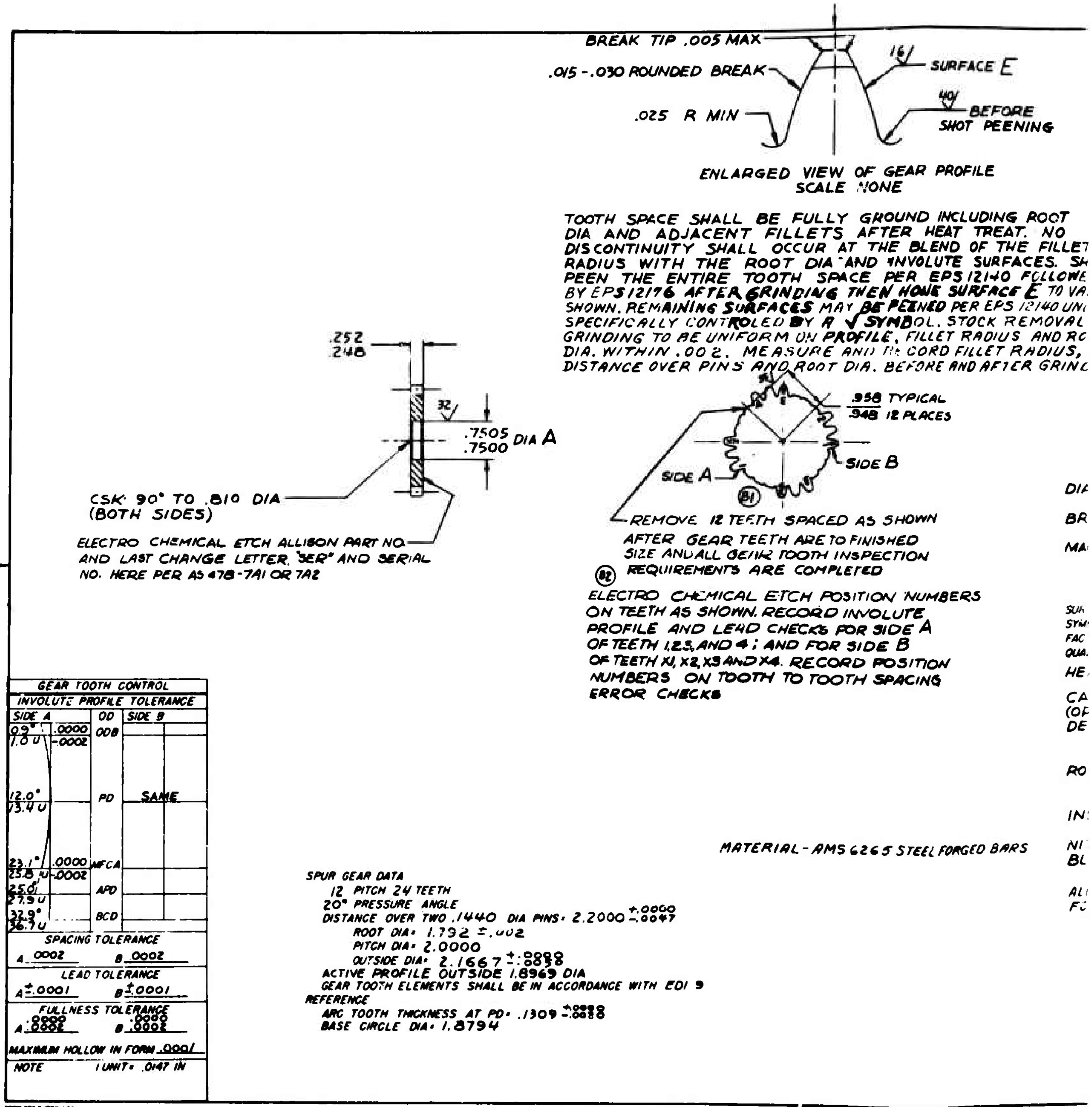

Figure 112. Fatigue Test Gear Configuration 2—EX-78773.

A

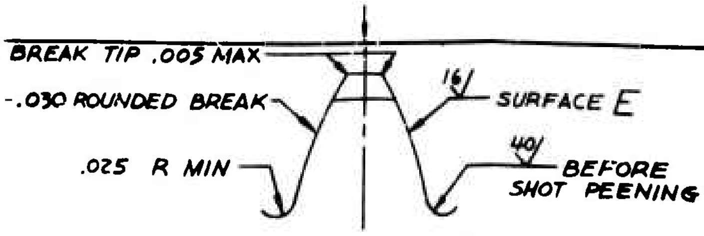

ENLARGED VIEW OF GEAR PROFILE
SCALE NONE

OTH SPACE SHALL BE FULLY GROUND INCLUDING ROOT
A AND ADJACENT FILLETS AFTER HEAT TREAT. NO
SCONTINUITY SHALL OCCUR AT THE BLEND OF THE FILLET
DIUS WITH THE ROOT DIA AND INVOLUTE SURFACES. SHOT
EN THE ENTIRE TOOTH SPACE PER EPS 12140 FOLLOWED
EPS 12176 AFTER GRINDING THEN HONE SURFACE E TO VALUE
OWN. REMAINING SURFACES MAY BE PEENED PER EPS 12140 UNLESS
ECIFICALLY CONTROLED BY A √ SYMBOL. STOCK REMOVAL BY
INDING TO BE UNIFORM ON PROFILE, FILLET RADIUS AND ROOT
A. WITHIN .002. MEASURE AND RECORD FILLET RADIUS,
TANCE OVER PINS AND ROOT DIA. BEFORE AND AFTER GRINDING.

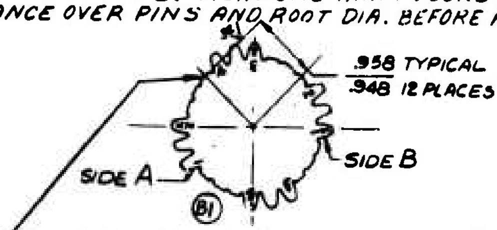

REMOVE 12 TEETH SPACED AS SHOWN
AFTER GEAR TEETH ARE TO FINISHED
SIZE AND ALL GEAR TOOTH INSPECTION
(B2) REQUIREMENTS ARE COMPLETED

ELECTRO CHEMICAL ETCH POSITION NUMBERS
ON TEETH AS SHOWN. RECORD INVOLUTE
PROFILE AND LEAD CHECKS FOR SIDE A
OF TEETH 1,2,3, AND 4; AND FOR SIDE B
OF TEETH X1, X2, X3 AND X4. RECORD POSITION
NUMBERS ON TOOTH TO TOOTH SPACING
ERROR CHECKS

DIA A SHALL BE CONCENTRIC WITH PD WITHIN .002 TIR

BREAK SHARP EDGES .010 UOS

MACHINE ALL OVER.

SURFACE CHARACTERISTICS NOT CONTROLLED BY A √
SYMBOL SHALL BE COMMENSURATE WITH GOOD MANU-
FACTURING PRACTICES WHICH PRODUCE ACCEPTABLE
QUALITY LEVELS.

HEAT TREAT PER EPS 202

CASE HARDEN GEAR TEETH OUTSIDE 1.570 DIA
(OPTIONAL TO CASE HARDEN ALL OVER) EFFECTIVE CASE
DEPTHS AS FOLLOWS:
.020-.030 BEFORE FINISHING
.015-.030 AFTER FINISHING
ROCKWELL HARDNESS – CASE C58 MIN
CORE C34 MIN

INSPECT PER EIS 985 (MAGNETIC)

MATERIAL - AMS 6265 STEEL FORGED BARS

NITAL ETCH PER EIS 1510 THEN
BLACK OXIDE PER AMS 2485

ALL DIMENSIONS TO BE MET AFTER PROCESSING
FORGING SHALL CONFORM TO EDI 138 AND EIS 502

?000 $^{+.0000}_{-.0047}$

ANCE WITH EDI 9

?8

2—EX-78773.

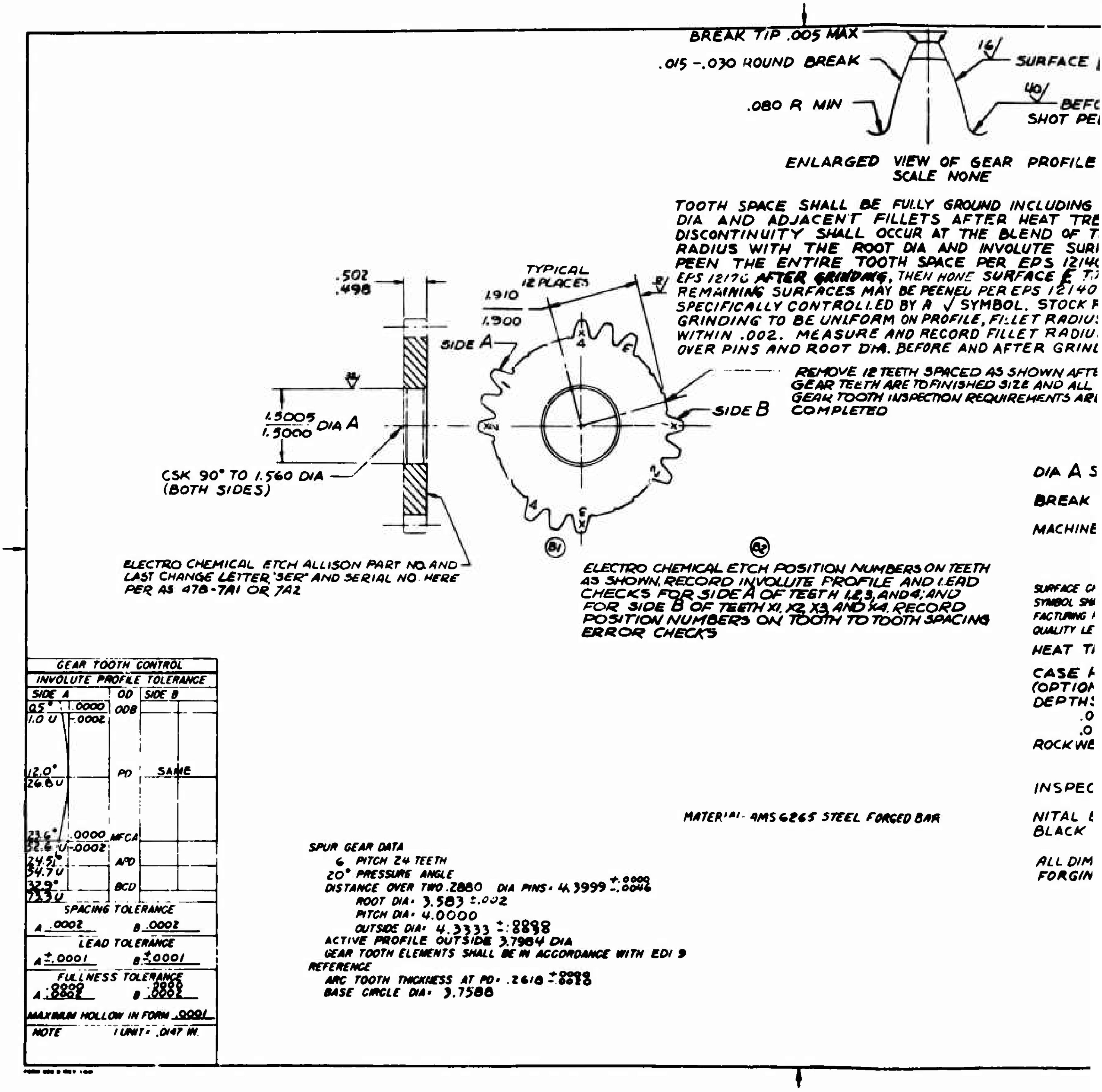

Figure 113. Fatigue Test Gear Configuration 3—EX-78774.

A

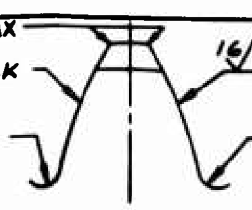

ENLARGED VIEW OF GEAR PROFILE
SCALE NONE

TOOTH SPACE SHALL BE FULLY GROUND INCLUDING ROOT DIA AND ADJACENT FILLETS AFTER HEAT TREAT. NO DISCONTINUITY SHALL OCCUR AT THE BLEND OF THE FILLET RADIUS WITH THE ROOT DIA AND INVOLUTE SURFACES. SHOT PEEN THE ENTIRE TOOTH SPACE PER EPS 12140 FOLLOWED BY EPS 12170 AFTER GRINDING, THEN HONE SURFACE E TO VALUE SHOWN. REMAINING SURFACES MAY BE PEENED PER EPS 12140 UNLESS SPECIFICALLY CONTROLLED BY A √ SYMBOL. STOCK REMOVAL BY GRINDING TO BE UNIFORM ON PROFILE, FILLET RADIUS AND ROOT DIA. WITHIN .002. MEASURE AND RECORD FILLET RADIUS, DISTANCE OVER PINS AND ROOT DIA. BEFORE AND AFTER GRINDING.

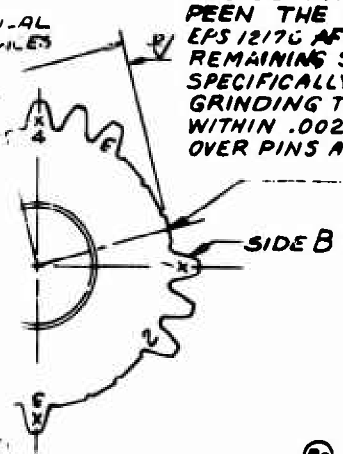

REMOVE 12 TEETH SPACED AS SHOWN AFTER GEAR TEETH ARE TO FINISHED SIZE AND ALL GEAR TOOTH INSPECTION REQUIREMENTS ARE COMPLETED

DIA A SHALL BE CONCENTRIC WITH PD WITHIN .002 TIR

BREAK SHARP EDGES .010 UOS

MACHINE ALL OVER.

ELECTRO CHEMICAL ETCH POSITION NUMBERS ON TEETH AS SHOWN. RECORD INVOLUTE PROFILE AND LEAD CHECKS FOR SIDE A OF TEETH 1,2,3, AND 4; AND FOR SIDE B OF TEETH X1, X2, X3, AND X4. RECORD POSITION NUMBERS ON TOOTH TO TOOTH SPACING ERROR CHECKS

SURFACE CHARACTERISTICS NOT CONTROLLED BY A √ SYMBOL SHALL BE COMMENSURATE WITH GOOD MANUFACTURING PRACTICES WHICH PRODUCE ACCEPTABLE QUALITY LEVELS.

HEAT TREAT PER EPS 202

CASE HARDEN GEAR TEETH OUTSIDE 3.340 DIA (OPTIONAL TO CASE HARDEN ALL OVER) EFFECTIVE CASE DEPTHS AS FOLLOWS:
.035 -.045 BEFORE FINISHING
.030 -.045 AFTER FINISHING
ROCKWELL HARDNESS - CASE C58 MIN
CORE C34 MIN

INSPECT PER EIS 985 (MAGNETIC)

MATERIAL- AMS 6265 STEEL FORGED BAR

NITAL ETCH PER EIS 1510 THEN BLACK OXIDE PER AMS 2485

ALL DIMENSIONS TO BE MET AFTER PROCESSING
FORGING SHALL CONFORM TO EDI 138 AND EIS 502

- 3999 $^{+.0000}_{-.0046}$

...DANCE WITH EDI 9

3—EX-78774.

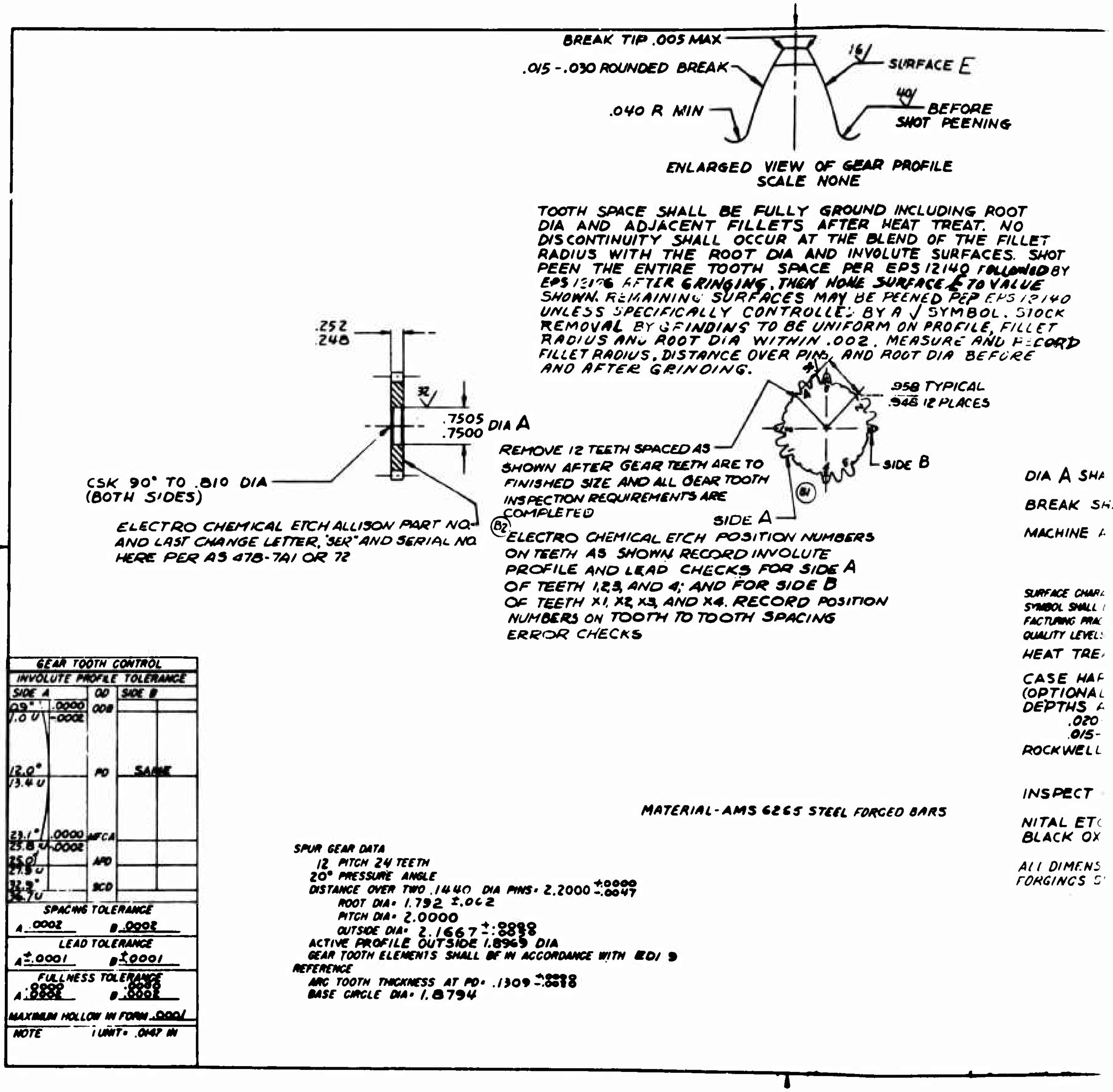

Figure 114. Fatigue Test Gear Configuration 4—EX-78775.

A

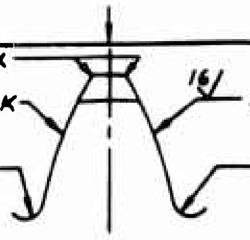

ENLARGED VIEW OF GEAR PROFILE
SCALE NONE

OTH SPACE SHALL BE FULLY GROUND INCLUDING ROOT
A AND ADJACENT FILLETS AFTER HEAT TREAT. NO
SCONTINUITY SHALL OCCUR AT THE BLEND OF THE FILLET
DIUS WITH THE ROOT DIA AND INVOLUTE SURFACES. SHOT
EN THE ENTIRE TOOTH SPACE PER EPS 12140 FOLLOWED BY
S 12176 AFTER GRINDING, THEN HONE SURFACE E TO VALUE
OWN. REMAINING SURFACES MAY BE PEENED PER EPS 12140
LESS SPECIFICALLY CONTROLLED BY A √ SYMBOL. STOCK
EMOVAL BY GRINDING TO BE UNIFORM ON PROFILE, FILLET
ADIUS AND ROOT DIA WITHIN .002. MEASURE AND RECORD
LET RADIUS, DISTANCE OVER PINS, AND ROOT DIA BEFORE
VD AFTER GRINDING.

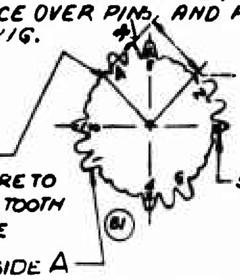

E 12 TEETH SPACED AS
AFTER GEAR TEETH ARE TO
ED SIZE AND ALL GEAR TOOTH
TION REQUIREMENTS ARE
LETED

RO CHEMICAL ETCH POSITION NUMBERS
ETH AS SHOWN. RECORD INVOLUTE
ILE AND LEAD CHECKS FOR SIDE A
ETH 1,2,3, AND 4; AND FOR SIDE B
ETH X1, X2, X3, AND X4. RECORD POSITION
ERS ON TOOTH TO TOOTH SPACING
OR CHECKS

MATERIAL-AMS 6265 STEEL FORGED BARS

.2000 $^{+.0000}_{-.0047}$

A
RDANCE WITH EDI 9

318

DIA A SHALL BE CONCENTRIC WITH PD WITHIN .002 TIR

BREAK SHARP EDGES .010 UOS

MACHINE ALL OVER.

SURFACE CHARACTERISTICS NOT CONTROLLED BY A √ SYMBOL SHALL BE COMMENSURATE WITH GOOD MANUFACTURING PRACTICES WHICH PRODUCE ACCEPTABLE QUALITY LEVELS.

HEAT TREAT PER EPS 202

CASE HARDEN GEAR TEETH OUTSIDE 1.570 DIA
(OPTIONAL TO CASE HARDEN ALL OVER) EFFECTIVE CASE
DEPTHS AS FOLLOWS:
.020-.030 BEFORE FINISHING
.015-.030 AFTER FINISHING
ROCKWELL HARDNESS - CASE C58 MIN
CORE C34 MIN

INSPECT PER EIS 985 (MAGNETIC)

NITAL ETCH PER EIS 1510 THEN
BLACK OXIDE PER AMS 2485

ALL DIMENSIONS TO BE MET AFTER PROCESSING
FORGINGS SHALL CONFORM TO EDI 138 AND EIS 502

n 4—EX-78775.

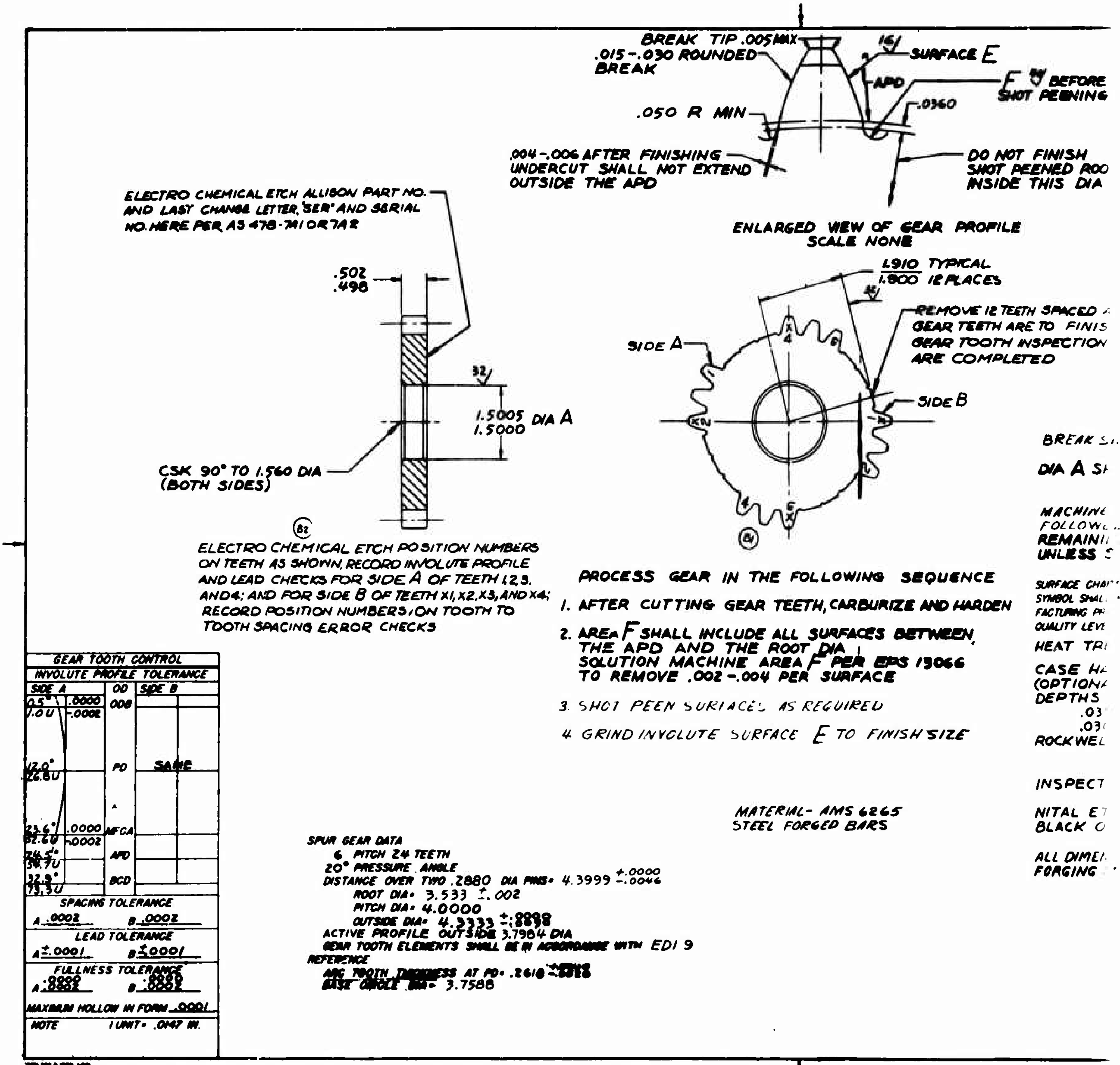

Figure 115. Fatigue Test Gear Configuration 5—EX-78776.

A

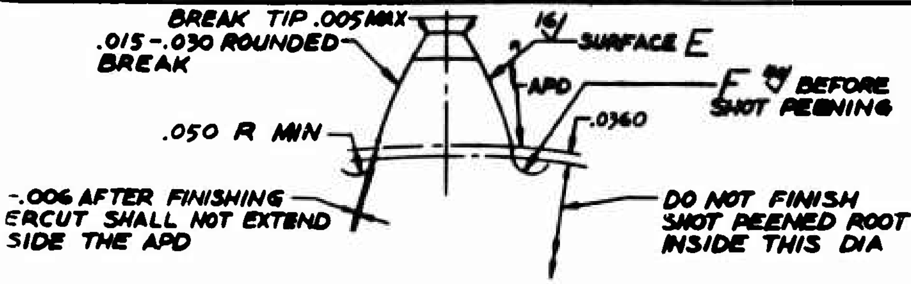

ENLARGED VIEW OF GEAR PROFILE
SCALE NONE

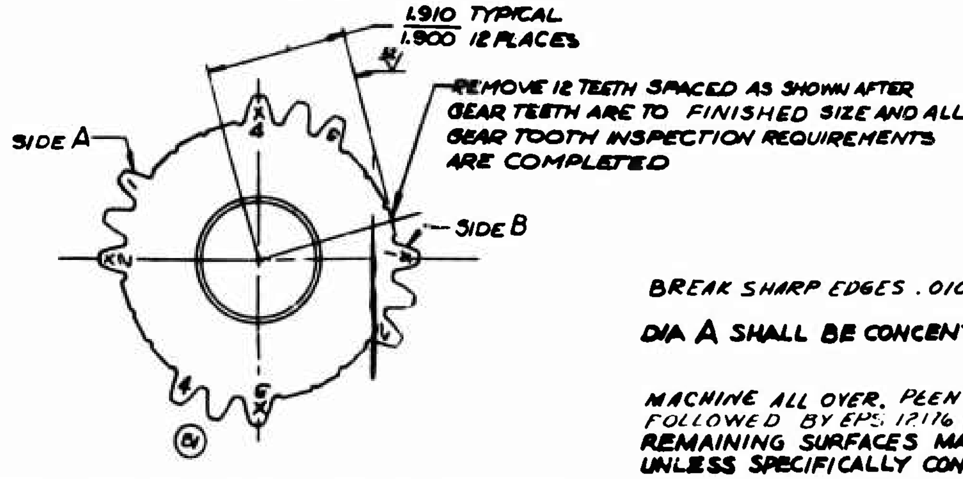

VIA A

PROCESS GEAR IN THE FOLLOWING SEQUENCE

1. AFTER CUTTING GEAR TEETH, CARBURIZE AND HARDEN
2. AREA F SHALL INCLUDE ALL SURFACES BETWEEN THE APD AND THE ROOT DIA. SOLUTION MACHINE AREA F PER EPS 13066 TO REMOVE .002-.004 PER SURFACE
3. SHOT PEEN SURFACES AS REQUIRED
4. GRIND INVOLUTE SURFACE E TO FINISH SIZE

MATERIAL- AMS 6265
STEEL FORGED BARS

VS. 4.3999 $^{+.0000}_{-.0046}$

38
4 DIA
ACCORDANCE WITH EDI 9

BREAK SHARP EDGES .010 UOS

DIA A SHALL BE CONCENTRIC WITH PD WITHIN .002 TIR

MACHINE ALL OVER. PEEN GEAR TEETH PER EPS 12140 FOLLOWED BY EPS 12176
REMAINING SURFACES MAY BE PEENED PER EPS 12140 UNLESS SPECIFICALLY CONTROLLED BY A √ SYMBOL

SURFACE CHARACTERISTICS NOT CONTROLLED BY A √ SYMBOL SHALL BE COMMENSURATE WITH GOOD MANUFACTURING PRACTICES WHICH PRODUCE ACCEPTABLE QUALITY LEVELS.

HEAT TREAT PER EPS 202

CASE HARDEN GEAR TEETH OUTSIDE 3.340 DIA (OPTIONAL TO CASE HARDEN ALL OVER) EFFECTIVE CASE DEPTHS AS FOLLOWS:
.035-.045 BEFORE FINISHING
.030-.045 AFTER FINISHING
ROCKWELL HARDNESS - CASE C58 MIN
CORE C34 MIN

INSPECT PER EIS 985 (MAGNETIC)

NITAL ETCH PER EIS 1510 THEN BLACK OXIDE PER AMS 2485

ALL DIMENSIONS TO BE MET AFTER PROCESSING
FORGING SHALL CONFORM TO EDI 138 AND EIS 502

tion 5—EX-78776.

B

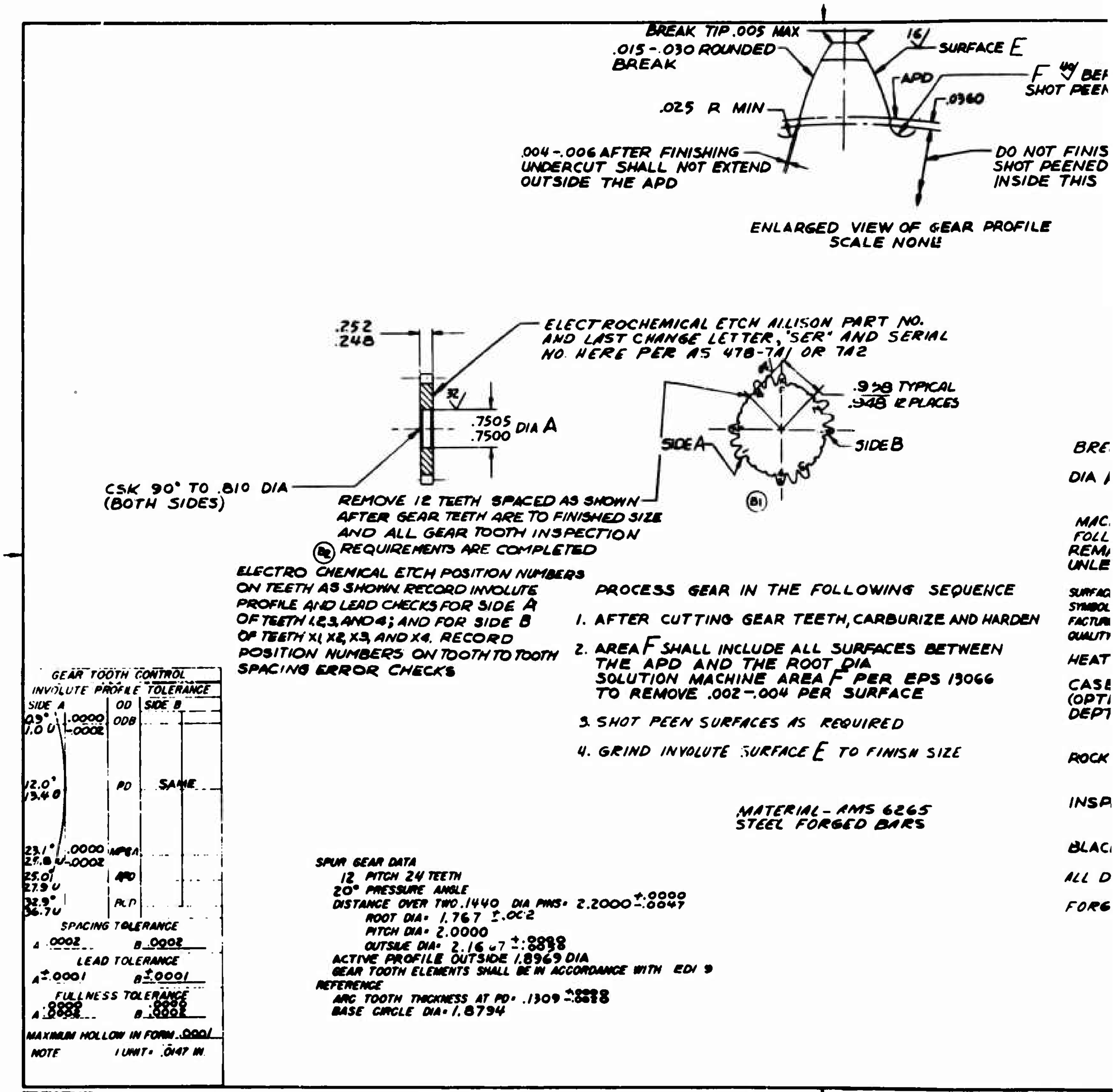

Figure 116. Fatigue Test Gear Configuration 6—EX-78777.

A

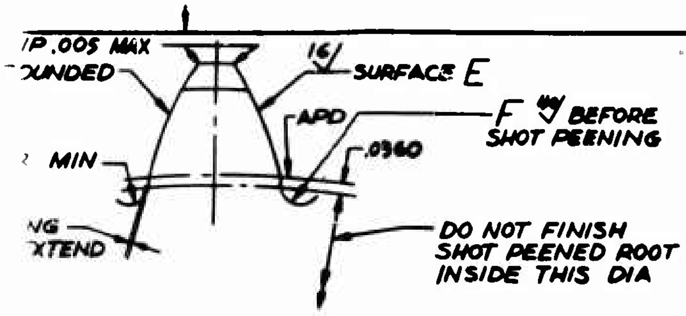

ENLARGED VIEW OF GEAR PROFILE
SCALE NONE

-TCH ALLISON PART NO.
ETTER, 'SER' AND SERIAL
478-741 OR 742

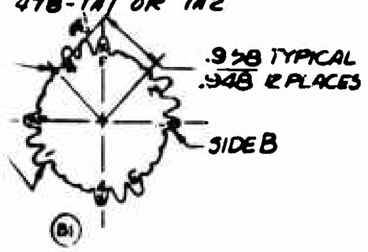

-R IN THE FOLLOWING SEQUENCE
-G GEAR TEETH, CARBURIZE AND HARDEN
INCLUDE ALL SURFACES BETWEEN
D THE ROOT DIA
CHINE AREA F PER EPS 13066
002-.004 PER SURFACE
RFACES AS REQUIRED
E SURFACE E TO FINISH SIZE

MATERIAL - AMS 6265
STEEL FORGED BARS

BREAK SHARP EDGES .010 UOS

DIA A SHALL BE CONCENTRIC WITH PD WITHIN .002 TIR

MACHINE ALL OVER. PEEN GEAR TEETH PER EPS 12140
FOLLOWED BY EPS 12176
REMAINING SURFACES MAY BE PEENED PER EPS 12140
UNLESS SPECIFICALLY CONTROLLED BY A √ SYMBOL

SURFACE CHARACTERISTICS NOT CONTROLLED BY A √
SYMBOL SHALL BE COMMENSURATE WITH GOOD MANU-
FACTURING PRACTICES WHICH PRODUCE ACCEPTABLE
QUALITY LEVELS.

HEAT TREAT PER EPS 202

CASE HARDEN GEAR TEETH OUTSIDE 1.570 DIA
(OPTIONAL TO CASE HARDEN ALL OVER) EFFECTIVE CASE
DEPTHS AS FOLLOWS:
.020-.030 BEFORE FINISHING
.015-.030 AFTER FINISHING
ROCKWELL HARDNESS - CASE C58 MIN
CORE C34 MIN

INSPECT PER EIS 985 (MAGNETIC)

BLACK OXIDE PER AMS 2485

ALL DIMENSIONS TO BE MET AFTER PROCESSING

FORGINGS SHALL CONFORM TO EDI 138 AND EIS 502

B

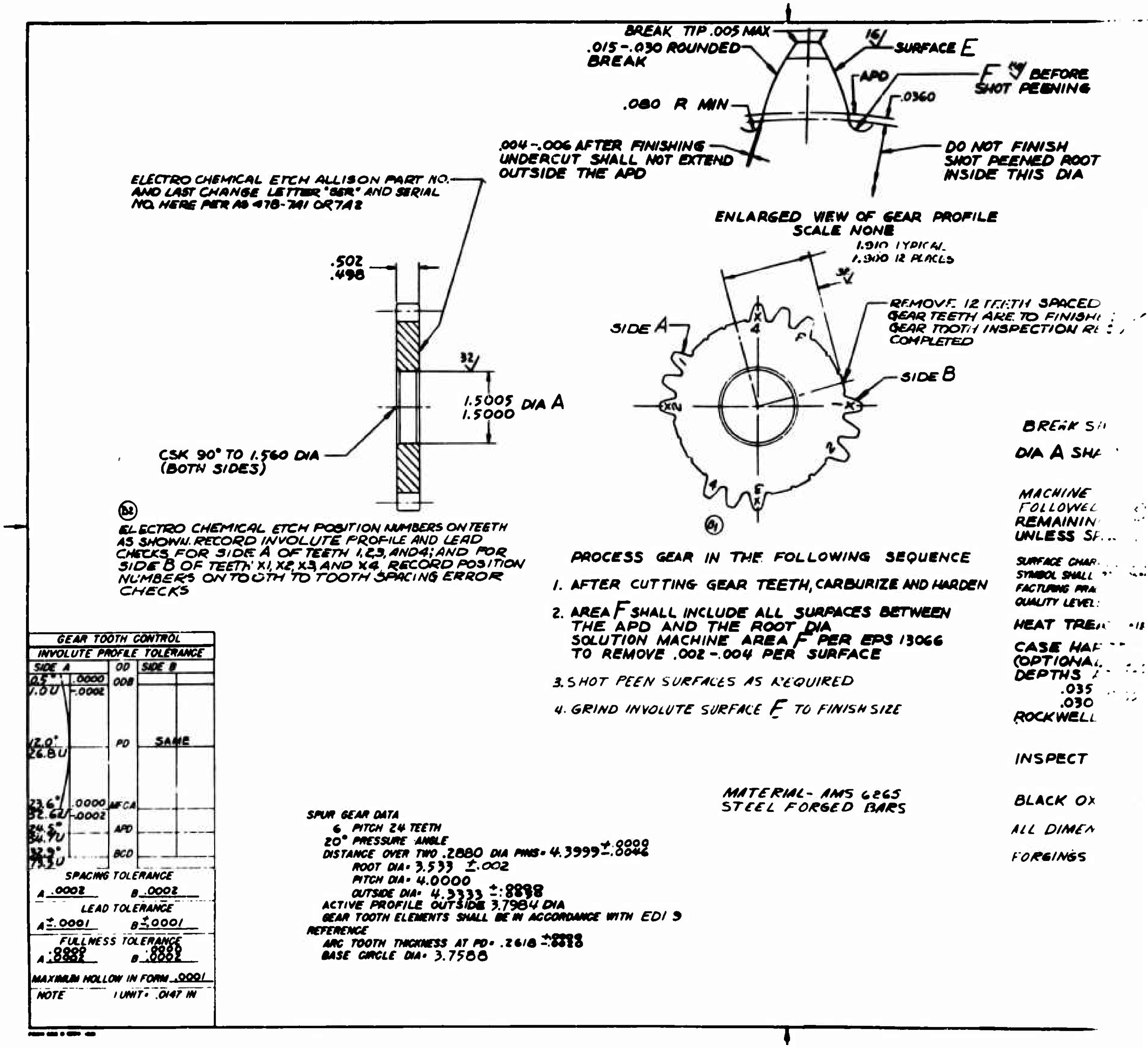

Figure 117. Fatigue Test Gear Configuration 7—EX-78778.

A

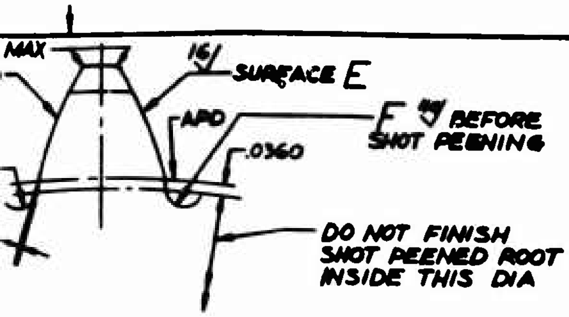

LARGED VIEW OF GEAR PROFILE
SCALE NONE

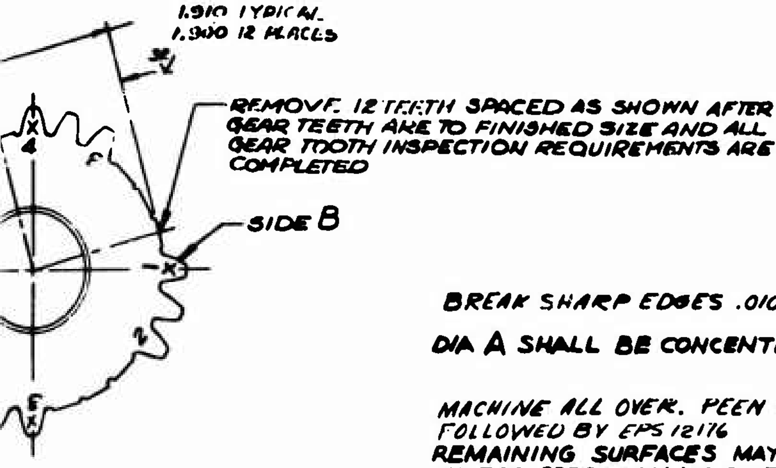

HE FOLLOWING SEQUENCE

R TEETH, CARBURIZE AND HARDEN

E ALL SURFACES BETWEEN
ROOT DIA
AREA F PER EPS 13066
04 PER SURFACE

AS REQUIRED

ACE E TO FINISH SIZE

ATERIAL- AMS 6265
TEEL FORGED BARS

BREAK SHARP EDGES .010 UOS

DIA A SHALL BE CONCENTRIC WITH PD WITHIN .002 TIR

MACHINE ALL OVER. PEEN GEAR TEETH PER EPS 12140
FOLLOWED BY EPS 12176
REMAINING SURFACES MAY BE PEENED PER EPS12140
UNLESS SPECIFICALLY CONTROLLED BY A √ SYMBOL

SURFACE CHARACTERISTICS NOT CONTROLLED BY A √
SYMBOL SHALL BE COMMENSURATE WITH GOOD MANU-
FACTURING PRACTICES WHICH PRODUCE ACCEPTABLE
QUALITY LEVELS.

HEAT TREAT PER EPS 202

CASE HARDEN GEAR TEETH OUTSIDE 3.340 DIA
(OPTIONAL TO CASE HARDEN ALL OVER) EFFECTIVE CASE
DEPTHS AS FOLLOWS:
.035-.045 BEFORE FINISHING
.030-.045 AFTER FINISHING
ROCKWELL HARDNESS - CASE C58 MIN
CORE C34 MIN

INSPECT PER EIS 985 (MAGNETIC)

BLACK OXIDE PER AMS 2485

ALL DIMENSIONS TO BE MET AFTER PROCESSING

FORGINGS SHALL CONFORM TO EDI 138 AND EIS 502

B

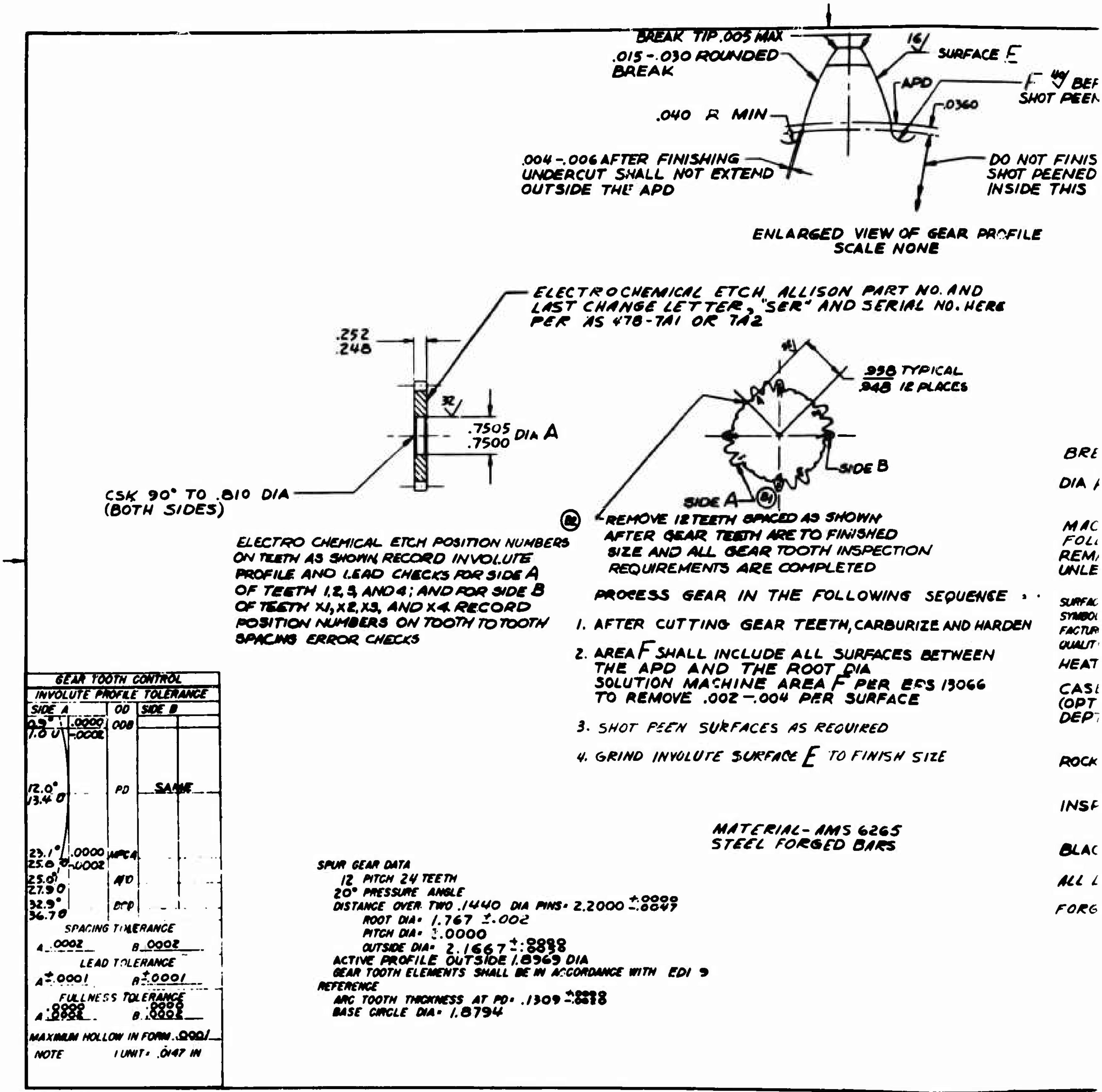

Figure 118. Fatigue Test Gear Configuration 8—EX-78779.

A

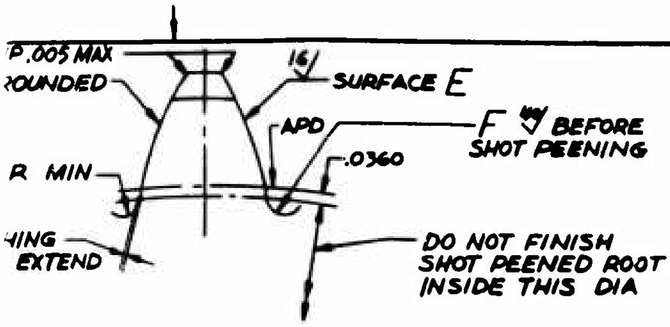

ENLARGED VIEW OF GEAR PROFILE
SCALE NONE

ETCH ALLISON PART NO. AND
TER, "SER" AND SERIAL NO. HERE
R 7A2

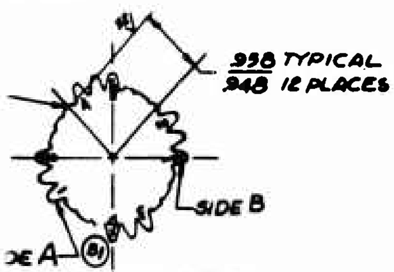

EETH SPACED AS SHOWN
? TEETH ARE TO FINISHED
L GEAR TOOTH INSPECTION
NTS ARE COMPLETED

'AR IN THE FOLLOWING SEQUENCE : ·

'ING GEAR TEETH, CARBURIZE AND HARDEN

. INCLUDE ALL SURFACES BETWEEN
ND THE ROOT DIA
ACHINE AREA F PER EPS 13066
.002 -.004 PER SURFACE

SURFACES AS REQUIRED

TE SURFACE E TO FINISH SIZE

MATERIAL - AMS 6265
STEEL FORGED BARS

BREAK SHARP EDGES .010 U05

DIA A SHALL BE CONCENTRIC WITH PD WITHIN .002 TIR

MACHINE ALL OVER. PEEN GEAR TEETH PER EPS 12140
FOLLOWED BY EPS 12176
REMAINING SURFACES MAY BE PEENED PER EPS 12140
UNLESS SPECIFICALLY CONTROLLED BY A √ SYMBOL

SURFACE CHARACTERISTICS NOT CONTROLLED BY A √
SYMBOL SHALL BE COMMENSURATE WITH GOOD MANU-
FACTURING PRACTICES WHICH PRODUCE ACCEPTABLE
QUALITY LEVELS.

HEAT TREAT PER EPS 202

CASE HARDEN GEAR TEETH OUTSIDE 1.570 DIA
(OPTIONAL TO CASE HARDEN ALL OVER) EFFECTIVE CASE
DEPTHS AS FOLLOWS:
.020-.030 BEFORE FINISHING
.015-.030 AFTER FINISHING
ROCKWELL HARDNESS - CASE C58 MIN
CORE C34 MIN

INSPECT PER EIS 985 (MAGNETIC)

BLACK OXIDE PER AMS 2485

ALL DIMENSIONS TO BE MET AFTER PROCESSING

FORGINGS SHALL CONFORM TO EDI 138 AND EIS 502

3779.

B

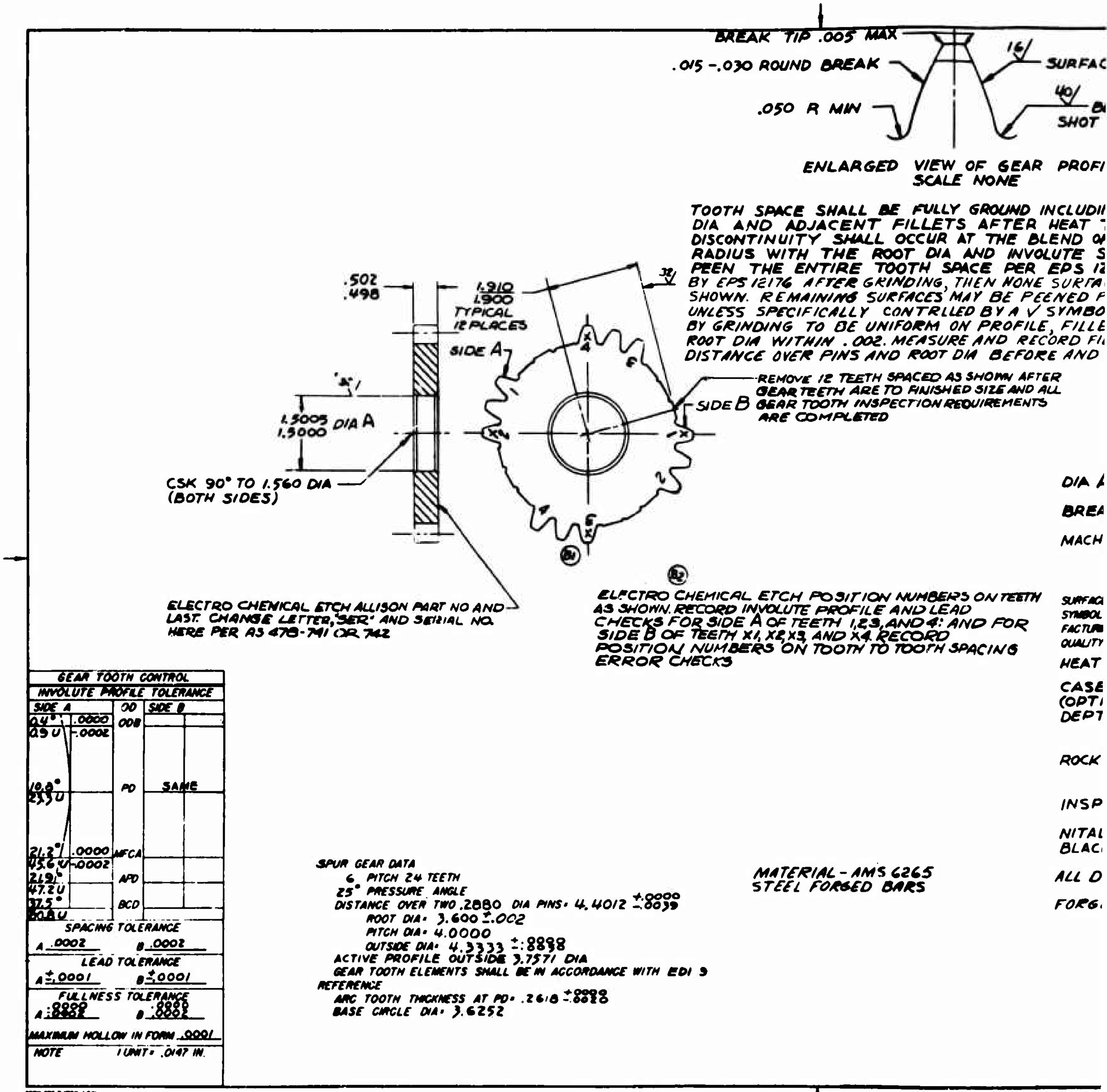

Figure 119. Fatigue Test Gear Configuration 9—EX-78780.

A

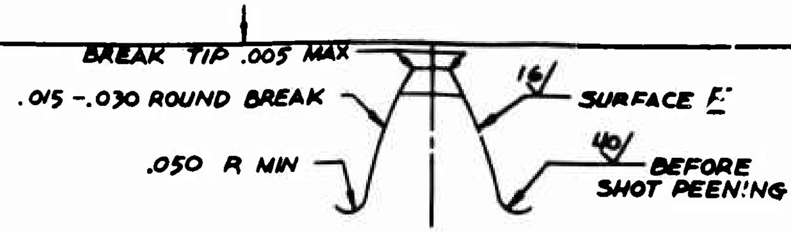

ENLARGED VIEW OF GEAR PROFILE
SCALE NONE

TOOTH SPACE SHALL BE FULLY GROUND INCLUDING ROOT DIA AND ADJACENT FILLETS AFTER HEAT TREAT. NO DISCONTINUITY SHALL OCCUR AT THE BLEND OF THE FILLET RADIUS WITH THE ROOT DIA AND INVOLUTE SURFACES. SHOT PEEN THE ENTIRE TOOTH SPACE PER EPS 12140 FOLLOWED BY EPS 12176 AFTER GRINDING, THEN HONE SURFACE E TO VALUE SHOWN. REMAINING SURFACES MAY BE PEENED PER EPS 12140 UNLESS SPECIFICALLY CONTRLLED BY A √ SYMBOL. STOCK REMOVAL BY GRINDING TO BE UNIFORM ON PROFILE, FILLET RADIUS AND ROOT DIA WITHIN .002. MEASURE AND RECORD FILLET RADIUS, DISTANCE OVER PINS AND ROOT DIA BEFORE AND AFTER GRINDING

REMOVE 12 TEETH SPACED AS SHOWN AFTER GEAR TEETH ARE TO FINISHED SIZE AND ALL GEAR TOOTH INSPECTION REQUIREMENTS ARE COMPLETED

DIA A SHALL BE CONCENTRIC WITH PD WITHIN .002 TIR

BREAK SHARP EDGES .010 UOS

MACHINE ALL OVER.

82

TRO CHEMICAL ETCH POSITION NUMBERS ON TEETH
OWN. RECORD INVOLUTE PROFILE AND LEAD
KS FOR SIDE A OF TEETH 1,2,3, AND 4: AND FOR
B OF TEETH X1, X2, X3, AND X4. RECORD
TION NUMBERS ON TOOTH TO TOOTH SPACING
OR CHECKS

SURFACE CHARACTERISTICS NOT CONTROLLED BY A √ SYMBOL SHALL BE COMMENSURATE WITH GOOD MANUFACTURING PRACTICES WHICH PRODUCE ACCEPTABLE QUALITY LEVELS.

HEAT TREAT PER EPS 202

CASE HARDEN GEAR TEETH OUTSIDE 3.340 DIA (OPTIONAL TO CASE HARDEN ALL OVER) EFFECTIVE CASE DEPTHS AS FOLLOWS:
.035 -.045 BEFORE FINISHING
.030 -.045 AFTER FINISHING
ROCKWELL HARDNESS - CASE C58 MIN
CORE C34 MIN

INSPECT PER EIS 985 (MAGNETIC)

NITAL ETCH PER EIS 1510 THEN BLACK OXIDE PER AMS 2485

MATERIAL - AMS 6265
STEEL FORGED BARS

.0000
.0039

ALL DIMENSIONS TO BE MET AFTER PROCESSING

FORGING TO CONFORM TO EDI 138 AND EIS 502

WITH EDI 9

9—EX-78780.

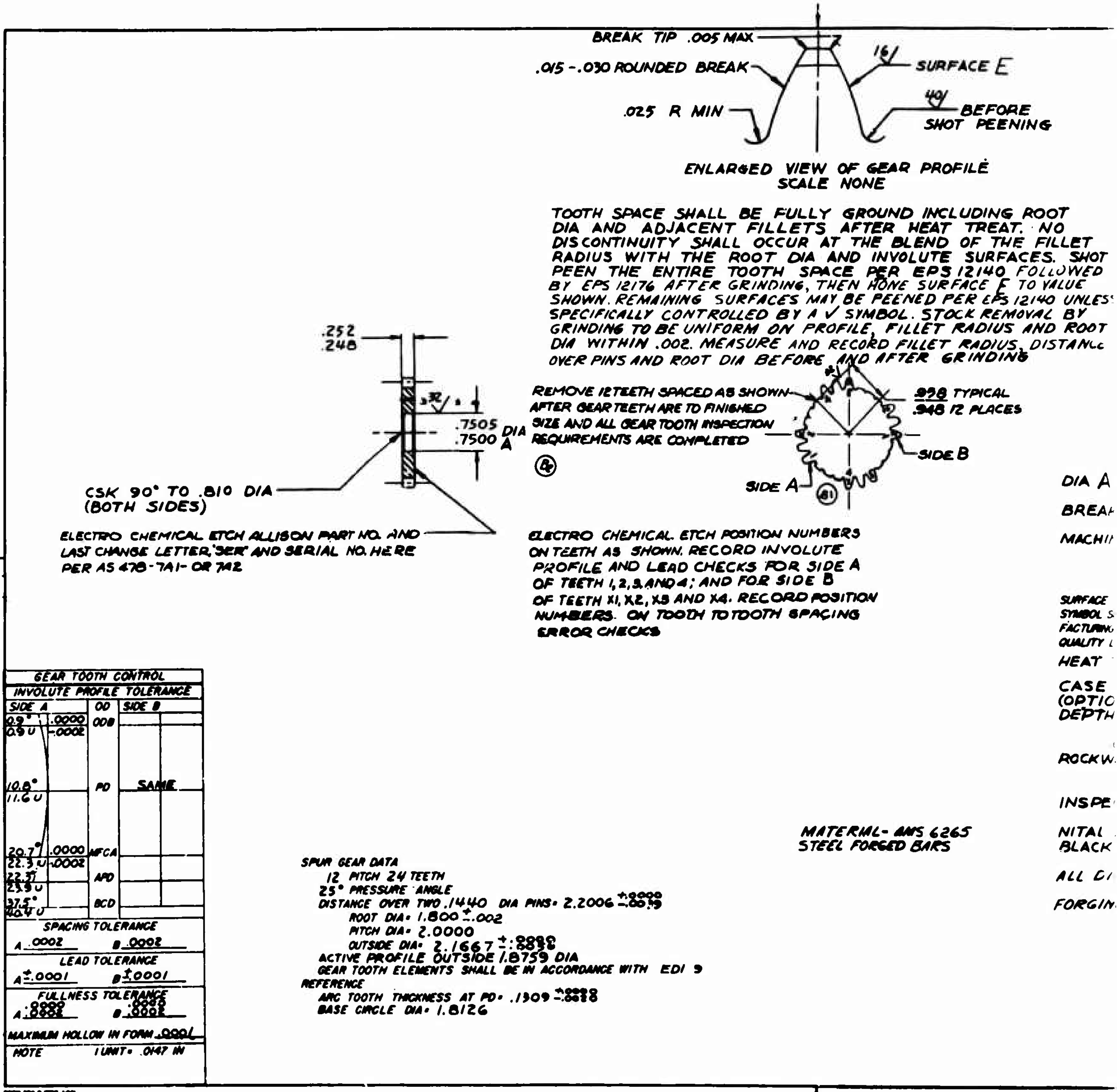

Figure 120. Fatigue Test Gear Configuration 10—EX-78781.

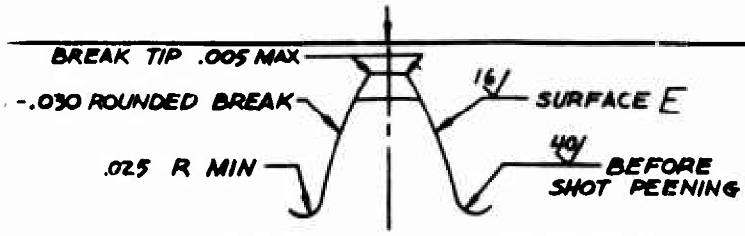

ENLARGED VIEW OF GEAR PROFILE
SCALE NONE

)OTH SPACE SHALL BE FULLY GROUND INCLUDING ROOT
'A AND ADJACENT FILLETS AFTER HEAT TREAT. NO
SCONTINUITY SHALL OCCUR AT THE BLEND OF THE FILLET
ADIUS WITH THE ROOT DIA AND INVOLUTE SURFACES. SHOT
'EEN THE ENTIRE TOOTH SPACE PER EPS 12140 FOLLOWED
EPS 12176 AFTER GRINDING, THEN HONE SURFACE E TO VALUE
IOWN. REMAINING SURFACES MAY BE PEENED PER EPS 12140 UNLESS
'ECIFICALLY CONTROLLED BY A √ SYMBOL. STOCK REMOVAL BY
'INDING TO BE UNIFORM ON PROFILE, FILLET RADIUS AND ROOT
A WITHIN .002. MEASURE AND RECORD FILLET RADIUS, DISTANCE
'R PINS AND ROOT DIA BEFORE AND AFTER GRINDING

OVE 12 TEETH SPACED AS SHOWN
? GEAR TEETH ARE TO FINISHED
AND ALL GEAR TOOTH INSPECTION
IIREMENTS ARE COMPLETED

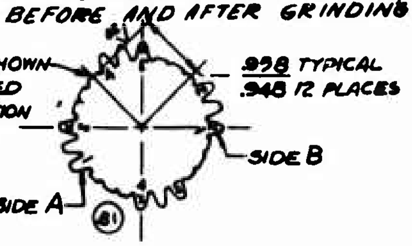

TRO CHEMICAL ETCH POSITION NUMBERS
TEETH AS SHOWN. RECORD INVOLUTE
)FILE AND LEAD CHECKS FOR SIDE A
TEETH 1,2,3,AND 4; AND FOR SIDE B
TEETH X1, X2, X3 AND X4. RECORD POSITION
MBERS ON TOOTH TO TOOTH SPACING
ROR CHECKS

MATERIAL- AMS 6265
STEEL FORGED BARS

2.2006 +.0000 -.0039

DIA
:ORDANCE WITH EDI 9

.0088 .0018

DIA A SHALL BE CONCENTRIC WITH PD WITHIN .002 TIR

BREAK SHARP EDGES .010 UOS

MACHINE ALL OVER.

SURFACE CHARACTERISTICS NOT CONTROLLED BY A √
SYMBOL SHALL BE COMMENSURATE WITH GOOD MANU-
FACTURING PRACTICES WHICH PRODUCE ACCEPTABLE
QUALITY LEVELS.

HEAT TREAT PER EPS 202

CASE HARDEN GEAR TEETH OUTSIDE 1.570 DIA
(OPTIONAL TO CASE HARDEN ALL OVER) EFFECTIVE CASE
DEPTHS AS FOLLOWS:
.020-.030 BEFORE FINISHING
.015-.030 AFTER FINISHING
ROCKWELL HARDNESS - CASE C58 MIN
CORE C34 MIN

INSPECT PER EIS 985 (MAGNETIC)

NITAL ETCH PER EIS 1510 THEN
BLACK OXIDE PER AMS 2485

ALL DIMENSIONS TO BE MET AFTER PROCESSING

FORGINGS SHALL CONFORM TO EDI 138 AND EIS 502

tion 10—EX-78781.

B

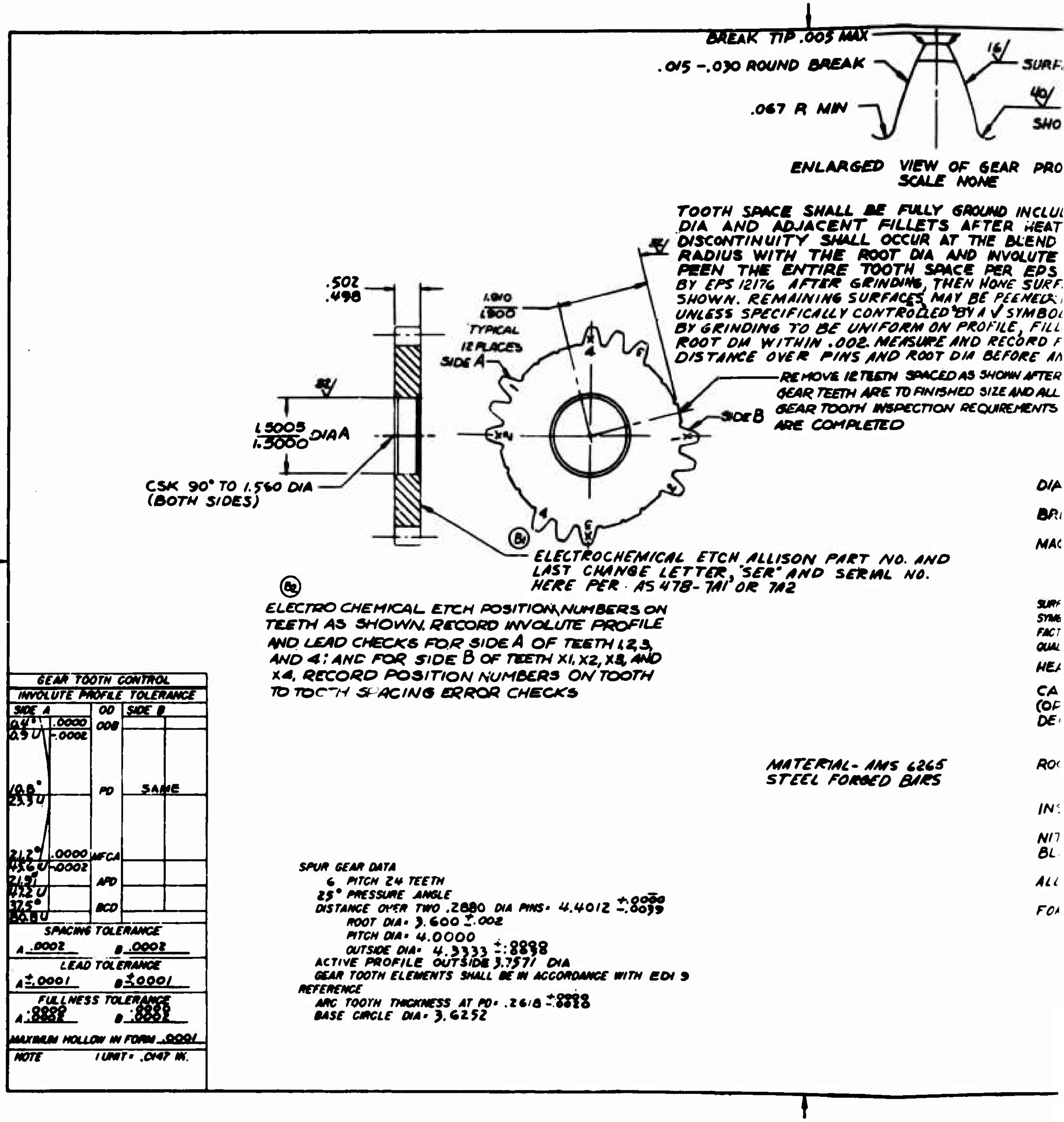

Figure 121. Fatigue Test Gear Configuration 11—EX-78782.

A

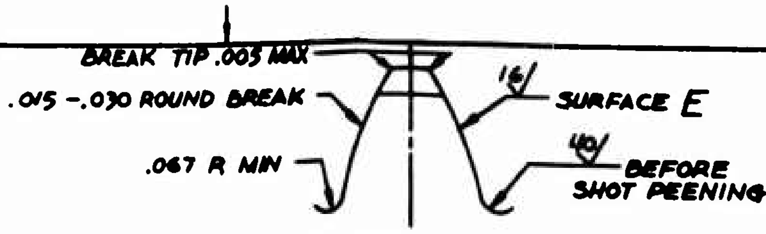

ENLARGED VIEW OF GEAR PROFILE
SCALE NONE

TOOTH SPACE SHALL BE FULLY GROUND INCLUDING ROOT DIA AND ADJACENT FILLETS AFTER HEAT TREAT. NO DISCONTINUITY SHALL OCCUR AT THE BLEND OF THE FILLET RADIUS WITH THE ROOT DIA AND INVOLUTE SURFACES. SHOT PEEN THE ENTIRE TOOTH SPACE PER EPS 12140 FOLLOWED BY EPS 12176 AFTER GRINDING, THEN HONE SURFACE E TO VALUE SHOWN. REMAINING SURFACES MAY BE PEENED PER EPS 12140 UNLESS SPECIFICALLY CONTROLLED BY A √ SYMBOL. STOCK REMOVAL BY GRINDING TO BE UNIFORM ON PROFILE, FILLET RADIUS AND ROOT DIA WITHIN .002. MEASURE AND RECORD FILLET RADIUS, DISTANCE OVER PINS AND ROOT DIA BEFORE AND AFTER GRINDING

REMOVE 12 TEETH SPACED AS SHOWN AFTER GEAR TEETH ARE TO FINISHED SIZE AND ALL GEAR TOOTH INSPECTION REQUIREMENTS ARE COMPLETED

CHEMICAL ETCH ALLISON PART NO. AND
ANGE LETTER, "SER" AND SERIAL NO.
R · AS 478-7A1 OR 7A2

ERS ON
PROFILE
TH 1,2,3,
XS, AND
TOOTH

MATERIAL- AMS 6265
STEEL FORGED BARS

+.0000
-.0039

WITH EDI 9

DIA A SHALL BE CONCENTRIC WITH PD WITHIN .002 TIR

BREAK SHARP EDGES .010 UOS

MACHINE ALL OVER.

SURFACE CHARACTERISTICS NOT CONTROLLED BY A √ SYMBOL SHALL BE COMMENSURATE WITH GOOD MANUFACTURING PRACTICES WHICH PRODUCE ACCEPTABLE QUALITY LEVELS.

HEAT TREAT PER EPS 202

CASE HARDEN GEAR TEETH OUTSIDE 3.340 DIA (OPTIONAL TO CASE HARDEN ALL OVER) EFFECTIVE CASE DEPTHS AS FOLLOWS:
.035 -.045 BEFORE FINISHING
.030 -.045 AFTER FINISHING
ROCKWELL HARDNESS - CASE C58 MIN
CORE C34 MIN

INSPECT PER EIS 985 (MAGNETIC)

NITAL ETCH PER EIS 1510 THEN BLACK OXIDE PER AMS 2485

ALL DIMENSIONS TO BE MET AFTER PROCESSING

FORGING SHALL CONFORM TO EDI 138 AND EIS 502

1—EX-78782.

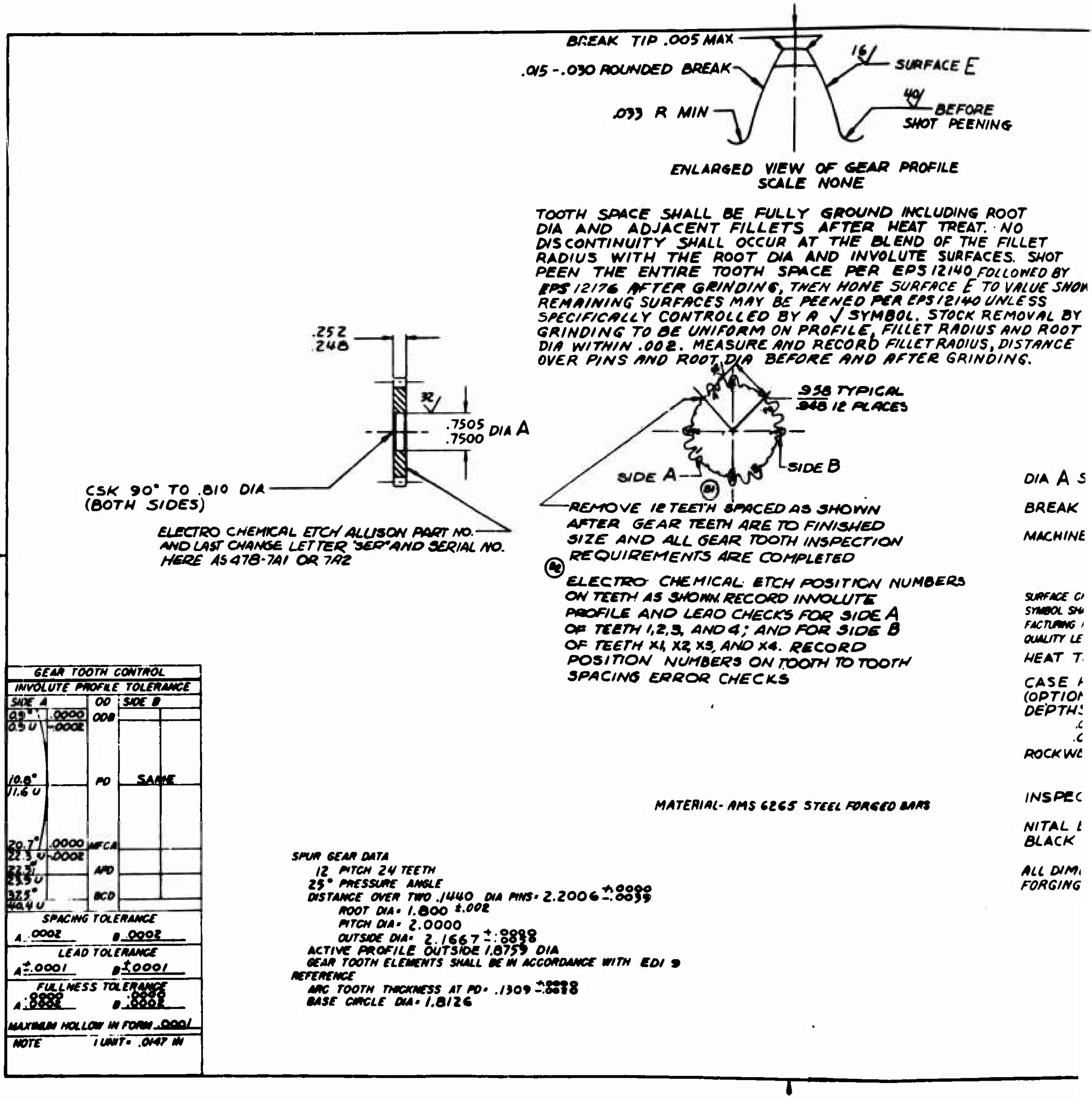

Figure 122. Fatigue Test Gear Configuration 12—EX-78783.

A

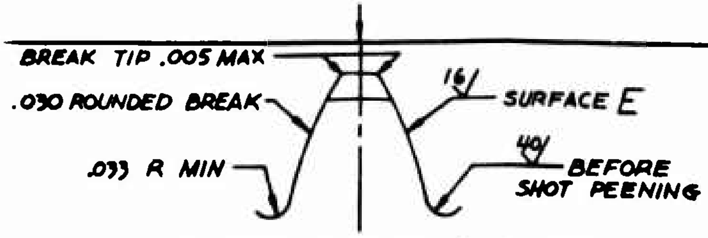

ENLARGED VIEW OF GEAR PROFILE
SCALE NONE

ᴐTH SPACE SHALL BE FULLY GROUND INCLUDING ROOT AND ADJACENT FILLETS AFTER HEAT TREAT. NO CONTINUITY SHALL OCCUR AT THE BLEND OF THE FILLET ᴐIUS WITH THE ROOT DIA AND INVOLUTE SURFACES. SHOT ·N THE ENTIRE TOOTH SPACE PER EPS 12140 FOLLOWED BY S 12176 AFTER GRINDING, THEN HONE SURFACE E TO VALUE SHOWN. ·MAINING SURFACES MAY BE PEENED PER EPS 12140 UNLESS CIFICALLY CONTROLLED BY A √ SYMBOL. STOCK REMOVAL BY ·INDING TO BE UNIFORM ON PROFILE, FILLET RADIUS AND ROOT WITHIN .002. MEASURE AND RECORD FILLET RADIUS, DISTANCE R PINS AND ROOT DIA BEFORE AND AFTER GRINDING.

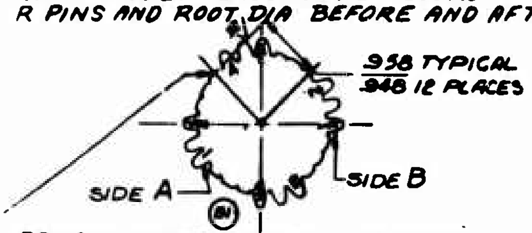

REMOVE 12 TEETH SPACED AS SHOWN AFTER GEAR TEETH ARE TO FINISHED SIZE AND ALL GEAR TOOTH INSPECTION REQUIREMENTS ARE COMPLETED

ELECTRO CHEMICAL ETCH POSITION NUMBERS ON TEETH AS SHOWN. RECORD INVOLUTE PROFILE AND LEAD CHECKS FOR SIDE A OF TEETH 1,2,3, AND 4; AND FOR SIDE B OF TEETH X1, X2, X3, AND X4. RECORD POSITION NUMBERS ON TOOTH TO TOOTH SPACING ERROR CHECKS

MATERIAL- AMS 6265 STEEL FORGED BARS

2006 $^{+.0000}_{-.0039}$

·DANCE WITH EDI 9

·28

DIA A SHALL BE CONCENTRIC WITH PD WITHIN .002 TIR

BREAK SHARP EDGES .010 UOS

MACHINE ALL OVER.

SURFACE CHARACTERISTICS NOT CONTROLLED BY A √ SYMBOL SHALL BE COMMENSURATE WITH GOOD MANUFACTURING PRACTICES WHICH PRODUCE ACCEPTABLE QUALITY LEVELS.

HEAT TREAT PER EPS 202

CASE HARDEN GEAR TEETH OUTSIDE 1.570 DIA (OPTIONAL TO CASE HARDEN ALL OVER) EFFECTIVE CASE DEPTHS AS FOLLOWS:

.020-.030 BEFORE FINISHING
.015-.030 AFTER FINISHING

ROCKWELL HARDNESS - CASE C58 MIN
CORE C34 MIN

INSPECT PER EIS 985 (MAGNETIC)

NITAL ETCH PER EIS 1510 THEN BLACK OXIDE PER AMS 2485

ALL DIMENSIONS TO BE MET AFTER PROCESSING
FORGING SHALL CONFORM TO EDI 138 AND EIS 502

tion 12—EX-78783.

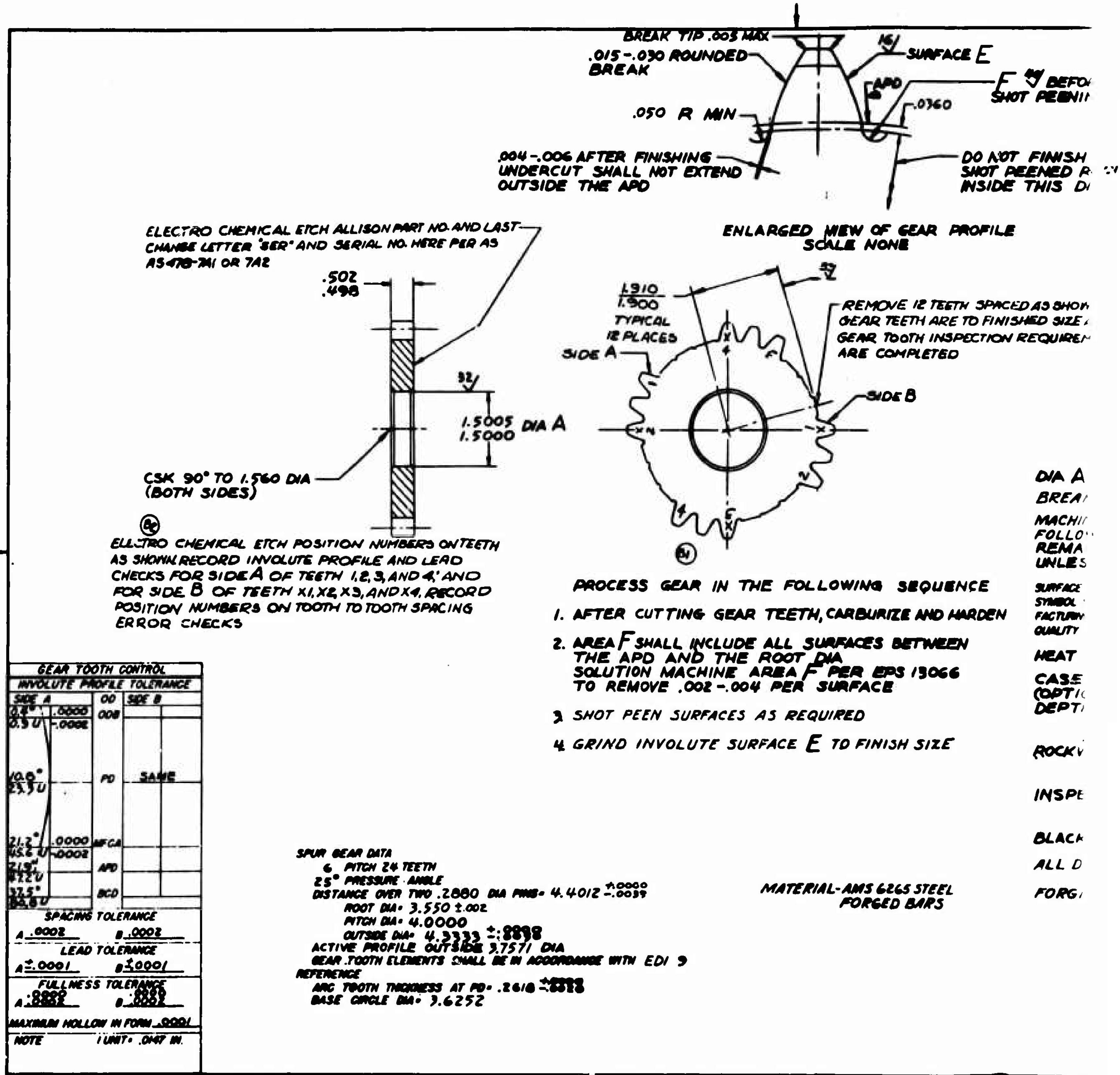

Figure 123. Fatigue Test Gear Configuration 13—EX-78784.

A

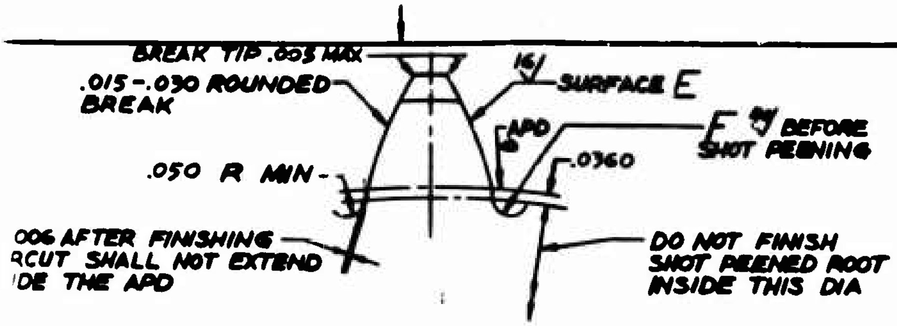

ENLARGED VIEW OF GEAR PROFILE
SCALE NONE

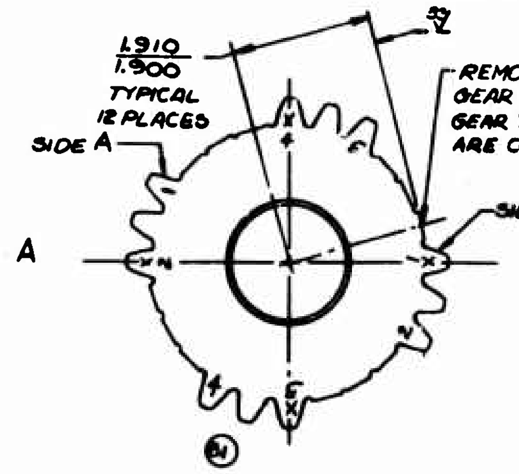

PROCESS GEAR IN THE FOLLOWING SEQUENCE

1. AFTER CUTTING GEAR TEETH, CARBURIZE AND HARDEN
2. AREA F SHALL INCLUDE ALL SURFACES BETWEEN THE APD AND THE ROOT DIA SOLUTION MACHINE AREA F PER EPS 13066 TO REMOVE .002-.004 PER SURFACE
3. SHOT PEEN SURFACES AS REQUIRED
4. GRIND INVOLUTE SURFACE E TO FINISH SIZE

$4.4012^{+.0000}_{-.0039}$

MATERIAL-AMS 6265 STEEL
FORGED BARS

DIA
CORDANCE WITH EDI 9

DIA A SHALL BE CONCENTRIC WITH PD WITHIN .002 TIR

BREAK SHARP EDGES .010 UOS

MACHINE ALL OVER. PEEN GEAR TEETH PER EPS 12140 FOLLOWED BY EPS 12176
REMAINING SURFACES MAY BE PEENED PER EPS 12140 UNLESS SPECIFICALLY CONTROLLED BY A √ SYMBOL

SURFACE CHARACTERISTICS NOT CONTROLLED BY A √ SYMBOL SHALL BE COMMENSURATE WITH GOOD MANUFACTURING PRACTICES WHICH PRODUCE ACCEPTABLE QUALITY LEVELS.

HEAT TREAT PER EPS 202

CASE HARDEN GEAR TEETH OUTSIDE 3.340 DIA (OPTIONAL TO CASE HARDEN ALL OVER) EFFECTIVE CASE DEPTHS AS FOLLOWS:
.035-.045 BEFORE FINISHING
.030-.045 AFTER FINISHING
ROCKWELL HARDNESS - CASE C58 MIN
CORE C34 MIN

INSPECT PER EIS 985 (MAGNETIC)

BLACK OXIDE PER AMS 2485

ALL DIMENSIONS TO BE MET AFTER PROCESSING

FORGING SHALL CONFORM TO EDI 138 AND EIS 502

ration 13—EX-78784.

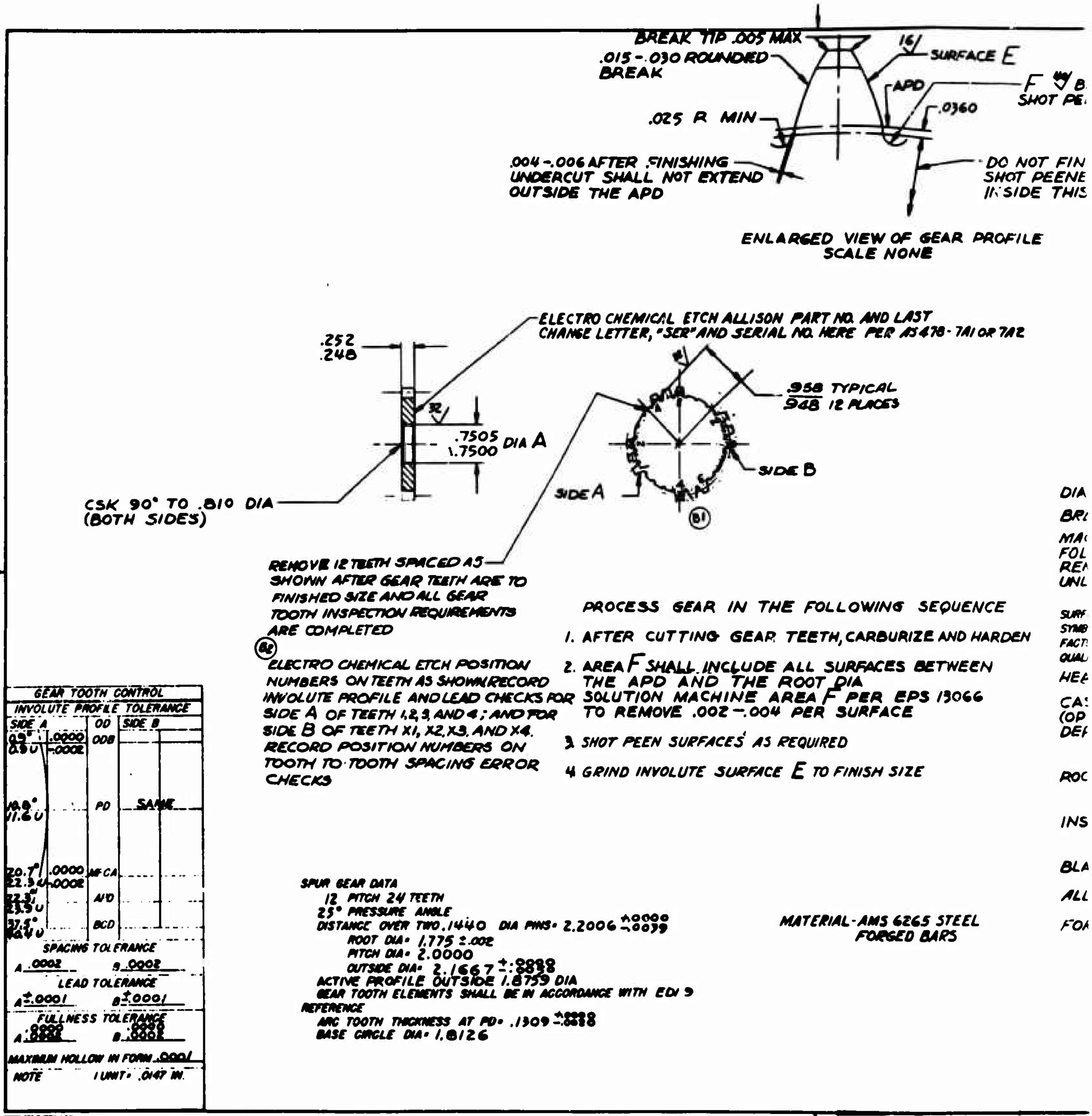

Figure 124. Fatigue Test Gear Configuration 14--EX-78785.

A

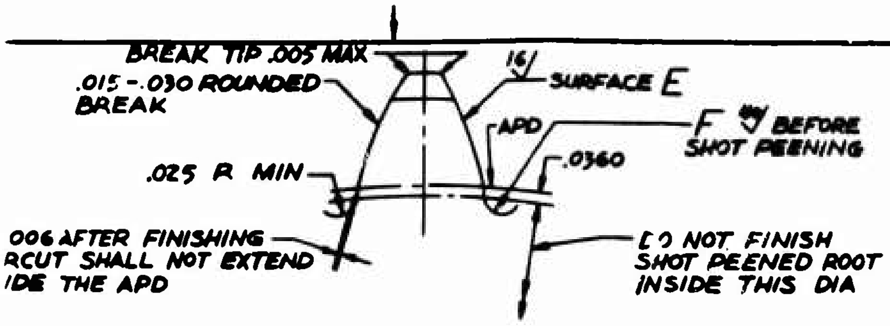

ENLARGED VIEW OF GEAR PROFILE
SCALE NONE

ECTRO CHEMICAL ETCH ALLISON PART NO. AND LAST
ANGE LETTER, "SER" AND SERIAL NO. HERE PER AS478-7A1 OR 7A2

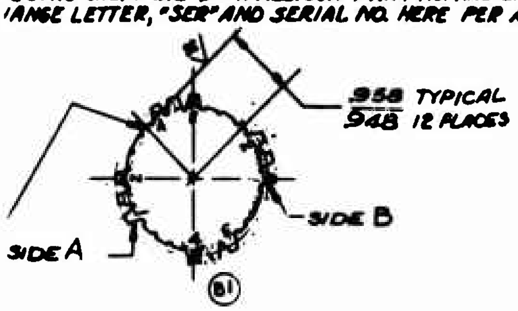

PROCESS GEAR IN THE FOLLOWING SEQUENCE

1. AFTER CUTTING GEAR TEETH, CARBURIZE AND HARDEN
2. AREA F SHALL INCLUDE ALL SURFACES BETWEEN THE APD AND THE ROOT DIA
OR SOLUTION MACHINE AREA F PER EPS 13066 TO REMOVE .002-.004 PER SURFACE
3. SHOT PEEN SURFACES AS REQUIRED
4. GRIND INVOLUTE SURFACE E TO FINISH SIZE

2.2006 $^{+.0000}_{-.0039}$

MATERIAL-AMS 6265 STEEL
FORGED BARS

DIA
CORDANCE WITH EDI 9

$^{+.0000}_{-.0018}$

DIA A SHALL BE CONCENTRIC WITH PD WITHIN .002 TIR

BREAK SHARP EDGES .010 UOS

MACHINE ALL OVER. PEEN GEAR TEETH PER EPS 12140
FOLLOWED BY EPS 12176
REMAINING SURFACES MAY BE PEENED PER EPS 12140
UNLESS SPECIFICALLY CONTROLLED BY A √ SYMBOL

SURFACE CHARACTERISTICS NOT CONTROLLED BY A √
SYMBOL SHALL BE COMMENSURATE WITH GOOD MANU-
FACTURING PRACTICES WHICH PRODUCE ACCEPTABLE
QUALITY LEVELS.

HEAT TREAT PER EPS 202

CASE HARDEN GEAR TEETH OUTSIDE 1.570 DIA
(OPTIONAL TO CASE HARDEN ALL OVER) EFFECTIVE CASE
DEPTHS AS FOLLOWS:
.020-.030 BEFORE FINISHING
.015-.030 AFTER FINISHING
ROCKWELL HARDNESS - CASE C58 MIN
CORE C34 MIN

INSPECT PER EIS 985 (MAGNETIC)

BLACK OXIDE PER AMS 2485

ALL DIMENSIONS TO BE MET AFTER PROCESSING

FORGING SHALL CONFORM TO EDI 138 AND EIS 502

tion 14—EX-78785.

B

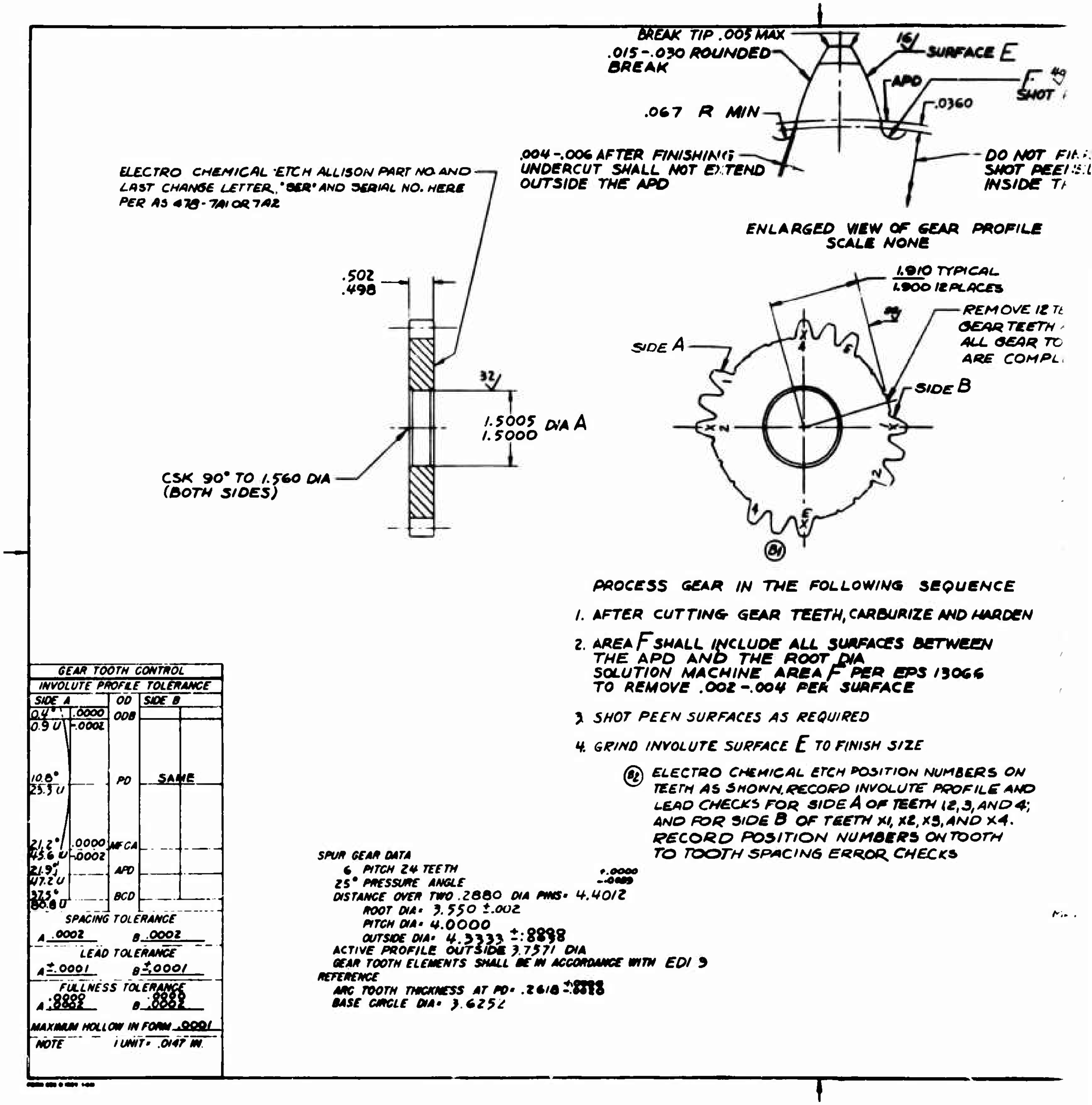

Figure 125. Fatigue Test Gear Configuration 15—EX-78786.

A

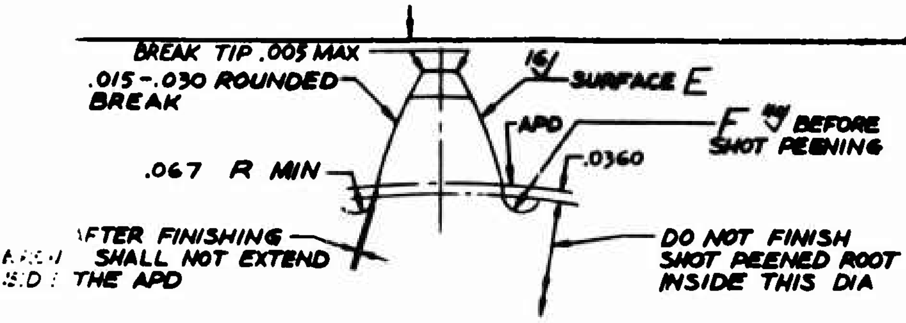

ENLARGED VIEW OF GEAR PROFILE
SCALE NONE

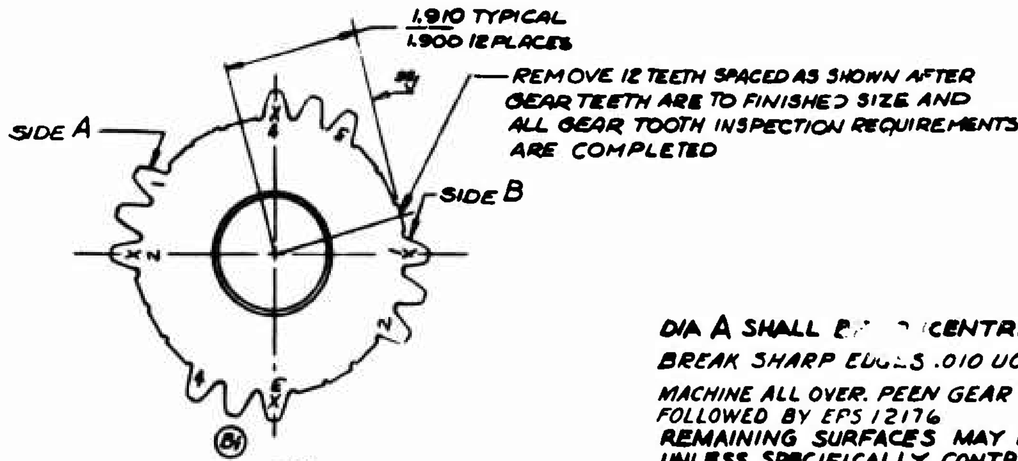

PROCESS GEAR IN THE FOLLOWING SEQUENCE

AFTER CUTTING GEAR TEETH, CARBURIZE AND HARDEN

AREA F SHALL INCLUDE ALL SURFACES BETWEEN THE APD AND THE ROOT DIA
OLUTION MACHINE AREA F PER EPS 13066
O REMOVE .002-.004 PER SURFACE

SHOT PEEN SURFACES AS REQUIRED

GRIND INVOLUTE SURFACE E TO FINISH SIZE

(B2) ELECTRO CHEMICAL ETCH POSITION NUMBERS ON TEETH AS SHOWN. RECORD INVOLUTE PROFILE AND LEAD CHECKS FOR SIDE A OF TEETH 1,2,3, AND 4; AND FOR SIDE B OF TEETH X1, X2, X3, AND X4. RECORD POSITION NUMBERS ON TOOTH TO TOOTH SPACING ERROR CHECKS

.0000
-.0089
012

NCE WITH EDI 9

DIA A SHALL BE CONCENTRIC WITH PD WITHIN .002 TIR

BREAK SHARP EDGES .010 UOS

MACHINE ALL OVER. PEEN GEAR TEETH PER EPS 12140 FOLLOWED BY EPS 12176
REMAINING SURFACES MAY BE PEENED PER EPS 12140 UNLESS SPECIFICALLY CONTROLLED BY A √ SYMBOL

SURFACE CHARACTERISTICS NOT CONTROLLED BY A √ SYMBOL SHALL BE COMMENSURATE WITH GOOD MANUFACTURING PRACTICES WHICH PRODUCE ACCEPTABLE QUALITY LEVELS.

HEAT TREAT PER EPS 202

CASE HARDEN GEAR TEETH OUTSIDE 3.340 DIA (OPTIONAL TO CASE HARDEN ALL OVER) EFFECTIVE CASE DEPTHS AS FOLLOWS:
.035-.045 BEFORE FINISHING
.030-.045 AFTER FINISHING
ROCKWELL HARDNESS - CASE C58 MIN
CORE C34 MIN

INSPECT PER EIS 985 (MAGNETIC)

BLACK OXIDE PER AMS 2485

ALL DIMENSIONS TO BE MET AFTER PROCESSING

FORGING SHALL CONFORM TO EDI 138 AND EIS 502

MATERIAL: AMS 6265 STEEL
FORGED BARS

n 15—EX-78786.

B

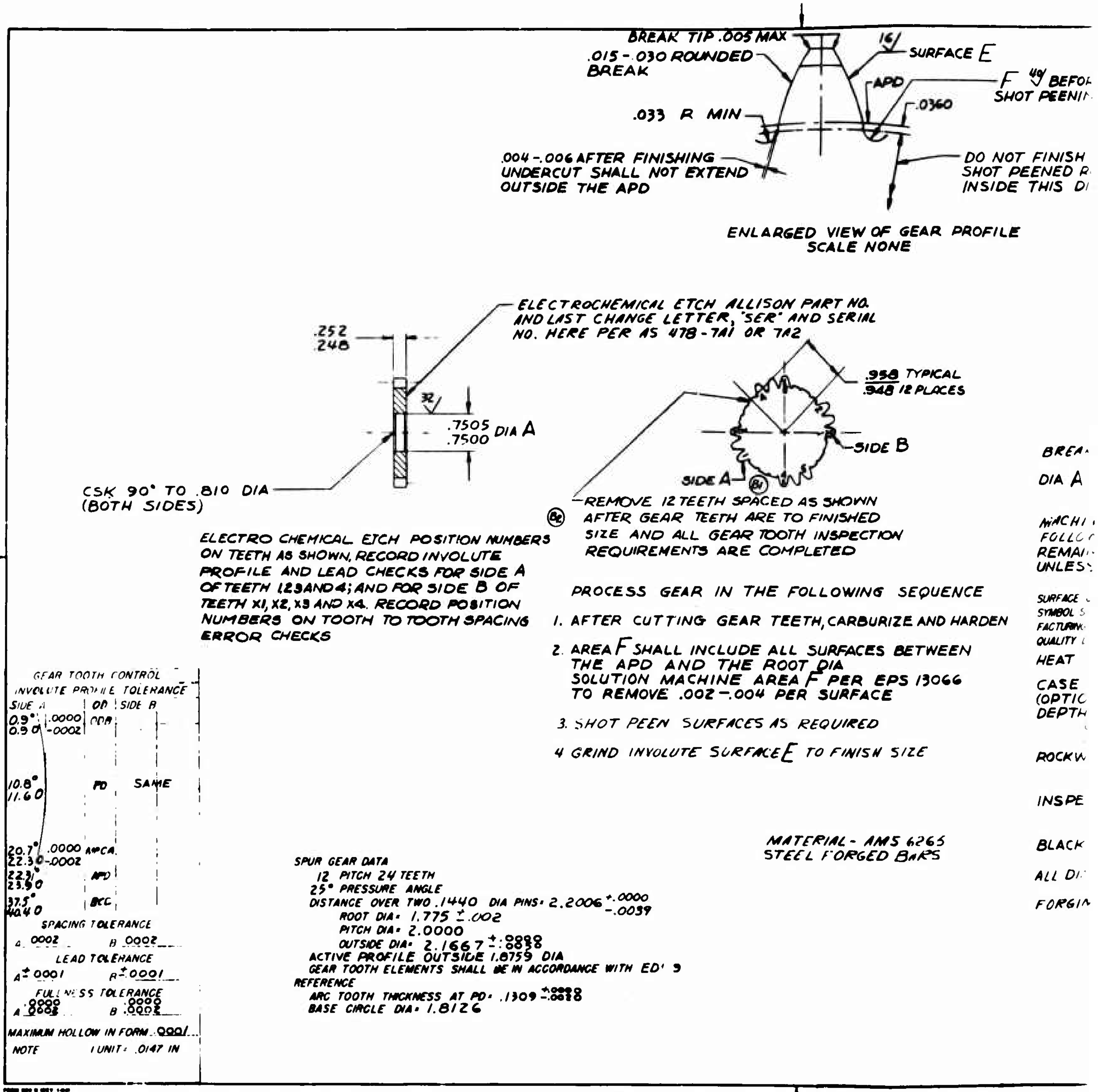

Figure 126. Fatigue Test Gear Configuration 16—EX-78787.

A

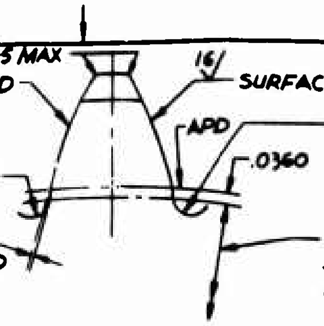

ENLARGED VIEW OF GEAR PROFILE
SCALE NONE

CTROCHEMICAL ETCH ALLISON PART NO.
LAST CHANGE LETTER, 'SER' AND SERIAL
HERE PER AS 478-7A1 OR 7A2

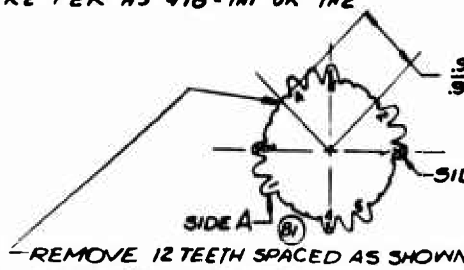

REMOVE 12 TEETH SPACED AS SHOWN
B2 AFTER GEAR TEETH ARE TO FINISHED SIZE AND ALL GEAR TOOTH INSPECTION REQUIREMENTS ARE COMPLETED

PROCESS GEAR IN THE FOLLOWING SEQUENCE

1. AFTER CUTTING GEAR TEETH, CARBURIZE AND HARDEN
2. AREA F SHALL INCLUDE ALL SURFACES BETWEEN THE APD AND THE ROOT DIA
   SOLUTION MACHINE AREA F PER EPS 13066 TO REMOVE .002-.004 PER SURFACE
3. SHOT PEEN SURFACES AS REQUIRED
4. GRIND INVOLUTE SURFACE E TO FINISH SIZE

MATERIAL - AMS 6265
STEEL FORGED BARS

2.2006 $^{+.0000}_{-.0039}$

DIA
CORDANCE WITH EDI 9

$^{+.0000}_{-.0018}$

BREAK SHARP EDGES .010 UOS

DIA A SHALL BE CONCENTRIC WITH PD WITHIN .002 TIR

MACHINE ALL OVER. PEEN GEAR TEETH PER EPS 12140 FOLLOWED BY EPS 12176
REMAINING SURFACES MAY BE PEENED PER EPS 12140 UNLESS SPECIFICALLY CONTROLLED BY A √ SYMBOL

SURFACE CHARACTERISTICS NOT CONTROLLED BY A √ SYMBOL SHALL BE COMMENSURATE WITH GOOD MANUFACTURING PRACTICES WHICH PRODUCE ACCEPTABLE QUALITY LEVELS.

HEAT TREAT PER EPS 202

CASE HARDEN GEAR TEETH OUTSIDE 1.570 DIA (OPTIONAL TO CASE HARDEN ALL OVER) EFFECTIVE CASE DEPTHS AS FOLLOWS:
.020-.030 BEFORE FINISHING
.015-.030 AFTER FINISHING
ROCKWELL HARDNESS - CASE C58 MIN
CORE C34 MIN

INSPECT PER EIS 985 (MAGNETIC)

BLACK OXIDE PER AMS 2485

ALL DIMENSIONS TO BE MET AFTER PROCESSING

FORGINGS SHALL CONFORM TO EDI 138 AND EIS 502

ration 16—EX-78787.

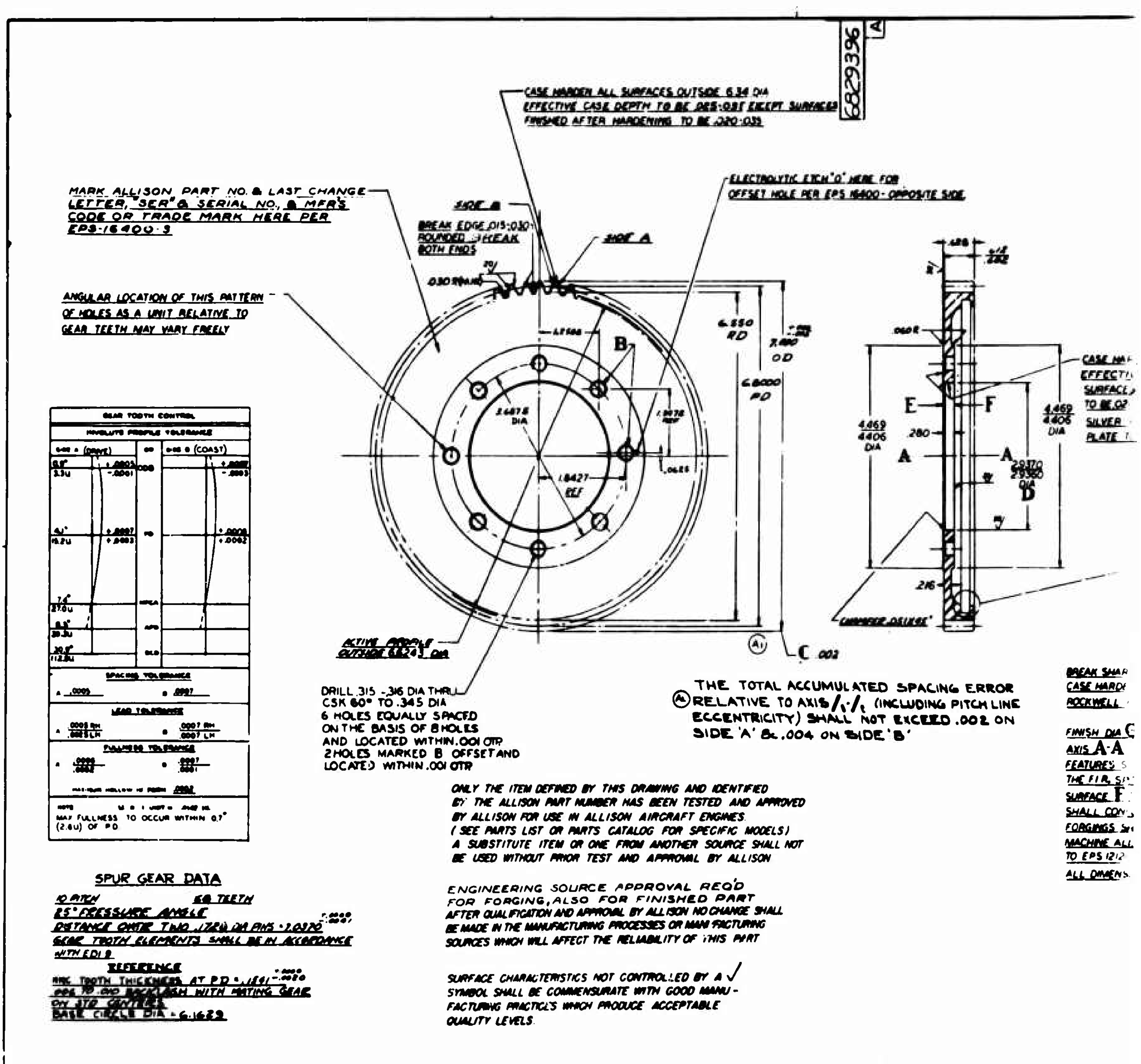

Figure 127. Main Accessory Drive Spur Gear (6829396).

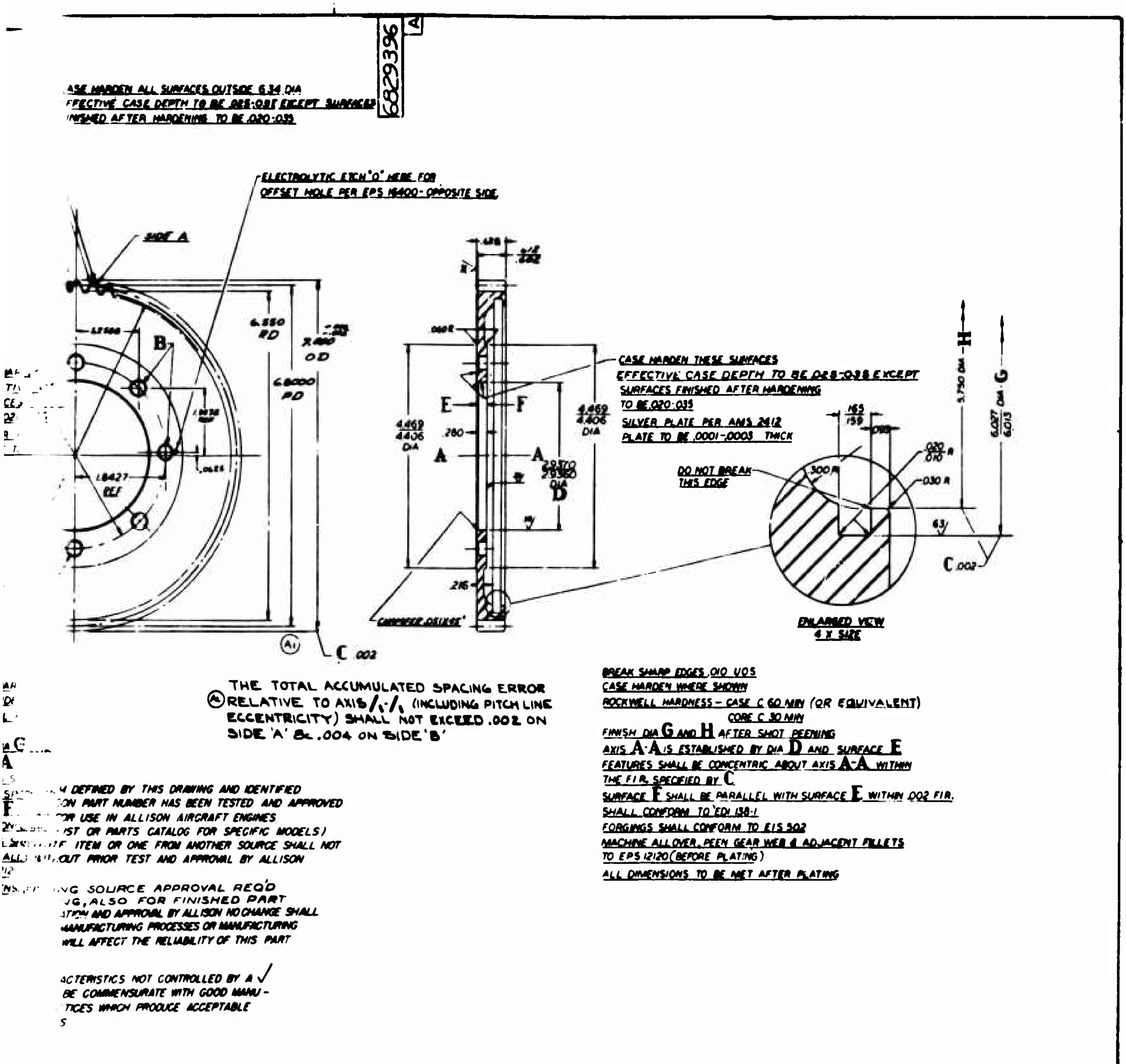

ur Gear (6829396).

B

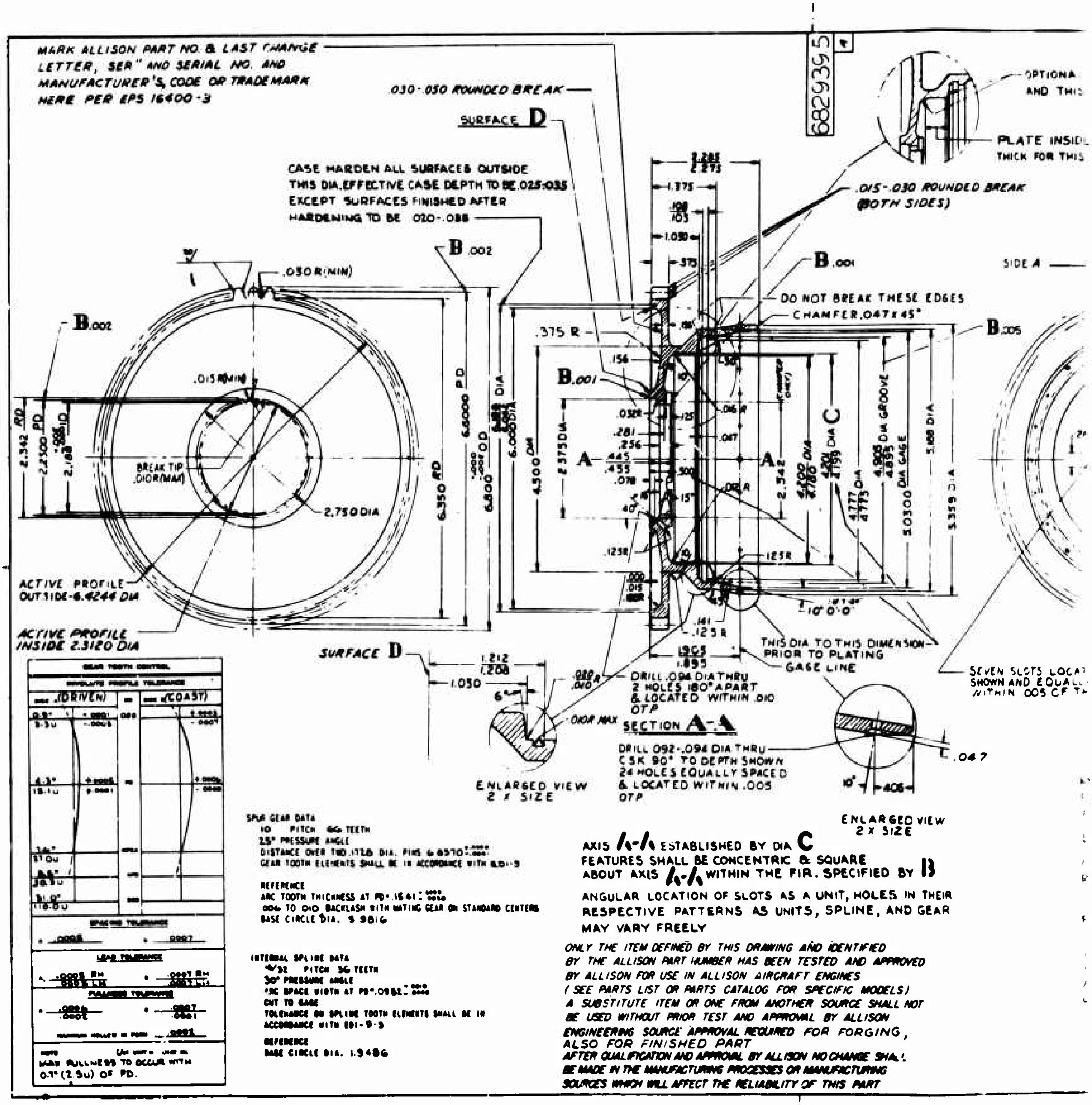

Figure 128. Propeller Brake Outer Member (6829395).

A

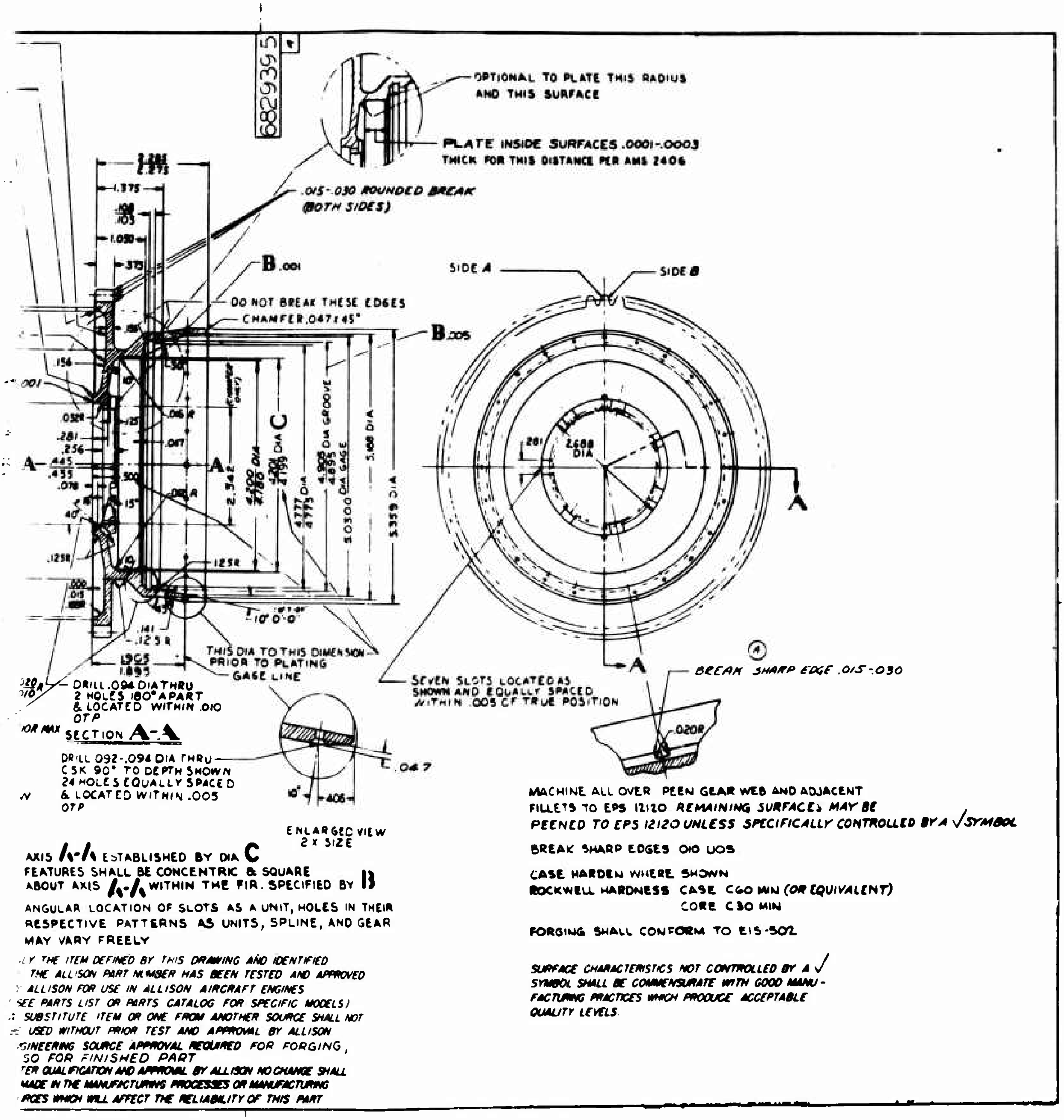

ber (6829395).

B

APPENDIX II

SAMPLE PROCESS ROUTING SHEETS

This appendix consists of sample process routing sheets for a full form ground fillet gear (EX-78772, Figure 129) and for a protuberant hobbed gear (EX-78776, Figure 130). The processing routings for all 16 fatigue test gear part numbers were identical except for the changes required by the two root fillet configurations, as shown in these samples, and for the difference in carburized case depth required by the two diametral pitches.

ROUTE SHEET

SHEET 1 OF 5	PART NAME: FATIGUE TEST GEAR	PART OR TOOL NUMBER: EX-78772	REV
		NEXT ASSEMBLY NUMBER	REV
WRITTEN BY: — DATE: 9-8-65	MATERIAL SPEC – SIZE: AMS 6265 Forged Bar 5" dia. x 1" long	DRAWING NUMBER	REV
APPROVED BY: — DATE: —	MATERIAL SUBSTITUTION	MODEL NO: EX-78772	REV: B

OPER NO	DEPT	OPERATION	TOOL NO	TOOL CODE	MACHINE
1	856S	Machine to Sketch Oper. 1 and deburr.			Lathe
3	819	Inspect and attach serial number. Start log of PCI 8000 and required information. Forward parts to Dept. 846.			
5	846	Hold until all 16 lots of gears are ready to core harden.			
7	862F	Harden at 1750° and temper per EPS 202 and PCI 8000 for control. C34 - C38. CAUTION: Core harden all 16 lots of gears at same time.			Furnace
9	859	Gritblast.			
11	819	Rockwell and magnaflux.			
13	856S	Machine to sketch Oper. #13 and deburr. Transfer tag.			Lathe

Figure 129. Typical Routing Sheet for Full Form Ground Fillet Gear, EX-78772 (Sheet 1 of 9).

ROUTE SHEET

SHEET 2 OF 5		PART NAME: Same as Sheet #1	PART OR TOOL NUMBER: EX-78772	REV
WRITTEN BY	DATE 9-9-65	MATERIAL SPEC – SIZE	NEXT ASSEMBLY NUMBER	REV
APPROVED BY	DATE	MATERIAL SUBSTITUTION	DRAWING NUMBER	REV
			MODEL NO	REV

OPER NO	DEPT	OPERATION	TOOL NO	TOOL CODE	MACHINE
15	858	Grind to sketch oper. #15 and deburr. Transfer tag.			Grind
17	854	Rough hob to 4.4367 + .000 - .002" over (2) .288" dia. pins. Hob (5) pieces of this P/N at same time. CAUTION: Use proper hob. Deburr. Transfer tag.	8-17429 SPT 2603	Bush Hob	Gear Hob
19	854	Round break gear teeth .031 - .046."			
21	819	Gear Lab. Inspect and forward to Dept. 846. Etch S/N on part for heat treat operations.			
23	846	Hold until all (16) lots of gears are ready for carburizing.			
25	862F	Carburize and anneal per EPS 202 - .035 - .045" effective case depth. Use PCI 8000 for control. CAUTION: Carburize (8) lots of gears requiring this case depth at the same time.			Furnace

Figure 129. Typical Routing Sheet for Full Form Ground Fillet Gear, EX-78772 (Sheet 2 of 9).

ROUTE SHEET

SHEET 3 OF 5		PART NAME: Same as Sheet #1	PART OR TOOL NUMBER: EX-78772	REV
WRITTEN BY	DATE 9-9-65	MATERIAL SPEC – SIZE	NEXT ASSEMBLY NUMBER	REV
APPROVED BY	DATE	MATERIAL SUBSTITUTION	DRAWING NUMBER	REV
			MODEL NO	REV

OPER NO	DEPT	OPERATION	TOOL NO	TOOL CODE	MACHINE
27	862C	Copper plate all over per PCI 2001. Copper plate (16) lots of gears at the same time.			Plating
29	862F	Harden and temper per EPS-202 and PCI 8000 for control. CAUTION: All (16) lots of gears to be heat treated at the same time.			Furnace
31	859	Gritblast.			
33	862C	Strip copper plating per PCI 2001. Strip all (16) lots of gears at the same time.			Plating
35	859	Mask and shotblast gear teeth only with 80 grit chilled shot.			
37	819	Rockwell and magnaflux.			
38	819	Gear Lab. Inspect gear and record information.			
39	858	Grind to sketch Oper. #39 and deburr. Transfer tag. See that S/N is etched back on part after grinding.	8-17428	Arbor	Grind

Figure 129. Typical Routing Sheet for Full Form Ground Fillet Gear, EX-78772 (Sheet 3 of 9).

ROUTE SHEET

SHEET 4 OF 5	PART NAME Same as Sheet #1	PART OR TOOL NUMBER EX-78772	REV
WRITTEN BY / DATE	MATERIAL SPEC – SIZE	NEXT ASSEMBLY NUMBER	REV
APPROVED BY / DATE	MATERIAL SUBSTITUTION	DRAWING NUMBER	REV
		MODEL NO	REV

OPER NO	DEPT	OPERATION	TOOL NO	TOOL CODE	MACHINE
41	819	Remove metal tag and etch S/N on web.			
43	862F	Stress relieve per EPS 202 and PCI 8000.			Furnace
45	866	Etch mark teeth per B/P.			Sub Assy
47	819	Gear Lab. Inspect pin size, root dia., root radius and record.			
49	854	Finish grind gear to 4.3999-4.3979"dia. over (2) .288"dia. pins. Grind (5) pieces of this P/N at the same time. Use 10" grinding wheel TA46G10VB. Down feed .0005 - .001"max. per pass of grinding wheel. Transfer tag.	8-17428 8-17627	Arbor Forms	P & W Gear Grind
50	819	Gear lab inspect gear and record information.			
51	862F	Stress relieve per EPS 202 and PCI 8000.			Furnace
53	862C	Nital etch per EIS 1510.			Plating
54	819	Red line 4 teeth.			

Figure 129. Typical Routing Sheet for Full Form Ground Fillet Gear, EX-78772 (Sheet 4 of 9).

ROUTE SHEET

SHEET 5 OF 5	PART NAME: Same as Sheet #1	PART OR TOOL NUMBER: EX-78772	REV
WRITTEN BY / DATE: 9-9-65	MATERIAL SPEC – SIZE	NEXT ASSEMBLY NUMBER	REV
APPROVED BY / DATE	MATERIAL SUBSTITUTION	DRAWING NUMBER	REV
		MODEL NO	REV

OPER NO	DEPT	OPERATION	TOOL NO	TOOL CODE	MACHINE
55	859	Mask and shot peen gear teeth only per EPS 12140 followed by EPS 12176. Shot peen (16) lots of gears at the same time if possible; if not, shot peen consecutively with one setup.			
57	854	Finish hone gear. Use 280 grit hone.	8-17428 SPT-2606	Arbor Hone	Gear Hone
59	819	Inspect gear and record information.			
61	854	Mount (5) pieces on arbor, matching marked teeth. Remove (12) teeth per B/P. Down feed .0005 - .001" max. per pass of grinding wheel.	8-17428	Arbor	Gear Grind
63	862F	Stress relieve per EPS 202 and PCI 8000.			Furnace
65	819	Magnaflux.			
67	819	Inspect for black oxide.			
69	IPO BC5	Black oxide per AMS-2485.			
71	819	Inspect and identify.			

Figure 129. Typical Routing Sheet for Full Form Ground Fillet Gear, EX-78772 (Sheet 5 of 9).

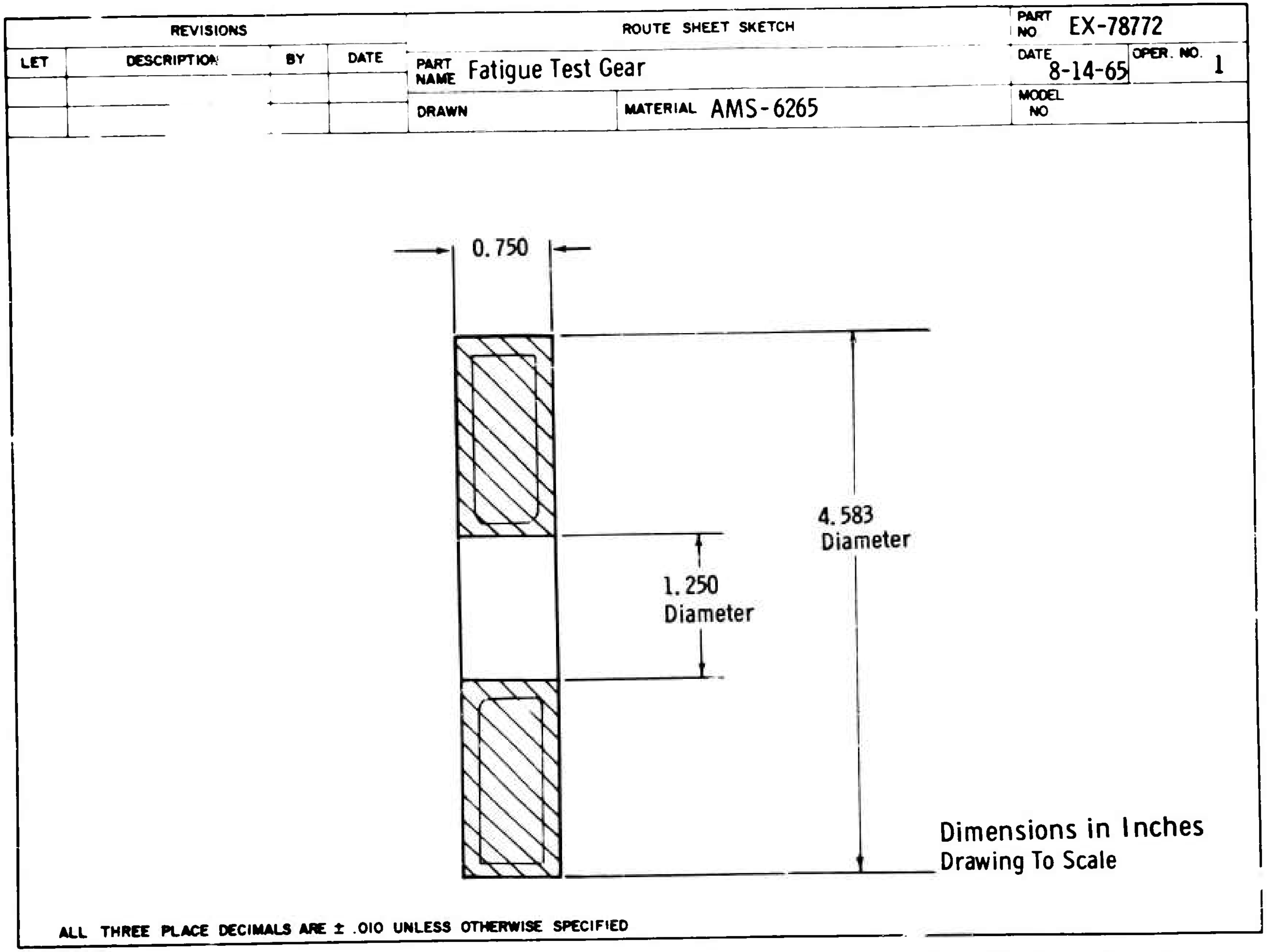

Figure 129. Typical Routing Sheet for Full Form Ground Fillet Gear, EX-78772 (Sheet 6 of 9).

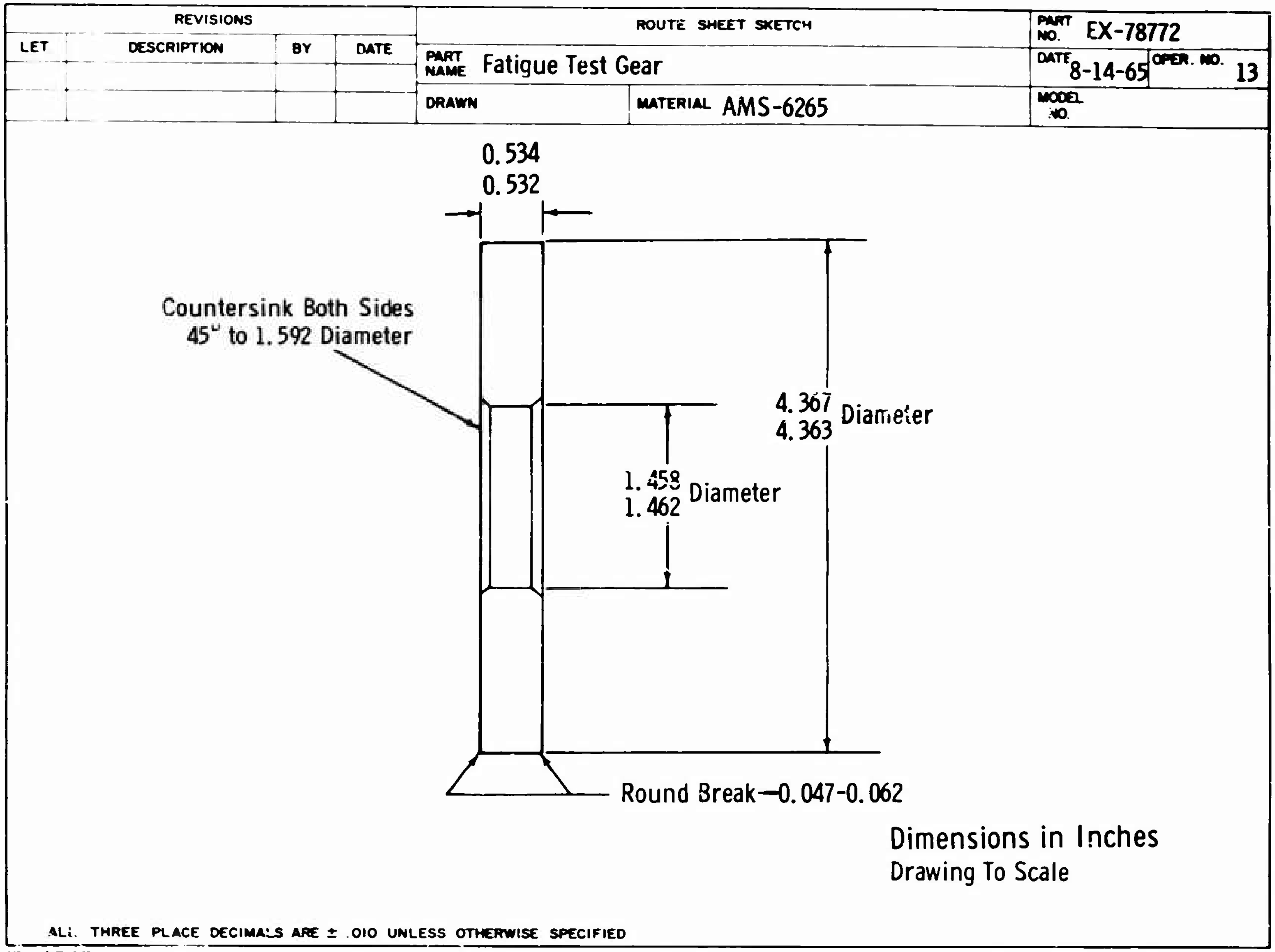

Figure 129. Typical Routing Sheet for Full Form Ground Fillet Gear, EX-78772 (Sheet 7 of 9).

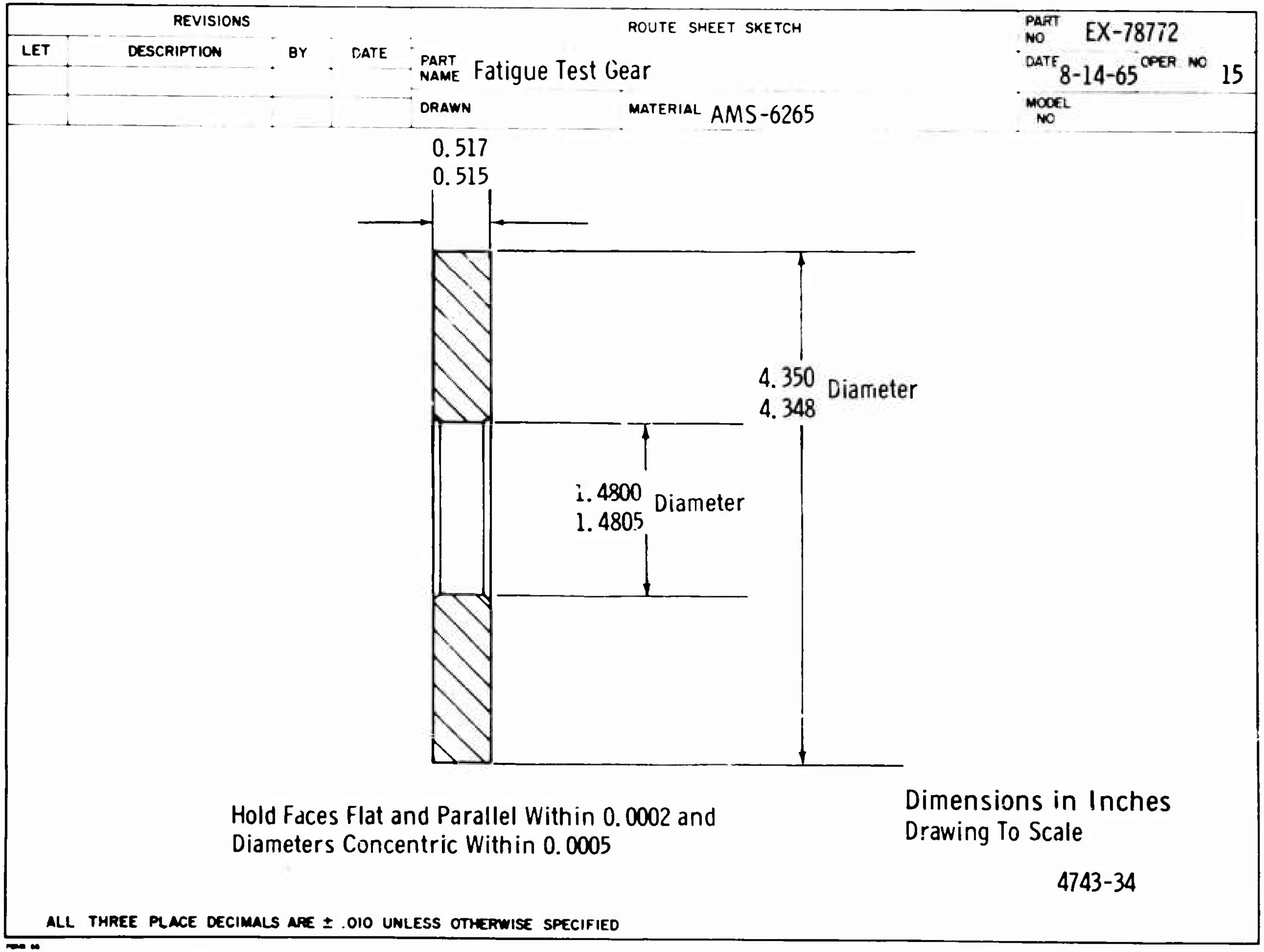

Figure 129. Typical Routing Sheet for Full Form Ground Fillet Gear, EX-78772 (Sheet 8 of 9).

REVISIONS				ROUTE SHEET SKETCH		PART NO. EX-78772	
LET.	DESCRIPTION	BY	DATE	PART NAME Fatigue Test Gear		DATE 8-14-65	OPER. NO. 39
				DRAWN	MATERIAL AMS-6265	MODEL NO	

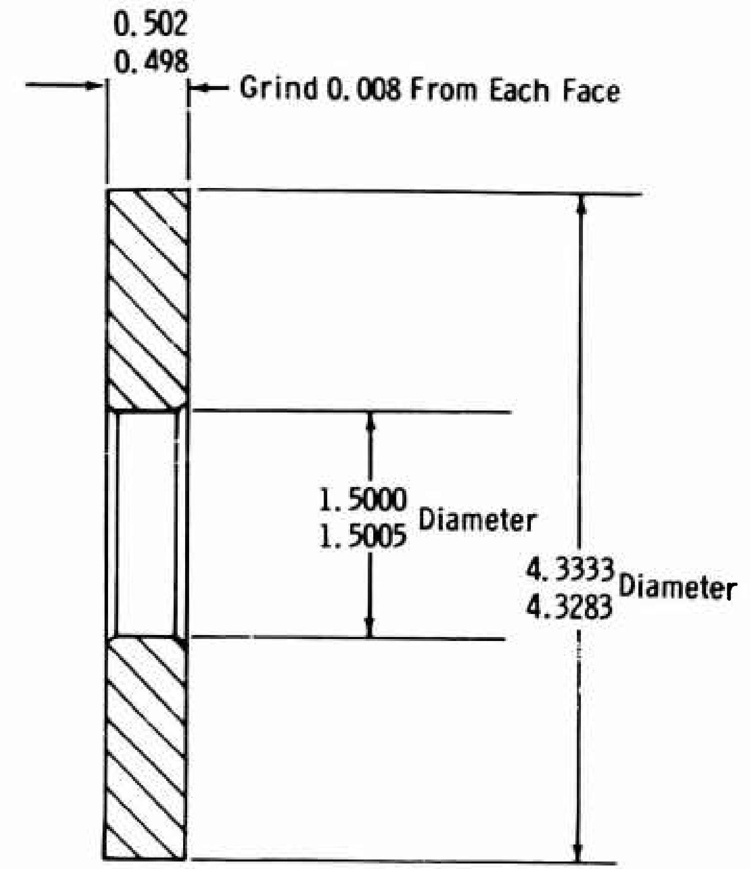

True to Pitch Diameter of Gear
Use Arbor for OD Grind
Faces Must Be Flat and Parallel Within 0.0002

Dimensions in Inches
Drawing To Scale

ALL THREE PLACE DECIMALS ARE ± .010 UNLESS OTHERWISE SPECIFIED

Figure 129. Typical Routing Sheet for Full Form Ground Fillet Gear, EX-78772 (Sheet 9 of 9).

ROUTE SHEET

SHEET 1 OF 5	PART NAME: FATIGUE TEST GEAR	PART OR TOOL NUMBER: EX-78776	REV
WRITTEN BY:	DATE: 9-8-65	MATERIAL SPEC – SIZE: AMS 6265 Forged Bar 5" dia x 1" long	NEXT ASSEMBLY NUMBER:	REV
APPROVED BY:	DATE:	MATERIAL SUBSTITUTION:	DRAWING NUMBER:	REV
			MODEL NO: EX-78776	REV: B

OPER NO	DEPT	OPERATION	TOOL NO	TOOL CODE	MACHINE
1	856S	Machine to sketch Oper. 1 and deburr.			Lathe
3	819	Inspect and attach serial number. Start log of PCI 8000 and required information. Forward parts to Dept. 846.			
5	846	Hold until all 16 lots of gears are ready to core harden.			
7	862F	Harden at 1750° and temper per EPS 202 and PCI 8000 for control. C34-C38. CAUTION: Core harden all 16 lots of gears at same time.			Furnace
9	859	Grit blast.			
11	819	Rockwell and magnaflux.			
13	856S	Machine to sketch Oper. #13 and deburr. Transfer tag.			Lathe

Figure 130. Typical Routing Sheet for Protuberant Hobbed Gear, EX-78776 (Sheet 1 of 9).

ROUTE SHEET

SHEET 2 OF 5		PART NAME: Same as Sheet #1	PART OR TOOL NUMBER: EX 78776	REV
WRITTEN BY	DATE 9-9-65	MATERIAL SPEC – SIZE	NEXT ASSEMBLY NUMBER	REV
APPROVED BY	DATE	MATERIAL SUBSTITUTION	DRAWING NUMBER	REV
			MODEL NO	REV

OPER NO	DEPT	OPERATION	TOOL NO	TOOL CODE	MACHINE
15	858	Grind to sketch Oper. #15 and deburr. Transfer tag.			Grind
17	854	Rough hob to 4.4367 + .000 - .002" over (2) .288" dia. pins. Hob 5 pcs. of this P/N at same time. CAUTION: Use proper hob. Deburr. Transfer tag.	8-17429 SPT-2604	Bush Hob	Gear Hob
19	854	Round break gear teeth .031 - .046"			
21	819	Gear Lab. Inspect and forward to Dept. 846. Etch serial number for heat treat operations.			
23	846	Hold until all 16 lots of gears are ready for carburizing.			
25	862F	Carburize and anneal per EPS 202 .035-.045" effective case depth. Use FCI 8000 for control. CAUTION: Carburize 8 lots of gears requiring this case depth at the same time.			Furnace

Figure 130. Typical Routing Sheet for Protuberant Hobbed Gear, EX-78776 (Sheet 2 of 9).

ROUTE SHEET

SHEET 3 OF 5		PART NAME: Same as Sheet #1	PART OR TOOL NUMBER: EX 78776	REV
			NEXT ASSEMBLY NUMBER	REV
WRITTEN BY	DATE 9-9-65	MATERIAL SPEC – SIZE	DRAWING NUMBER	REV
APPROVED BY	DATE	MATERIAL SUBSTITUTION	MODEL NO	REV

OPER NO	DEPT	OPERATION	TOOL NO	TOOL CODE	MACHINE
27	862C	Copper plate all over per PCI 2001. Copper plate 16 lots of gears at the same time.			Plating
29	862F	Harden and temper per EPS 202 and PCI 8000 for control. CAUTION: All 16 lots of gears to be heat treated at the same time.			Furnace
31	859	Gritblast.			
33	862C	Strip copper plating per PCI 2001. Strip all 16 lots of gears at the same time.			Plating
35	859	Shotblast gear teeth with 80 grit chilled shot.			
37	819	Rockwell and magnaflux.			
38	819	Gear Lab. Inspect gear and record information.			

Figure 130. Typical Routing Sheet for Protuberant Hobbed Gear, EX-78776 (Sheet 3 of 9).

ROUTE SHEET

SHEET 4 OF 5	PART NAME: Same as sheet #1			PART OR TOOL NUMBER: EX-78776	REV
				NEXT ASSEMBLY NUMBER	REV
WRITTEN BY	DATE: 9-9-[illegible]5	MATERIAL SPEC – SIZE		DRAWING NUMBER	REV
APPROVED BY	DATE	MATERIAL SUBSTITUTION		MODEL NO	REV

OPER NO	DEPT	OPERATION	TOOL NO	TOOL CODE	MACHINE
39	862C	Mask and solution machine gear teeth only per EPS 13066, .002" max. stock removal. Solution machine 8 lots of gears requiring this operation at the same time, or as near alike as possible, removing the same amount of stock on all lots.			
40	819	Gear Lab. Inspect gear and reword information.			
41	859	Mask and shot peen gear teeth only per EPS-12140 followed by EPS 12176. Shot peen 10 lots of gears at the same time if possible; if not, shot peen consecutively with one setup.			
43	858	Grind per sketch Oper. #43 and deburr. Transfer tag. Etch S/N on part after grinding.	8-17428	Arbor	Grind
45	819	Remove metal tag and etch S/N on web.			
47	862F	Stress relieve per EPS 202 and PCI 8000.			Furnace
49	866	Etch mark gear teeth per B/P.			Sub Assy

Figure 130. Typical Routing Sheet for Protuberant Hobbed Gear, EX-78776 (Sheet 4 of 9).

ROUTE SHEET

SHEET 5 OF 5	PART NAME: Same as Sheet #1	PART OR TOOL NUMBER: EX 78776	REV
WRITTEN BY	DATE: 9-9-65	MATERIAL SPEC – SIZE	NEXT ASSEMBLY NUMBER	REV
APPROVED BY	DATE	MATERIAL SUBSTITUTION	DRAWING NUMBER	REV
			MODEL NO	REV

OPER NO	DEPT	OPERATION	TOOL NO	TOOL CODE	MACHINE
51	854	Finish grind gear. Grind 5 pieces of this P/N at the same time. Deburr. Use 8.66" dia. wheel 38A605KVBE. Down feed .0005 - .001" max. per pass of grinding wheel.	8-17428 8-17459	Arbor Pitch Block	Maag Gear Grind
52	819	Gear Lab. Inspect gear and record information and red line 4 teeth.			
53	862F	Stress relieve per EPS 202 and PCI 8000.			Furnace
54	862C	Nital etch per EIS 1510			Plating
55	854	Mount 5 pieces on arbor matching marked teeth. Remove 12 teeth per B/P. Down feed .0005-.001" max.	8-17428	Arbor	Gear Grind
57	862F	Stress relieve per EPS 202 and PCI 8000.			Furnace
59	819	Magnaflux			
61	819	Inspect for black oxide.			
63	IPO BC5	Black oxide per AMS 2485.			
65	819	Inspect and identify.			

Figure 130. Typical Routing Sheet for Protuberant Hobbed Gear, EX-78776 (Sheet 5 of 9).

REVISIONS				ROUTE SHEET SKETCH		PART NO. EX-78776
LET.	DESCRIPTION	BY	DATE	PART NAME Fatigue Test Gear		DATE 8-14-65 OPER. NO. 1
				DRAWN	MATERIAL AMS-6265	MODEL NO.

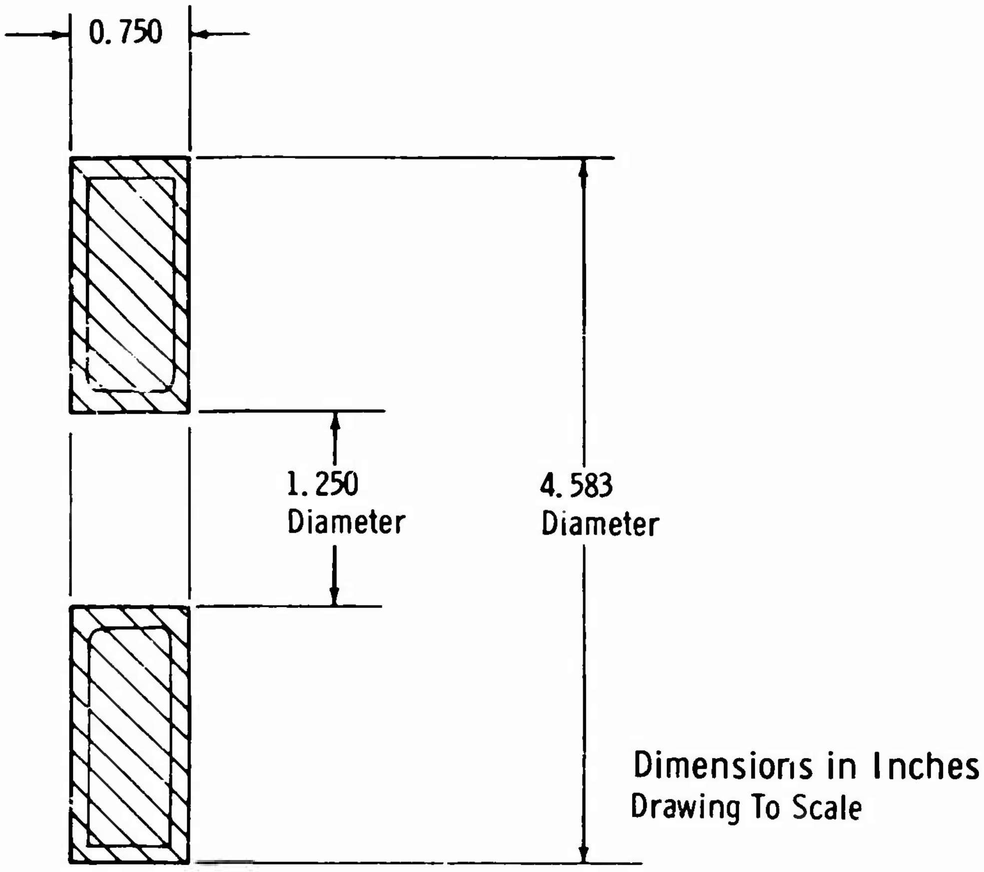

ALL THREE PLACE DECIMALS ARE ± .010 UNLESS OTHERWISE SPECIFIED

Figure 130. Typical Routing Sheet for Protuberant Hobbed Gear, EX-78776 (Sheet 6 of 9).

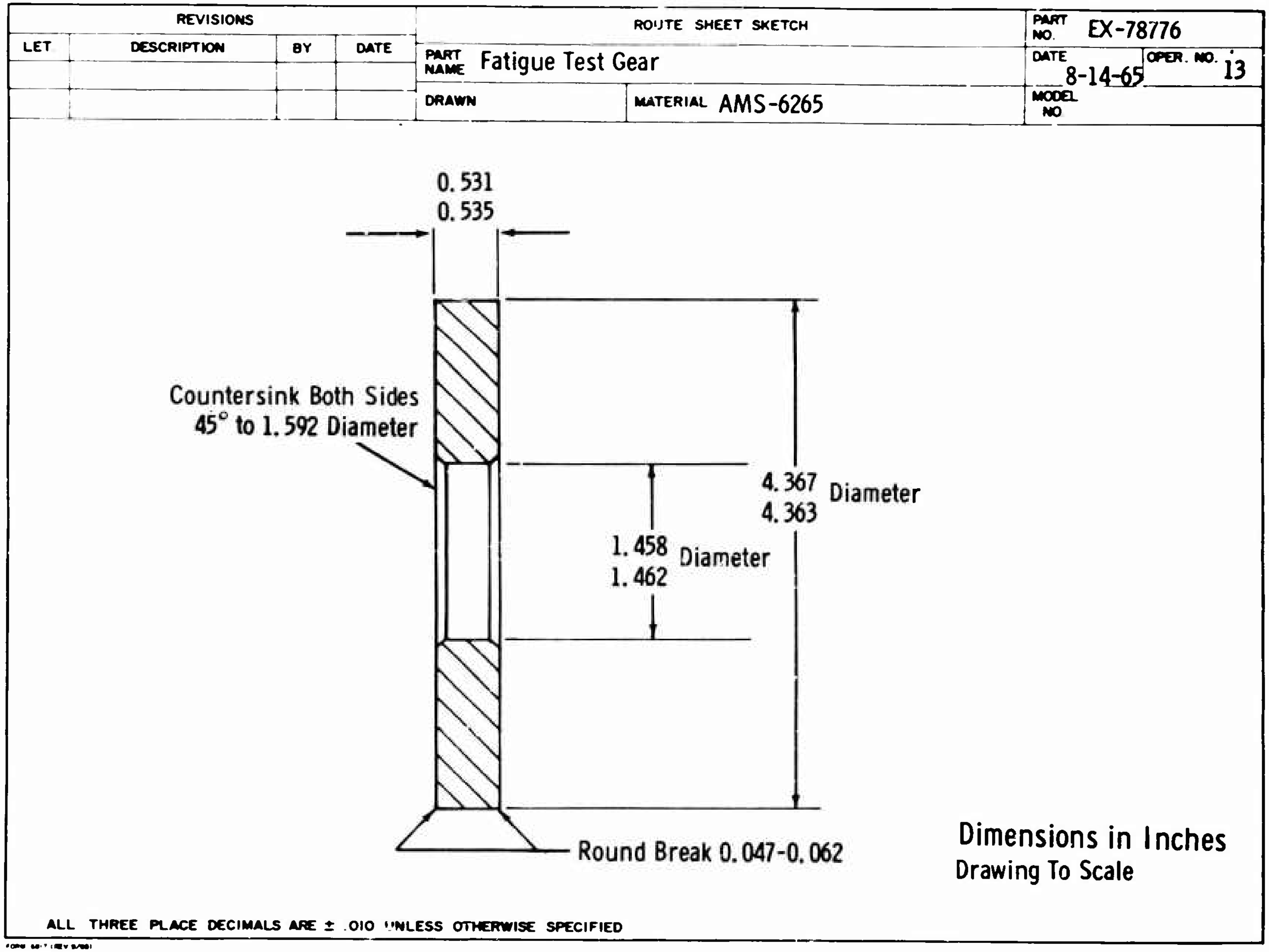

Figure 130. Typical Routing Sheet for Protuberant Hobbed Gear, EX-78776 (Sheet 7 of 9).

REVISIONS				ROUTE SHEET SKETCH		
LET.	DESCRIPTION	BY	DATE	PART NAME Fatigue Test Gear		PART NO. EX-78776
						DATE 8-14-65 / OPER. NO. 15
				DRAWN	MATERIAL AMS-6265	MODEL NO.

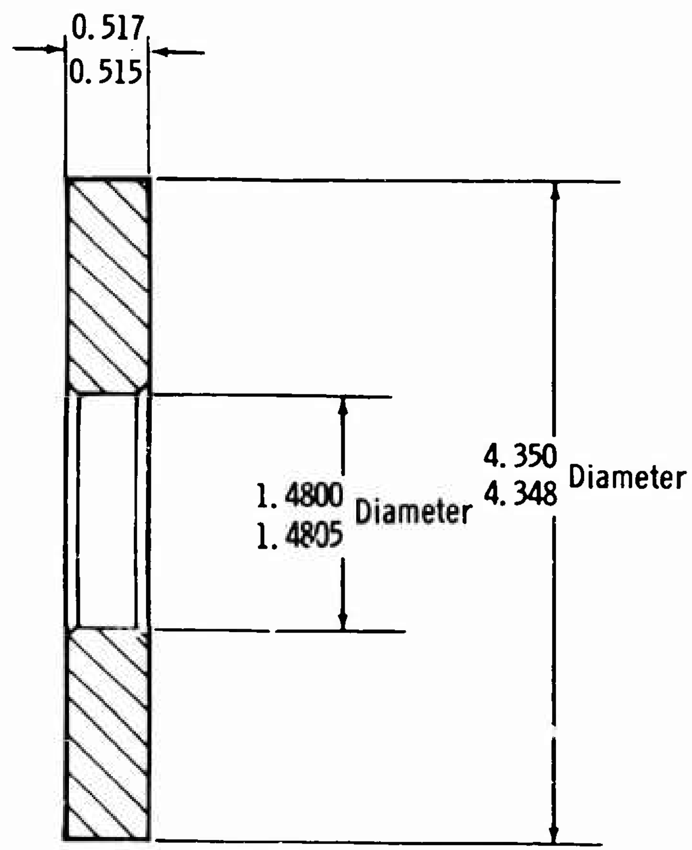

Hold Faces Flat and Parallel Within 0.0002 and Diameters Concentric Within 0.0005

Dimensions in Inches
Drawing To Scale

ALL THREE PLACE DECIMALS ARE ± .010 UNLESS OTHERWISE SPECIFIED

Figure 130. Typical Routing Sheet for Protuberant Hobbed Gear, EX-78776 (Sheet 8 of 9).

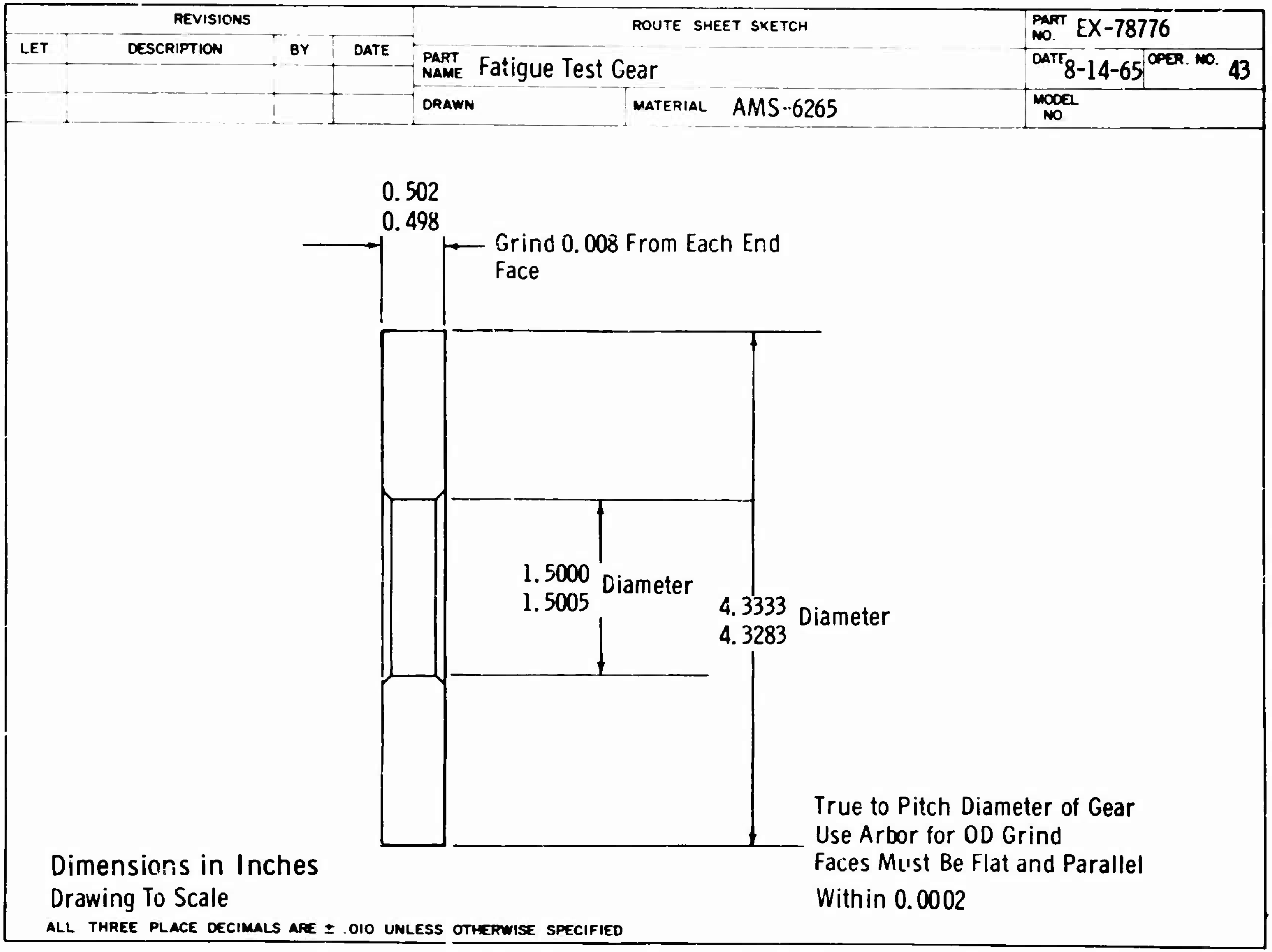

Figure 130. Typical Routing Sheet for Protuberant Hobbed Gear, EX-78776 (Sheet 9 of 9).

BLANK PAGE

APPENDIX III

MATHEMATICAL DESCRIPTION OF STATISTICAL TREATMENT OF TEST DATA

This appendix consists of a detailed description of the mathematical model developed to linearize the test data, its substantiation, its use to determine an endurance limit, and the determination of the variability associated with this endurance limit. A description of the method used to determine the significance of main effects and interactions for the four designed experiment variables is included. Finally, a mathematical equation developed to assign numerical values to the four geometric factors studied is described.

DERIVATION OF S/N CURVE

Analytical Model

There were two requisites for the mathematical model; it should linearize the relationship between cycles-to-failure and stress to define the endurance limit accurately, and it should make the variance of the transformed cycles equal within the range of interest for stress to make tests of significance meaningful.

The mathematical model developed is:

$$\text{Life}_T = \left(\frac{1}{K}\right)^C = A + Bx$$

where

K	= kilocycles to failure
x	= applied stress
C	= linearizing parameter
A and B	= constants to be determined by the least squares fitting method

The model was checked against two relatively large sets of data. The transformed data are plotted in Figures 131 and 132. The points and the fitted curve are presented in conventional S/N format in Figures 133 and 134. The linearity of the transformed data is evident by inspection. The homogeneity of variances was checked using Bartlett's test. The stress (or strength) at infinite life is clearly shown at $\text{Life}_T = \left(\frac{1}{K}\right)^C = 0.$

The value of C was selected by trial and error because of time limitations. Further development work is suggested to automate the optimization of C and to investigate an alternate transformation, $\text{Life}_T = \frac{1}{\log (CK)}$

Treatment of Runouts

Runout data were used in one of two ways. If only runouts occurred at any one stress level, the runouts were treated as failures at 10^9 cycles. Where both runouts and failures occurred at a stress level for any configuration, the data were plotted on normal probability paper using mean ranks to plot the cumulative probability. The points were fitted with a straight line with a slope that best fit all sets of data. The cycles at 50-percent failure represented the average life for all teeth tested at that stress level for the configuration. This value of life, weighted for the associated number of failed teeth, was used in the least squares fit of the complete S/N line.

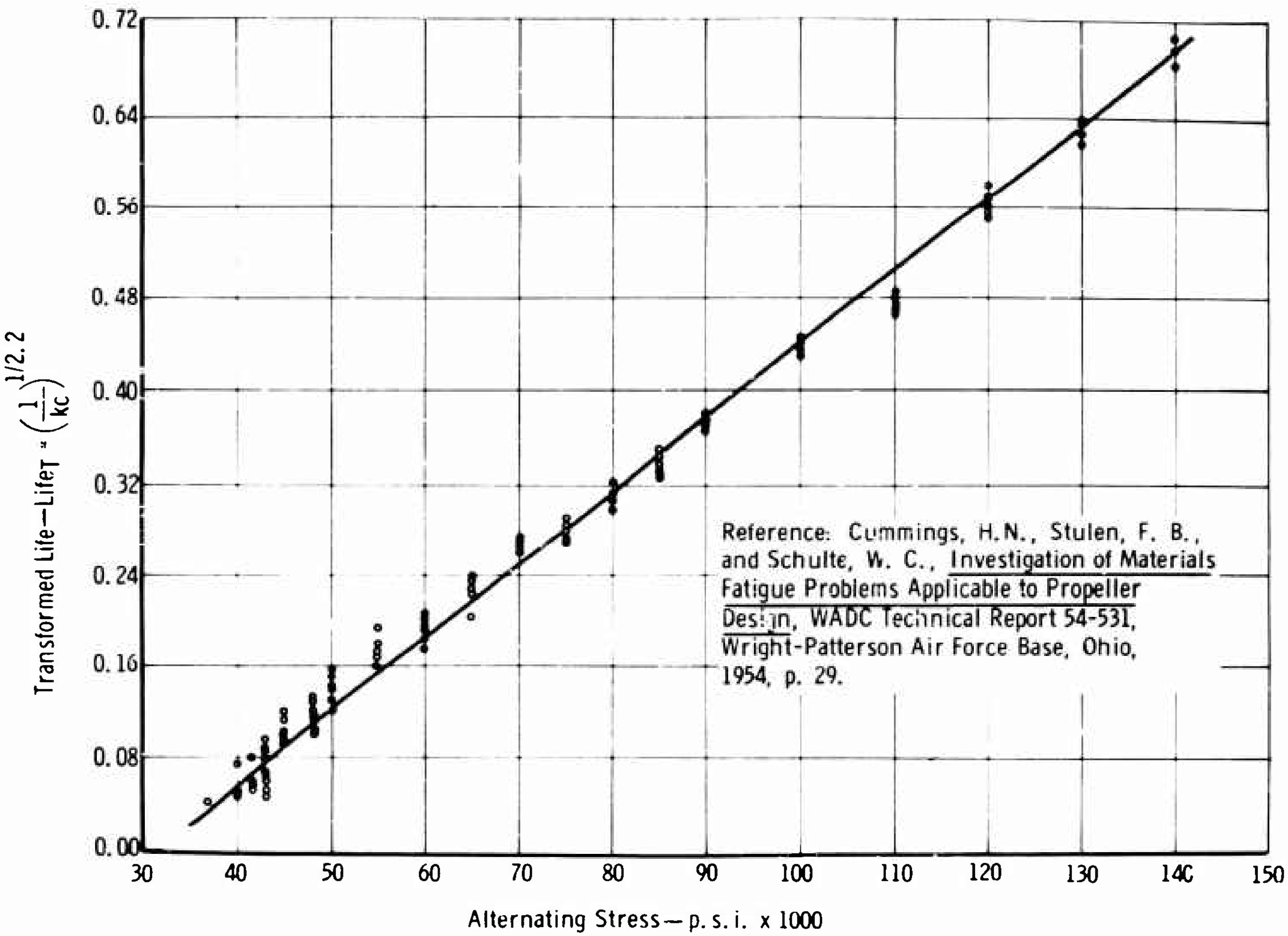

Figure 131. Results of R. R. Moore Tests on Notched 4340 Steel.

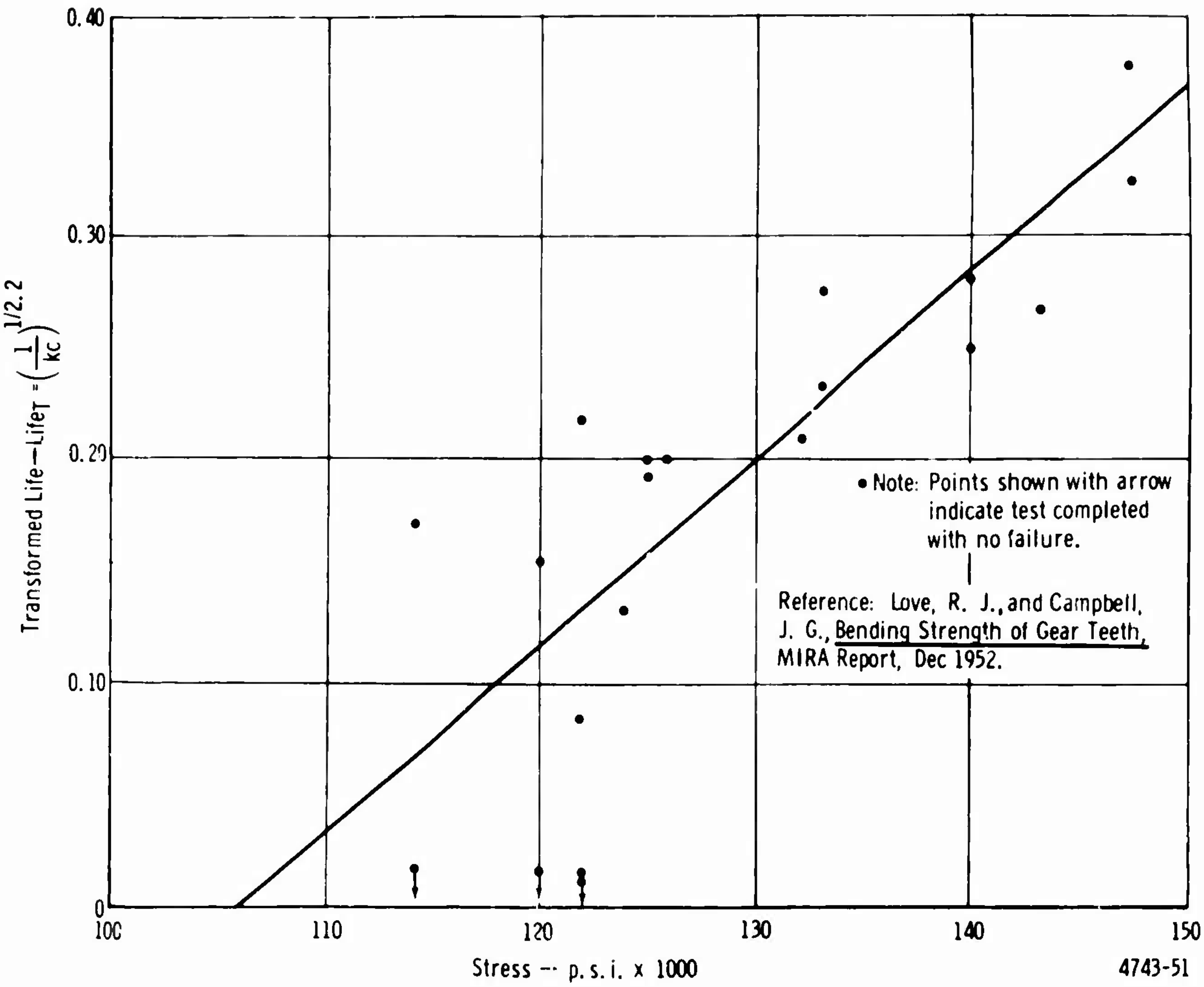

Figure 132. Transformed Gear Tooth Fatigue Data—British Steel EN 39A.

Analysis

The least squares fit of the S/N line for each combination of gear factors represents a solution to the equation $Life_T = A + Bx$. Recalling that the endurance limit occurs at $Life_T = 0$, it follows that $A + Bx = 0$ at this point. Subtracting A from both sides of the equation and dividing through by B, and since A is negative, the value of x at the endurance limit is simply A/B.

Each endurance limit A/B has a measure of variability associated with it. This variability is indicated by the scatter in test points about the line, which results from inherent variability in material, processing, and testing factors. The variability or variance, $(\sigma_{A/B})^2$, of each intercept was derived through error propagation techniques (reference 20):

$$(\sigma_{A/B})^2 = \frac{1}{B^2}\sigma_A^2 + \frac{A^2}{B^4}\sigma_B^2 + \frac{2A}{B^3}\sigma_{AB}^2$$

where the components σ_A^2, σ_B^2, and σ_{AB}^2 represent the variance of A, variance of B, and covariance of A and B, respectively. The variances of A, B, and the covariance

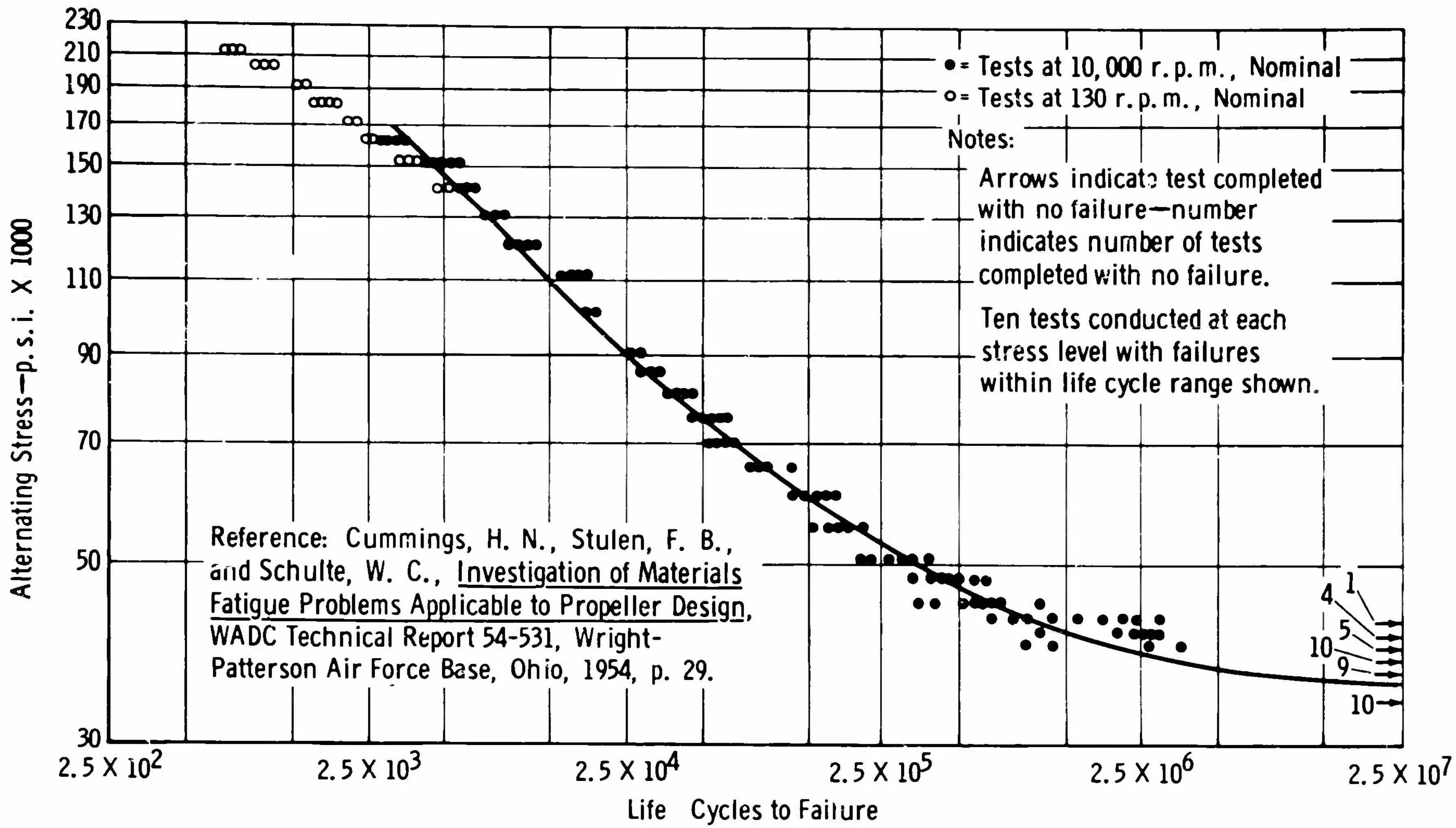

Figure 133. R. R. Moore Rotating Bending Test Data.

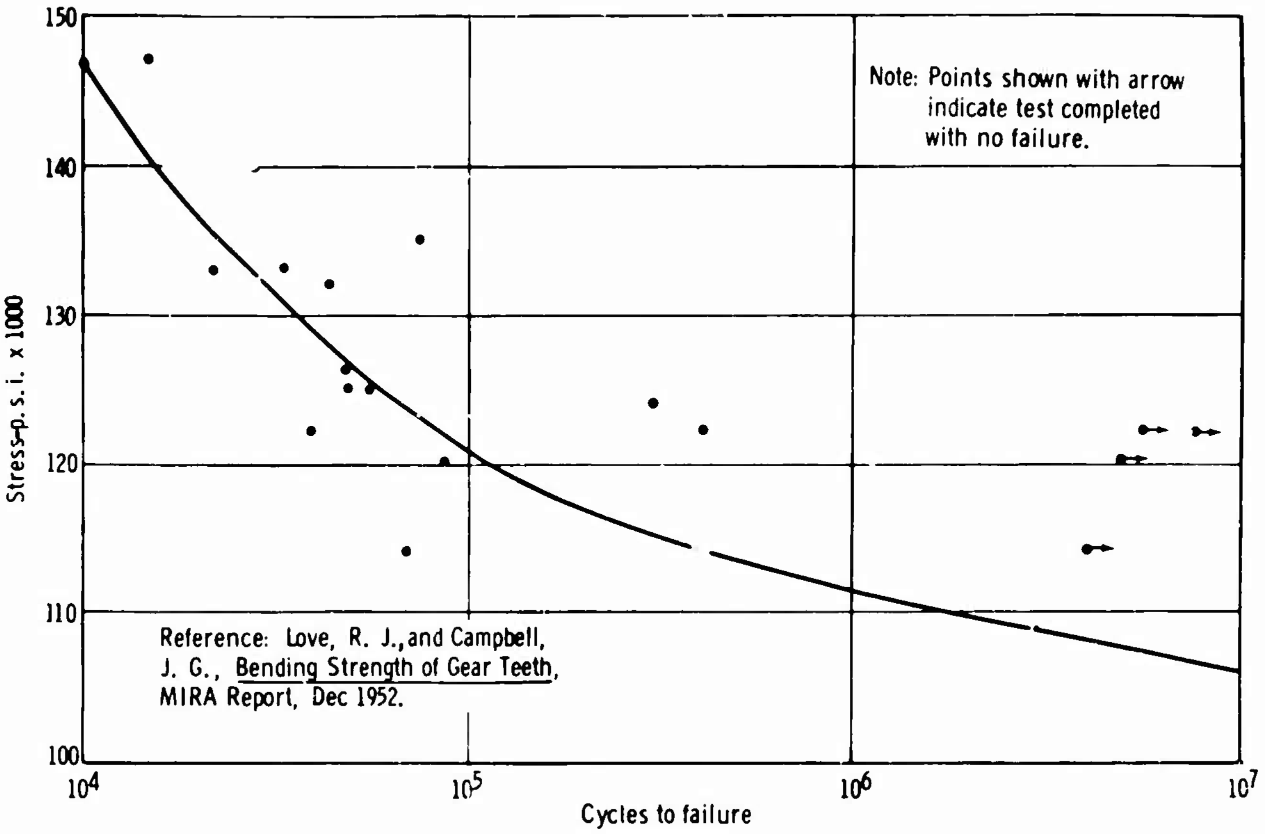

Figure 134. Gear Tooth Fatigue Data—British Steel EN 39A.

of A and B were evaluated using the techniques presented in reference 3. Briefly, a matrix arising from the least squares solution of A and B is set up and inverted. The inverse elements of the least squares matrix, when multiplied by the variance, $S_e^2 = \frac{\Sigma(\text{Life}_T - A - Bx)^2}{n-2}$ (where n is the number of test points defining the line) associated with regression, are the variances of A, B, and the covariance of A and B.

To test the significance of main effects and interactions, linear combinations of the 16 endurance limits were computed and then divided by the appropriate standard deviation. The linear combination divided by the standard deviation constitutes the criterion for "t" tests of significance.

STATISTICAL TESTS OF SIGNIFICANCE

The concept of statistical tests of significance arises because of the inherent variability associated with any type of testing. In particular, the variability associated with fatigue testing is large.

If repeat fatigue tests are made under identical test conditions, the computed endurance limits will not be identical, but will be distributed about the average of the computed values. If one or more test conditions are changed (i.e., geometric factors), a criterion may be set up to determine if the magnitude of the change in endurance limits is larger than can be expected due to chance alone—at a preselected probability level.

The criterion established was the "t" test, where "t" is the observed difference in endurance limits generated from two different test conditions. These test conditions were then divided by the standard deviation of the difference:

$$"t" = \frac{EL_1 - EL_2}{\sqrt{S_1^2 + S_2^2}}$$

where

EL_1 = the endurance limit associated with the first test condition

EL_2 = the endurance limit associated with the second test condition

S_1^2 and S_2^2 = the variances associated with the respective endurance limits

The critical "t" value is a number based on degrees of freedom (related to number of data points), and some preselected significance level α (an arbitrary risk of making a wrong conclusion). The degrees of freedom for the gear test program was approximately 50. The significance level was selected as $\alpha = 0.05$. Therefore, if the computed "t" was equal to or greater than 2.0, it was concluded that the factor evaluated caused a real (or significant) change in endurance limit. For the mathematical sense, α is defined as the probability that a "t" value larger than the critical "t" will result if the evaluated geometric factor has no true effect on endurance limit; therefore, if a "t" larger than the critical "t" is computed, the odds are 19 to 1 that the effect is real.

Some modification of the "t" tests of significance was necessary because of unequal sample sizes in the 16 combinations of the four geometric factors. The resulting "t" tests are set up by first obtaining the difference between weighted average associated with low and high values assigned to the geometric factors, and then dividing by an approximate standard deviation.

$$"t" = \frac{\left(\frac{\Sigma W_L \, EL_L}{\Sigma W_L} - \frac{\Sigma W_H \, EL_H}{\Sigma W_H}\right)}{\sqrt{\frac{1}{64} \sum_{i=1}^{16} \sigma_i^2}}$$

where

W = sample size
EL = endurance limit
L = low
H = high

The undefined indices of summation include run numbers to which low values and high values, respectively, have been assigned for the evaluation of any factor or interaction.

Confidence intervals are also based on the same critical "t" values and variances used in tests of significance. Confidence intervals are set up by the equations:

$$LL = EL - "t"_{\alpha/2} \times S_{EL}$$

$$UL = EL + "t"_{\alpha/2} \times S_{EL}$$

For mathematical terms, the probability is $(1-\alpha)$ that the resulting interval will contain the true endurance limit.

An example of a test of significance is provided for the main effect—diametral pitch. For convenience, the following notation is defined:

	High	Low
a = diametral pitch	12	6
b = pressure angle, degrees	25	20
c = root radius	Large	Small
d = fillet configuration	Full form	Protuberance

By convention, the presence of a letter (associated with a geometric factor) indicates that the high value is assigned to that factor. The absence of a letter indicates that the low level is assigned to that factor. Further, (1) means that the low level is assigned to all factors. Thus, the configuration ab means gears of 12 diametral pitch, 25-degree pressure angle, small radius, and protuberance ground.

To test the significance of diametral pitch using the notation developed, a linear combination of 16 computed endurance limits was set up.

$$L = 1/8 \left[a + ab + ac + abc + ad + abd + acd + abcd\right] -$$

$$1/8 \left[(1) + b + c + bc + d + bd + cd + bcd\right]$$

The first group contains all gear configurations of 12 diametral pitch, and the second group contains all configurations of 6 diametral pitch.

The variance of L, which is the same for all tests, is:

$$L^2 = \frac{1}{64}\left[\sigma_a^2 + \sigma_{ab}^2 + \ldots + \sigma_{abcd}^2\right] + \frac{1}{64}\left[\sigma_{(1)}^2 + \ldots + \sigma_{bcd}^2\right]$$

A "t" test of significance is set up by dividing L by the standard deviation of σ_L or "t" $= \frac{L}{\sigma_L}$.

The four main effects, all two-factor interactions and all three-factor interactions, were tested using this method. The exact linear combination for any specified effect or interaction is found in reference 14 or 29.

PREDICTIVE EQUATION BASED ON TEST RESULTS

A second objective in the analysis of gear tooth fatigue failures was to develop a single predictive equation incorporating numerical values assigned to the geometric factors in addition to the basic applied load. The technique is as follows:

1. Define a linear mathematical model

$$Life_T = A + Bx$$

where

$Life_T = (1/K)^{1/2.2}$
K = kilocycles to failure
x = unit stress

2. Redefine the geometric factors

	Factor	Range
U1 =	pressure angle, degrees	20 - 25
U2 =	diametral pitch	6 - 12
U3 =	dedendum	1.20 - 1.40
U4 =	$\frac{\text{minimum fillet radius}}{\text{maximum fillet radius}}$, inch	0.49 - 0.80

The coefficients A and B in the linear model are defined by the geometric factors as follows:

$$A = (a0 + a1\ U1 + \ldots + a4\ U4 + a5\ U1\ U2 + \ldots + a10\ U3\ U4 + a11\ U1\ U2\ U3 + \ldots + a14\ U2\ U3\ U4)$$

$$B = (b0 + b1\ U1 + \ldots + b14\ U2\ U3\ U4)$$

In terms of the refined coefficients, the expanded model is:

$$Life_T = (1/K)^{1/2.2} = (a0 + a1\ U1 + \ldots + a14\ U2\ U3\ U4) + (b0 + b1\ U1 + \ldots + b14\ U2\ U3\ U4)\ X$$

The individual coefficients were evaluated using the least squares technique.

The following geometric factors affect fatigue life and are listed in order of decreasing importance:

1. (Pressure angle × diametral pitch × dedendum) × load
2. Pressure angle × diametral pitch × dedendum
3. Pressure angle × diametral pitch
4. Pressure angle × dedendum × fillet radius
5. Pressure angle × fillet radius
6. Pressure angle × load
7. Pressure angle
8. Dedendum
9. Diametral pitch × dedendum
10. (Pressure angle × diametral pitch) × load
11. Dedendum × fillet radius

In terms of coding, the finalized equation is:

$$Life_T = (1/K)^{1/2.2} = 2.27864 - 5.47376 \times 10^{-2}\ (U1) - 1.18640\ (U3) - 8.97196 \times 10^{-3}\ (U1\ U2) + 1.20233 \times 10^{-1}\ (U1\ U4) -$$

$$3.67334 \times 10^{-2} (U2\ U3) + 4.43879 \times 10^{-1} (U3\ U4) +$$

$$9.11496 \times 10^{-3} (U1\ U2\ U3) - 1.17884 \times 10^{-1} (U1\ U3\ U4) (\text{load}) +$$

$$X \ \Big\{ -3.58085 \times 10^{-6} (U1) - 1.09015 \times 10^{-6} (U1\ U2) +$$

$$1.75948 \times 10^{-6} (U1\ U2\ U3) \Big\}$$

The standard deviation (σ_Y) associated with the predictive equation is 0.0656.

The equation can be used to predict transformed kilocycles only within the range of interest for applied load values and only within the range of values assigned to the geometric factors from which the equation was derived.

The most efficient use of the predictive equation can be obtained by first computing transformed kilocycles using observed values for the geometric factors and the applied load, and then converting to cycles or kilocycles, as desired. To obtain an approximate confidence interval for kilocycles to failure, add and subtract the quantity ($Z_{\alpha/2} \times 0.0656$) to and from the calculated Y = transformed kilocycles ($Z_{\alpha/2}$ is a confidence factor to be obtained from a table of areas for the normal distribution). These computed upper and lower limits are then transformed to kilocycles using the same procedures used to convert Y to kilocycles.

The equation, although derived from valid test data, is yet untried in the predictive sense. It may be that additional testing, at more than two levels per geometric factor, may be required to derive a mathematical model suitable for general usage in predicting gear failures.

BLANK PAGE

APPENDIX IV

AGMA CALCULATED STRESS VERSUS LIFE AND TRANSFORMED LIFE

This appendix consists of life versus AGMA calculated stress plots of the fatigue test data points for each of the 16 gear configurations. See Figures 135 through 150. The calculated mean S/N curve fitting the data points is drawn on each plot. Also included are transformed life versus AGMA calculated stress plots of the fatigue test data points for each of the 16 gear configurations. See Figures 151 through 166. Life and transformed life versus alternating stress (R. R. Moore) data are shown in Figures 167 and 168, respectively.

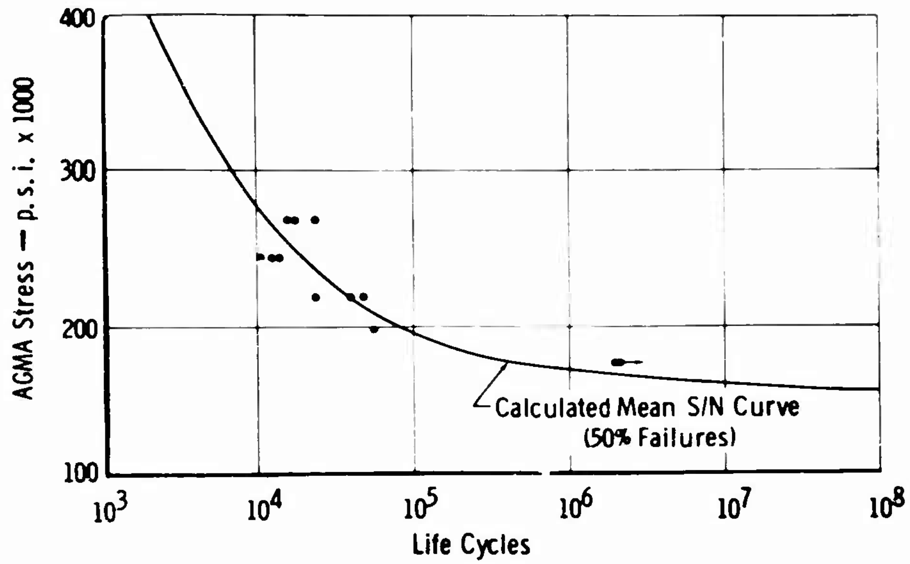

Figure 135. Fatigue Test Results–AGMA Stress Versus Life (EX-78772).

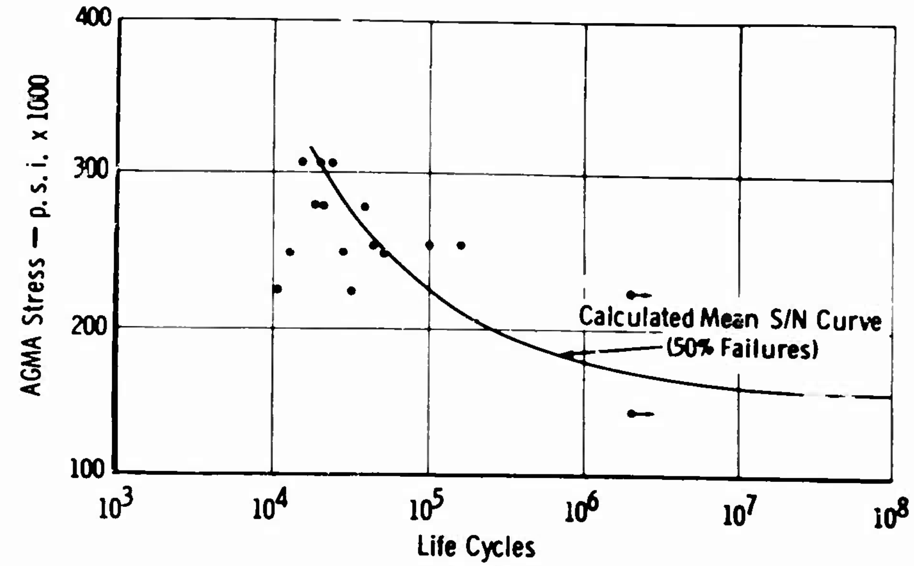

Figure 136. Fatigue Test Results–AGMA Stress Versus Life (EX-78773).

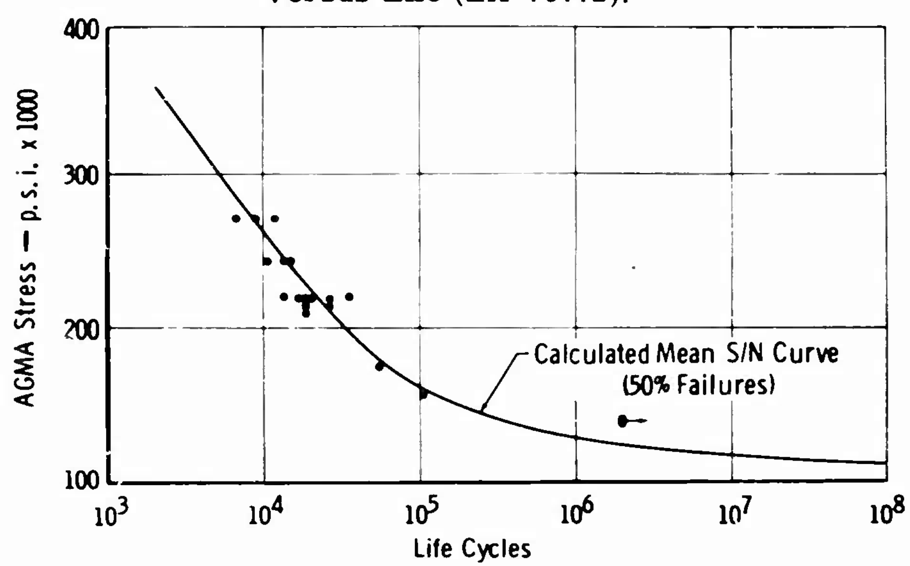

Figure 137. Fatigue Test Results–AGMA Stress Versus Life (EX-78774).

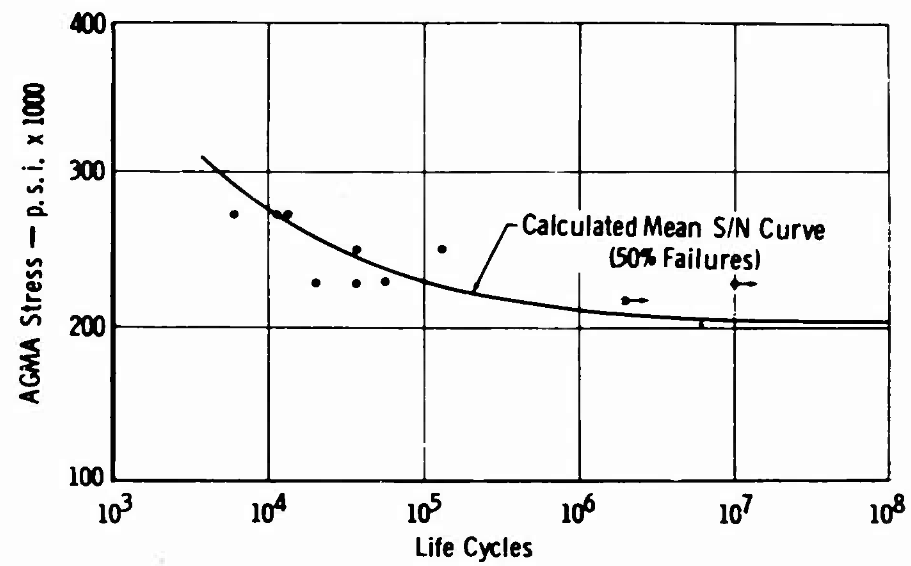

Figure 138. Fatigue Test Results–AGMA Stress Versus Life (EX-78775).

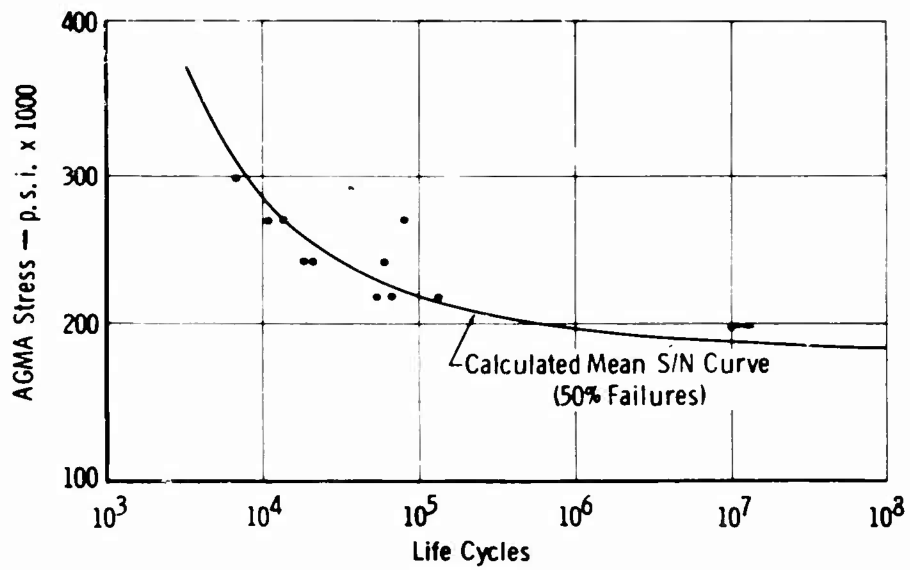

Figure 139. Fatigue Test Results–AGMA Stress Versus Life (EX-78776).

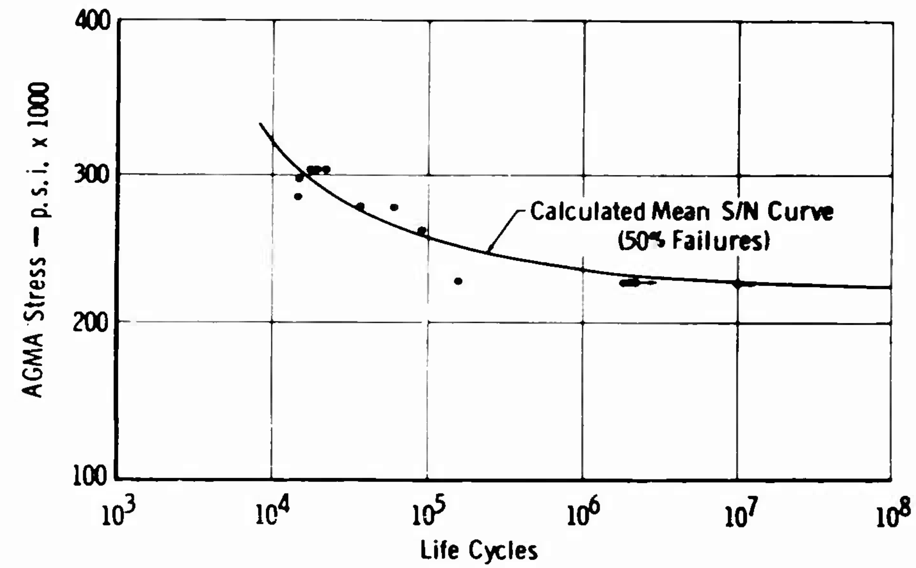

Figure 140. Fatigue Test Results–AGMA Stress Versus Life (EX-78777).

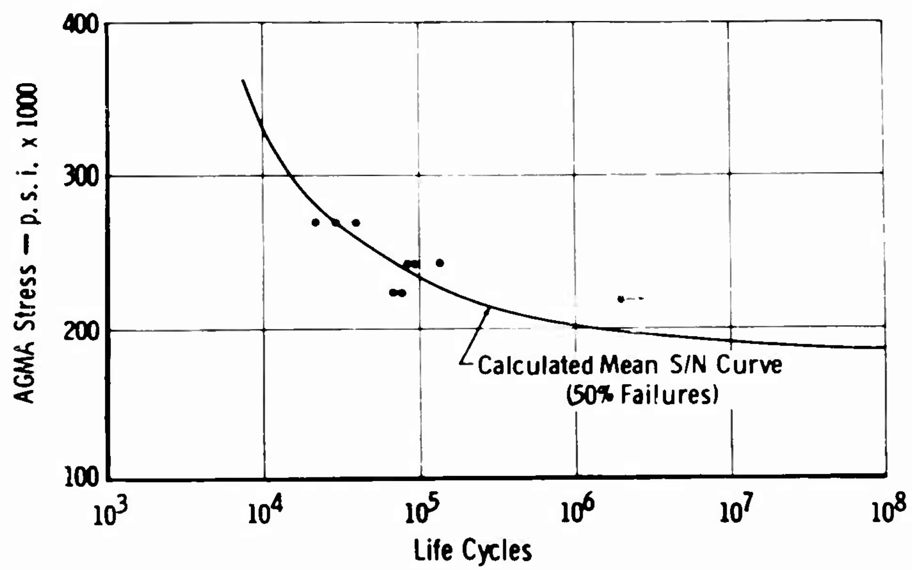

Figure 141. Fatigue Test Results–AGMA Stress Versus Life (EX-78778).

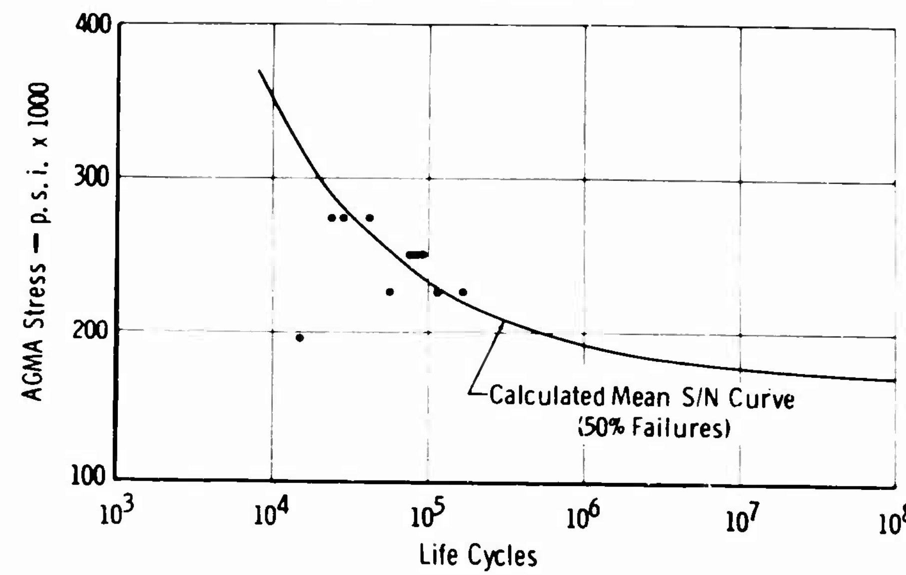

Figure 142. Fatigue Test Results–AGMA Stress Versus Life (EX-78779).

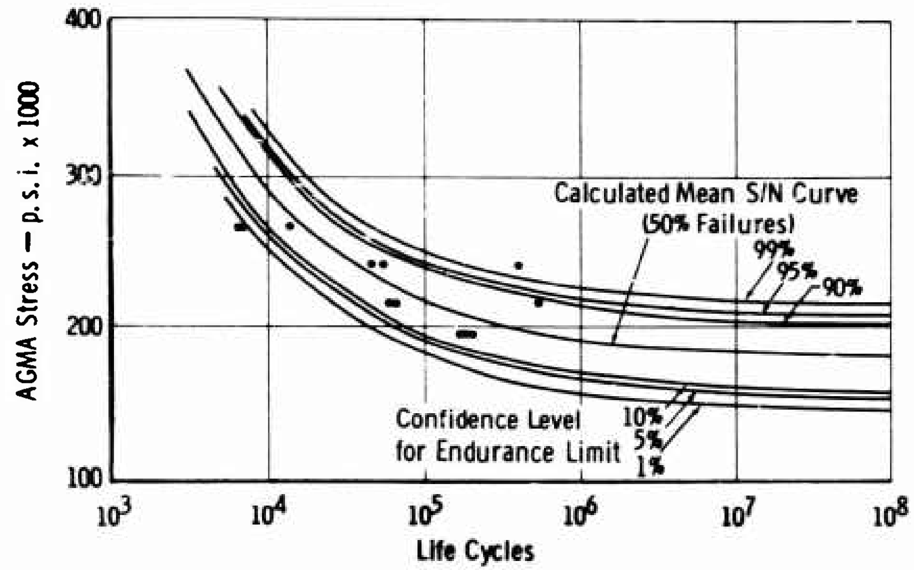

Figure 143. Fatigue Test Results -AGMA Stress Versus Life (EX-78780).

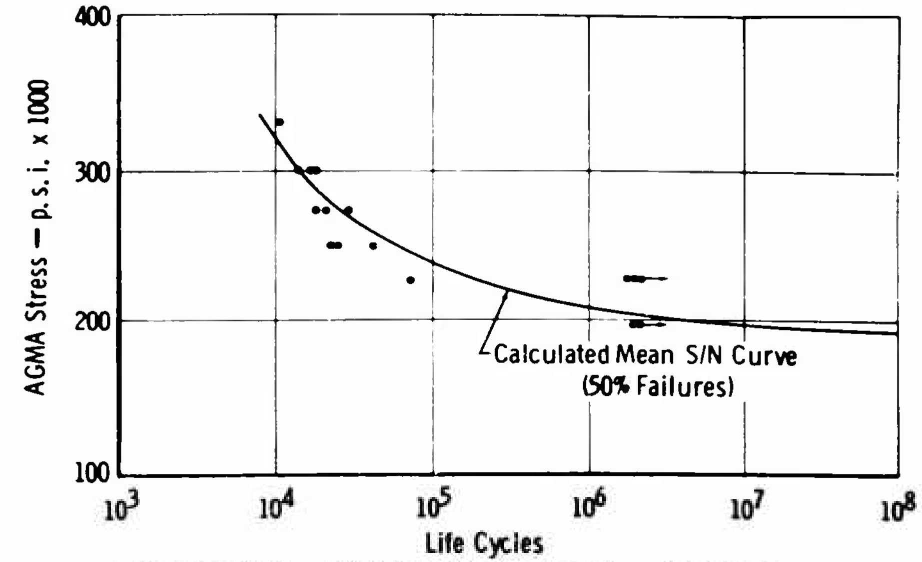

Figure 144. Fatigue Test Results–AGMA Stress Versus Life (EX-78781).

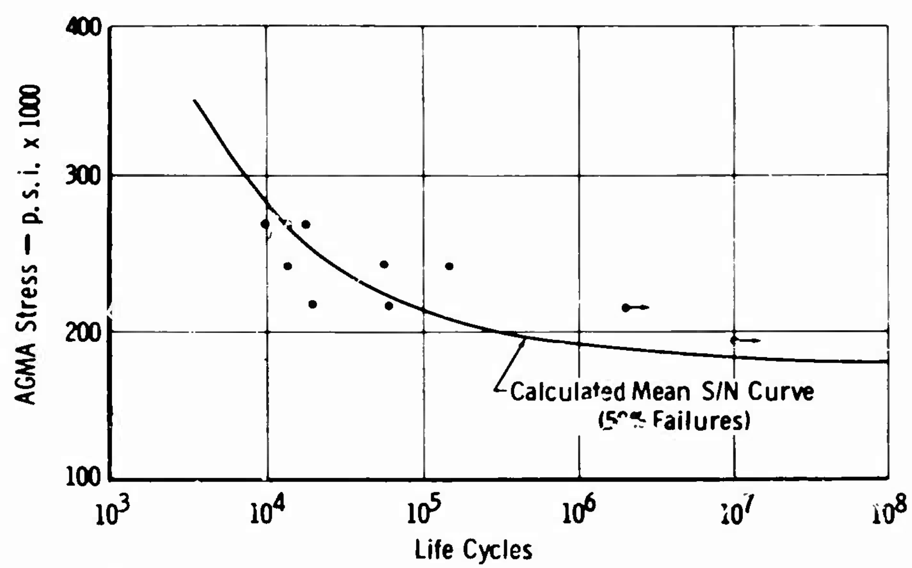

Figure 145. Fatigue Test Results–AGMA Stress Versus Life (EX-78782).

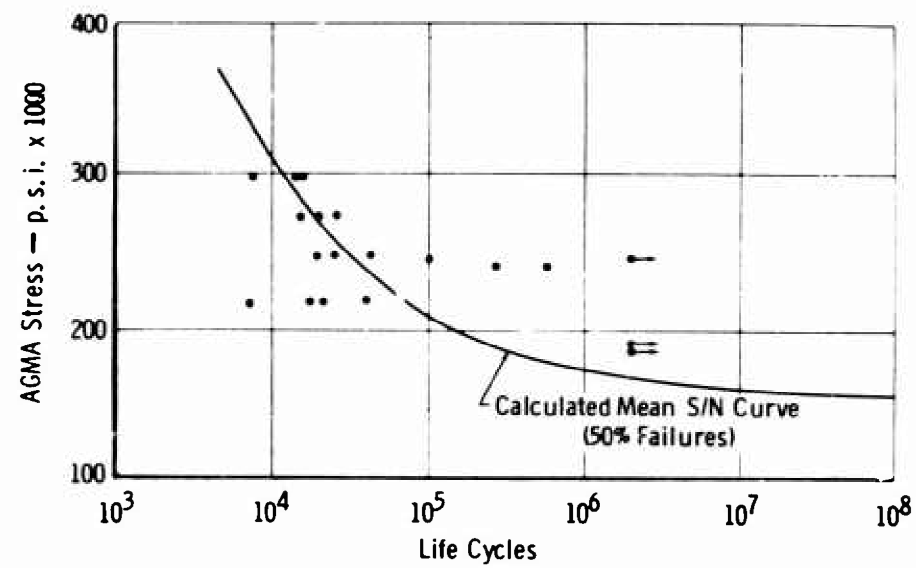

Figure 146. Fatigue Test Results–AGMA Stress Versus Life (EX-78783).

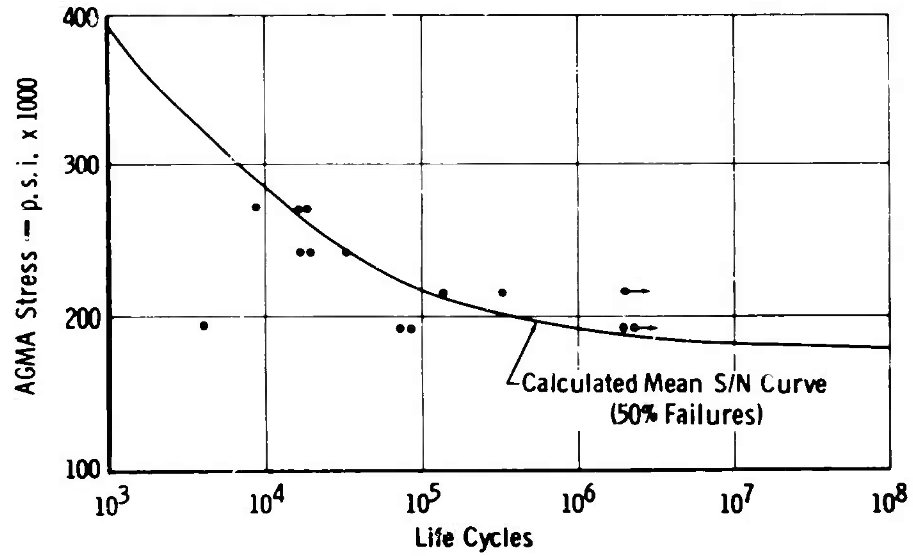

Figure 147. Fatigue Test Results–AGMA Stress Versus Life (EX-78784).

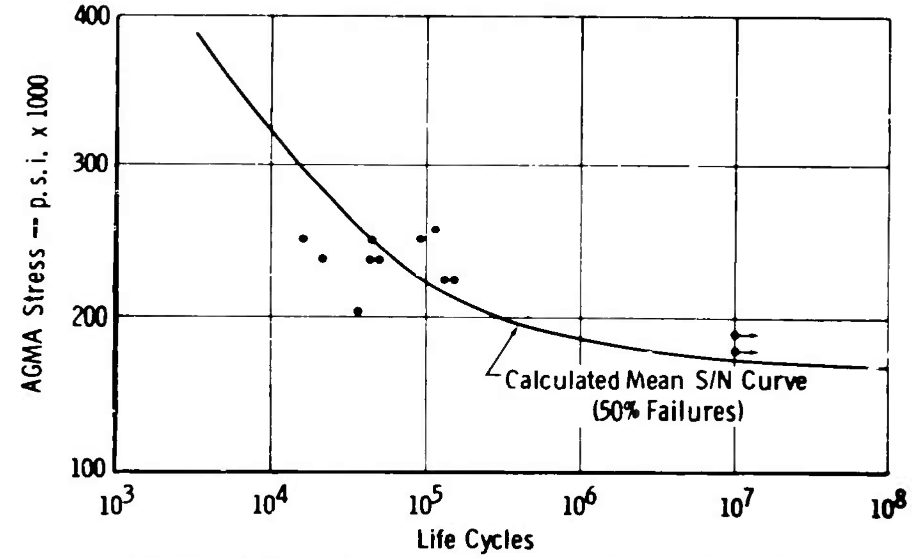

Figure 148. Fatigue Test Results–AGMA Stress Versus Life (EX-78785).

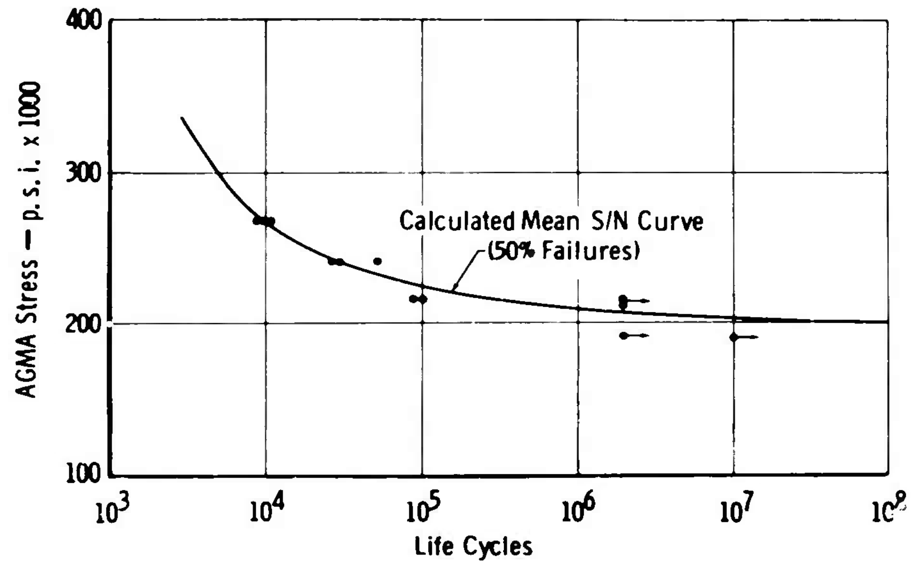

Figure 149. Fatigue Test Results–AGMA Stress Versus Life (EX-78786).

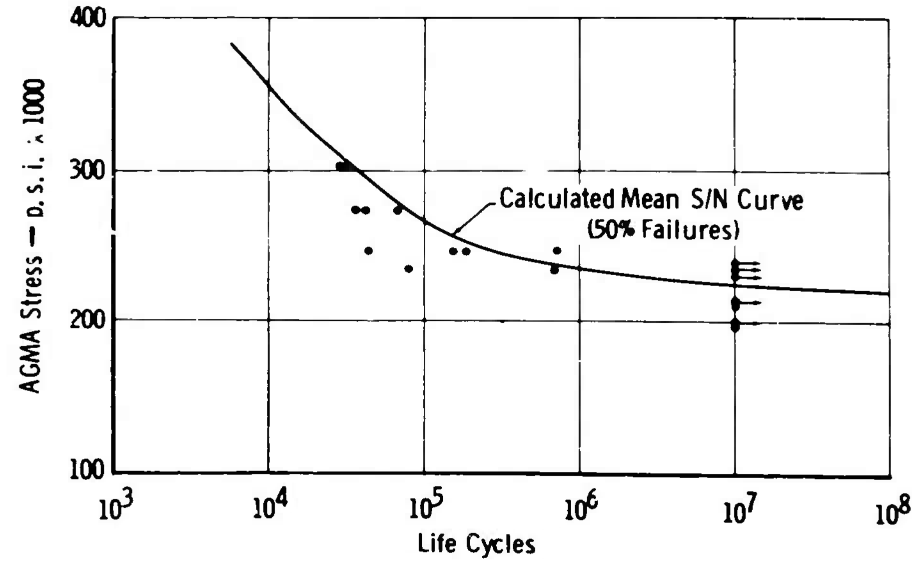

Figure 150. Fatigue Test Results–AGMA Stress Versus Life (EX-78787).

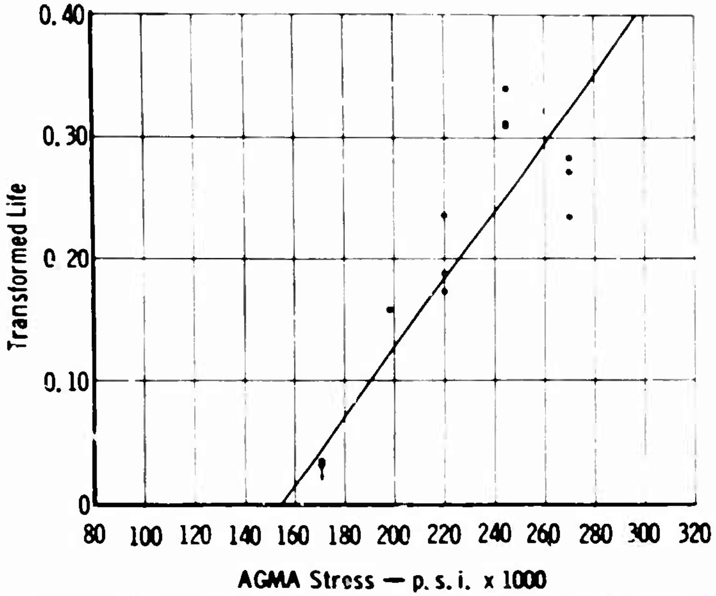

Figure 151. Fatigue Test Results–AGMA Stress Versus Transformed Life (EX-78772).

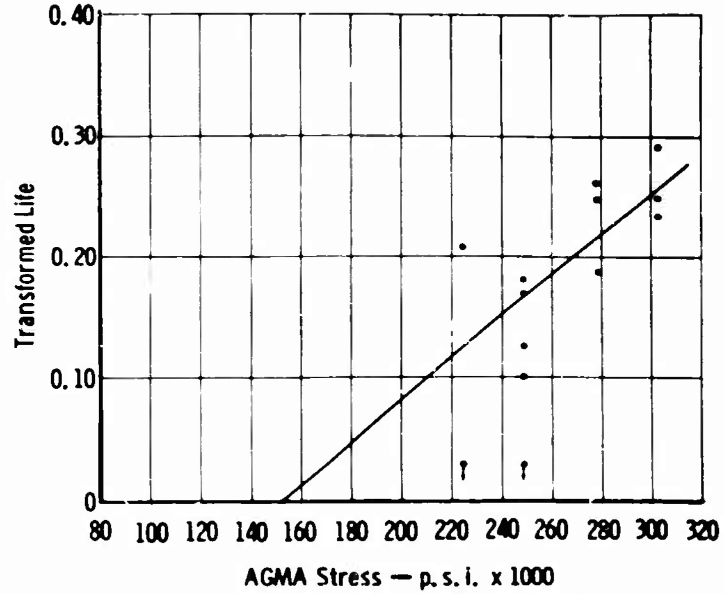

Figure 152. Fatigue Test Results–AGMA Stress Versus Transformed Life (EX-78773).

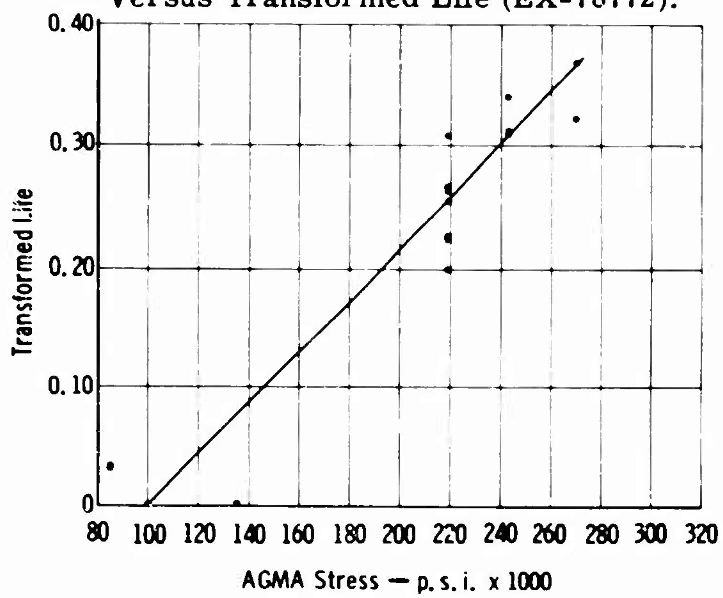

Figure 153. Fatigue Test Results–AGMA Stress Versus Transformed Life (EX-78774).

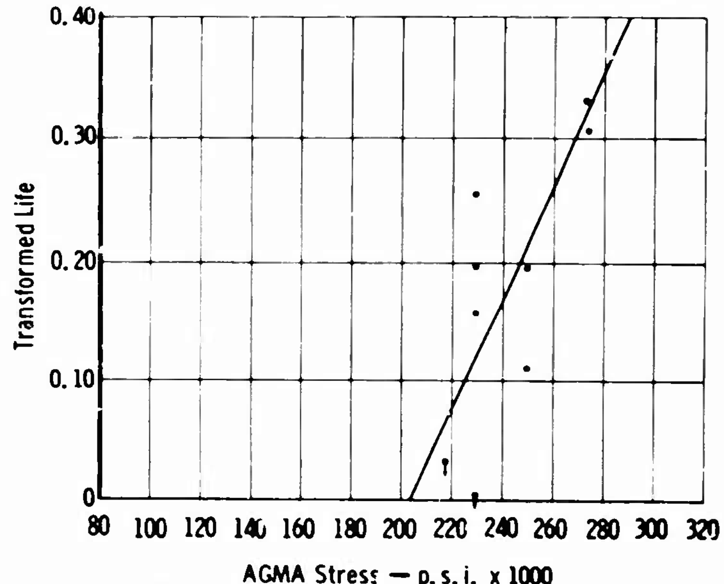

Figure 154. Fatigue Test Results–AGMA Stress Versus Transformed Life (EX-78775).

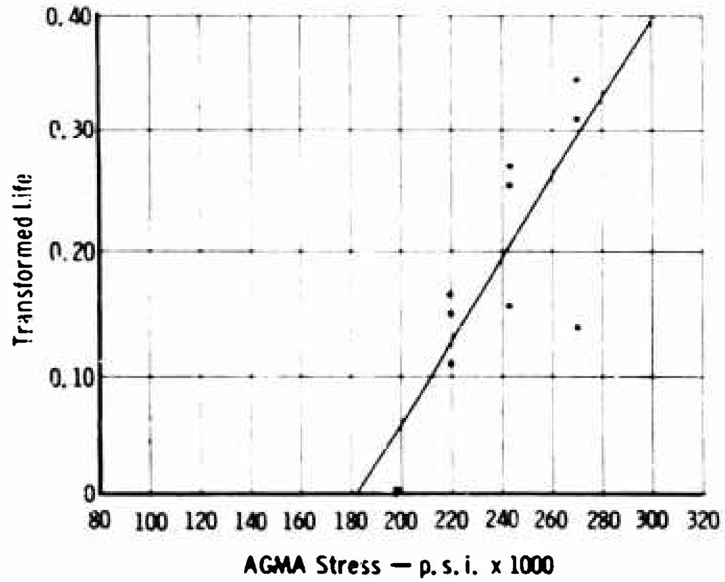

Figure 155. Fatigue Test Results–AGMA Stress Versus Transformed Life (EX-78776).

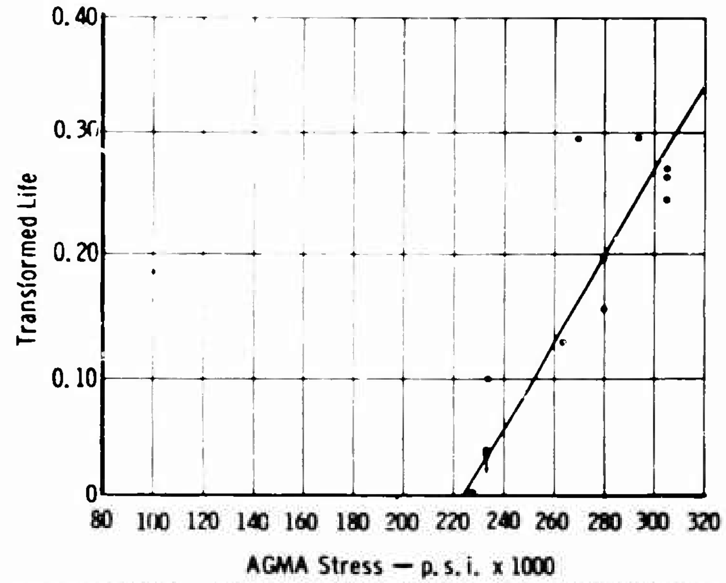

Figure 156. Fatigue Test Results–AGMA Stress Versus Transformed Life (EX-78777).

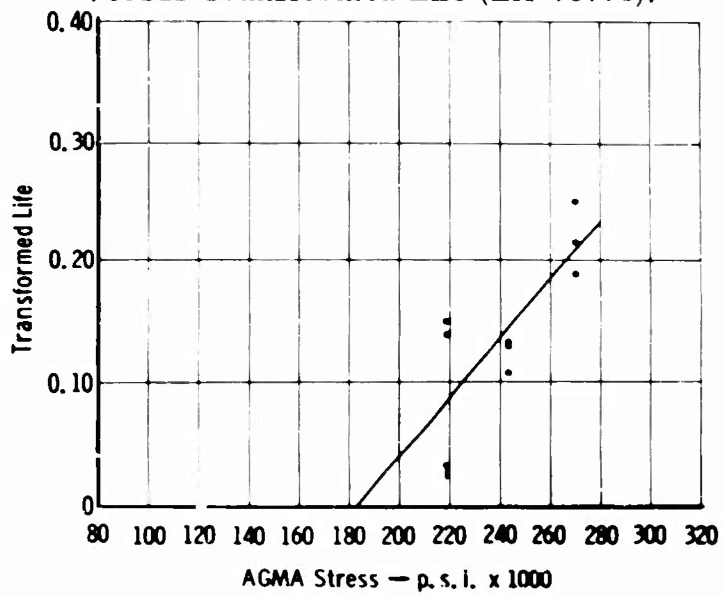

Figure 157. Fatigue Test Results–AGMA Stress Versus Transformed Life (EX-78778).

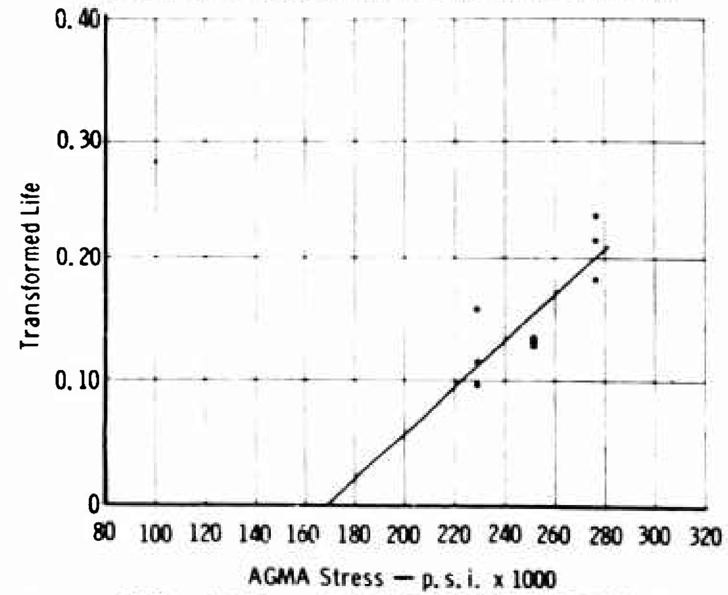

Figure 158. Fatigue Test Results–AGMA Stress Versus Transformed Life (EX-78779).

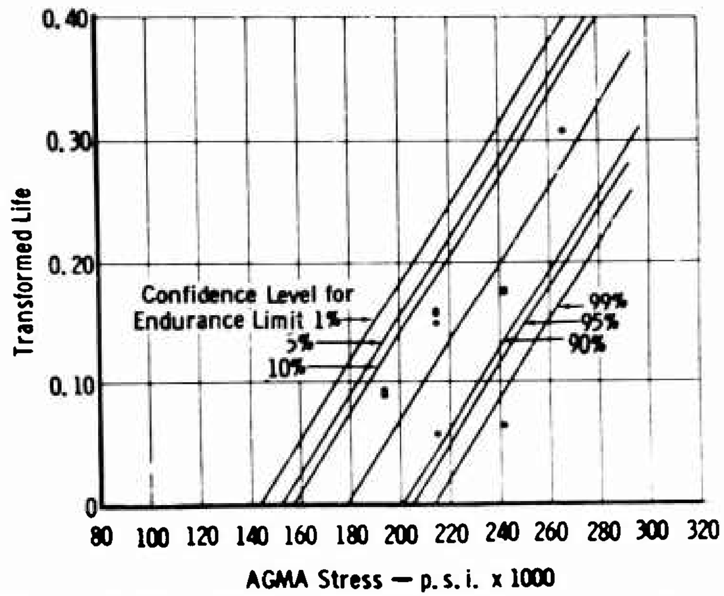

Figure 159. Fatigue Test Results–AGMA Stress Versus Transformed Life (EX-78780).

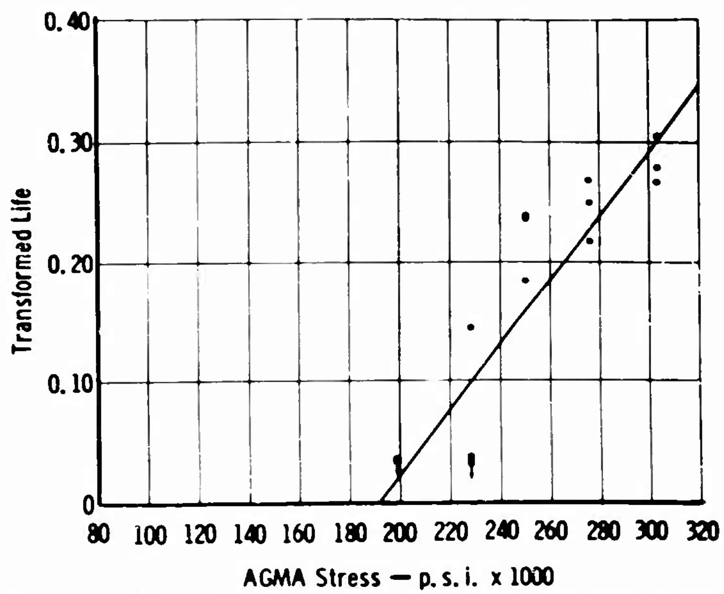

Figure 160. Fatigue Test Results–AGMA Stress Versus Transformed Life (EX-78781).

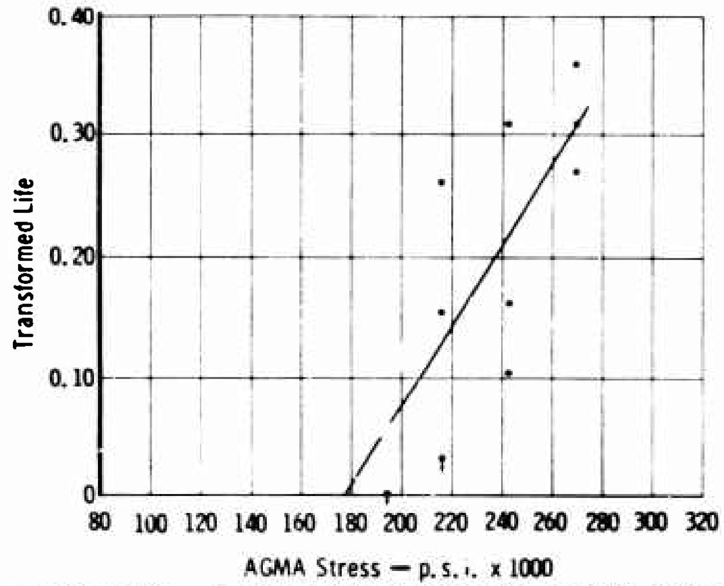

Figure 161. Fatigue Test Results–AGMA Stress Versus Transformed Life (EX-78782).

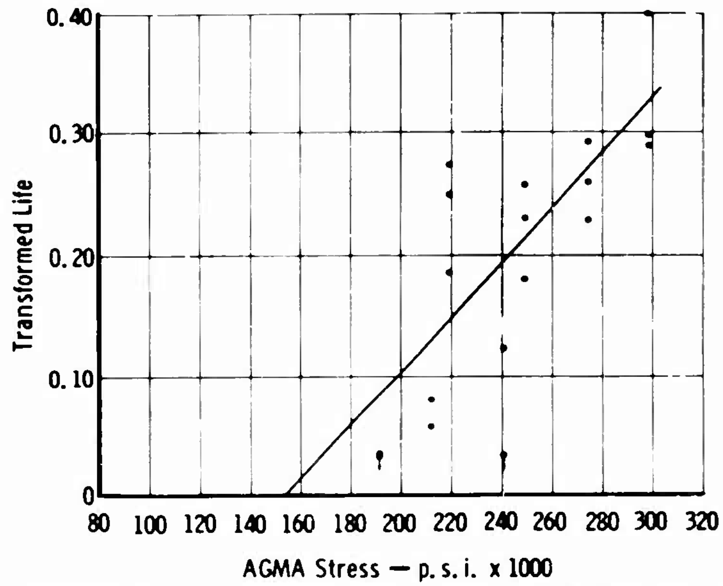

Figure 162. Fatigue Test Results–AGMA Stress Versus Transformed Life (EX-78783).

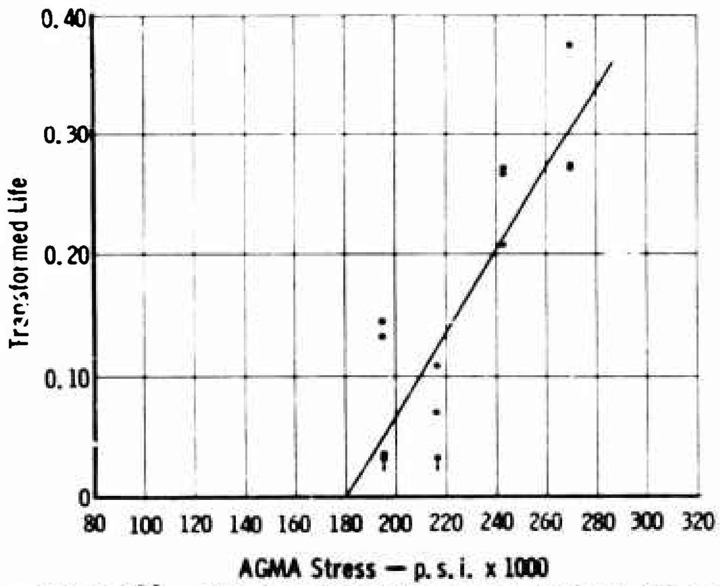

Figure 163. Fatigue Test Results–AGMA Stress Versus Transformed Life (EX-78784).

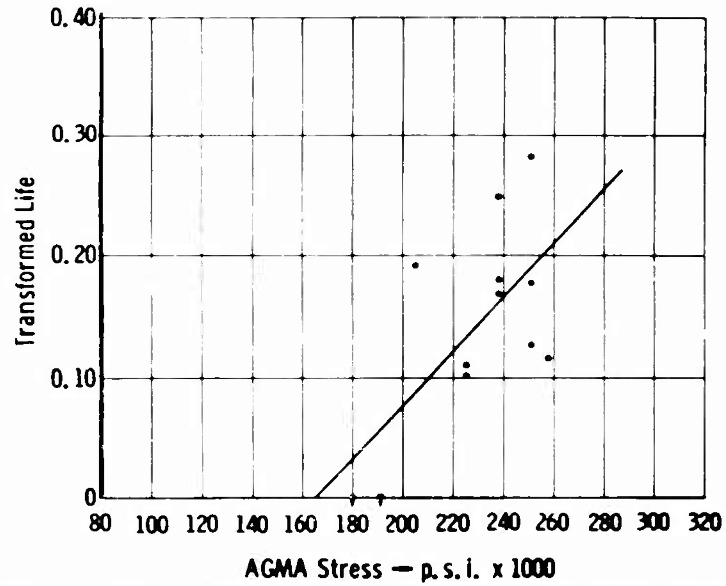

Figure 164. Fatigue Test Results–AGMA Stress Versus Transformed Life (EX-78785).

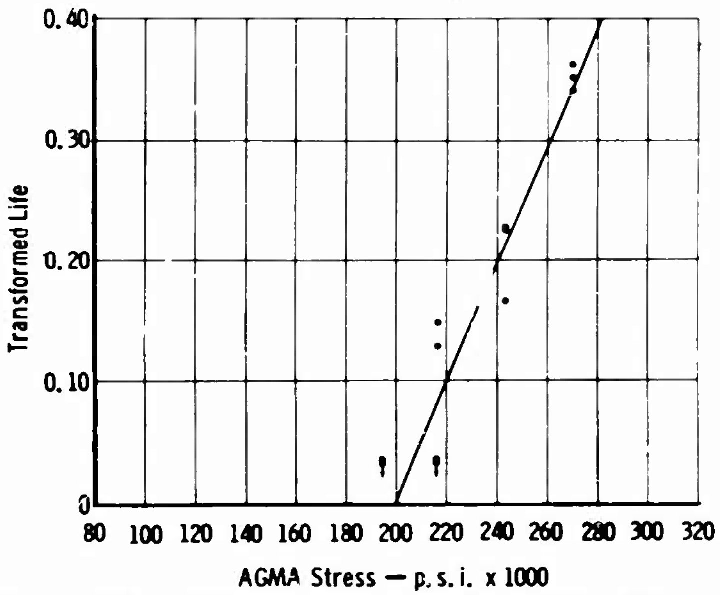

Figure 165. Fatigue Test Results–AGMA Stress Versus Transformed Life (EX-78786).

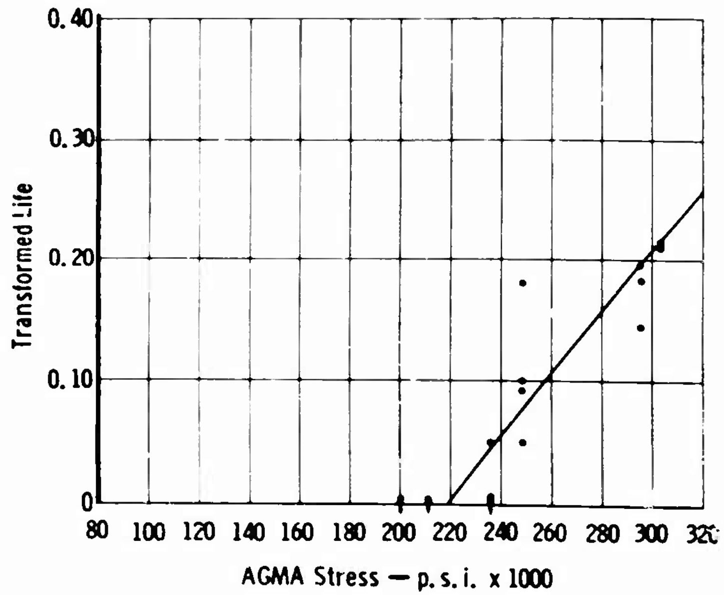

Figure 166. Fatigue Test Results–AGMA Stress Versus Transformed Life (EX-78787).

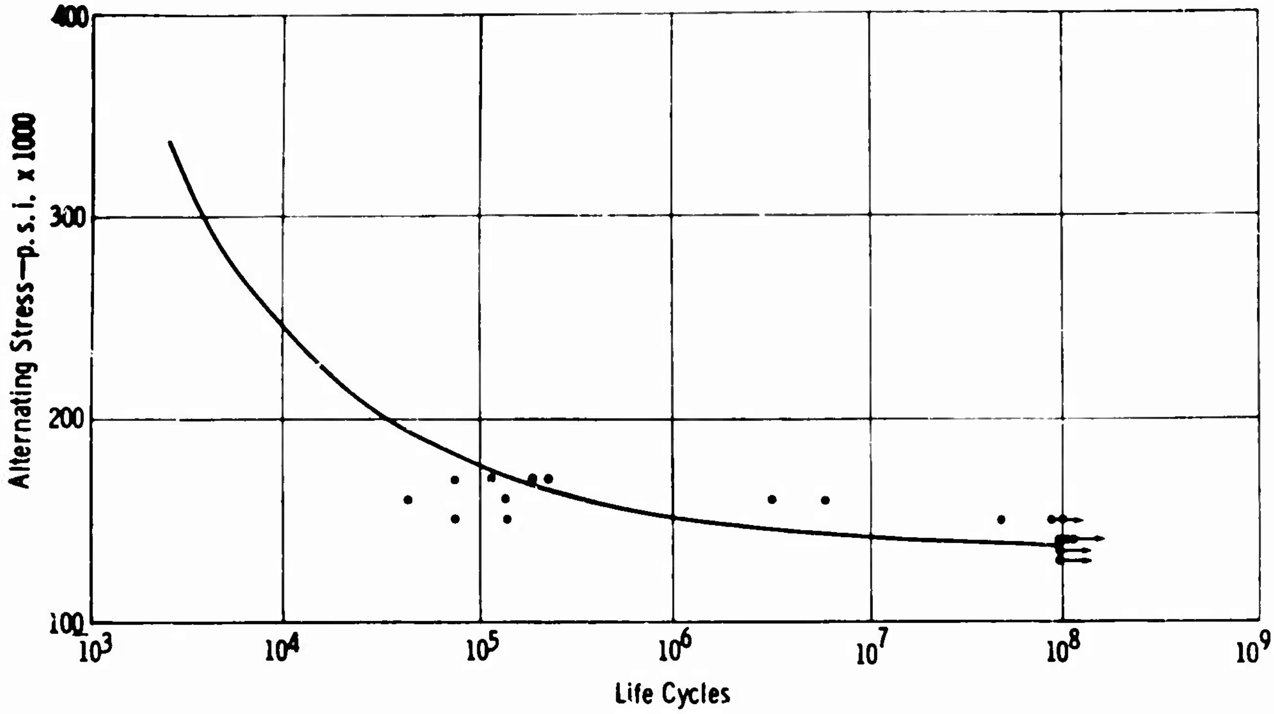

Figure 167. Fatigue Test Gear Life Data (R. R. Moore).

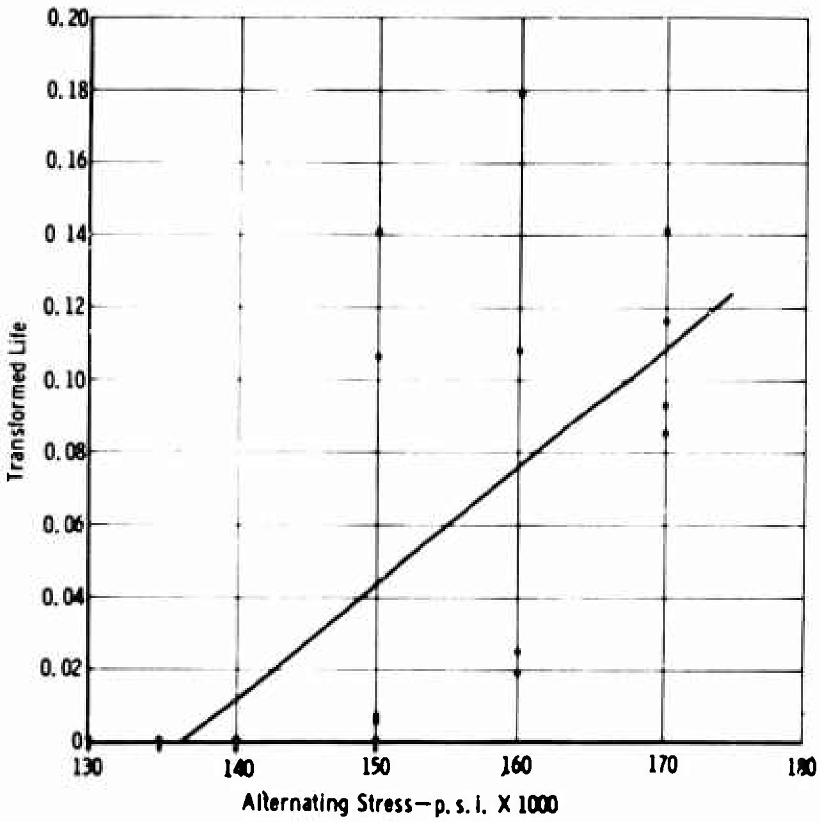

Figure 168. Fatigue Test Gear Transformed Life Data (R. R. Moore).

APPENDIX V

DESCRIPTION OF COMPUTER PROGRAM

This appendix consists of a complete description of the computer program and includes the program equations, input data sheet, source program print-out, and a sample problem. The equations are given in both engineering and computer program terms.

DESCRIPTION OF PROBLEM

Gear tooth bending strength is one of the major criteria in gear design. Gear tooth loading is cyclic in nature, therefore subjecting the material to fatigue. The critical section is close to the root diameter. Failure usually results in fracture of an entire tooth from the gear rim.

Calculation of gear tooth bending stress requires geometrically precise description of the root fillet contour and location of the critical section. The point of the involute tooth profile at which the transmitted load produces the maximum bending stress is also required. Knowledge of the mounting and operating conditions of the unit in which the gear is assembled is required to assess the increase in bending stress caused by misalignment, overloads, system dynamics, and centrifugal forces. Gear material ultimate strength and fatigue data must be known to convert the calculated stress to anticipated gear life.

The purpose of this program is to calculate gear tooth bending stress and gear life considering these factors.

METHOD OF SOLUTION

The gear tooth geometry has been developed using basic formulas available in the literature. The hob dimensions have been used to generate in the program the trochoidal fillet contour resulting on a finished gear from some gear processing procedures. A true radius fillet is used when a shaped contour is specified in the program input. The program uses an iteration routine to inscribe a parabola (per Lewis construction) and to locate its tangent point with the root fillet contour. The Lewis dimensional parameters for the weakest section thus obtained are then calculated. These parameters are then used in the AGMA formula as given in AGMA 220.02 (Appendix VI herein) to calculate a bending stress. A hoop stress at the root diameter is also calculated. The AGMA temperature factor and factor of safety are applied to the bending and hoop stresses, which are then combined by use of a modified Goodman diagram. The modified Goodman diagram is based on an ultimate strength and S/N curve determined for the material used and the gear tooth designs tested; they may be easily changed within the program. A life is also determined from the modified Goodman diagram.

COMPUTER TYPE AND PROGRAM LANGUAGE

The subject program is written in FORTRAN IV language for use on an IBM 7094 computer.

There must be four, five, or six cards per data set depending on data input for words 4 and 5 on Card 1. Data sets may be stacked. Computer running time will be approximately 0.1 minute per set of data.

INPUT DATA

A sample input data form is shown in Figure 169. Each set of data requires four, five, or six cards. A description of the cards follows.

Input Card 1

Word	Column	Description
1	1 - 5	Number of teeth—Pinion.
2	6 - 10	Number of teeth—Gear.
3	11 - 20	Nonstandard center distance (blank if standard gear set).
4	21 - 26	This must be one of the following beginning in Column 21: SHAPED HOBBED
—	27 - 29	These spaces left blank.
5	30	This must be one of the following in Column 30: 0—if pinion is hobbed 1—if gear is hobbed 2—if both pinion and gear are hobbed Blank--if "SHAPED" is in Column 21 through 26
6	31 - 40	Horsepower.
7	41 - 50	r.p.m. —Pinion.
8	51 - 55	Density—pounds/cubic inch.
9	56 - 60	Temperature factor.
10	61 - 65	Safety factor.
11	66 - 70	Load distribution factor.

Input Card 2

1	1 - 10	Pressure angle at the standard pitch diameter—degrees.
2	11 - 20	Diametral pitch at the standard pitch diameter.
3	21 - 25	Backlash—minimum.
4	26 - 30	Backlash—maximum.
5	31 - 40	Arc or chordal tooth thickness at the standard pitch diameter—minimum (pinion).
6	41 - 50	Arc or chordal tooth thickness at the standard pitch diameter—maximum (pinion).
7	51 - 60	Arc or chordal tooth thickness at the standard pitch diameter—minimum (gear).
8	61 - 70	Arc or chordal tooth thickness at the standard pitch diameter—maximum (gear).
—	71	This space is left blank.
9	72	This must be one of the following in Column 72: 0—if Columns 31 through 70 are arc tooth thickness 1—if Columns 31 through 70 are chordal tooth thickness

Input Card 3

1	1 - 10	Outside diameter—minimum (pinion).
2	11 - 20	Outside diameter—maximum (pinion).
3	21 - 30	Outside diameter—minimum (gear).
4	31 - 40	Outside diameter—maximum (gear).

IBM 7094 DATA SHEET

* SHAPED
* HOBBED

IDENTIFICATION NUMBER

EXAMPLE

No. OF TEETH PINION | GEAR	NONSTANDARD DISTANCE	*	HORSEPOWER	RPM - PINION	DENSITY LB/IN³ | K_T	K_R | K_m	1
PRESSURE ANGLE	DIAMETRAL PITCH	BACKLASH MIN | MAX	ARC OR CHORDAL (STD D_p) - MIN	TOOTH THK-PINION (STD D_p) - MAX	ARC OR CHORDAL (STD D_p) - MIN	TOOTH THK-GEAR (STD D_p) - MAX	2
OUTSIDE DIAMETER - PINION MIN	MAX	OUTSIDE DIAMETER - GEAR MIN	MAX	FACE WIDTH - MIN PINION	GEAR	MAX TIP BREAK PINION | GEAR	3
ROOT DIA - PINION MIN	MAX	ROOT DIA - GEAR MIN	MAX	FILLET RAD - MIN PINION | GEAR	MAX UNDERCUT PINION | GEAR	K_O | K_V	4
TOOTH THK (HTT)	ADDENDUM (HADD)	LEAD (HLEAD)	PRESSURE ANGLE (HPA)	TIP RADIUS (HTIPR)	HPW	SEE FIG 170 PINION	5
TOOTH THK (HTT)	ADDENDUM (HADD)	LEAD (HLEAD)	PRESSURE ANGLE (HPA)	TIP RADIUS (HTIPR)	HPW	SEE FIG 170 GEAR	6
							1
							2
							3
							4
							5
							6

Figure 169. Sample Input Data Form.

Word	Column	Description
5	41 - 50	Face width—minimum (pinion).
6	51 - 60	Face width—minimum (gear).
7	61 - 65	Maximum tip break (pinion).
8	66 - 70	Maximum tip break (gear).

Input Card 4

1	1 - 10	Root diameter—minimum (pinion).
2	11 - 20	Root diameter—maximum (pinion).
3	21 - 30	Root diameter—minimum (gear).
4	31 - 40	Root diameter—maximum (gear).
5	41 - 45	Fillet radius—minimum (pinion) (blank if pinion is hobbed).
6	46 - 50	Fillet radius—minimum (gear) (blank if gear is hobbed).
7	51 - 55	Maximum undercut (pinion) (blank if pinion is hobbed).
8	56 - 60	Maximum undercut (gear) (blank if gear is hobbed).
9	61 - 65	Overload factor.
10	66 - 70	Dynamic factor.

Input Card 5

This card is needed only when words 4 and 5 of Card 1 are given as "HOBBED" and "0" or "2," respectively. This card is for PINION only. See Figure 170.

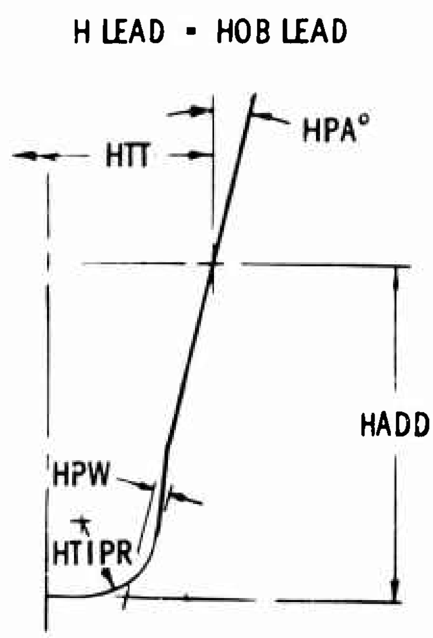

Figure 170. Standard or Protuberance Hob Form for Input.

Word	Column	Description
1	1 - 10	Hob tooth thickness.
2	11 - 20	Hob addendum.
3	21 - 30	Hob lead.
4	31 - 40	Hob pressure angle—degrees.
5	41 - 50	Hob tip radius—inches.
6	51 - 60	HPW. (See Figure 170.)

Input Card 6

This card is needed only when words 4 and 5 of Card 1 are given as "HOBBED" and "1" or "2," respectively. This card is for GEAR only and is the same format as input Card 5.

PROGRAM EQUATIONS

Computer program input symbols in both engineering (AGMA) and program terms are listed as follows.

AGMA	Program	Definition
NP	ANP	Number of teeth—pinion.
NG	ANG	Number of teeth—gear.
B_{MI}	BMIN	Backlash—minimum.
B_{MA}	BMAX	Backlash—maximum.
—	BRKP	Maximum tip break—pinion.
—	BRKG	Maximum tip break—gear.
C	CSTDIN	Standard center distance.
C_X	CNSTD	Nonstandard center distance.
—	CODE	See input fillout.
—	CUTTER	See input fillout.
D_{OMA}	DOGMA	Outside diameter—maximum (gear).
D_{OMI}	DOGMI	Outside diameter—minimum (gear).
d_{OMA}	DOPMA	Outside diameter—maximum (pinion).
d_{OMI}	DOPMI	Outside diameter—minimum (pinion).
DR_{MA}	DRGMA	Root diameter—maximum (gear).
DR_{MI}	DRGMI	Root diameter—minimum (gear).
dR_{MA}	DRPMA	Root diameter—maximum (pinion).
dR_{MI}	DRPMI	Root diameter—minimum (pinion).
FG_{MI}	FMING	Face width—minimum (gear).
Fp_{MI}	FMINP	Face width—minimum (pinion).
HP	HORSES	Horsepower.
—	L	See input fillout.
K_m	KM	Load distribution factor.
K_O	KO	Overload factor.
K_R	KR	Safety factor.
K_T	KT	Temperature factor.
K_V	KV	Dynamic factor.
η_P	RPMP	r.p.m.—pinion.
		Arc or chordal tooth thickness
t_{GMA} or tc_{GMA}	TGMAS	Maximum—gear.
t_{GMI} or tc_{GMI}	TGMIS	Minimum—gear.

AGMA	Program	Definition
t_{pMA} or tc_{PMA}	TPMAS	Maximum—pinion.
t_{pMI} or tc_{PMI}	TPMIS	Minimum—pinion.
r_{fGMI}	RFMIG	True root fillet radius—gear.
r_{fpMI}	RFMIP	True root fillet radius—pinion.
—	UCG	Maximum undercut—gear.
—	UCP	Maximum undercut—pinion.
a_C	HADD	Hob addendum.
L_C	HLEAD	Hob lead.
ϕ_C	HPA	Hob pressure angle.
—	HPW	Hob protuberance.
r_T	HTIPR	Hob tip radius.
t_c	HTT	Hob tooth thickness.

The computer program equations in both engineering (AGMA) and program terms follow. The basic geometric equations for gear teeth can be obtained or developed from textbooks.

AGMA	Program
$Pd_x = \dfrac{Np + NG}{2 \times C_x}$	$PDX = \dfrac{ANP + ANG}{2 \times CNSTD}$
$mg = \dfrac{NG}{Np}$	$AMG = \dfrac{ANG}{ANP}$
$Rmg = \dfrac{Np}{NG}$	$RMG = \dfrac{ANP}{ANG}$
$dp = \dfrac{Np}{Pnd}$	$DP = \dfrac{ANP}{PND}$
$db = dp \times COS\,\phi_\eta$	$DBP = DP \times FNCO$
$d_x = \dfrac{Np}{Pd_x}$	$DXP = \dfrac{ANP}{PDX}$
$D_G = \dfrac{NG}{Pnd}$	$DG = \dfrac{ANG}{PND}$
$Db = D_G \times COS\,\phi_\eta$	$DBG = DG \times FNCO$
$D_x = \dfrac{NG}{Pd_x}$	$DXG = \dfrac{ANG}{PDX}$
$d_{ODB} = d_{OMI} - 2 \times BRKp$	$DODBP = DOPMI - 2 \times BRKP$
$D_{ODB} = D_{OMI} - 2 \times BRKG$	$DODBG = DOGMI - 2 \times BRKG$
$\epsilon_{ECP} = \left[\left(\dfrac{d_{ODB}}{db}\right)^2 - 1\right]^{1/2}$	$EECP = \left[\left(\dfrac{DODBP}{DBP}\right)^2 - 1\right]^{1/2}$

AGMA	Program
$\epsilon_{BCG} = \left[\left(\frac{DODB}{Db}\right)^2 - 1\right]^{1/2}$	$EBCG = \left[\left(\frac{DODBG}{DBG}\right)^2 - 1\right]^{1/2}$
$\epsilon_{BCP} = (TAN\,\phi_x(mg + 1)) - (\epsilon_{BCG} \times mg)$	$EBCP = (FXTA(AMG + 1)) - (EBCG \times AMG)$
$\epsilon_{ECG} = (TAN\,\phi_x(Rmg + 1)) - (\epsilon_{ECP} \times Rmg)$	$EECG = (FXTA(RMG + 1)) - (EECP \times RMG)$
$\epsilon_{BSTCP} = \epsilon_{ECP} - \frac{2\pi}{NP}$	$EBSP = EECP - \frac{2 \times PI}{ANP}$
$\epsilon_{ESTCP} = \epsilon_{BCP} + \frac{2\pi}{NP}$	$EESP = EBCP + \frac{2 \times PI}{ANP}$
$\epsilon_{BSTCG} = \epsilon_{ECG} + \frac{2\pi}{NG}$	$EBSG + EECG + \frac{2 \times PI}{ANG}$
$\epsilon_{ESTCG} = \epsilon_{BCG} - \frac{2\pi}{NG}$	$EESG = EBCG - \frac{2 \times PI}{ANG}$
$\epsilon_{dOMA} = \left[\left(\frac{dOMA}{d_b}\right)^2 - 1\right]^{1/2}$	$E_{OPMA} = \left[\left(\frac{DOPMA}{DBP}\right)^2 - 1\right]^{1/2}$
$\epsilon_{DOMA} = \left[\left(\frac{DOMA}{D_b}\right)^2 - 1\right]^{1/2}$	$E_{OGMA} = \left[\left(\frac{DOGMA}{DBG}\right)^2 - 1\right]^{1/2}$
$d_{BC} = \left[\epsilon_{BCP}{}^2 + 1\right]^{1/2} db$	$DBCP = \left[EBCP^2 + 1\right]^{1/2} \times DBP$
$d_{BSTC} = \left[\epsilon_{BSTCP}{}^2 + 1\right]^{1/2} db$	$DBSP = \left[EBSP^2 + 1\right]^{1/2} \times DBP$
$d_{ESTC} = \left[\epsilon_{ESTCP}{}^2 + 1\right]^{1/2} db$	$DESP = \left[EESP^2 + 1\right]^{1/2} \times DBP$
$d_{EC} = \left[\epsilon_{ECP}{}^2 + 1\right]^{1/2} db$	$DECP = \left[EECP^2 + 1\right]^{1/2} \times DBP$
$D_{BC} = \left[\epsilon_{BCG}{}^2 + 1\right]^{1/2} Db$	$DBCG = \left[EBCG^2 + 1\right]^{1/2} \times DBG$
$D_{BSTC} = \left[\epsilon_{BSTCG}{}^2 + 1\right]^{1/2} Db$	$DBSG = \left[EBSG^2 + 1\right]^{1/2} \times DBG$
$D_{ESTC} = \left[\epsilon_{ESTCG}{}^2 + 1\right]^{1/2} Db$	$DESG = \left[EESG^2 + 1\right]^{1/2} \times DBG$
$D_{EC} = \left[\epsilon_{ECG}{}^2 + 1\right]^{1/2} Db$	$DECG = \left[EECG^2 + 1\right]^{1/2} \times DBG$

AGMA	Program
$m_{N_{max}} = NG\,(\epsilon_{OG} - TAN\,\phi_x) + (Np\,(\epsilon_{OP} - TAN\,\phi_x))/2\pi$	$AMP_{MA} = ANG\,(EOGMA - FXTA) + ANP\,(EOPMA - FXTA)/2\pi$
$m_{N_{min}} = NG\,(\epsilon_{BCG} - TAN\,\phi_x) + (NP\,(\epsilon_{ECP} - TAN\,\phi_x))/2\pi$	$AMP_{MI} = ANG\,(EBCG - FXTA) + ANP\,(EECP-FXTA)/2\pi$

See Figure 171.

AGMA	Program
$SIN\,(AN) = \dfrac{0.5\,t_c}{0.5\,D}$	$AN = \dfrac{0.5 \times TPMIS}{0.5 \times DP}$
$\widehat{AN} = ARC\,TAN\left(\dfrac{AN}{\sqrt{1 - AN^2}}\right)$	$AN = ATAN\left(\dfrac{AN}{\sqrt{1 - AN^2}}\right)$
$t = \widehat{AN} \times D$	$TPMIS = AN \times DP$
$t_x = D_x\left[\left(\left(\dfrac{t}{D}\right) + INV\,\phi\right) - INV\,\phi_x\right]$	$TPMIN = D \times P\left[\left(\left(\dfrac{TPMIS}{DP}\right) + ZF\right) - ZFX\right]$

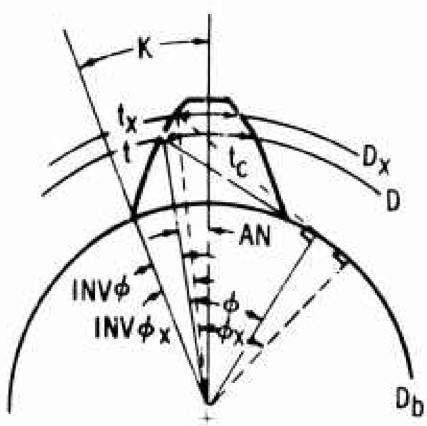

Figure 171. Arc and Chordal Tooth Thickness.

AGMA	Program
$\cos\phi_x = \frac{Db}{D_x}$	$F = \frac{DB}{DIA(I)}$
$\widehat{\phi_x} = \text{ARC TAN}\left(\frac{\sqrt{1-\phi_x^2}}{\phi_x}\right)$	$FRA(I) = ATAN\left(\frac{\sqrt{1-F^2}}{F}\right)$
$INV\,\phi_x = TAN(\phi_x) - \widehat{\phi_x}$	$ZF(I) = FTA(I) - FRA(I)$
$K = \frac{t}{D_x} + INV\,\phi_x$	$PK = \frac{TPMIN}{DXP} + ZFX$
$F = TAN(\phi) - K$	$F(I) = FPTA(I) - PK$
$D_V = \frac{Db}{COS(F)}$	$DVP(I) = \frac{DBP}{COS(F(I))}$

Basic Hob Data (See Figure 172.)

Program

$$TSA = \frac{\pi}{N}$$

$$DHPA = N \times \frac{HLEAD}{\pi}$$

$$HADDN = 0.5\,(DHPA - D_R)$$

$$HPAR = 0.017453293 \times HPA$$

$$HTTN = HTT + 2\,(HADDN - HADD)\,TAN\,(HPAR)$$

$$HTTR = 0.5 \times HTT - HADD \times TAN\,(HPAR)$$

$$HA = HTTR - \frac{HTIPR - HPW}{COS\,(HPAR)}$$

$$HRCTRX = HA + HTIPR \times TAN\,(HPAR)$$

$$RHPA = 0.5\,DHPA$$

$$HRCTRP = HADDN - HTIPR$$

$$\widehat{HPCA} = \text{ARC TAN}\left(\frac{HRCTRX}{HRCTRP}\right)$$

$$HYP = \sqrt{HRCTRX^2 + HRCTRP^2}$$

Wrap pitch line of hob around gear pitch circle by equal increments and calculate path of hob tip radius center. See Figure 173.

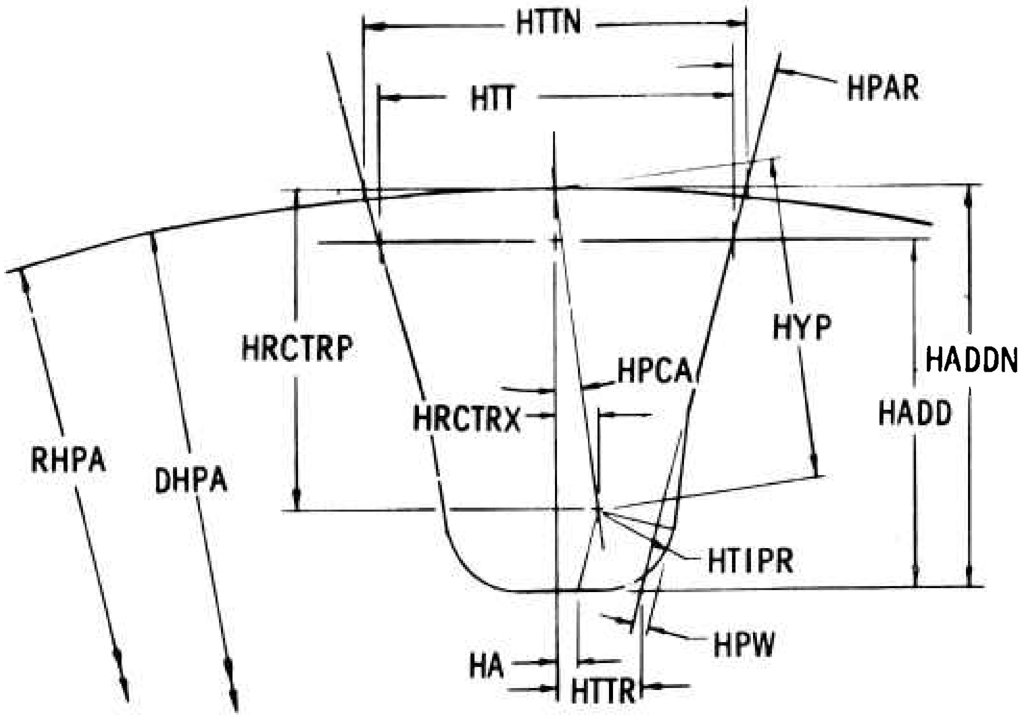

Figure 172. Standard or Protuberance Hob Form for Calculation.

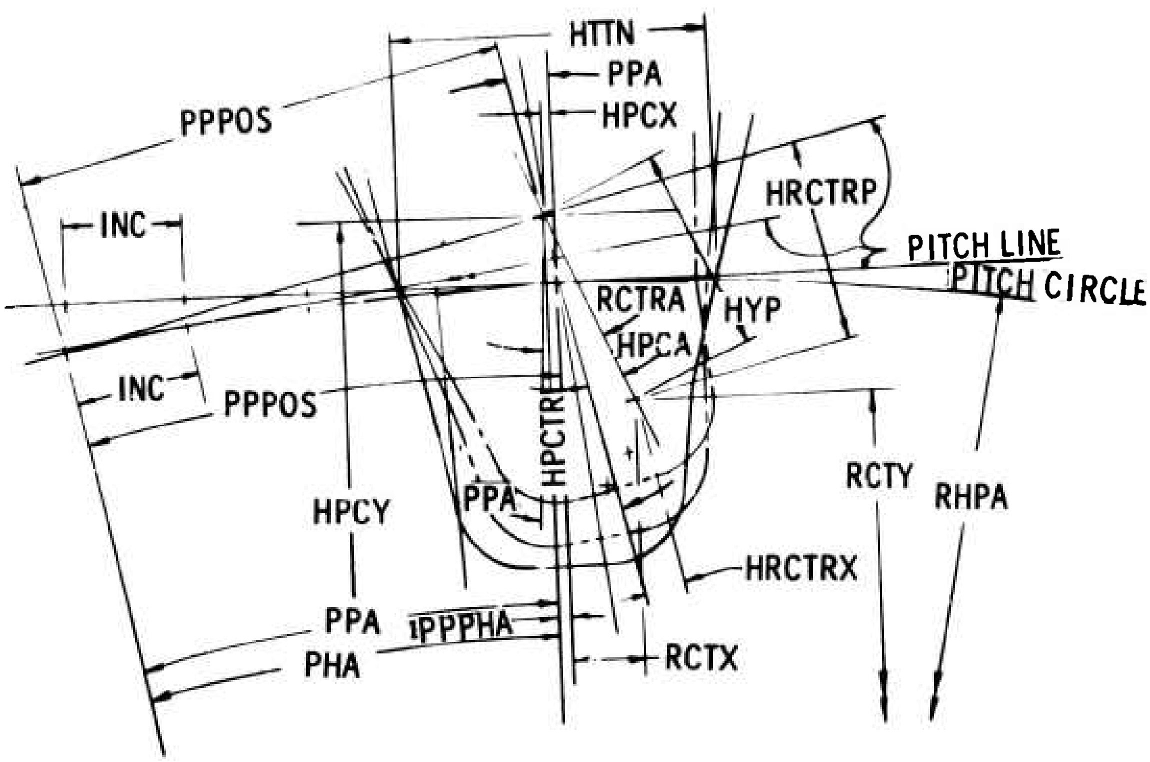

Figure 173. Tooth Generation by Hob.

Program

INC = 0.1 × HTTN (increment of change)

PPPOS = 0 (pitch point position—first time through increase PPPOS by increments each time)

$$PPA = \frac{PPPOS}{RHPA}$$

$$HPCTR = \sqrt{PPPOS^2 + RHPA^2}$$

$$\widehat{PHA} = \text{ARC TAN}\left(\frac{PPPOS}{RHPA}\right)$$

PPPHA = PPA - PHA

HPCX = HPCTR × SIN (PPPHA)

HPCY = HPCTR × COS (PPPHA)

RCTRA = HPCA + PPA

RCTX = HYP × SIN (RCTRA) - HPCX

RCTY = HPCY - HYP × COS (RCTRA)

Calculate points where hob tip radius is making final cut in fillet of gear. See Figure 174.

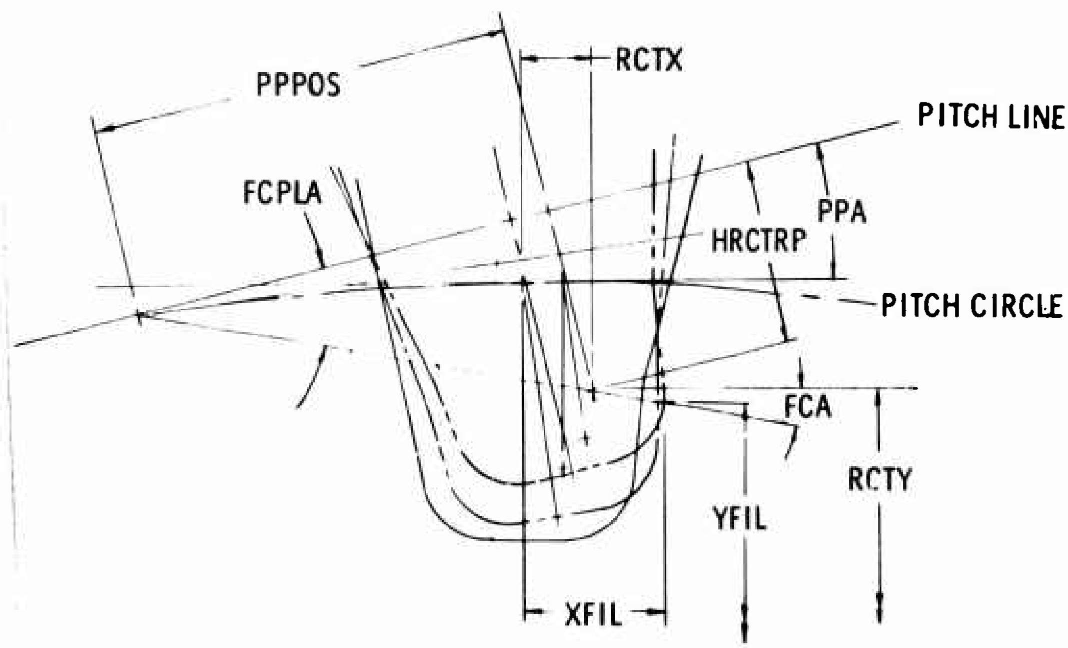

Figure 174. Fillet Generation by Hob.

$$\widehat{FCPLA} = \text{ARC TAN}\left(\frac{HRCTRP}{PPPOS}\right)$$

$$FCA = FCPLA - PPA$$

$$XFIL = RCTX + HTIPR \times COS(FCA)$$

$$YFIL = RCTY - HTIPR \times SIN(FCA)$$

Convert location of fillet points from center of tooth space to center of gear tooth. See Figure 175.

$$\widehat{FSA} = \text{ARC TAN}\left(\frac{XFIL}{YFIL}\right)$$

$$FTA = TSA - \widehat{FSA}$$

$$RFIL = \sqrt{XFIL^2 + YFIL^2}$$

$$XTFIL = RFIL \times SIN(FTA)$$

$$YTFIL = RFIL \times COS(FTA)$$

Find parabola for evaluating bending stress. See Figure 176.

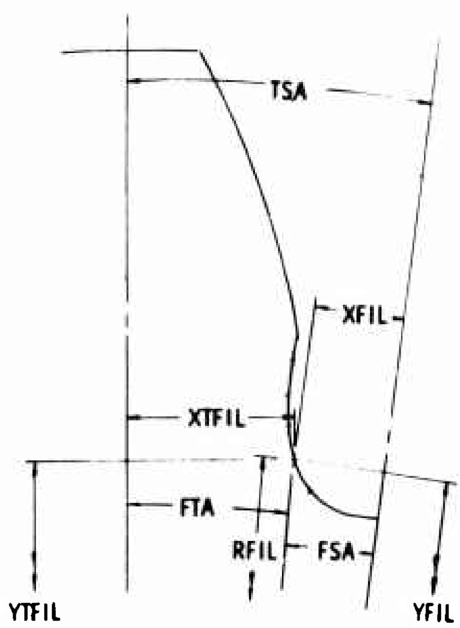

Figure 175. Generated Tooth Fillet.

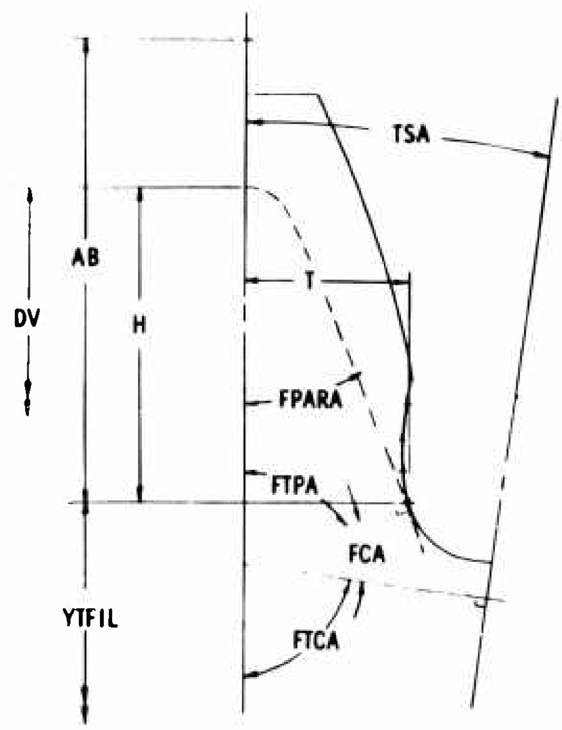

Figure 176. Trochoidal Fillet Inscribed Lewis Parabola.

Program

$$FTCA = \frac{\pi}{2} - TSA$$

$$FTPA = \pi - (FTCA + FCA)$$

$$FPARA = \frac{\pi}{2} - FTPA$$

$$AB = T \times TAN(FPARA)$$

$$H = 0.5\ DV - YTFIL$$

Reiterate for new T, H, and YTFIL values until AB = 2H is satisfied.

Find the radius of curvature of generated fillet tangent to parabola. See Figure 177.

$$SIDEA = YFIL - (RHPA - HADDN)$$

$$HYPA = \frac{SIDEA}{COS(FCA)}$$

$$ANGLEA = 0.5\left(\left(\frac{\pi}{2}\right) + FCA\right)$$

$$FILR = HYPA \times TAN(ANGLEA)$$

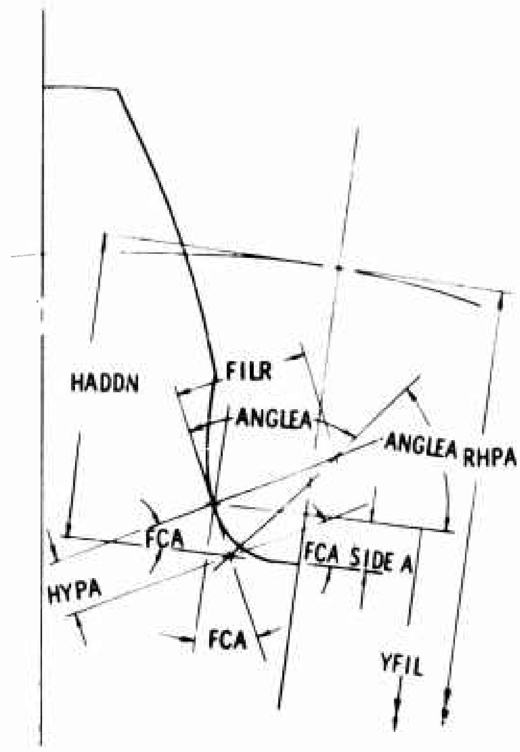

Figure 177. Radius of Curvature at Weakest Section.

Find X value from parabola and diameter of the weakest section of tooth. See Figure 178.

<u>Program</u>

$$ANGLED = ARC\ TAN \left(\frac{T}{H}\right)$$

$$ADJ = \frac{T}{SIN\ (ANGLED)}$$

$$XDIM = \frac{ADJ}{COS\ (ANGLED) - H}$$

$$DW = 2\sqrt{T^2 + YTFIL^2}$$

Find coordinates to center of true fillet radius. See Figures 179 and 180

$$H = \frac{DR}{2} + RF$$

When $\frac{DB}{2} \leq H$, then (Figure 179):

$$CPR = \frac{0.5\ DB}{H}$$

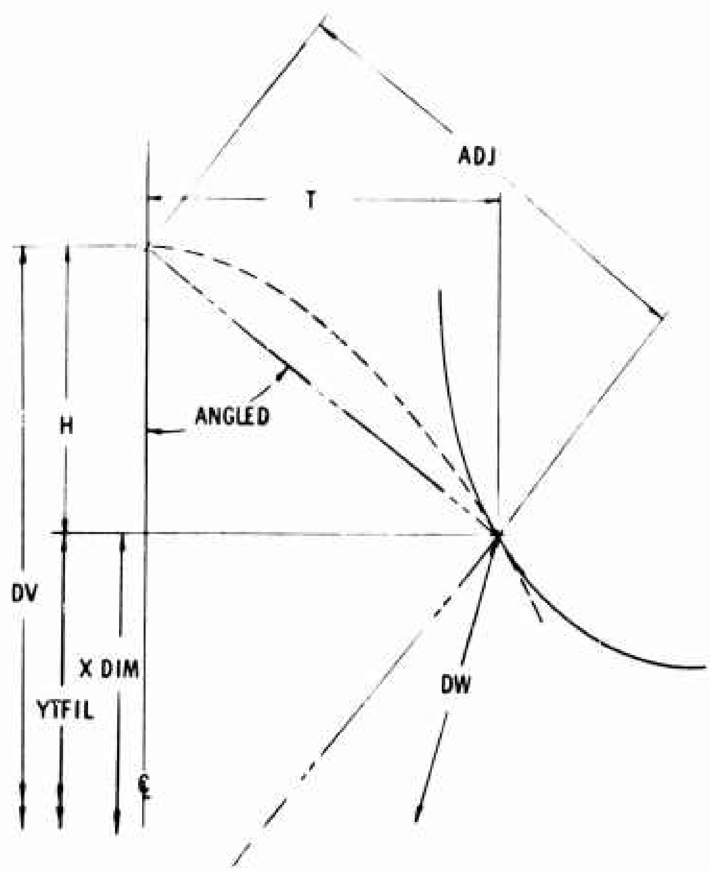

Figure 178. Diameter of Weakest Section and Lewis Y Value.

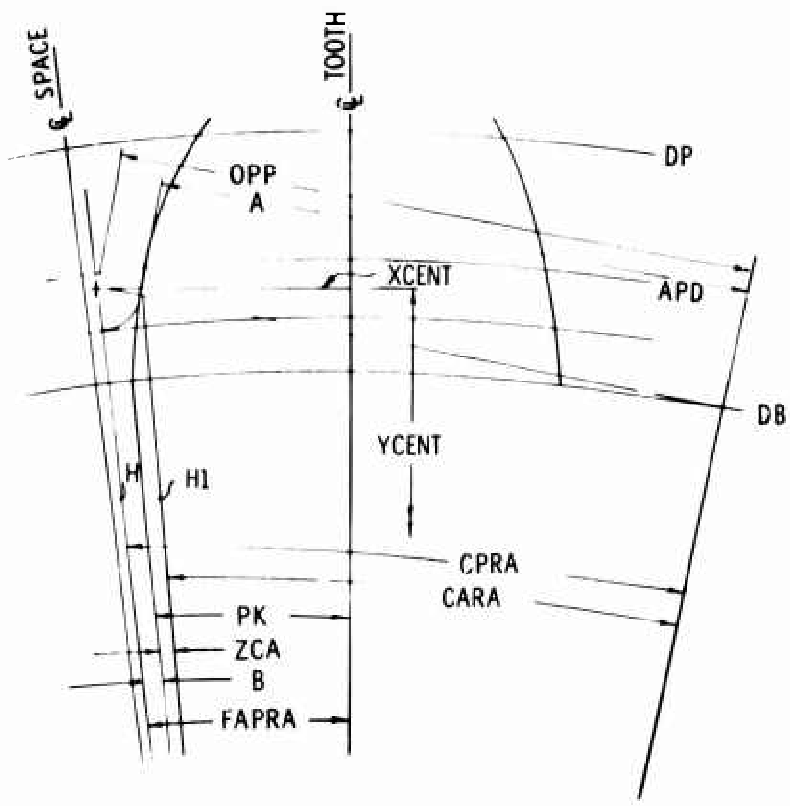

Figure 179. Coordinates at Center of True Fillet Radius—Base Circle Below Root Diameter.

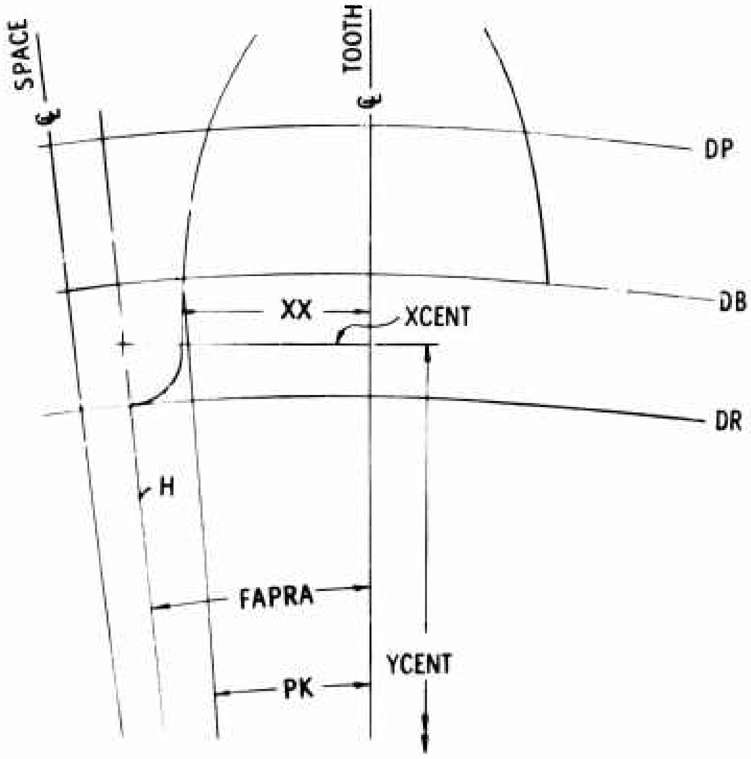

Figure 180. Coordinates at Center of True Fillet Radius—Base Circle Above Root Diameter.

Program

$$CPRA = \text{ARC TAN}\left(\frac{\sqrt{1 - CPR^2}}{CPR}\right)$$

$$OPP = \sqrt{H^2 - (0.5\ DB)^2}$$

$$A = OPP - RF$$

$$H1 = \sqrt{A^2 + (0.5\ DB)^2}$$

$$CA = \frac{0.5\ DB}{H1}$$

$$CARA = \text{ARC TAN}\left(\frac{\sqrt{1 - CA^2}}{CA}\right)$$

$$ZCA = \text{TAN}\ (CARA) - \widehat{CARA}$$

$$B = CPRA - CARA - ZCA$$

$$FAPRA = PK + B$$

$$XCENT = \text{SIN}\ (FAPRA) \times H$$

$$YCENT = \text{COS}\ (FAPRA) \times H$$

When $\frac{DB}{2} > H$, then (Figure 180):

$$XX = \left(\frac{DB}{2}\right) \text{SIN}\ (PK)$$

$$FAPSI = \frac{XX + RF}{H}$$

$$FAPRA = \text{ARC TAN}\left(\frac{FAPSI}{\sqrt{1 - FAPSI^2}}\right)$$

$$XCENT = \text{SIN}\ (FAPRA) \times H$$

$$YCENT = \text{COS}\ (FAPRA) \times H$$

Find parabola for evaluating bending stress. Also, find X value and diameter of weakest section. See Figure 181.

$ALPHA = 0.1$ (First time only)

$$V = \text{SIN}\ (ALPHA) \times RF$$

$$VI = \sqrt{RF^2 - V^2}$$

$$T = XCENT - VI$$

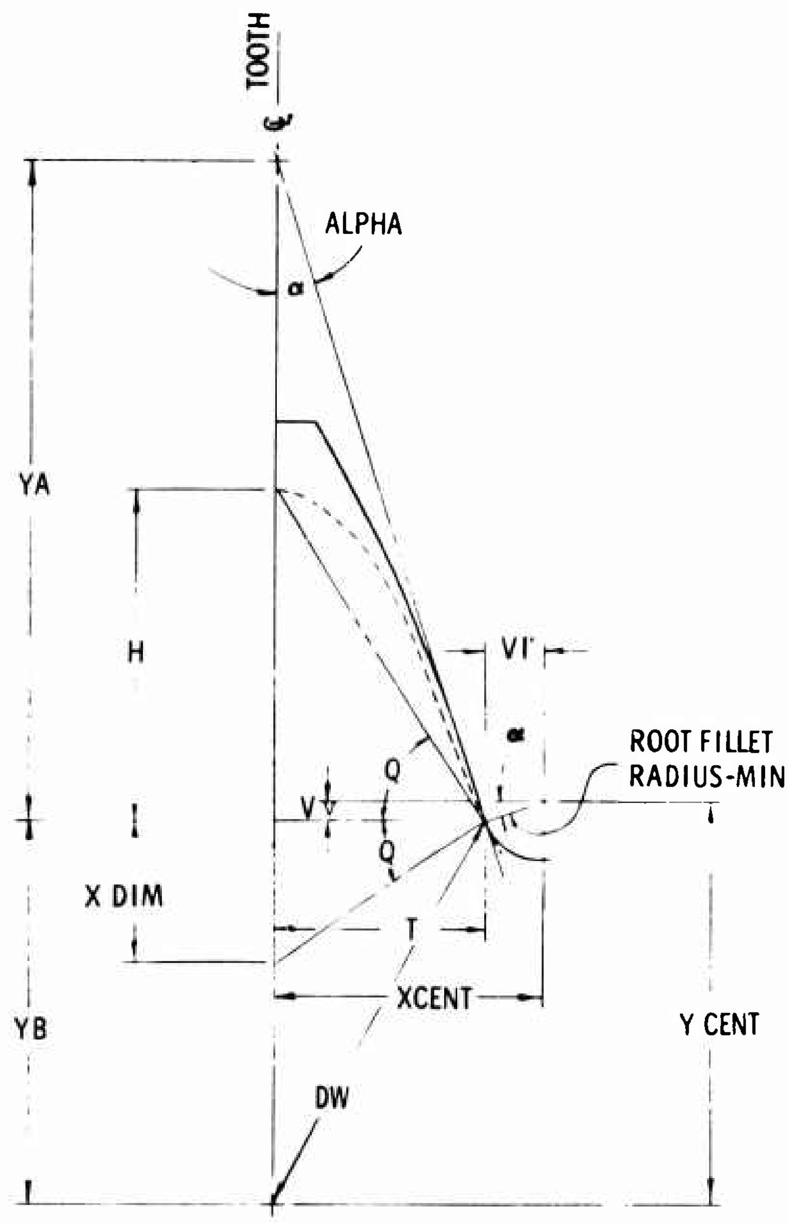

Figure 181. True Fillet Radius Inscribed Lewis Parabola.

Program

$$YA = \frac{T}{TAN\ (ALPHA)}$$

$$H = (RV - YCENT) + V$$

Reiterate for new value of ALPHA until YA = 2H is satisfied.

$$YB = YCENT - V$$

$$DW = \sqrt{YB^2 + T^2} \times 2$$

Program

$$Q = \text{ARC TAN}\left(\frac{H}{T}\right)$$

$$Q = \frac{\pi}{2} - Q$$

$$\text{XDIM} = T \times \text{TAN}(Q)$$

AGMA	Program
$T = \frac{63025 \times Hp}{\eta p}$	$TQ = \frac{63025 \times HORSES}{RPMP}$
$W_t = \frac{2 \times T}{\eta p}$	$WT = \frac{2 \times TQ}{RPMP}$
$G = \eta p \times R_{mg}$	$RPMG = RPMP \times RMG$
$S_h = \rho \frac{V^2}{g}$	$SHOOP = RHO \frac{V^2}{386.064}$
$b_1 = b - r_T$	$B1 = HADD - HTIPR$
$r_1 = \frac{b_1^2}{Rp + b_1}$	$R1 = \frac{B1^2}{RP + B1}$
$r_f = r_1 + r_T$	$RFMI = R1 + HTIPR$
$K_f = 0.22 + \left(\frac{T}{r_f}\right)^{0.20}\left(\frac{T}{h}\right)^{0.40}$	$KF = 0.22 + \left(\frac{T}{RFMI}\right)^{0.20}\left(\frac{T}{H}\right)^{0.40}$
$K_f = 0.18 + \left(\frac{T}{r_f}\right)^{0.15}\left(\frac{T}{h}\right)^{0.45}$	$KF = 0.18 + \left(\frac{T}{RFMI}\right)^{0.15}\left(\frac{T}{H}\right)^{0.45}$
$K_f = 0.14 + \left(\frac{T}{r_f}\right)^{0.11}\left(\frac{T}{h}\right)^{0.50}$	$KF = 0.14 + \left(\frac{T}{RFMI}\right)^{0.11}\left(\frac{T}{H}\right)^{0.50}$
$J = \frac{Y}{K_f \times m_\eta}$	$J = \frac{YAGMA}{KF \times MN}$
$S_t = \frac{W_t K_o}{K_v} \frac{Pd}{F} \frac{K_s K_m}{J}$	$SB = \frac{WT \times KO}{KV} \frac{PDX}{FMINP} \frac{KS \times KM}{J}$

Combine bending and centrifugal stress on the modified Goodman diagram. See Figure 182.

From S/N curve in Figure 183, find the life cycle endurance limit.

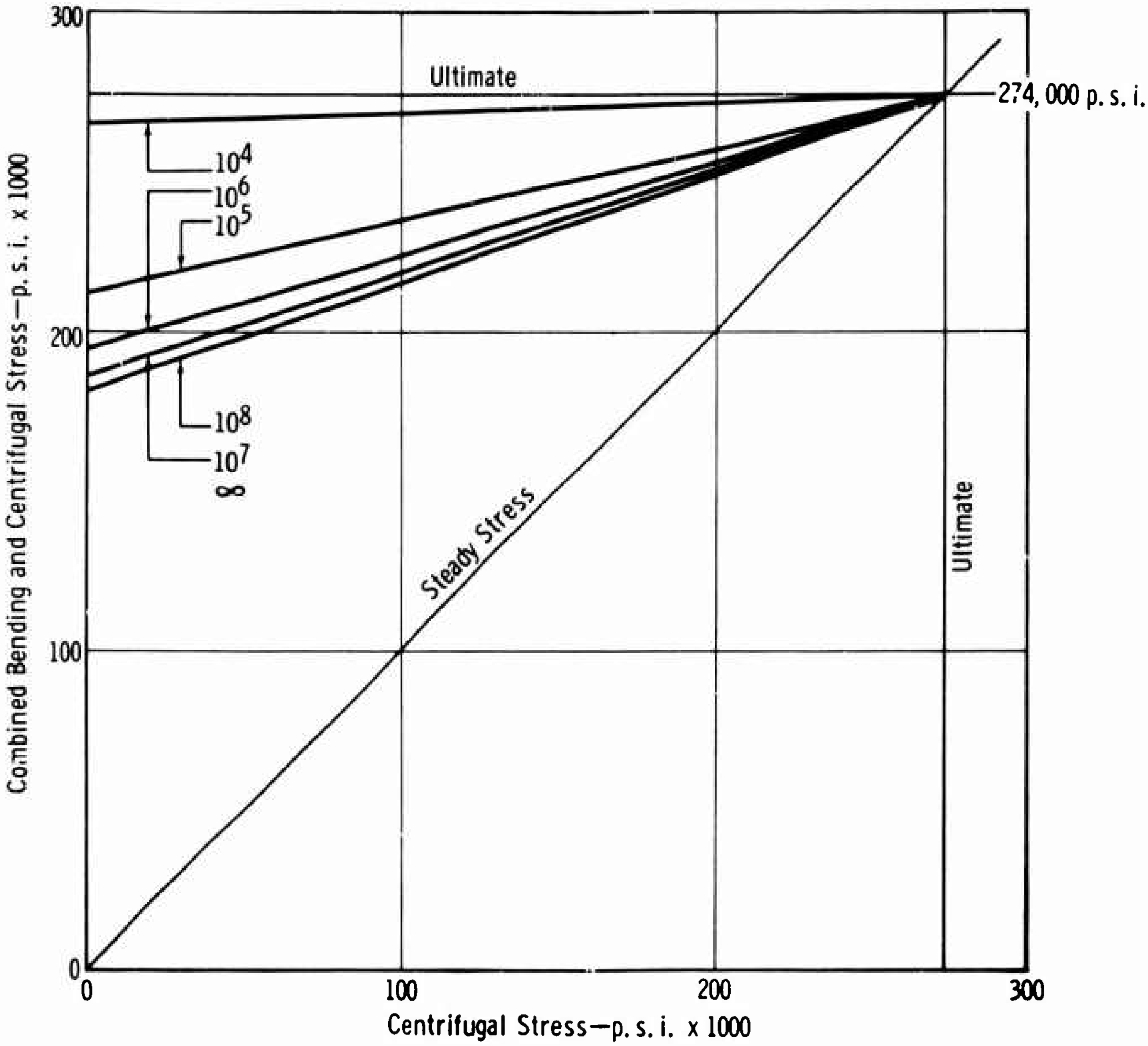

Figure 182. Modified Goodman Diagram Combining Centrifugal and Bending Stresses.

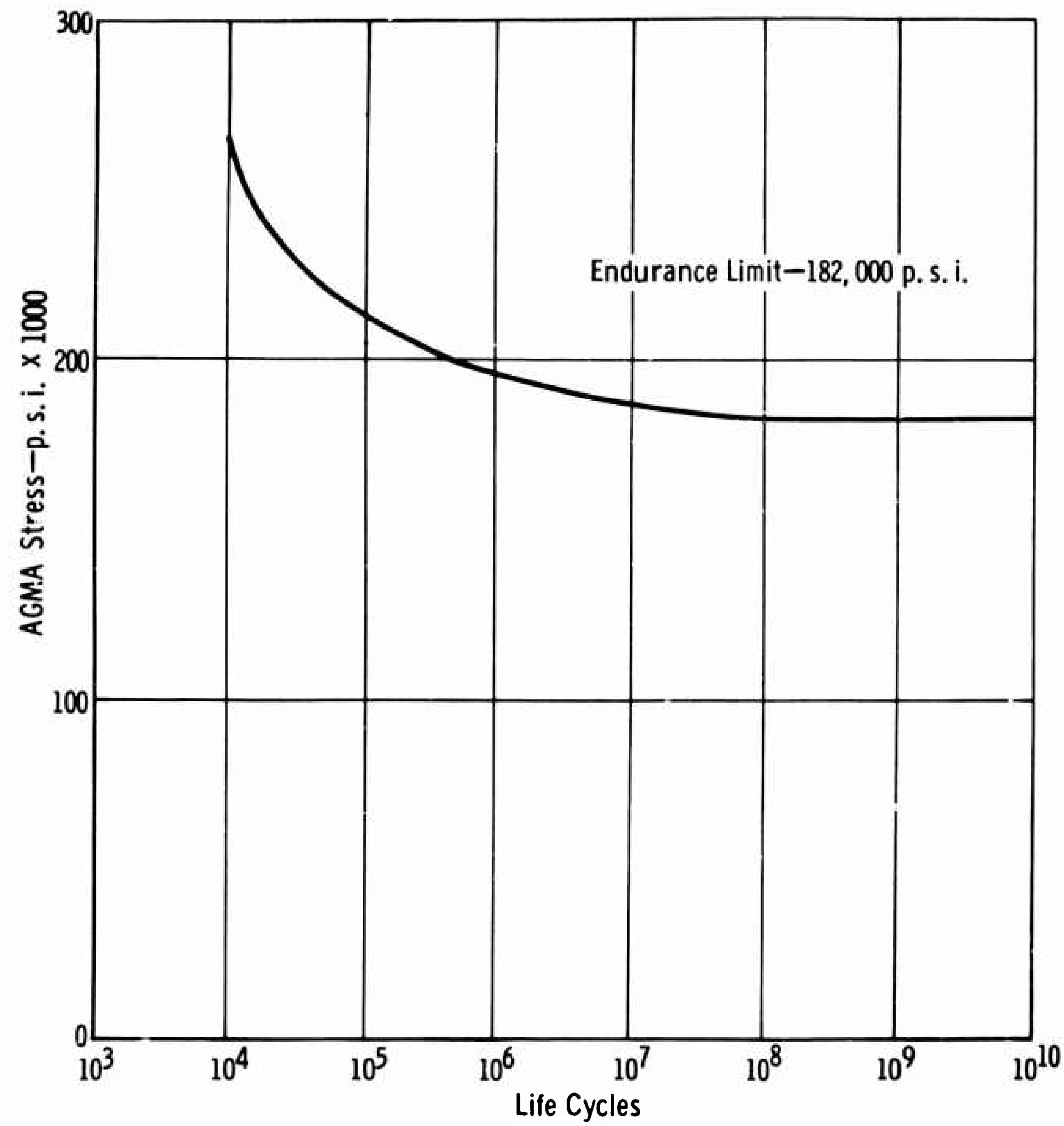

Figure 183. Fatigue Test Gear Endurance Strength for Computer Program.

SOURCE PROGRAM LISTING

The source program is listed on the following pages. Comment cards have been used to define generated symbols within the program. Several subroutines are used and are also listed.

SOURCE PROGRAM PRINT-OUT

```
C                         *  EXTERNAL SPUR GEARS - FOR   *
C                         *  EVALUATING BENDING STRESS   *
C                         *  PROGRAMED BY M.R. CHAPLIN   *
C                         *  ALLISON,DIV. OF GMC         *
C                         * * * * * * * * * * * * * * * *
C
      REAL KT,KR,KM,KO,KV,MN,JP,JG,KFP,KFG,KSP,KSG
      INTEGER CODE
      DIMENSION DIAP(6),DIAG(6),FPRA(6),FPDE(6),FPSI(6),FPCO(6),FPTA(6),
     *ZFP(6),FGRA(6),FGDE(6),FGSI(6),FGCO(6),FGTA(6),ZFG(6),
     *DVP(6),RVP(6),ALPHP(6),TP(6),HP(6),DWP(6),XDIMP(6),
     *DVG(6),RVG(6),ALPHG(6),TG(6),HG(6),DWG(6),XDIMG(6),
     *SBP(6),SBG(6),SBPHOP(6),SBGHOP(6),YPAGMA(6),YGAGMA(6),
     *FILRP(6),FILRG(6),XCYC(5),YPSI (5),         JP(5),JG(5),KFP(5),
     *KFG(5),Q1(12),Q3(12)
      EQUIVALENCE (DIAP(1),DBCP),(DIAP(2),DBSP),(DIAP(3),CP),
     *(DIAP(4),DXP),(DIAP(5),DESP),(DIAP(6),DECP),
     *(DIAG(1),DECG),(DIAG(2),DBSG),(DIAG(3),DG),(DIAG(4),DXG),
     *(DIAG(5),DESG),(DIAG(6),DECG)
C
C  LOGICAL UNIT/MODE (LIN=5  INPUT  5/BCD)
C                    (LOU=6  OUTPUT 6/BCD)
C
      LIN=5
      LOU=6
    1 READ (LIN,2) ANP,ANG,CNSTD,CUTTER,CODE,HORSES,RPMP,RHO,KT,KR,KM,
     *PHIN,PND,BMIN,BMAX,TPMIS,TPMAS,TGMIS,TGMAS,L,
     *DOPMI,DOPMA,DOGMI,DOGMA,FMINP,FMING,BRKP,BRKG,
     *DRPMI,DRPMA,DRGMI,DRGMA,RFMIP,RFMIG,UCP,UCG,KO,KV
    2 FORMAT (2F5.0,F10.0,A6,2X,I2,2F10.0,4F5.0/
     *2F10.0,2F5.0,4F10.0,I2/
     *6F10.0,2F5.0/
     *4F10.0,6F5.0)
C
      COMMON RHPA,HPCA,HYP,HRCTRP,        TSA,FCA,YFIL
C
      NP=ANP
      NG=ANG
C
C  DATA STATEMENTS  -  USED TO DEFINE VARIABLE TITLES FOR OUTPUT
C
      DATA (Q1(N),N=1,12) /6HBC (LP,6HC)      ,6HBSTC (,6HLPSTC),
     *6HPP (ST,6HD)      ,6HPP (OP,6H)       ,6HESTC (,6HHPSTC),
     *6HEC (HP,6HC)      /
      DATA (Q3(N),N=1,12) /6HBC (HP,6HC)      ,6HBSTC (,6HHPSTC),
     *6HPP (ST,6HD)      ,6HPP (OP,6H)       ,6HESTC (,6HLPSTC),
     *6HEC (LP,6HC)      /
C
      DATA SHAPED/6HSHAPED/
      DATA PINION,GEAR   /6HPINION,6HGEAR   /
C
      DATA (XCYC(M),M=1,5) /4.,5.,6.,7.,8./
      DATA (YPSI (M),M=1,5)/265000.,212000.,198000.,186000.,182000./
C
C                           * * * * * * * * * * *
C
C           RN   -- CONVERT FROM DEGREES TO RADIANS
C           DEGR -- CONVERT FROM RADIANS TO DEGREES
C
      RN=.017453293
      DEGR=57.2957795131
      PI=3.1415926535898
      IPHI=PHIN
```

```
      FNRA=PHIN*FN
      FNSI=SIN(FNRA)
      FNCO=COS(FNRA)
      FNTA=FNSI/FNCO
C
C  PDX          ---DIAMETRAL PITCH  (NON STD CENTERS)
C  CSTD         ---STD CENTER DISTANCE
C  FXRA         ---PHI X            (NON STD CENTERS)
C
      CSTD=(ANP&ANG)/(2.*PND)
      IF (CNSTD)              20,19,20
   19 CNSTD=CSTD
   20 PDX=(ANP&ANG)/(2.*CNSTD)
      FX=(CSTD*FNCO)/CNSTD
      FXRA=ATAN(SQRT(1.-(FX)**2)/FX)
      FXSI=SIN(FXRA)
      FXCO=COS(FXRA)
      FXTA=FXSI/FXCO
C
C  ZFN          ---INVOLUTE PHI     (STD CENTERS)
C  ZFX          ---INVOLUTE PHI     (NON STD CENTERS)
C
      IF (CNSTD - CSTD)       604,606,608
  604 WRITE (LOU,1000)
      GO TO 21
  606 WRITE (LOU,1001)
      GO TO 21
  608 WRITE (LOU,1002)
   21 WRITE (LOU,1004) NP,NG,CNSTD,CUTTER,CODE,HORSES,RPMP,RHO,KT,KR,KM
      IF (L)                  90,92,90
   90 WRITE (LOU,1005) PHIN,PND,BMIN,BMAX,TPMIS,TPMAS,YGMIS,TGMAS
      GO TO 94
   92 WRITE (LOU,1006) PHIN,PND,BMIN,BMAX,TPMIS,TPMAS,TGMIS,TGMAS
   94 WRITE (LOU,1007) DOPMI,DOPMA,DOGMI,DOGMA,FMINP,FMING,BRKP,BRKG,
     *DRPMI,DRPMA,DRGMI,DRGMA,RFMIP,RFMIG,UCP,UCG,KO,KV
      WRITE (LOU,2000)
      ZFN=FNTA-FNRA
      ZFX=FXTA-FXRA
C
C  AMG          ---GEAR RATIO
C  RMG          ---1/GEAR RATIO
C
      AMG=ANG/ANP
      RMG=ANP/ANG
C
C          PINION       GEAR
C          DP           DG            - STD PITCH DIA.
C          DBP          DBG           - BASE CIRCLE DIA.
C          DXP          DXG           - NON STD PITCH DIA.
C          DODBP        DODBG         - OUTSIDE DIA BREAK
C
      DP=ANP/PND
      DBP=DP*FNCO
      DXP=ANP/PDX
      DG=ANG/PND
      DBG=DG*FNCO
      DXG=ANG/PDX
      DODBP=DOPMI-(2.*BRKP)
      DODBG=DOGMI-(2.*BRKG)
C
C          PINION       GEAR
C          EECP         EECG          - EPSILON  END CONTACT
C          EBCP         EBCG          - EPSILON  BEGIN CONTACT
```

```
C           EBSP          EBSG          - EPSILON  BEGIN SINGLE TOOTH CONTACT
C           EESP          EESG          - EPSILON  END SINGLE TOOTH CONTACT
C           EOPMA         EOGMA         - EPSILON  OD MAX
C
      EECP=SQRT((DOCBP/CBP)**2-1.)
      EBCG=SQRT((CODBG/CBG)**2-1.)
      EBCP=(FXTA*(AMG&1.))-(EBCG*AMG)
      EECG=(FXTA*(RMG&1.))-(EECP*RMG)
      EBSP=EECP-((2.*PI)/ANP)
      EESP=EBCP&((2.*PI)/ANP)
      EBSG=EECG&((2.*PI)/ANG)
      EESG=EBCG-((2.*PI)/ANG)
      EOPMA=SQRT((DCPMA/DBP)**2-1.)
      EOGMA=SQRT((DOGMA/CBG)**2-1.)
C
C  DIAMETERS AT ENGAGEMENT CONDITIONS
C          PINION        GEAR
C          DBCP          CBCG          - BEGIN CONTACT
C          CBSP          CBSG          - BEGIN SINGLE TOOTH CONTACT
C          DESP          CESG          - END SINGLE TOOTH CONTACT
C          DECP          CECG          - END CONTACT
C
      DBCP=SQRT((EBCP)**2&1.)*DBP
      CBSP=SQRT((EBSP)**2&1.)*DBP
      DESP=SQRT((EESP)**2&1.)*DBP
      CECP=SQRT((EECP)**2&1.)*DBP
      CBCG=SQRT((EBCG)**2&1.)*DBG
      CBSG=SQRT((EBSG)**2&1.)*DBG
      CESG=SQRT((EESG)**2&1.)*DBG
      CECG=SQRT((EECG)**2&1.)*DBG
C
C  AMPMA          -- PROFILE CONTACT RATIO MAX
C  AMPMI          -- PROFILE CONTACT RATIO MIN
C
      AMPMA=((ANG*(EOGMA-FXTA))&(ANP*(EOPMA-FXTA)))/(2.*PI)
      AMPMI=((ANG*(EBCG -FXTA))&(ANP*(EECP -FXTA)))/(2.*PI)
C
      IF (L)                    80,82,80
C
C  CALCULATE ARC TOOTH THK. FROM CHORDAL THK.
C
   80 AN=(.5*TPMIS)/(.5*DP)
      AN=ATAN(AN/(SCRT(1.-(AN)**2)))
      TPMIS=AN*DP
      AN=(.5*TPMAS)/(.5*DP)
      AN=ATAN(AN/(SCRT(1.-(AN)**2)))
      TPMAS=AN*DP
      AN=(.5*TGMIS)/(.5*DG)
      AN=ATAN(AN/(SCRT(1.-(AN)**2)))
      TGMIS=AN*DG
      AN=(.5*TGMAS)/(.5*DG)
      AN=ATAN(AN/(SCRT(1.-(AN)**2)))
      TGMAS=AN*DG
C
C  CALCULATE ARC TOOTH THK. AT THE OPERATING PITCH DIA.  (DXP)
C
   82 TPMIN=DXP*(((TPMIS/DP)&ZFN)-ZFX)
      TPMAX=DXP*(((TPMAS/DP)&ZFN)-ZFX)
      TGMIN=DXG*(((TGMIS/DG)&ZFN)-ZFX)
      TGMAX=DXG*(((TGMAS/DG)&ZFN)-ZFX)
C
C  CALCULATE PHI AND INVOLUTE PHI AT THE ENGAGEMENT CONDITIONS
C
```

```
      CALL PHI (CIAP,DEGR,FPRA,FPDE,FPSI,FPCO,FPTA,ZFP,DBP)
      CALL PHI (CIAG,DEGR,FGRA,FGDE,FGSI,FGCO,FGTA,ZFG,DBG)
C
C         PINION        GEAR
C         PK            GK        -      ANGLE FROM THE ORGIN OF THE
C                                     INVOLUTE TO THE CENTER LINE OF TOOTH
C         DVP           DVG       -   DIA. TO VERTEX OF PARABOLAS
C         RVP           RVG       -   RAD. TO VERTEX OF PARABOLAS
C
      PK=(TPMIN/DXP)&ZFX
      GK=(TGMIN/DXG)&ZFX
      DO 500 I=1,6
      F=FPTA(I)-PK
      DVP(I)=DBP/COS(F)
      RVP(I)=DVP(I)*.5
      F=FGTA(I)-GK
      DVG(I)=DBG/COS(F)
  500 RVG(I)=DVG(I)*.5
      IF (CUTTER.EQ.SHAPED)  GO TO 512
      IF (CODE - 1)          502,504,506
  502 CALL HOB (DXP,DRPMI,ANP,PI,RN,TP,HP,DWP,XDIMP,HADDP,HPWP,FILRP,
     *HTIPRP,DVP,6)
      GO TO 508
  504 CALL HOB (DXG,DRGMI,ANG,PI,RN,TG,HG,DWG,XDIMG,HADDG,HPWG,FILRG,
     *HTIPRG,DVG,6)
      GO TO 510
  506 CALL HOB (DXP,DRPMI,ANP,PI,RN,TP,HP,DWP,XDIMP,HADDP,HPWP,FILRP,
     *HTIPRP,DVP,6)
      CALL HOB (DXG,DRGMI,ANG,PI,RN,TG,HG,DWG,XDIMG HADDG,HPWG,FILRG,
     *HTIPRG,DVG,6)
      GO TO 514
  508 CALL XY (DBG,DRGMI,RFMIG,DEGR,GK,XG,YG)
      RFMG=RFMIG&UCG
      CALL WEAK (RVG,XG,YG,RFMG,ALPHG,TG,HG,DWG,XDIMG,6)
      GO TO 514
  510 CALL XY (DBP,DRPMI,RFMIP,DEGR,PK,XP,YP)
      RFMP=RFMIP&UCP
      CALL WEAK (RVP,XP,YP,RFMP,ALPHP,TP,HP,DWP,XDIMP,6)
      GO TO 514
  512 CALL XY (DBP,DRPMI,RFMIP,DEGR,PK,XP,YP)
      CALL XY (DBG,DRGMI,RFMIG,DEGR,GK,XG,YG)
      RFMP=RFMIP&UCP
      RFMG=RFMIG&UCG
      CALL WEAK (RVP,XP,YP,RFMP,ALPHP,TP,HP,DWP,XDIMP,6)
      CALL WEAK (RVG,XG,YG,RFMG,ALPHG,TG,HG,DWG,XDIMG,6)
C
  514 TQP=(63025.*HORSES)/RPMP
      RPMG=RPMP*RMG
      TQG=(63025.*HORSES)/RPMG
      WTP=(2.*TQP)/DXP
      WTG=(2.*TQG)/DXG
      DO 515 I=2,5
$JOB  CHAPLIN,M.        FT4   N84   7893   P57507   002   010   1
$EXECUTE        IBJOB
$IBJOB N84
$IBFTC N84
C                   * * * * * * * * * * * * * * * *
C                   *  STANDARD AND NON STANDARD  *
      A=FPTA(I)-PK
      BB=COS(A)/FXCO
      BBB=1.5/XDIMP(I)
      BBBB=(SIN(A)/COS(A))/(TP(I)*2.)
      YPAGMA(I)=FCX/(BB*(BBB-BBBB))
```

```
      A=FGTA(I)-CK
      BB=COS(A)/FXCO
      BBB=1.5/XCIMG(I)
      BBBB=(SIN(A)/COS(A))/(TG(I)*2.)
  515 YGAGMA(I)=FDX/(BB*(BBB-BBBB))
C
      MN=1.0
      IF (CUTTER.EQ.SHAPED)  GO TO 406
      IF (CODE - 1)          402,404,400
  400 B1=HADDP-HTIPRP
      R1=B1**2/((DP*.5)&B1)
      RFMIP=R1&HTIPRP
  404 B1=HADDG-HTIPRG
      R1=B1**2/((DG*.5)&B1)
      RFMIG=R1&HTIPRG
      GO TO 406
  402 B1=HADDP-HTIPRP
      R1=B1**2/((DP*.5)&B1)
      RFMIP=R1&HTIPRP
  406 IF (IPHI-20)           408,412,416
  408 DO 410 I=2,5
      KFP(I)=.22 & (((TP(I)*2.)/RFMIP)**.20 * ((TP(I)*2.)/HP(I))**.40)
  410 KFG(I)=.22 & (((TG(I)*2.)/RFMIG)**.20 * ((TG(I)*2.)/HG(I))**.40)
      GO TO 420
  412 DO 414 I=2,5
      KFP(I)=.18 & (((TP(I)*2.)/RFMIP)**.15 * ((TP(I)*2.)/HP(I))**.45)
  414 KFG(I)=.18 & (((TG(I)*2.)/RFMIG)**.15 * ((TG(I)*2.)/HG(I))**.45)
      GO TO 420
  416 DO 418 I=2,5
      KFP(I)=.14 & (((TP(I)*2.)/RFMIP)**.11 * ((TP(I)*2.)/HP(I))**.50)
  418 KFG(I)=.14 & (((TG(I)*2.)/RFMIG)**.11 * ((TG(I)*2.)/HG(I))**.50)
  420 DO 422 I=2,5
      JP(I)=YPAGMA(I)/(KFP(I)*MN)
      JG(I)=YGAGMA(I)/(KFG(I)*MN)
      KSP=1.
      KSG=1.
      SBP(I)=((WTP*KO)/KV)*(PDX/FMINP)*((KSP*KM)/JP(I))
  422 SBG(I)=((WTG*KO)/KV)*(PDX/FMING)*((KSG*KM)/JG(I))
      VP=PI*DRPMI*(RPMP/60.)
      SHOOPP=RHO*(VP**2/386.064)
      VG=PI*DRGMI*(RPMG/60.)
      SHOOPG=RHO*(VG**2/386.064)
      DO 426 I=2,5
      SBPHOP(I)=SBP(I)&SHOOPP
  426 SBGHOP(I)=SBG(I)&SHOOPG
C
C  BENDING & HOOP STRESS FROM MODIFIED GOODMAN DIAGRAM
C
      HOOPMA=274000.
      DO 522 I=2,5
      DIFFP=HOOPMA - SBPHOP(I)
      DIFFG=HOOPMA - SBGHOP(I)
      EP=HOOPMA-SHOOPP
      EG=HOOPMA-SHOOPG
      AP=(HOOPMA * DIFFP)/EP
      AG=(HOOPMA * DIFFG)/EG
      SBPHOP(I)=HOOPMA-AP
  522 SBGHOP(I)=HOOPMA-AG
C
      IF (SBPHOP(5) - 274000.)         526,526,524
  524 WRITE (LOU,1003) PINION
  526 IF (SBGHOP(2) - 274000.)         530,530,528
  528 WRITE (LOU,1003) GEAR
```

```
 530 IF (SBPHOP(5)-182000.) 624,624,626
 624 WRITE (LOU,1008) PINION
     GO TO 628
 626 CALL CISCOT (SBPHCP(5),DUMA,YPSI,XCYC,DUMB,-31,5,0,EXP)
 628 IF (SBGHOP(2)-182000.) 630,630,632
 630 WRITE (LOU,1008) GEAR
     GO TO 609
 632 CALL CISCCT (SBGHCP(2),DUMA,YPSI,XCYC,DUMB,-31,5,0,EXG)
C
 609 WRITE (LOU,1009) PINION,GEAR
     N=3
     DO 201 I=2,5
     WRITE (LOU,1010) C1(N),Q1(N&1),SBPHOP(I),Q3(N),Q3(N&1),SBGHOP(I)
 201 N=N&2
     WRITE (LOU,999) PINION,GEAR
 999 FORMAT (///26X36HB E N D I N G   S T R E S S   (AGMA)//21X,A6,28X
    *,A6)
     N=3
     DO 202 I=2,5
     WRITE (LOU,1010) C1(N),Q1(N&1),SBP(I),Q3(N),Q3(N&1),SBG(I)
 202 N=N&2
     WRITE (LOU,9999) SHOOPP,SHOOPG
9999 FORMAT (///20X11HHOOP STRESS/10X6HPINION23X4HGEAR/F19.4,15XF12.4)
     IF (SBPHOP(5)-182000.) 612,612,610
 610 WRITE (LOU,1011) PINION,EXP
 612 IF (SBGHOP(2)-182000.) 1,1,614
 614 WRITE (LOU,1011) GEAR,EXG
1000 FORMAT(1H134X23HNON STANDARD SPUR GEARS/35X25HDECREASED CENTER DIS
    *TANCE)
1001 FORMAT(1H134X19HSTANDARD SPUR GEARS/35X24HSTANDARD CENTER DISTANCE
    *)
1002 FORMAT(1H134X23HNON STANDARD SPUR GEARS/35X25HINCREASED CENTER DIS
    *TANCE)
1003 FORMAT(///5X15HBENDING STRESS A6, 9H AT HPSTC/4X31HEXCEEDS ULTIMAT
    *E OF 274000. PSI)
1004 FORMAT (///35X35HI N P U T   D A T A   S E C T I O N///5X
    *15HNUMBER OF TEETH9X6HCENTER9X        1H*7X4HCODE7X2HHP11X3HRPM5X
    *7HDENSITY6X2HKT7X2HKR7X2HKM/5X15HPINION     GEAR8X
    *8HDISTANCE39X        18HPINION   LB/CU. IN/5XI4,6XI4,F17.6,8XA6,
    *2XI2,1X2F14.4,4F9.4)
1005 FORMAT (/5X8HPRESSURE5X9HDIAMETRAL9X8HBACKLASH8X25HCHORDAL TOOTH T
    *HK -PINION6X23HCHORDAL TOOTH THK -GEAR/5X5HANGLE8X5HPITCH11X3HMIN
    *6X3HMAX6X25HMIN      (STD  PD)      MAX6X24HMIN      (STD  PD)      MAX
    */F14.6,F13.6,F11.4,F9.4,F13.6,3X2F14.6,F15.6)
1006 FORMAT (/5X8HPRESSURE5X9HDIAMETRAL9X8HBACKLASH8X21HARC TOOTH THK -
    *PINION10X19HARC TOOTH THK -GEAR/5X5HANGLE8X5HPITCH11X3HMIN6X3HMAX
    *6X21HMIN     (STD PD)    MAX10X20HMIN     (STD PD)  MAX /F14.6,F13.6,
    *F11.4,F9.4,2F13.6,7X2F11.6)
1007 FORMAT (//5X20HOUTSIDE DIA - PINION9X20HOUTSIDE DIA  -  GEAR7X
    *18HFACE WIDTH  -  MIN4X13HMAX TIP BREAK/5X3HMIN14X3HMAX9X3HMIN14X
    *3HMAX7X6HPINION8X4HGEAR4X6HPINION3X4HGEAR/3X2F11.6,7X2F11.6,5X
    *2F10.6,3X2F7.4//5X20HROOT DIA     - PINION9X20HROOT DIA      -  GEAR
    *7X18HFILLET RADIUS -MIN4X13HMAX  UNDERCUT5X2HKO7X2HKV/5X3HMIN14X
    *3HMAX9X3HMIN14X3HMAX7X6HPINION8X4HGEAR4X6HPINION3X4HGEAR/3X
    *2F11.6,7X2F11.6,1X2F12.6,3X2F7.4,2F9.4)
1008 FORMAT (///5X15HBENDING STRESS-A6,17H-AT HPSTC IS LESS/4X
    *56HTHAN THE ENDURANCE LIMIT OF 182000. PSI - INFINITE LIFE.)
1009 FORMAT(///26X27HB E N D I N G   S T R E S S3X10H(COMBINED)//
    *21X,A6,28X,A6)
1010 FORMAT (10X,2A6,F15.4,5X,2A6,F15.4)
1011 FORMAT (//5X12HLIFE CYCLES ,A6,19H 10 TO A EXPONET OF,F7.2)
2000 FORMAT (1H134X37HO U T P U T   D A T A   S E C T I O N)
     GO TO 1
```

```
      END
$IBFTC PHI.
C  SUBROUTINE PHI -CALC. PRESSURE ANGLES AND INVOLUTE ANGLES AT
C  ENGAGEMENT CONDITIONS
C
      SUBROUTINE PHI (DIA,DEGR,FRA,FDE,FSI,FCO,FTA,ZF,DB)              PHI    1
      DIMENSION DIA(6),FRA(6),FDE(6),FSI(6),FCO(6),FTA(6),ZF(6)        PHI    2
      DO 10 I=1,6                                                      PHI    3
      F=DB/DIA(I)                                                      PHI    4
      FRA(I)=ATAN(SQRT(1.-(F)**2)/F)                                   PHI    5
      FDE(I)=FRA(I)*DEGR                                               PHI    6
      FSI(I)=SIN(FRA(I))                                               PHI    7
      FCO(I)=COS(FRA(I))                                               PHI    8
      FTA(I)=FSI(I)/FCO(I)                                             PHI    9
      ZF(I)=FTA(I)-FRA(I)                                              PHI   10
   10 CONTINUE                                                         PHI   11
      RETURN                                                           PHI   12
      END                                                              PHI   13
$IBFTC XY.
C  SUBROUTINE XY --CALCULATES COORDINATES TO CENTER OF FILLET RADIUS   XY     1
C                                                                      XY     2
      SUBROUTINE XY (DB,DR,RF,DEGR,PK,          X,Y)                   XY     3
      H=(DR/2.)&RF                                                     XY     4
      IF ((DB/2.)-H)           10,10,12                                XY     5
   10 CPR=(DB/2.)/H                                                    XY     6
      CPRA=ATAN(SQRT(1.-(CPR)**2)/CPR)                                 XY     7
      OPP=SQRT((H)**2-(DB/2.)**2)                                      XY     8
      A=OPP-RF                                                         XY     9
      H1=SQRT((A)**2&(DB/2.)**2)                                       XY    10
      CA=(DB/2.)/H1                                                    XY    11
      CARA=ATAN(SQRT(1.-(CA)**2)/CA)                                   XY    12
      ZCA=(SIN(CARA)/COS(CARA))-CARA                                   XY    13
      B=(CPRA-CARA)-ZCA                                                XY    14
      FAPRA=PK&B                                                       XY    15
   11 X=SIN(FAPRA)*H                                                   XY    17
      Y=COS(FAPRA)*H                                                   XY    18
      RETURN                                                           XY    19
   12 XX=(DB/2.)*SIN(PK)                                               XY    20
      FAPSI=(XX&RF)/H                                                  XY    21
      FAPRA=ATAN(FAPSI/(SQRT(1.-(FAPSI)**2)))                          XY    22
      GO TO 11                                                         XY    24
      END                                                              XY    25
$IBFTC WEAK.
C     SUBROUTINE WEAK CALCS. THE DIA. OF THE WEAKEST SECTION (DW) BY
C   INSCRIBING THE LARGEST PARABOLA THAT WILL FIT THE GEAR TOOTH SHAPE.
C
      SUBROUTINE WEAK (RV,XCENT,YCENT,RF,ALPHA,T,H,DW,XDIM,NOD)        WEAK   1
      DIMENSION RV(6),ALPHA(6),T(6),H(6),XDIM(6),DW(6)                 WEAK   2
      DO 10 I=1,NOD                                                    WEAK   3
      ALPHA(I)=.1                                                      WEAK   4
      DELTA=.1                                                         WEAK   5
  144 V=SIN(ALPHA(I))*RF                                               WEAK   6
      V1=SQRT((RF)**2-(V)**2)                                          WEAK   7
C       T --  HALF CHORD AT THE WEAKEST SECTION                        WEAK   8
      T(I)=XCENT-V1                                                    WEAK   9
      YA=T(I)/(SIN(ALPHA(I))/COS(ALPHA(I)))                            WEAK  10
C       H --  TOOTH HEIGHT FROM WEAKEST SECTION TO VERTEX OF PARABOLA  WEAK  11
      H(I)=(RV(I)-YCENT)&V                                             WEAK  12
      YAP=YA*.5                                                        WEAK  13
      IF (YAP - H(I))          146,150,148                             WEAK  14
  146 ALPHA(I)=ALPHA(I)-DELTA                                          WEAK  15
      DELTA=.1*DELTA                                                   WEAK  16
      IF (.0000001-DELTA)   144,150,150                                WEAK  17
```

```
  148 ALPHA(I)=ALPHA(I)&DELTA                                          WEAK  18
      GO TO 144                                                        WEAK  19
  150 YB=YCENT-V                                                       WEAK  20
C        DW  --  WEAKEST SECTION DIAMETER                              WEAK  21
      DW(I)=SQRT((YB)**2&(T(I))**2)*2.                                 WEAK  22
      C=ATAN(H(I)/T(I))                                                WEAK  23
      C=1.57079623-Q                                                   WEAK  24
C        XDIM-      X DIMENSION                                        WEAK  25
      XDIM(I)=T(I)*(SIN(Q)/COS(Q))                                     WEAK  26
   10 CONTINUE                                                         WEAK  27
      RETURN                                                           WEAK  28
      END                                                              WEAK  29
$IBFTC HCB.
C  SUBROUTINE HOB  --
C
C
      SUBROUTINE HOB (DX,DRPM,ANP,PI,RN,T,H,DW,XDIM,HADD,HPW,FILR,     HOB    1
     *HTIPR,DVP,NOD)
      DIMENSION DVP(6),XDIM(6),DW(6),T(6),H(6),PI(6),YYFIL(6),DIAP(6), HOB    2
     *DIAG(6),FILR(6)                                                  HOB    3
      EQUIVALENCE (DIAP(1),DBCP),(DIAP(2),DBSP),(DIAP(3),DP),(DIAP(4),       70
     *DXP),(DIAP(5),DESP),(DIAP(6),DECP),(DIAG(1),DBCG),(DIAG(2),           80
     *DBSG),(DIAG(3),DG),(DIAG(4),DXG),(DIAG(5),DESG),(DIAG(6),DECG)        90
C  LOGICAL UNIT/MODE  (LIN=5  INPUT 5/BCD)
C                     (LOU=6  OUTPUT 6/BCD)
C
      LIN=5                                                            HOB    4
      LOU=6                                                            HOB    5
      READ (LIN,2) HTT,HADD,HLEAD,HPA,HTIPR,HPW                        HOB    6
    2 FORMAT (6F10.0)                                                  HOB    7
      COMMON RHPA,HPCA,HYP,HRCTRP,      TSA,FCA,YFIL                   HOB    8
      WRITE (LOU,1008) HTT,HADD,HLEAD,HPA,HTIPR,HPW                    HOB    9
 1008 FORMAT (//3X9HHOB  DATA//5X21HTOOTH THK.   ADDENDUM7X4HLEAD4X    HOB
     *24HPRESSURE ANGLE  TIP RAD.7X3HHPW/6F13.6)                       HOB
      REAL INC                                                         HOB    7
      TSA=PI/ANP                                                       HOB    8
      DHPA=(ANP*HLEAD)/PI                                              HOB    9
      HADDN=.5*(DHPA-DRPMI)                                            HOB   10
      HPAR=HPA*RN                                                      HOB   11
      HTTN=HTT&2.*(HADDN-HADD)*TAN(HPAR)                               HOB   12
      HTTR=.5*HTT-HADD*TAN(HPAR)                                       HOB   13
      HA=HTTR-(HTIPR-HPW)/COS(HPAR)                                    HOB   14
      HRCTRX=HA&HTIPR*TAN(HPAR)                                        HOB   15
      RHPA=.5*DHPA                                                     HOB   16
      HRCTRP=HADD-HTIPR                                                HOB   17
      HPCA=ATAN(HRCTRX/HRCTRP)                                         HOB   18
      HYP=HRCTRP/COS(HPCA)                                             HOB   19
C  FIND PARABOLA TANGENT TO GENERATED FILLET                           HOB   20
      FTCA=(PI/2.)-TSA                                                 HOB   21
      DO 25 I=1,NOD                                                    HOB   22
      INC=.1*HTTN                                                      HOB   23
      PPPOS=0.                                                         HOB   24
    5 PPPOS=PPPOS&INC                                                  HOB   25
      CALL GENFIL (PPPOS, T(I),YYFIL(I),DW(I),FCA,HTIPR)               HOB   26
      FTPA=PI-(FTCA&FCA)                                               HOB   27
      FPARA=(PI/2.)-FTPA                                               HOB   28
      AB= T(I)/TAN(FPARA)                                              HOB   29
      H(I)=.5*DVP(I)-YYFIL(I)                                          HOB   30
      K=1000000.*(AB-2.*H(I))                                          HOB   31
      IF (K)             5,15,10                                       HOB   32
   10 PPPOS=PPPOS-INC                                                  HOB   33
      INC=.1*INC                                                       HOB   34
      GO TO 5                                                          HOB   35
```

```
   15 PI(I)= T(I)**2/(2.*H(I))                                       HOB   36
C FIND RADIUS OF CURVATURE OF GENERATED FILLET AT TANGENT OF PARABOLA  HOB   37
      SIDEA=YFIL&HADON-RHPA                                           HOB   38
      HYPA=SIDEA/COS(FCA)                                             HOB   39
      ANGLEA=.5*((PI/2.)&FCA)                                         HOB   40
      FILR(I)=HYPA*TAN(ANGLEA)                                        HOB   41
C FIND  --X-- VALUE FOR PARABOLA                                      HOB   42
      ANGLED=ATAN( T(I)/H(I))                                         HOB   43
      ADJ= T(I)/SIN(ANGLED)                                           HOB   44
   25 XDIM(I)=ADJ/COS(ANGLED)-H(I)                                    HOB   45
      RETURN                                                          HOB   46
      END                                                             HOB   47
$IBFTC GENFI.
C   SUBROUTINE GENFIL  -
C
C
      SUBROUTINE GENFIL (PPPOS,XTFIL,YTFIL,DFIL,FCA,HTIPR)            GENFIL 1
      DIMENSION DIAP(6),DIAG(6)
      EQUIVALENCE (DIAP(1),DBCP),(DIAP(2),DBSP),(DIAP(3),CP),(DIAP(4),      70
     *DXP),(DIAP(5),DESP),(DIAP(6),DECP),(DIAG(1),DBCG),(DIAG(2),           80
     *DBSG),(DIAG(3),DG),(DIAG(4),DXG),(DIAG(5),DESG),(DIAG(6),DECG)       90
      COMMON RHPA,HPCA,HYP,HRCTRP,      TSA,FCA,YFIL                  HOB    8
      PPA=PPPOS/RHPA                                                  GENFIL 3
      PHA=ATAN(PPA)                                                   GENFIL 4
      HPCTR=RHPA/COS(PHA)                                             GENFIL 5
      PPPHA=PPA-PHA                                                   GENFIL 6
      HPCX=HPCTR*SIN(PPPHA)                                           GENFIL 7
      HPCY=HPCTR*COS(PPPHA)                                           GENFIL 8
      RCTRA=HPCA&PPA                                                  GENFIL 9
      RCTX=HYP*SIN(RCTRA)-HPCX                                        GENFIL10
      RCTY=HPCY-HYP*COS(RCTRA)                                        GENFIL11
      IF (PPPOS)       10,10,5                                        GENFIL
   10 XFIL=RCTX                                                       GENFIL
      YFIL=RCTY-HTIPR                                                 GENFIL
      GO TO 15                                                        GENFIL
    5 FCPLA=ATAN(HRCTRP/PPPOS)                                        GENFIL12
      FCA=FCPLA-PPA                                                   GENFIL13
      XFIL=RCTX&HTIPR*COS(FCA)                                        GENFIL14
      YFIL=RCTY-HTIPR*SIN(FCA)                                        GENFIL15
   15 FSA=ATAN(XFIL/YFIL)                                             GENFIL16
      FTA=TSA-FSA                                                     GENFIL17
      RFIL=YFIL/COS(FSA)                                              GENFIL18
      XTFIL=RFIL*SIN(FTA)                                             GENFIL19
      YTFIL=RFIL*COS(FTA)                                             GENFIL20
      DFIL=2.0*RFIL                                                   GENFIL21
      RETURN                                                          GENFIL22
      END                                                             GENFIL23
$IBFTC DISCOD  LIST
CDISCOT                                                               DISC0010
      SUBROUTINE DISCOT (XA,ZA,TABX,TABY,TABZ,NC,NY,NZ,ANS)           DISC0020
      DIMENSION TABX(500),TABY(500),TABZ(500),NPX(8),NPY(8),YY(8)     DISC0030
      CALL UNS (NC,IA,IDX,IDZ,IMS)                                    DISC0050
      IF (NZ-1) 5,5,10                                                DISC0060
    5 CALL DISSER (XA,TABX,1,NY,IDX,NN)                               DISC0070
      NNN=IDX&1                                                       DISC0080
      CALL LAGRAN (XA,TABX(NN),TABY(NN),NNN,ANS)                      DISC0090
      GO TO 70                                                        DISC0100
   10 ZARG=ZA                                                         DISC0110
      IP1X=IDX&1                                                      DISC0120
      IP1Z=IDZ&1                                                      DISC0130
      IF (IA)    15,25,15                                             DISC0140
   15 IF (ZARG-TABZ(NZ))    25,25,20                                  DISC0150
   20 ZARG=TABZ(NZ)                                                   DISC0160
```

```
   25 CALL CISSER (ZARG,TABZ,1,NZ,IDZ,NPZ)                                DISC0170
      NX=NY/NZ                                                            DISC0180
      NPZL=NPZ&IEZ                                                        DISC0190
      I=1                                                                 DISC0200
      IF (IMS)     3C,30,4C                                               DISC0210
   30 CALL CISSER (XA,TABX,1,NX,IDX,NPX)                                  DISC0220
      DO 35  JJ=NPZ,NPZL                                                  DISC0230
      NPY(I)=(JJ-1)*NX&NPX(1)                                             DISC0240
      NPX(I)=NPX(1)                                                       DISC0250
   35 I=I&1                                                               DISC0260
      GO TO 50                                                            DISC0270
   40 CO 45 JJ=NPZ,NPZL                                                   DISC0280
      IS=(JJ-1)*NX&1                                                      DISC0290
      CALL CISSER (XA,TABX,IS,NX,IDX,NPX(I))                              DISC0300
      NPY(I)=NPX(I)                                                       DISC0310
   45 I=I&1                                                               DISC0320
   50 CO 55  I=1,IP1Z                                                     DISC0330
      NLOC=NPX(I)                                                         DISC0340
      NLOCY=NPY(I)                                                        DISC0350
   55 CALL LAGRAN (XA,TABX(NLOC),TABY(NLOCY),IP1X,YY(I))                  DISC0360
      CALL LAGRAN (ZARG,TABZ(NPZ),YY,IP1Z,ANS)                            DISC0370
   70 RETURN                                                              DISC0380
      END                                                                 DISC0390
$IBFTC LAGRAD  LIST
CLAGRAN                                                                   LAGR0010
      SUBROUTINE LAGRAN (XA,X,Y,N,ANS)                                    LAGR0020
      DIMENSION X(200),Y(200)                                             LAGR0030
      SUM=0.0                                                             LAGR0050
      DO 3   I=1,N                                                        LAGR0060
      PROD=Y(I)                                                           LAGR0070
      CO 2 J=1,N                                                          LAGR0080
      A=X(I)-X(J)                                                         LAGR0090
      IF (A)    1,2,1                                                     LAGR0100
    1 B=(XA-X(J))/A                                                       LAGR0110
      PROD=PROD*E                                                         LAGR0120
    2 CONTINUE                                                            LAGR0130
    3 SUM=SUM&PROD                                                        LAGR0140
      ANS=SUM                                                             LAGR0150
      RETURN                                                              LAGR0160
      END                                                                 LAGR0170
$IBFTC UNSD    LIST
CUNS                                                                      UNS 0010
      SUBROUTINE UNS (IC,IA,IDX,IDZ,IMS)                                  UNS 0020
      IF (IC)     5,5,10                                                  UNS 0030
    5 IMS=1                                                               UNS 0040
      NC=-IC                                                              UNS 0050
      GO TO 15                                                            UNS 0060
   10 IMS=0                                                               UNS 0070
      NC=IC                                                               UNS 0080
   15 IF (NC-100)   20,25,25                                              UNS 0090
   20 IA=0                                                                UNS 0100
      GC TO 30                                                            UNS 0110
   25 IA=1                                                                UNS 0120
      NC=NC-100                                                           UNS 0130
   30 IDX=NC/10                                                           UNS 0140
      IDZ=NC-IDX*10                                                       UNS 0150
      RETURN                                                              UNS 0160
      END                                                                 UNS 0170
$IBFTC CISSED  LIST
CCISSER                                                                   DISS0010
      SUBROUTINE CISSER (XA,TAB,I,NX,ID,NPX)                              DISS0020
      DIMENSION TAB(200C)                                                 DISS0030
      NPT=IC&1                                                            DISS0050
```

```
      NPB=NPT/2                                                         DISS0060
      NPU=NPT-NPB                                                       DISS0070
      IF (NX-NPT)   10,5,10                                             DISS0080
    5 NPX=1                                                             DISS0090
      RETURN                                                            DISS0100
   10 NLOW=I&NPB                                                        DISS0110
      NUPP=I&NX-(NPU&1)                                                 DISS0120
      DO 15 II=NLOW,NUPP                                                DISS0130
      NLOC=II                                                           DISS0140
      IF (TAB(II)-XA)   15,20,20                                        DISS0150
   15 CONTINUE                                                          DISS0160
      NPX=NUPP-NPB&1                                                    DISS0170
      RETURN                                                            DISS0180
   20 NL=NLOC-NPB                                                       DISS0190
      NU=NL&ID                                                          DISS0200
      DO 25  JJ=NL,NU                                                   DISS0210
      NDIS=JJ                                                           DISS0220
      IF (TAB(JJ)-TAB(JJ&1))   25,30,25                                 DISS0230
   25 CONTINUE                                                          DISS0240
      NPX=NL                                                            DISS0250
      RETURN                                                            DISS0260
   30 IF (TAB(NDIS)-XA)   40,35,35                                      DISS0270
   35 NPX=NDIS-ID                                                       DISS0280
      RETURN                                                            DISS0290
   40 NPX=NDIS&1                                                        DISS0300
      RETURN                                                            DISS0310
      END                                                               DISS0320
$DATA
32.0 100.0           SHAPED    3755.0    13820.0   .283 1.1451.0  1.0
25.0      6.0        .012 .018 .2778     .2808     .2278     .2308      0
5.702     5.707      16.929    16.934    2.545     2.490     .020 .020
4.954     4.974      16.1800   16.2000   .030 .030 .0   .0   1.0  1.450
```

SAMPLE PROBLEM

IBM 7094 DATA SHEET **STD & NON STD EXTERNAL SPUR GEARS BENDING STRESS**

* SHAPED
* HOBBED

IDENTIFICATION NUMBER

EXAMPLE

No. OF TEETH PINION GEAR 32.0 100.0	NON STD CENTER DISTANCE	*	X	HORSEPOWER 3755.5	RPM PINION 13820.0	DENSITY LB/IN³ .283 | K_T 1.145	K_R 1.0 | K_m 1.0		1
PRESSURE ANGLE 25.0	DIAMETRAL PITCH 6.0	BACKLASH MIN MAX .012 .018	ARC OR CHORDAL (STD D_p)-MIN .2778	TOOTH THK PINION (STD D_p)-MAX .2808	ARC OR CHORDAL (STD D_p)-MIN .2278	TOOTH THK GEAR (STD D_p)-MAX .2308	1 2		2
OUTSIDE DIAMETER-PINION MIN 5.702	MAX 5.707	OUTSIDE DIAMETER-GEAR MIN 16.929	MAX 16.934	FACE WIDTH-MIN PINION 2.545	GEAR 2.490	MAX TIP BREAK PINION GEAR .020 .020			3
ROOT DIAMETER-PINION MIN 4.954	MAX 4.974	ROOT DIAMETER GEAR MIN 16.180	MAX 16.934	FILLET RAD-MIN PINION GEAR .030 .030	MAX UNDERCUT PINION GEAR .0 .0	K_o 1.0 | K_v 1.00			4
TOOTH THK (HTT)	ADDENDUM (HADD)	LEAD (HLEAD)	PRESSURE ANGLE (HPA)	TIP RADIUS (HTIPR)	HPW	SEE FIGURE 170 PINION			5
TOOTH THK (HTT)	ADDENDUM (HADD)	LEAD (in LEAD)	PRESSURE ANGLE (HPA)	TIP RADIUS (HTIPR)	HPW	SEE FIGURE 170 GEAR			6
									1
									2
									3
									4
									5
									6

INPUT DATA SHEET

STANDARD SPUR GEARS
STANDARD CENTER DISTANCE

I N P U T   D A T A   S E C T I O N

NUMBER OF TEETH PINION	GEAR	NON STD CENTER DISTANCE	*	CODE	HP	RPM PINION	DENSITY LB/CU. IN
32	100	11.000000	SHAPED	-C	3755.0000	13870.0000	0.2330

PRESSURE ANGLE	DIAMETRAL PITCH	BACKLASH MIN	BACKLASH MAX	ARC TOOTH THK -PINION MIN	(STD PD)	ARC TOOTH THK -PINION MAX	ARC TOOTH MIN	(STD
25.000000	6.000000	0.0120	0.0180	0.277800		0.280800	0.227900	

OUTSIDE DIA - PINION MIN	OUTSIDE DIA - PINION MAX	OUTSIDE DIA - GEAR MIN	OUTSIDE DIA - GEAR MAX	FACE WIDTH - MIN PINION	FACE WIDTH - MIN GEAR	MAX TIP BR PINION	G
5.702000	5.707000	16.929000	16.934000	2.545000	2.490000	0.0200	0.(

ROOT DIA - PINION MIN	ROOT DIA - PINION MAX	ROOT DIA - GEAR MIN	ROOT DIA - GEAR MAX	FILLET RADIUS -MIN PINION	FILLET RADIUS -MIN GEAR	MAX UNDER PINION	G
4.954000	4.974000	16.180000	16.200000	0.030000	0.030000	0.0000	0.0

BENDING STRESS-PINION-AT HPSTC IS LESS
THAN THE ENDURANCE LIMIT OF 182000. PSI - INFINATE LIFE.

BENDING STRESS-GEAR -AT HPSTC IS LESS
THAN THE ENDURANCE LIMIT OF 182000. PSI - INFINATE LIFE.

B E N D I N G   S T R E S S

PINION		GEAR	
BSTC (LPSTC)	32696.3555	BSTC (HPSTC)	125957.7188
PP (STD)	68065.4707	PP (STD)	94310.6230
PP (OP)	68065.4707	PP (OP)	94310.6230
ESTC (HPSTC)	123804.7285	ESTC (LPSTC)	24721.3926

B E N D I N G   S T R E S S   (AGMA)

PINION		GEAR	
BSTC (LPSTC)	31572.2649	BSTC (HPSTC)	121227.6045
PP (STD)	65725.4014	PP (STD)	90768.9580
PP (OP)	65725.4014	PP (OP)	90768.9580
ESTC (HPSTC)	119548.3613	ESTC (LPSTC)	23793.0264

HOOP STRESS

PINION	GEAR
9420.0336	10289.5746

OUTPUT SHEET

A

STANDARD SPUR GEARS
STANDARD CENTER DISTANCE

I N P U T   D A T A   S E C T I O N

ON STD CENTER DISTANCE	*	CODE	HP	RPM PINION	DENSITY LB/CU. IN	KT	KR	KM
11.000000	SHAPED	-C	3755.0000	13820.0000	0.2330	1.1450	1.0000	1.0000

BACKLASH MIN	BACKLASH MAX	ARC TOOTH THK -PINION MIN	(STD PD)	MAX	ARC TOOTH THK -GEAR MIN	(STD PD)	MAX
0.0120	0.0180	0.277800		0.280800	0.227800		0.2 ?800

OUTSIDE DIA - GEAR MIN	MAX	FACE WIDTH - MIN PINION	GEAR	MAX TIP BREAK PINION	GEAR
16.929000	16.934000	2.545000	2.490000	0.0200	0.0200

ROOT DIA - GEAR MIN	MAX	FILLET RADIUS -MIN PINION	GEAR	MAX UNDERCUT PINION	GEAR	KO	KV
16.180000	16.200000	0.030000	0.030000	0.0000	0.0000	1.0000	1.0000

-AT HPSTC IS LESS
IT OF 182000. PSI - INFINATE LIFE.

-AT HPSTC IS LESS
IT OF 182000. PSI - INFINATE LIFE.

B E N D I N G   S T R E S S

N		GEAR
32696.3555	BSTC (HPSTC)	125957.7188
68065.4707	PP (STD)	94310.6230
68065.4707	PP (OP)	94310.6230
123804.7285	ESTC (LPSTC)	24721.3926

B E N D I N G   S T R E S S   (AGMA)

N		GEAR
31572.2649	BSTC (HPSTC)	121227.6045
65725.4014	PP (STD)	90768.9580
65725.4014	PP (OP)	90768.9580
119548.3613	ESTC (LPSTC)	23793.0264

TRESS

GEAR
10289.5746

OUTPUT SHEET

B

APPENDIX VI

AGMA STANDARD 220.02

Following is a reprint of "Tentative AGMA Standard for Rating the Strength of Spur Gear Teeth," by permission of V. C. Sears, American Gear Manufacturers Association.

FOREWORD

This standard is for rating the strength of spur gear teeth. It contains the following:

BASIC RATING FORMULA

This section enumerates the factors known to affect strength. Numerical values are presented for those factors which have been evaluated by analytical means, test results or field experience. Suggestions are made for the factors which are not now capable of being expressed accurately. New knowledge and more definite measurement of these parameters will continually necessitate revisions and improvements.

In addition to the above, it is contemplated to publish design practices, such as AGMA 220.02A, having specific application under the heading of:

DESIGN PRACTICES FOR SPECIALIZED APPLICATIONS

It is recognized that it is sometimes desirable to provide simplified design practice data applicable to a specialized field of application. These individual design practices will enable enclosed speed reducer, mill gear, aircraft or other specialized product designers to record the modifications and limitations they wish to use.

Basic data illustrating the coordination of rating for all types of gears is contained in Tentative Information Sheet AGMA 225.01, "Strength of Spur, Helical, Herringbone and Bevel Gear Teeth.".

The first draft of the revision to this standard was prepared by the committee in September, 1955. It was approved by the AGMA membership as of April 7, 1963.

Tables or other self-supporting sections may be quoted or extracted in their entirety. Credit lines should read: "Extracted from AGMA Standard for Rating the Strength of Spur Gear Teeth (AGMA 220.02), with the permission of the publisher, the American Gear Manufacturers Association, One Thomas Circle, Washington, D. C. 20005".

Personnel of

Gear Rating Committee

Technical Division

January, 1964

E. J. Wellauer, Chairman, The Falk Corp., Milwaukee, Wis.

D. L. Borden, The Falk Corp., Milwaukee, Wis.
W. Coleman, Gleason Works, Rochester, New York
D. W. Dudley, General Electric Co., West Lynn, Mass.
J. H. Glover, Ford Motor Co., Dearborn, Michigan
I. Koenig, Hewitt-Robins, Inc., Chicago, Illinois
C. F. Schwan, Reliance Electric & Engineering Co., Cleveland, Ohio
J. C. Straub, Wheelabrator Corp., Mishawaka, Indiana
F. A. Thoma, De Laval Turbine, Inc., Trenton, New Jersey
N. A. Wilson, Morgan Construction Co., Worcester, Mass.
G. L. Scott, AGMA, Washington, D. C.

TENTATIVE
AGMA STANDARD
STRENGTH OF SPUR GEAR TEETH

Basic Rating Formula

1. Scope

1.1 This standard presents the fundamental formulas for the strength of spur gear teeth. It includes all of the factors which are known to affect gear tooth strength. This standard is based on Information Sheet AGMA 225.01 and is therefore coordinated with strength ratings for helical and bevel gears.

1.2 Both pinion and gear teeth must be checked for bending strength rating to account for differences in geometry factors, material properties, and numbers of tooth contact cycles under load.

1.3 Other AGMA standards contain numerical values to be used to rate gears for specific applications. These should be consulted when applicable.

1.4 Where no applicable specific AGMA standard is established, numerical values may be estimated for the factors in the fundamental formula and an approximate stren[illegible]d.

1.5 The formu[illegible] this reference apply to external gears unless otherwise noted.

1.6 The symbols used, wherever applicable, conform to Standard AGMA 111.03 "Letter Symbols for Gear Engineering" (ASA B6.5-1954) and "Letter Symbols for Mechanics of Solid Bodies" (ASA Z10.3-1948).

2. Fundamental Bending Stress Formula

2.1 The basic equation for the bending stress in a gear is calculated as follows:

$$s_t = \frac{W_t K_o}{K_v} \frac{P_d}{F} \frac{K_s K_m}{J}$$

Where:

s_t = calculated tensile bending stress at the root of the tooth, psi

Load
- W_t = transmitted tangential load at operating pitch dia. lbs. (see Section 4).
- K_o = overload factor (see Section 9)
- K_v = dynamic factor (see Section 8)

Tooth Size
- P_d = diametral pitch
- F = face width, in.

Stress Distribution
- K_s = size factor (see Section 7)
- K_m = Load distribution factor (see Section 6)
- J = geometry factor (see Section 5)

2.1.1 Note that the above equation is divided into three groups of terms, the first of which is concerned with the load, the second with tooth size, and the third with stress distribution.

2.2 The relation of calculated stress to allowable stress is:

$$s_t \leq \frac{s_{at}\, K_L}{K_R\, K_T}$$

Where:

s_{at} = allowable bending stress for material, psi (see Section 13)

s_t = calculated bending stress, psi (see paragraph 2.1)

K_L = life factor (see Section 11)

K_T = temperature factor (see Section 12)

K_R = factor of safety (see Section 10)

3. Fundamental Power Formula

3.1 In preparing handbook data, for gear designs already developed, the following formula can be used to directly calculate the power which can be transmitted by a given gear set:

$$P_{at} = \frac{n_P\, d\, K_v}{126{,}000\, K_o}\ \frac{F}{K_m}\ \frac{J}{K_s\, P_d}\ \frac{s_{at}\, K_L}{K_R\, K_T}$$

Where:

P_{at} = allowable power of gear set, hp

n_P = pinion speed, rpm

d = operating pitch diameter of pinion, in.

4. Transmitted Tangential Load

4.1 The transmitted tangential load is calculated directly from the power transmitted by the gear set. (When operating near a critical speed of the drive, a careful analysis of conditions must be made.) When the transmitted load is not uniform, consideration should be given not only to the peak load and its anticipated number of cycles, but also to intermediate loads and their number of cycles.

4.2 The transmitted tangential load is:

$$W_t = \frac{33{,}000\, P}{v_t} = \frac{2T}{d} = \frac{126{,}000\, P}{n_P\, d}$$

Where:

P = power transmitted, hp

T = pinion torque, lb.in.

v_t = pitch line velocity, fpm

5. Geometry Factor — J

5.1 The geometry factor evaluates the shape of the tooth, the position at which the most damaging load is applied, stress concentration due to geometric shape and the sharing of load.

5.2 See Appendix A for a further discussion of spur gear geometry factors, and paper AGMA 229.07, "Spur and Helical Gear Geometry Factors."

5.3 Accurate spur gears develop the most critical stress when load is applied at the highest point of the tooth where a single pair of teeth is carrying all the load. Less accurate spur gears, having errors that prevent two pairs of teeth from sharing the load, may be stressed most heavily when load is applied at the tip. Figures 1A and 1B show the geometry factor for equal addendum involute spur gears of 20 deg and 25 deg pressure angle. In these curves, it is assumed that the theoretical stress concentration factor is not affected seriously by surface finish, plasticity, residual stresses or other factors.

5.3.1 Table 1 shows the variation in base pitch between the gear and pinion which determines whether or not load sharing exists in 20 degree pressure angle spur gears.

6. Load Distribution Factor — K_m

6.1 The load distribution factor depends upon the combined effect of:

1. misalignment of axes of rotation
2. lead deviations
3. elastic deflection of shafts, bearings and housing.

6.2 Figures 2 and 3 illustrate misalignment and its effect on load distribution.

6.3 The effect of different rates of spur gear misalignment is shown in Figure 4.

6.4 When the misalignment is known, use Figure 4 to select K_m. F_m represents the face width having just 100 per cent contact for a given tangential load and alignment error. Generally F_m should exceed F.

6.5 Manufacturers of precision gears with face widths greater than 6 inches generally find it necessary to control misalignment by other means than allowed rates of misalignment. To handle such cases, Table 2 shows appropriate values of K_m.

6.6 When the estimated or actual misalignment is not known, the K_m factor may be obtained from Table 3.

7. Size Factor — K_s

7.1 The size factor reflects non-uniformity of material properties. It depends primarily on:

1) tooth size;

2) diameter of parts;

3) ratio tooth size to diameter of part;

4) face width;

5) area of stress pattern;

6) ratio of case depth to tooth size;

7) hardenability and heat treatment of materials.

7.2 The size factor may be taken as unity for most spur gears provided a proper choice of steel is made for the size of the parts and the case depth or hardness pattern is adequate.

7.3 Standard size factors for spur gear teeth have not yet been established for cases where there is a detrimental size effect. In such cases a size factor greater than unity should be used.

Table 1 Limiting Error in Action for Steel Spur Gear

(Variation in Base Pitch)

Number of Pinion Teeth	Allowable Error When Teeth Share Load*					Amount of Error When Teeth Fail to Share Load**				
	Load Per In. of Face					Load Per In. of Face				
	500 lb.	1,000 lb.	2,000 lb.	4,000 lb.	8,000 lb.	500 lb.	1,000 lb.	2,000 lb.	4,000 lb.	8,000 lb.
15	0.0004	0.0007	0.0014	0.0024	0.0042	0.0006	0.0011	0.0023	0.0039	0.0064
20	0.0003	0.0006	0.0011	0.0020	0.0036	0.0006	0.0011	0.0023	0.0039	0.0064
25	0.0002	0.0005	0.0009	0.0017	0.0030	0.0006	0.0011	0.0023	0.0039	0.0064

* Use upper curves on Fig. 1 — highest point of single tooth loading.

** Use lower curve of Fig. 1 — tip loading.

8. Dynamic Factor — K_v

8.1 The dynamic factor depends on:

1) effect of tooth spacing and profile errors.

2) effect of pitch line and rotational speeds.

3) inertia and stiffness of all rotating elements.

4) transmitted load per inch of face.

5) tooth stiffness.

8.2 Figure 5 shows some of the dynamic factors that are commonly used.

Curve No. 1 — To be used with high precision shaved or ground spur gears where the effect of the items listed in paragraph 8.1 are such that no appreciable dynamic load is developed.

Curve No. 2 — To be used with high precision shaved or ground spur gears when the items listed in paragraph 8.1 can develop a dynamic load.

Curve No. 3 — To be used with spur gears finished by hobbing or shaping.

8.3 When milling cutters are used to cut the teeth or inaccurate teeth are generated, lower dynamic factors than shown must be used since the dynamic factor reflects the effect of inaccuracies in profile, tooth spacing and runout.

9. Overload Factor — K_o

9.1 The overload factor makes allowances for the roughness or smoothness of operation of both the driving and driven apparatus. Specific overload factors can only be established after considerable field experience is gained in a particular application.

9.2 In determining the overload factor, consideration should be given to the fact that many prime movers develop momentary overload torques appreciably greater than those determined by the nameplate ratings of either the prime mover or the driven apparatus.

9.3 In the absence of specific overload factors, the values in Table 4 should be used.

AGMA STANDARD
STRENGTH OF SPUR GEAR TEETH

Table 2 Load Distribution Factor for Precision Wide-Face Spur Gears — K_m

Ratio of $\frac{F}{d}$	Contact	Load Distribution Factor — K_m
1.0 or less	95% face width contact obtained at 1/3 torque	1.4 at 1/3 torque
	95% face width contact obtained at full torque	1.1 at full torque
	75% face width contact obtained at 1/3 torque	1.8 at 1/3 torque
	95% face width contact obtained at full torque	1.3 at full torque
	35% face width contact obtained at 1/3 torque	2.5 at 1/3 torque
	95% face width contact obtained at full torque	1.9 at full torque
	20% face width contact obtained at full torque	4.0 at 1/3 torque
	75% face width contact obtained at full torque	2.5 at full torque
	Teeth are crowned	
	35% face width contact at 1/3 torque	2.5 at 1/3 torque
	85% face width contact at full torque	1.7 at full torque
over 1 less than 2	Calculated combined twist and bending of pinion not over .001 in. over entire face	
	Pinion not over 250 Bhn hardness	
	75% contact obtained at 1/3 torque	2.0 at 1/3 torque
	95% contact obtained at full torque	1.4 at full torque
	Calculated combined twist and bending of pinion not over .0007 in. over entire face	
	Pinion not over 350 Bhn hardness	
	75% contact obtained at 1/3 torque	2.0 at 1/3 torque
	95% contact obtained at full torque	1.4 at full torque
	30% contact obtained at 1/3 torque	4.0 at 1/3 torque
	75% contact obtained at full torque	3.0 at full torque

Table 3 Load Distribution Factor — K_m

Condition of Support	Face Width, in.			
	2 in. Face and Under	6 in. Face	9 in. Face	16 in. Face and Over
Accurate mountings, low bearing clearances, minimum elastic deflection, precision gears	1.3	1.4	1.5	1.8
Less rigid mountings, less accurate gears, contact across full face	1.6	1.7	1.8	2.0
Accuracy and mounting such that less than full face contact exists	over 2.0			

Table 4 Overload Factors* — K_o

Power Source	Load on Driven Machine		
	Uniform	Moderate Shock	Heavy Shock
Uniform	1.00	1.25	1.75 or higher
Light Shock	1.25	1.50	2.00 or higher
Medium Shock	1.50	1.75	2.25 or higher

* Note that this table is for speed decreasing drives only. For speed increasing drives add

$$0.01 \left(\frac{N_G}{N_P}\right)^2$$ to the factors in Table 4.

Where:

N_P = number of teeth in the pinion

N_G = number of teeth in the gear.

9.4 Service factors have been established where field data is available for specific applications. These service factors include not only the overload factor, but also the life factor and factor of safety. Service factors for many applications are listed in other AGMA Standards, and should be used whenever available. If a specific service factor is used in place of the overload factor K_o, use a value of 1.0 for K_R and K_L.

10. Factor of Safety — K_R

10.1 The factor of safety is introduced in this equation to offer the designer an opportunity to design for high reliability or, in some instances, to design for a calculated risk. Table 5 shows a suggested list of factors of safety to be applied to the fatigue strength of the material rather than to the tensile strength. For this reason, the values are much smaller than customarily used in other branches of machine design.

10.1.1 Failure in the following table does not mean an immediate failure under applied load, but rather a shorter life than the minimum specified.

Table 5 Factors of Safety — K_R

Fatigue Strength

Requirements of Application	K_R
High Reliability	1.50 or higher
Fewer than 1 failure in 100	1.00
Fewer than 1 failure in 3	0.70

10.2 Table 6 shows safety factors to be applied to the yield strength of the material. These values must be applied to the maximum peak load to which the gears are subjected.

Table 6 Factors of Safety — K_R

Yield Strength

Requirements of Application	K_R
High Reliability	3.00 or higher
Industrial	1.33

11. Life Factor — K_L

11.1 The life factor adjusts the allowable loading for the required number of cycles. Table 7 shows typical values, for use with the allowable stress values of Figure 6 or Table 8.

Table 7 Life Factor — K_L

Number of Cycles	K_L			
	160 Bhn	250 Bhn	450 Bhn	case carb.*
Up to 1,000	1.6	2.4	3.4	2.7
10,000	1.4	1.9	2.4	2.0
100,000	1.2	1.4	1.7	1.5
1 million	1.1	1.1	1.2	1.1
10 million and over	1.0	1.0	1.0	1.0

* case carburized 55-63 R_c

12. Temperature Factor — K_T

12.1 When gears operate at oil or gear blank temperatures not exceeding 250 degree F, K_T is generally taken as unity. In some instances, it is necessary to use a K_T value greater than unity for case carburized gears at a temperature above 160 degree F. One basis of correction is:

$$K_T = \frac{460 + T_F}{620}$$

Where:

T_F = The peak operating oil temperature in degrees Fahrenheit.

13. Allowable Bending Stress — s_{at} and s_{ay}

13.1 An allowable design bending stress for unity application factor and 10 million cycles of load application is determined by field experience, for each material and condition of that material. This stress is designated s_{at}.

13.2 The allowable stress for gear materials varies considerably with heat treatment, forging or casting practice, material composition, and with various surface treatments.

13.3 Frequently, shot peening permits a higher allowable stress to be used.

13.4 The allowable fatigue design stress for steel is shown in Figure 6. These values are suggested for general design purposes.

13.5 The allowable fatigue design stress for surface hardened steel and other materials is shown in Table 8.

13.6 Use 70 per cent of the s_{at} values for idler gears and other gears where the teeth are loaded in both directions.

13.7 When the gear is subjected to infrequent momentary high overloads the maximum allowable stress is determined by the allowable yield properties rather than the fatigue strength of the material. This stress is designated as s_{ay}. Figure 7 shows suggested values for allowable yield strength, for through hardened steel. In these cases the design should be checked to make certain that the teeth are not permanently deformed. When yield is the governing stress, the stress concentration factor is sometimes considered ineffective.

Table 8 Allowable Fatigue Design Stress — s_{at}

Material	Material Hardness, min.	s_{at}-psi
Steel		
Case Carburized and Hardened	55 R_c	55-65,000
Induction or Flame Hardened		
Hard Root	300 Bhn	use values from Fig. 6
Unhardened Root	—	22,000
Cast Iron		
AGMA Grade 20	—	5,000
AGMA Grade 30	175 Bhn	8,500
AGMA Grade 40	200 Bhn	13,000

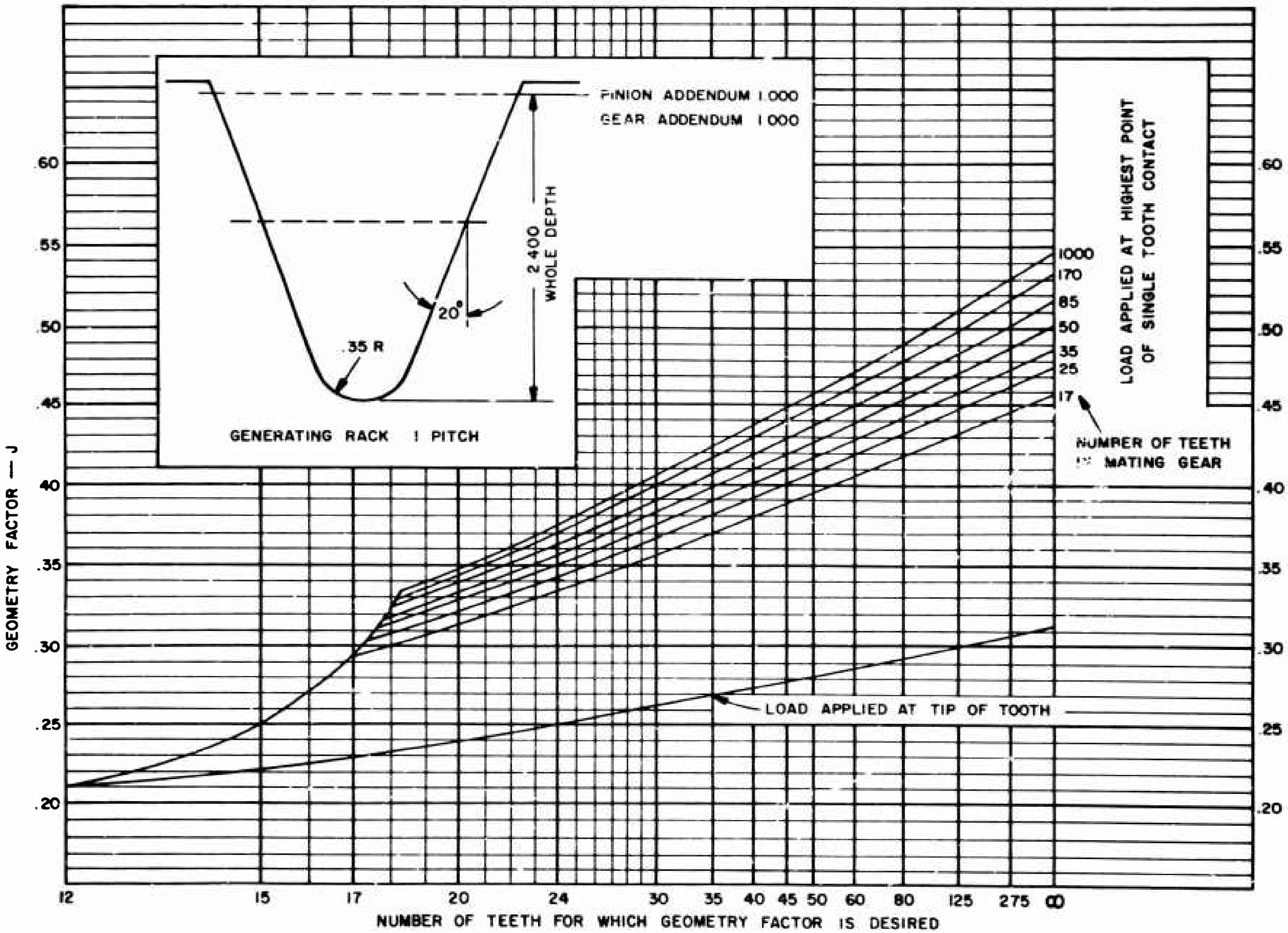

FIG. 1A GEOMETRY FACTORS — 20° SPUR — STANDARD ADDENDUM

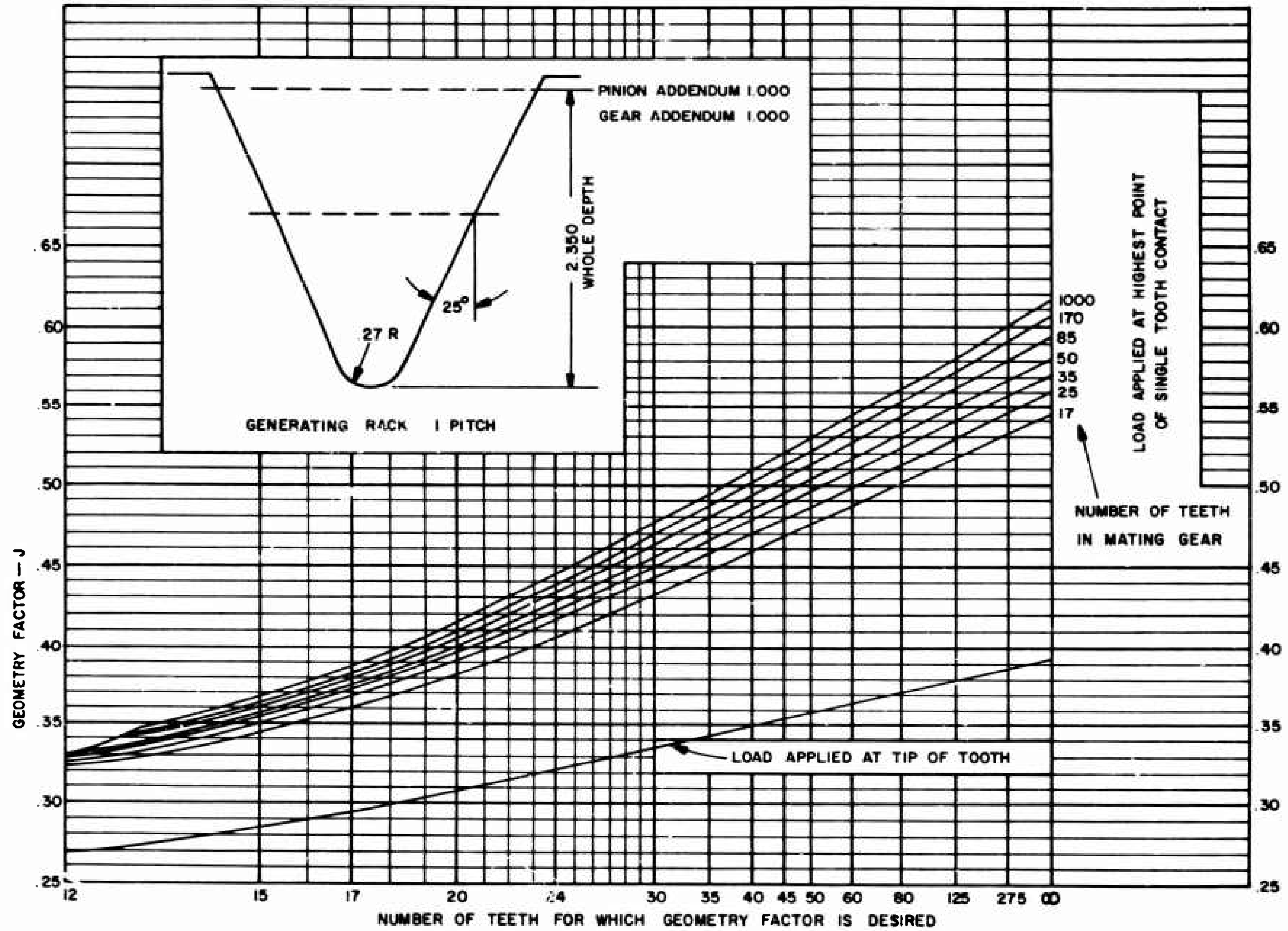

FIG. 1B GEOMETRY FACTORS — 25° SPUR — STANDARD ADDENDUM

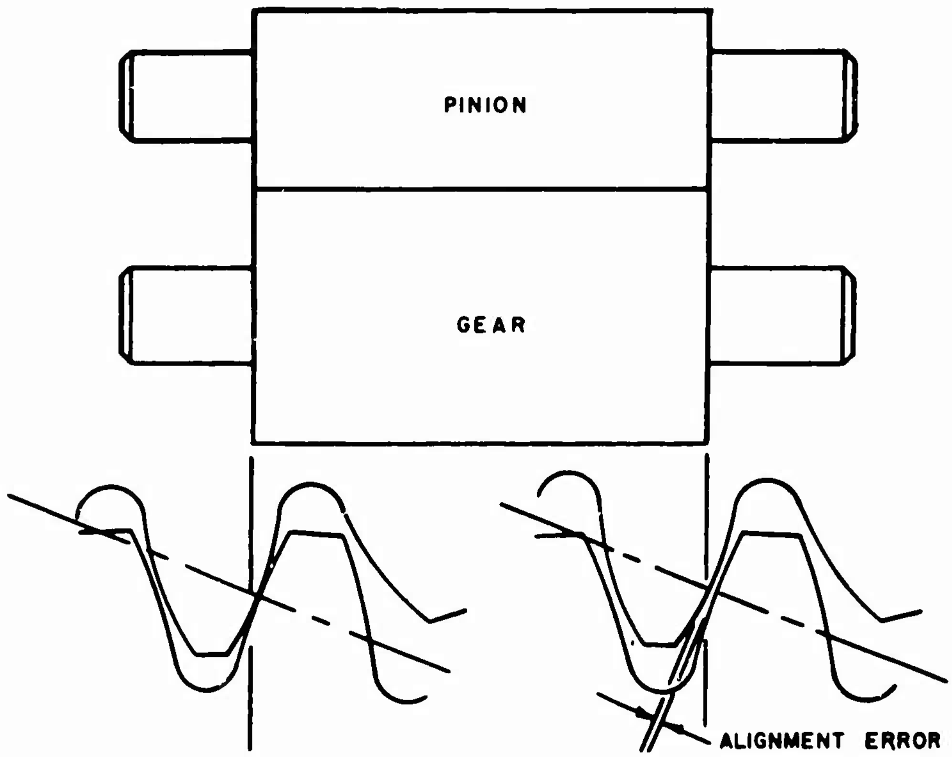

FIG. 2 EXAMPLE OF A PINION AND GEAR MISALIGNED UNDER NO LOAD. TEETH CONTACT AT LEFT HAND END AND ARE OPEN AT RIGHT HAND END.

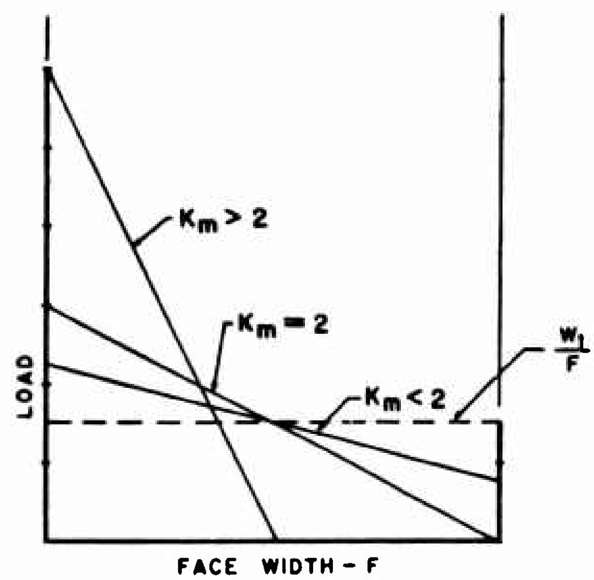

FIG. 3 LOAD DISTRIBUTION ACROSS FACE WIDTH FOR VARIOUS CONTACT CONDITIONS

$C_e = \frac{W_t}{1000e}$	W_t = TANGENTIAL LOAD - LBS e = ALIGNMENT ERROR INCHES/INCH

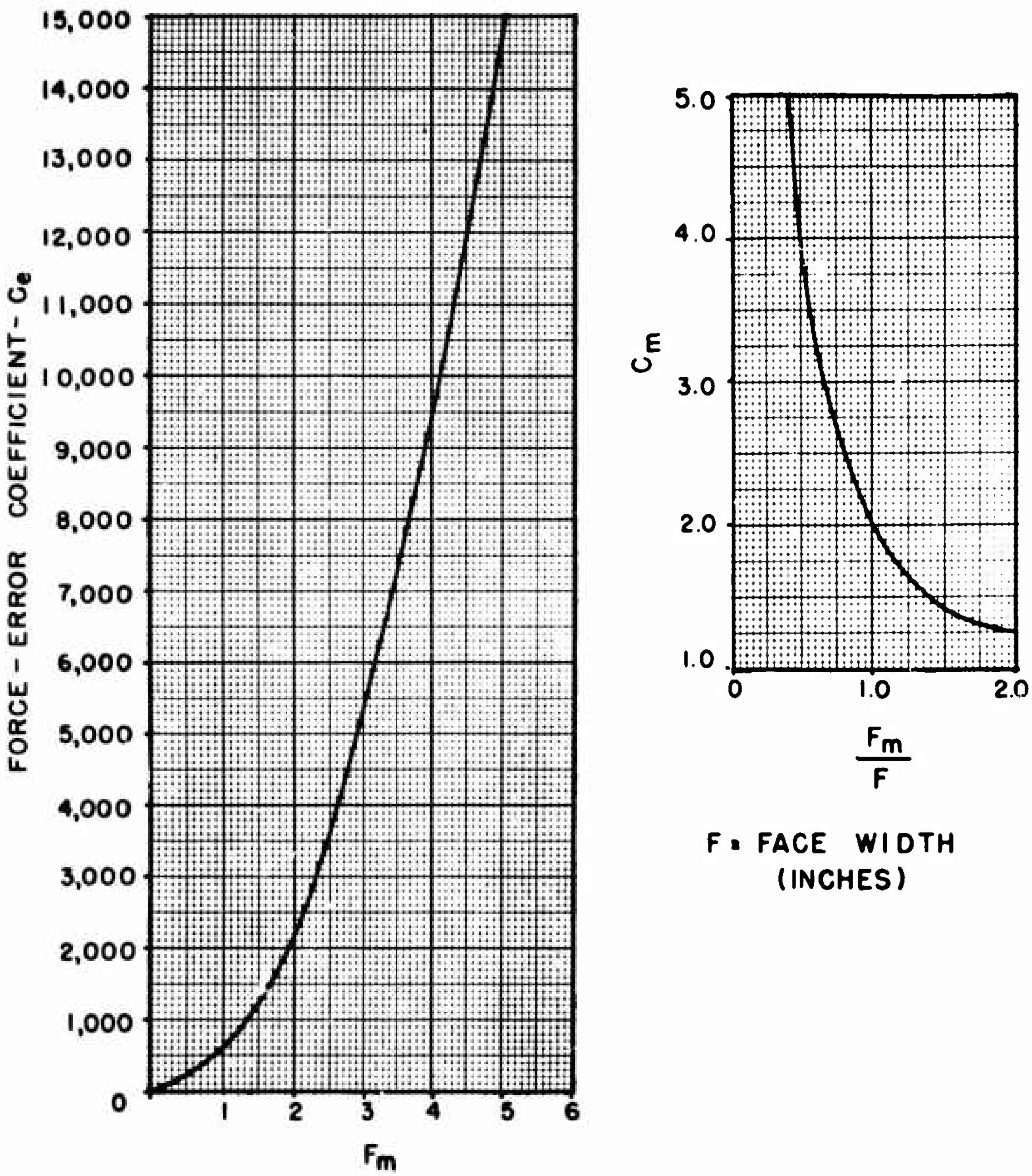

FIG. 4 SPUR GEAR LOAD DISTRIBUTION FACTOR — K_m

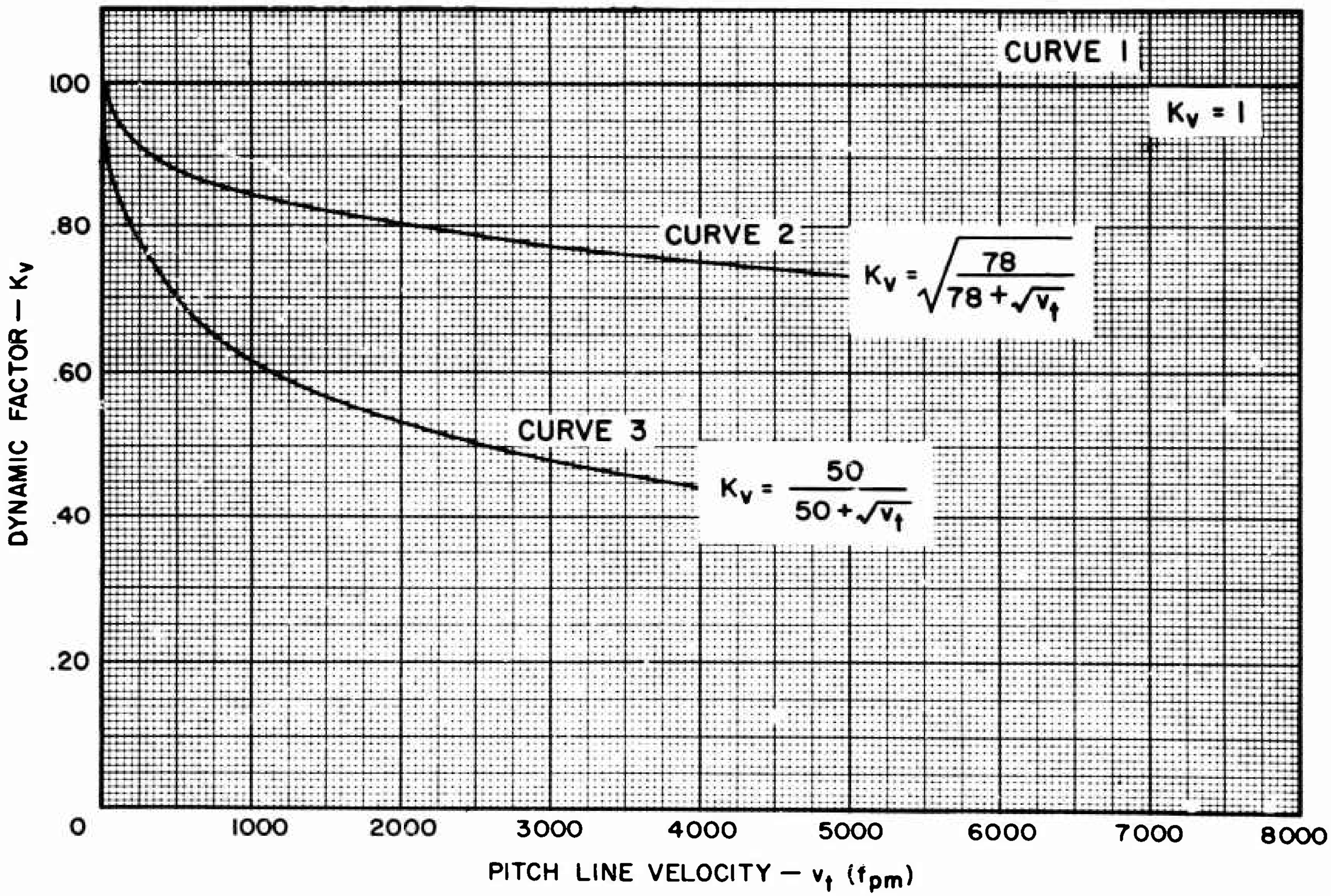

FIG. 5 DYNAMIC FACTOR — K_v

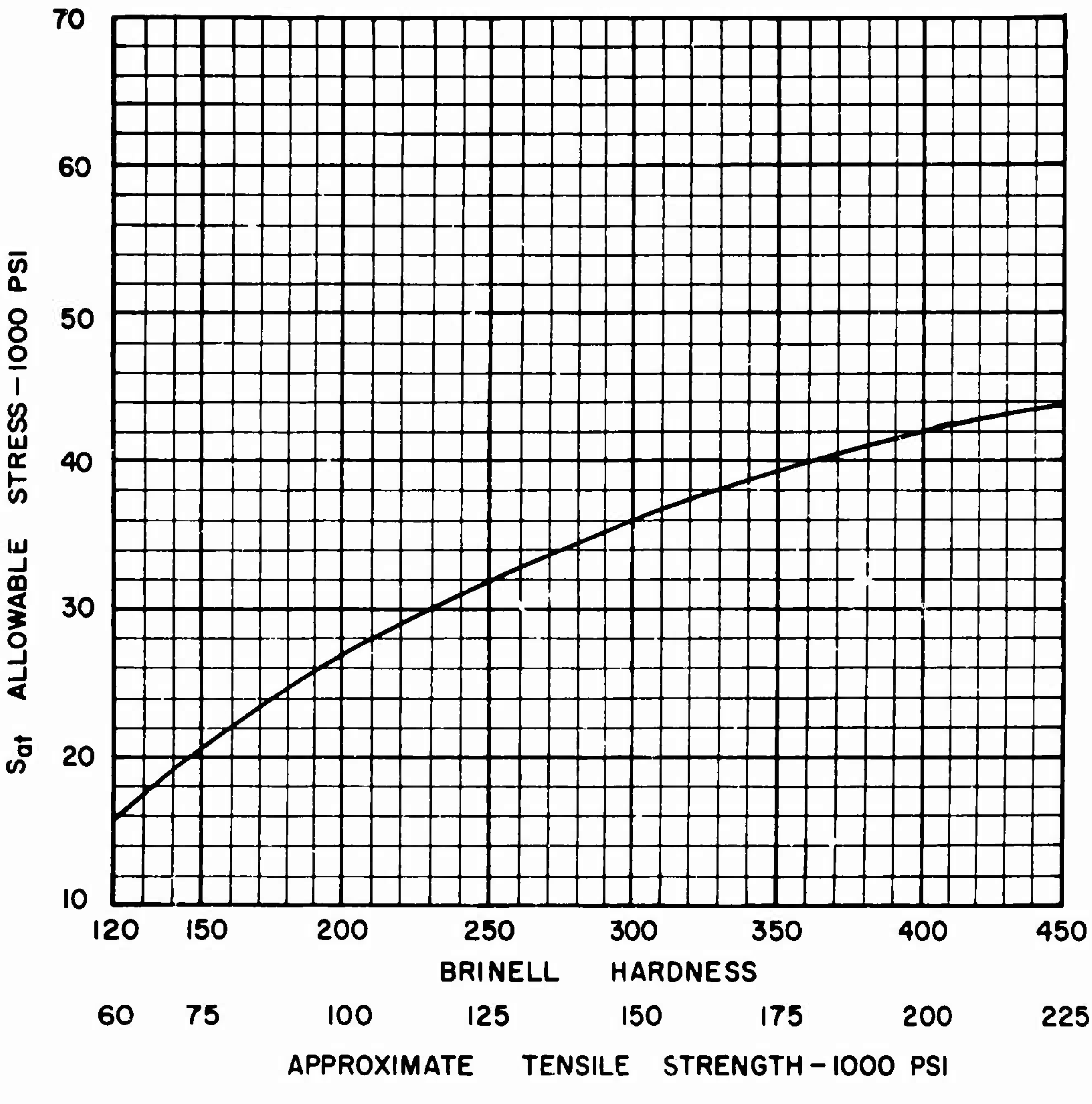

FIG. 6 ALLOWABLE FATIGUE STRESS FOR STEEL GEARS—S_{at}

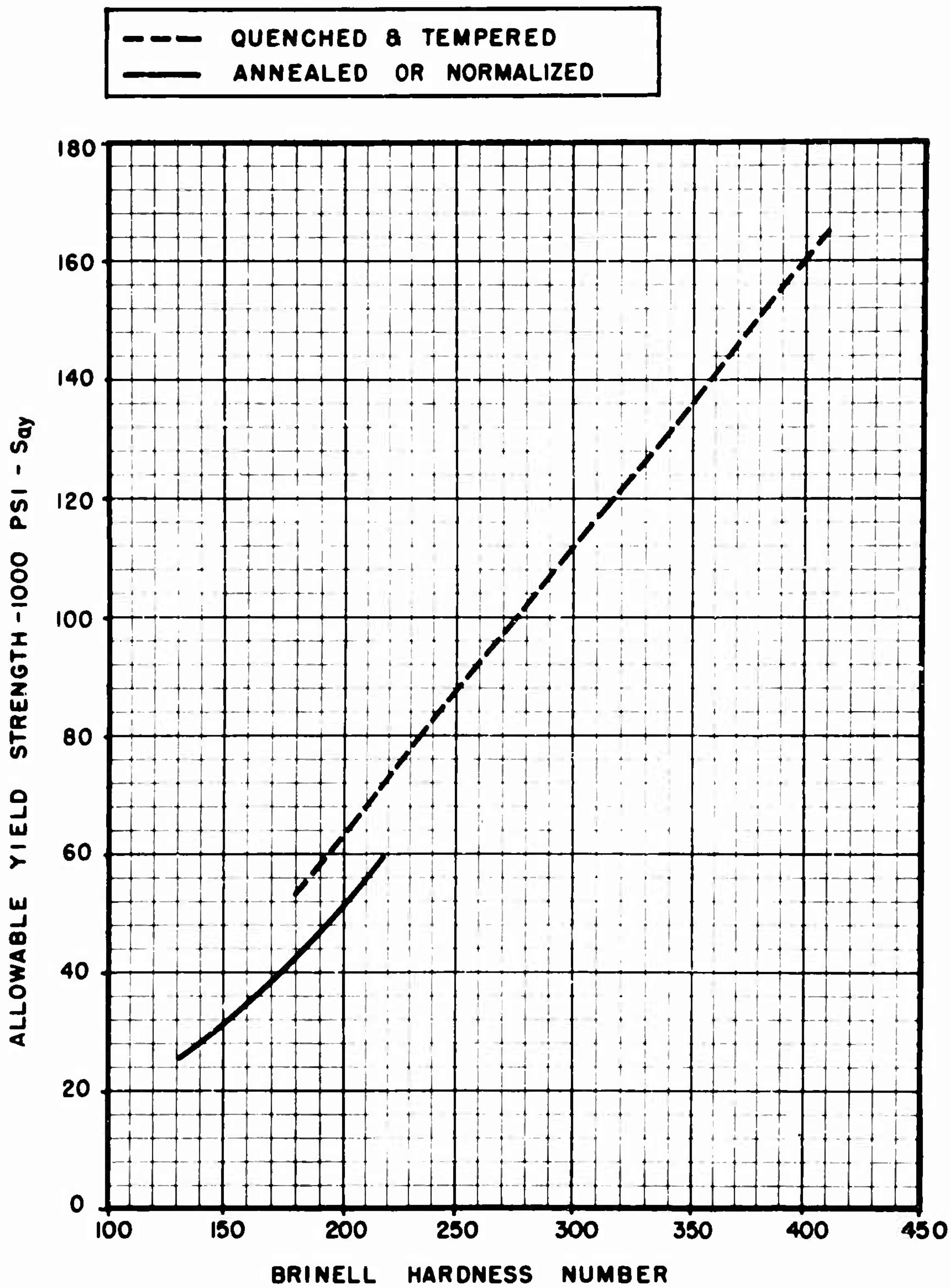

FIG. 7 ALLOWABLE YIELD STRENGTH - S_{ay}

APPENDIX A

SPUR GEAR GEOMETRY FACTOR

1. Geometry Factor — J

$$J = \frac{Y}{K_f \; m_N}$$

Where:

J = geometry factor

Y = tooth form factor

K_f = stress correction factor

m_N = load sharing ratio

2. Tooth Form Factor — Y

2.1 Y is determined for the most critical position of load application. This is at the tip of the tooth when load sharing does not exist and usually at the highest load position for single tooth contact when load sharing does exist.

2.2 The Y factor, which considers both the tangential (bending) and radial (compressive) components of the load is calculated as follows:

$$Y = \frac{1}{\dfrac{\cos \phi_L}{\cos \phi}\left(\dfrac{1.5}{X} - \dfrac{\tan \phi_L}{t}\right)}$$

Where:

ϕ = pressure angle

2.3 Use the following procedure to determine Y.

2.3.1 Lay out a generated tooth profile at a scale of one diametral pitch (P_d), as shown in Figures A1 and A2.

2.3.2 When load sharing exists (Fig. A1), lay a scale tangent to the base circle and locate the position where the distance from the intersection point with the pitch circle to the intersection point with the profile equals distance z_c – inches (obtained from Figures A3 or A4). This locates line *aa*.

2.3.3 When load sharing does not exist (Fig. A2), draw line *aa* through point *p* and tangent to the base circle. This locates line *aa*.

2.3.4 Through point *f* draw line *bb* perpendicular to the tooth center line. The included angle between lines *aa* and *bb* is angle ϕ_L.

2.3.5 Draw line *cde* tangent to the tooth fillet radius (r_f) at *e*, intersecting line *bb* at *d* and the tooth center line at *c* so that *cd* = *de*.

2.3.6 Draw line *fe*.

2.3.7 Through point *e* draw a line perpendicular to *fe*, intersecting the tooth center line at *n*.

2.3.8 Through point *e*, draw a line *me* perpendicular to the tooth center line.

2.3.9 Measure the following from the tooth layout:

mn = X – inches

me = $t/2$ – inches

angle ϕ_L

2.3.10 Calculate form factor Y.

3. Stress Correction Factor — K_f

3.1 Stress correction factor depends on:

1) effective stress concentration;

2) location of load;

3) plasticity effects;

4) residual stress effects;

5) material composition effects;

6) surface finish:

a) resulting from gear production

b) resulting from service.

7) Hertz stress effects;

8) size effect;

9) end of tooth effects.

3.2 The following stress correction factor is that of Dolan and Broghamer and only includes the effects of items 1 and 2.

$$K_f = H + \left(\frac{t}{r_f}\right)^J \left(\frac{t}{h}\right)^L$$

Where:

H, J and L are obtained from Table A-1. For other pressure angles, the values of H, J and L can be obtained by interpolation and extrapolation.

Table A-1 Values for H, J and L

Pressure Angle	H	J	L
14½°	0.22	0.20	0.40
20°	0.18	0.15	0.45
25°	0.14	0.11	0.50

h = distance fm measured from the layout — inches

$\frac{t}{2}$ = distance me measured from the layout — inches

$r_f = r_1 + r_T$

Where:

r_T = edge radius of tool — inches. For a cutter with chamfered teeth, take $r_T = 0$.

$$r_1 = \frac{b_1^2}{R_o + b_1}$$

Where:

R_o = the relative radius of curvature of the pitch circle of the gear and the pitch line or pitch circle of the generating tool. For generation by a rack or hob, R_o equals the pitch radius R of the gear being generated. For generation by a pinion-shaped cutter, $1/R_o = 1/R + 1/R_c$, where R_c is the pitch radius of the cutter.

$b_1 = b - r_T$

Where:

b = dedendum — inches

3.3 Plasticity reduces the effect of stress concentration and is partially measured by the life factor of Table 7. When more accurate data such as notch sensitivity values are available, they may be used.

3.4 If more exact values for the stress correction factor are available, they may be used.

4. Load Sharing Ratio — m_N

4.1 Load sharing ratio is influenced by profile contact ratio.

4.2 The most critical position of spur gear load application normally occurs when only one tooth is in contact.

Therefore, $m_N = 1.0$.

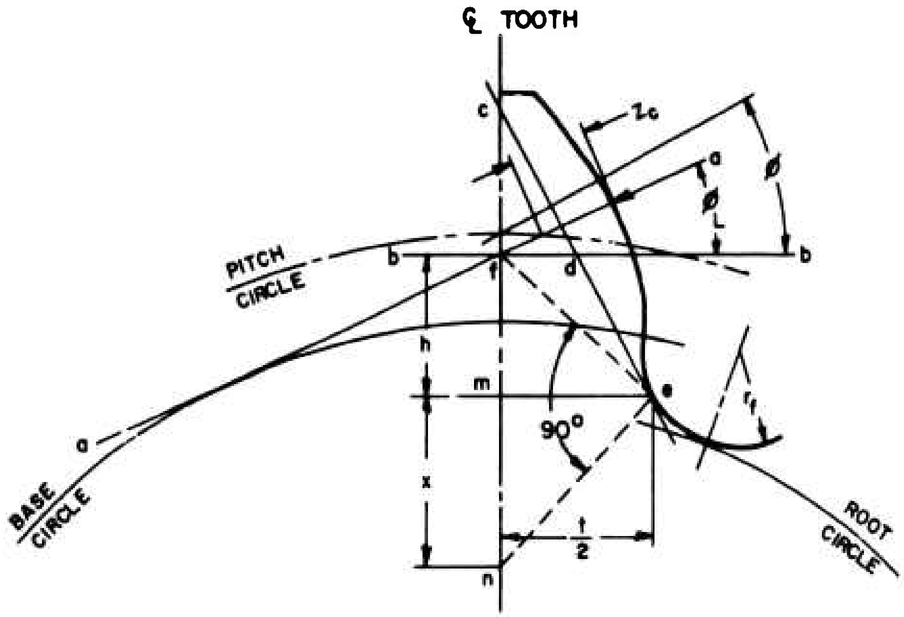

LOAD AT HIGHEST POINT FOR SINGLE TOOTH CONTACT

FIG. A-1 TOOTH FORM FACTOR LAYOUT WITH LOAD SHARING

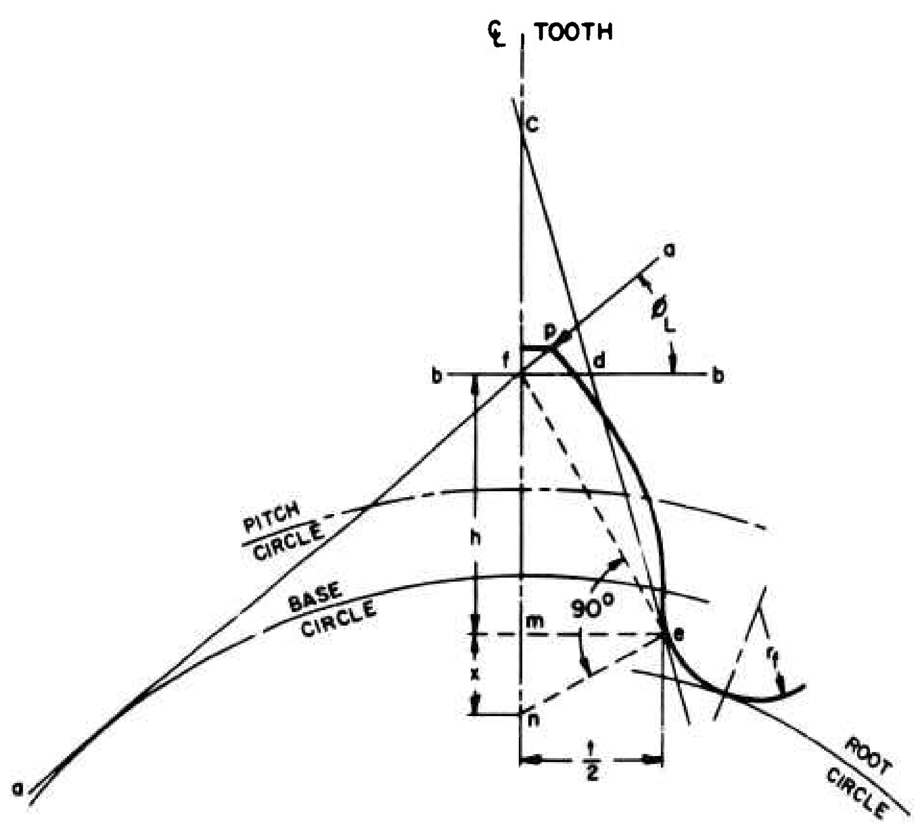

TIP LOADING

FIG. A-2 TOOTH FORM FACTOR LAYOUT WITHOUT LOAD SHARING

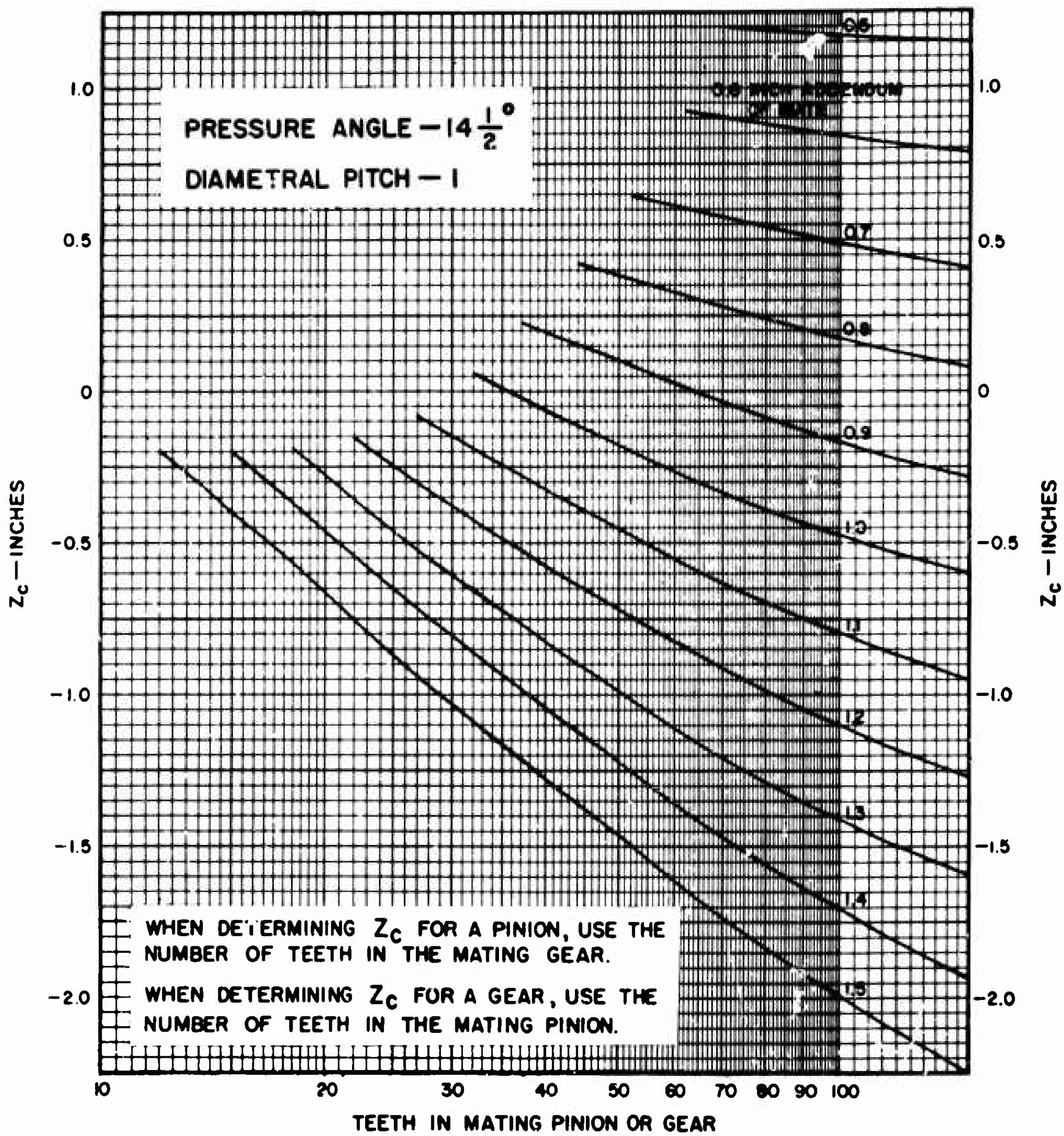

FIG. A-3 Z_C — FOR HIGHEST POINT OF SINGLE TOOTH CONTACT WHEN LOAD SHARING EXISTS BETWEEN TEETH

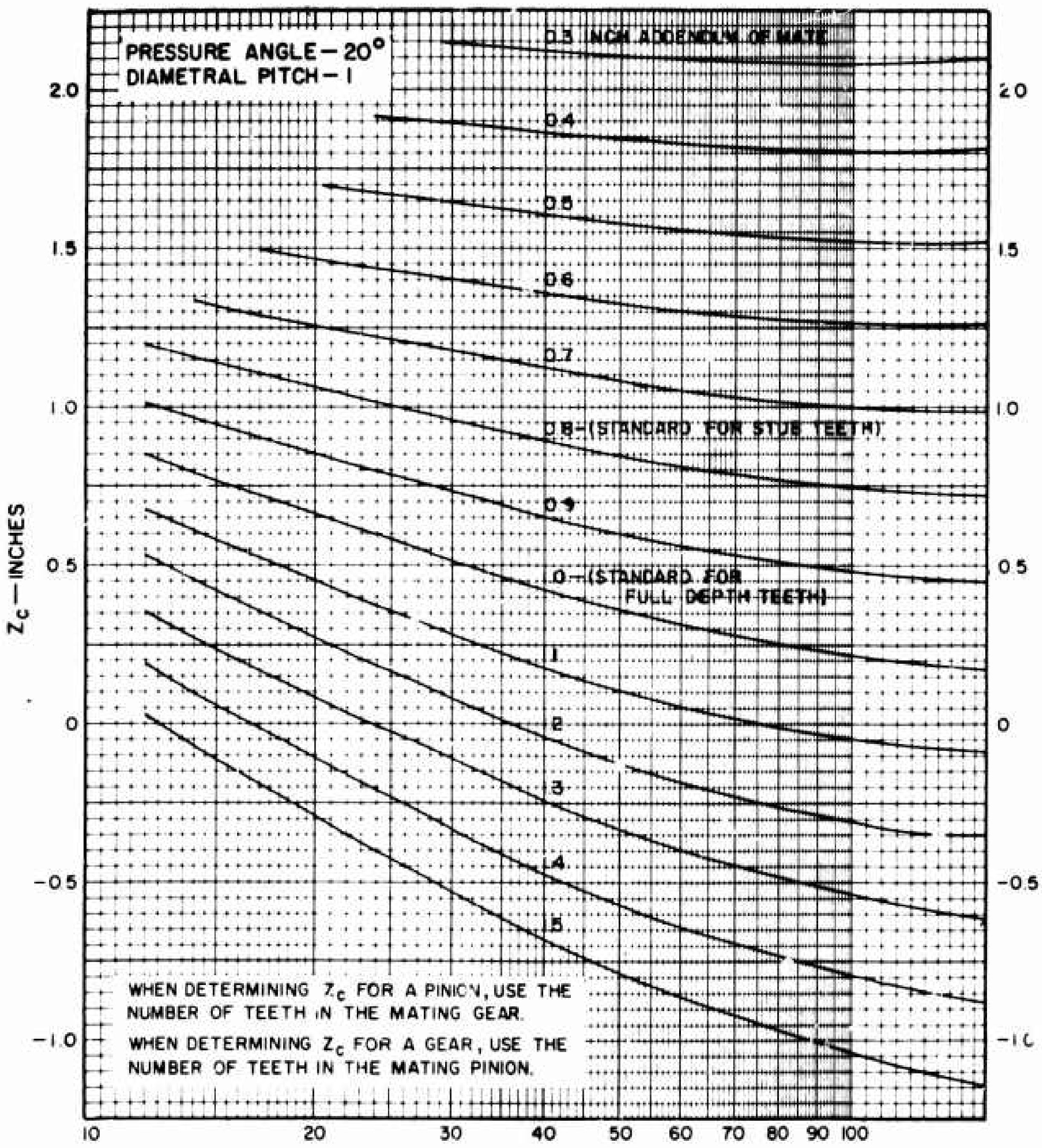

FIG. A-4 Z_c — FOR HIGHEST POINT OF SINGLE TOOTH CONTACT WHEN LOAD SHARING EXISTS BETWEEN TEETH

The user of this Standard (AGMA 220.02) may find these other AGMA Standards of value as reference data:

A more complete list of AGMA Standards published by the American Gear Manufacturers Association is available upon request.

Unclassified

Security Classification

DOCUMENT CONTROL DATA - R&D

(Security classification of title, body of abstract and indexing annotation must be entered when the overall report is classified)

1. ORIGINATING ACTIVITY *(Corporate author)* Allison Division of General Motors Post Office Box 894 Indianapolis, Indiana 46206	2a. REPORT SECURITY CLASSIFICATION Unclassified 2b. GROUP

3. REPORT TITLE

ADVANCEMENT OF SPUR GEAR DESIGN TECHNOLOGY

4. DESCRIPTIVE NOTES *(Type of report and inclusive dates)*

Final Report (29 June 1965 through 28 July 1966)

5. AUTHOR(S) *(Last name, first name, initial)*

McIntire, Wayne L.
Malott, Richard C.

6. REPORT DATE	7a. TOTAL NO. OF PAGES	7b. NO. OF REFS
December 1966	296	62

8a. CONTRACT OR GRANT NO. Contract DA44-177-AMC-318(T) b. PROJECT NO. Task 1M121401D14414 c. d.	9a. ORIGINATOR'S REPORT NUMBER(S) USAAVLABS Technical Report 66-85 9b. OTHER REPORT NO(S) *(Any other numbers that may be assigned this report)* Allison EDR 4743

10. AVAILABILITY/LIMITATION NOTICES

Distribution of this document is unlimited.

11. SUPPLEMENTARY NOTES	12. SPONSORING MILITARY ACTIVITY Department of the Army U.S. Army Aviation Materiel Laboratories Fort Eustis, Virginia 23604

13. ABSTRACT

An analytical and experimental study to evaluate factors for accurate appraisal of gear tooth bending strength is described. A design analysis consisting of a thorough review of current methods of calculating bending strength is presented. Experimental evaluation of strain gage measured stresses, photostress patterns, and a dynamic test at high speed are also presented for substantiation of the theoretical stress analysis. Results from a designed static fatigue test are presented to evaluate the effect of four geometric variables, i.e., diametral pitch, pressure angle, fillet radius size, and fillet configuration. A final computer program is described to calculate bending stress as substantiated by design analysis, experimental evaluation, and static fatigue test. It is shown that the thorough consideration of geometric variables permits a more precise assessment of bending strength for life expectance of lightweight aircraft gearing.

DD FORM 1 JAN 64 1473

Unclassified

Security Classification